ASSESSMENT OF METEOROLOGICAL AND HYDROLOGICAL DROUGHTS USING STATIONARY AND NON-STATIONARY INDICES FOR TWO CONTRASTING CLIMATE REGIONS IN INDIA

Thesis

Submitted in partial fulfilment of the requirements for the degree of

DOCTOR OF PHILOSOPHY

by

ARYA SAJEEV

DEPARTMENT OF WATER RESOURCES AND OCEAN ENGINEERING

NATIONAL INSTITUTE OF TECHNOLOGY KARNATAKA

SURATHKAL, MANGALURU – 575 025

SEPTEMBER, 2024

ASSESSMENT OF METEOROLOGICAL AND HYDROLOGICAL DROUGHTS USING STATIONARY AND NON-STATIONARY INDICES FOR TWO CONTRASTING CLIMATE REGIONS IN INDIA

Thesis

Submitted in partial fulfilment of the requirements for the degree of

DOCTOR OF PHILOSOPHY

by

ARYA SAJEEV

Under the Guidance of

Dr. SUBRAHMANYA KUNDAPURA

DEPARTMENT OF WATER RESOURCES AND OCEAN ENGINEERING

NATIONAL INSTITUTE OF TECHNOLOGY KARNATAKA

SURATHKAL, MANGALURU – 575 025

SEPTEMBER, 2024

DECLARATION

By the Ph.D. Research Scholar

I hereby *declare* that the Research Thesis entitled **Assessment of Meteorological and Hydrological Droughts Using Stationary and Non-Stationary Indices for Two Contrasting Climate Regions in India** which is being submitted to the **National Institute of Technology Karnataka, Surathkal** in partial fulfilment of the requirements for the award of the Degree of **Doctor of Philosophy** in **Water Resources Engineering** is a *bonafide report of the research work* carried out by me. The material contained in this Research Thesis has not been submitted to any University or Institution for the award of any degree.

04/09/2024

187082AM002, Arya Sajeev

(Register Number, Name & Signature of the Research Scholar)

Department of Water Resources and Ocean Engineering

Place: **NITK-Surathkal**

Date: 04/09/2024

CERTIFICATE

This is to certify that the Research Thesis entitled **Assessment of Meteorological and Hydrological Droughts Using Stationary and Non-Stationary Indices for Two Contrasting Climate Regions in India** submitted by **Arya Sajeev** (187082AM002) as the record of the research work carried out by her, is *accepted as the Research Thesis submission* in partial fulfilment of the requirements for the award of degree of **Doctor of Philosophy**.

04/09/24

Dr. Subrahmanya Kundapura

Research Guide

(Name and Signature with Date and Seal)

Dept. of Water Resources & Ocean Engineering ★ NITK Surathkal

Varija K
4.9.24

Chairman – DRPC

(Signature with Date and Seal)

Chairman (DPGC)
Dept. of Water Resources & Ocean Engineering

ACKNOWLEDGEMENTS

First and foremost, I would like to express my deepest gratitude to my advisor, **Dr. Subrahmanya Kundapura**, Faculty of Water Resources Engineering, Department of Water Resources and Ocean Engineering, NITK, Surathkal, for invaluable guidance, feedback, and constant encouragement throughout the research. His dedication to excellence has been a source of inspiration and his constructive feedback has significantly improved the quality of my work. I am particularly grateful for the time he devoted to discussing some important topics and for his thorough review of my thesis.

I am immensely thankful to **Prof. Mahesha A, Prof. Amba Shetty, Prof. Dodamani B M, and Prof. Varija K**, the successive Heads of the Department of Water Resources and Ocean Engineering, NITK, for the kind support and encouragement extended by them. I am grateful to all faculty members of the Department of Water Resources and Ocean Engineering, for their kind support and encouragement, throughout my tenure as a research scholar in the Department.

I am profoundly grateful to **Dr. Manu**, Department of Water Resources and Ocean Engineering and **Dr. Anupama Surenjan**, Department of Civil Engineering, the members of my Research Progress Assessment Committee, for their valuable suggestions and the encouragement provided at various stages of this work. I extend my sincere thanks **Dr. Azoni**, Department of Civil Engineering, former member of my Research Progress Assessment Committee for the insightful comments and encouragement.

I sincerely thank **Mr. Seetharama, Mr. Vishwanath Poojary, Mr. Shrikanth, Mrs. Prathima, Mr. Anil Kumar, Ms. Sweekritha, Mrs. Ashwija P Shetty, Mr. Shashidhar, Mr. Harish, Mr. Dheeraj**, and other non-teaching staff of the department for their invaluable assistance in ensuring the smooth progress of my research work.

I would like to express my gratitude to Director **Prof. B Ravi**, Former Directors **Prof. Prasad Krishna, Prof. Udaykumar R. Yaragatti** and **Prof. K Uma Maheshwar Rao**, Dean Academic, Staff of Office of Dean Academics, Associate Dean (PG&R) of NITK Surathkal, for their support and providing access to the institutional

infrastructure facilities. I would like to thank the Ministry of Education for the funding that made this research possible.

Special thanks to **Dr. Surajit** for his invaluable wisdom and continuous inspiration. I am also thankful to my dear friends **Dinesh, Partha, Biruk, Apoorva, Alka, Priyanka, Nithya, Elisuba, Chinmay, Sarannya, Shill, Aruni, Ashi, Tom, Dinu, Rony, Amala, Binoy, Charu, Anjali, Gangus, Roshu, Manj, Nivs, Uma, Anu, Chandana, Shankar, and other colleagues** for their unwavering support, companionship, and for making this journey memorable.

I would like to take a moment to express my deepest appreciation and heartfelt gratitude to my beloved family members, my parents **Smt. Ajitha, Shri. Sajeev**, grandmother **Smt. Thankamma** and my brother **Mr. Amal**. You are the pillars of strength and the guiding lights in my life. Your unwavering love, endless sacrifices, and boundless encouragement have been the foundation of my journey. I owe everything to my parents, whose values of hard work, perseverance, and compassion have shaped who I am today. Your sacrifices and understanding have empowered me to pursue my dreams with confidence. This achievement is as much yours as it is mine, and I dedicate it to you with all my love and gratitude.

My heartfelt thanks to my dear husband, **Mr. Sandeep**, for being my mentor, and constant support throughout this journey. I am deeply grateful for your constant presence as my pillar of strength. This achievement is as much yours as it is mine, and I look forward to celebrating many more milestones together. I am deeply grateful to my beloved in-laws, **Smt. Margaret** and **Shri. Jans**, for their unwavering support and love. Thanks to my brothers-in-law, **Mr. Richie** and **Mr. Deepak**, for their constant support. I am also thankful to dear **Ammachi** for her boundless love.

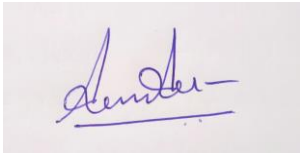

With love and affection

Arya Sajeev

ABSTRACT

Only a few researchers have incorporated climate change in drought indices calculations. This research attempts to build non-stationary indices for assessing meteorological drought in two different climate zones of India: the arid Saurashtra and Kutch and humid-tropical Coastal Karnataka. Time and climate indices are considered as covariates to develop non-stationary models using the Generalized Additive Model in Location, Scale, and Shape (GAMLSS) for the period, 1951-2004. A comparative study has been conducted to assess the statistical performance of stationary and non-stationary models on various time scales (3-,6-,12- and 24- months). The best model is selected to conduct copula-based bivariate drought analysis. For this purpose, drought properties such as drought severity, duration, and peak are calculated. The annual and seasonal rainfall departures are also analysed, and more rainfall-deficient years are detected in Saurashtra and Kutch regions than in Coastal Karnataka. The non-stationary index performed better in capturing drought properties in statistical analysis over both the study areas at all time scales. The non-stationary drought index shows better consistency with historical drought and flood events than the stationary index. The impact of rainfall and drought on the yield of major crops in study areas is also analysed. The yield loss rate of bajra significantly correlates with Non-stationary Standardized Precipitation Index (NSPI) in Saurashtra and Kutch, whereas rice yield has no significant correlation with the index in Coastal Karnataka.

Co-occurrence and joint return periods are calculated and compared with univariate return periods. A significant difference is observed between bivariate and univariate return periods, and more risk is detected in Saurashtra and Kutch than in Coastal Karnataka. Drought forecasting is crucial in water resource management and agricultural planning, particularly in regions vulnerable to water scarcity. Hence, the efficacy of various time-series forecasting models, including Autoregressive Integrated Moving Average (ARIMA), Feed-forward Neural Network (FNN), Recurrent Neural Network (RNN), as well as hybrid combinations such as ARIMA-FNN, ARIMA-RNN, FNN-ARIMA, and RNN-ARIMA, for predicting drought indices at different time scales (3, 6, 12, and 24 months) is performed in Saurashtra and Kutch. The effectiveness of the models is evaluated through Correlation Coefficient (CC), R-squared (R^2), Mean

Square Error (MSE), Mean Absolute Error (MAE), and Relative Absolute Error (RAE). FNN exhibits superior performance as a standalone model across all time scales considered, and scale 24 was the best-performing time scale with a Correlation Coefficient of 0.874 and R^2 of 0.911. However, further improvements in forecast accuracy are observed at all time scales when incorporating ARIMA as a post-processing step in the hybrid FNN-ARIMA model. Notably, FNN-ARIMA emerges as the top-performing model among all evaluated approaches, demonstrating its effectiveness in capturing the complex temporal dynamics of drought phenomena. This research emphasizes the significance of hybrid forecasting techniques, especially the combination of neural networks with traditional time-series models, in enhancing drought prediction accuracy. The findings contribute to the advancement of forecasting methodologies for better-informed decision-making in water resource management and agricultural sectors, thereby aiding in mitigating the impacts of drought events on vulnerable regions.

Comparative analyses of meteorological and hydrological droughts using non-stationary indices have not been explored yet. The other objective of this research is to develop non-stationary indices for assessing meteorological and hydrological droughts in the Shetrunji River basin in Saurashtra region, India, from 1971 to 2015. The statistical performance of stationary and non-stationary models has been compared across various time scales (3-,6-,12- and 24- months), and the results indicate that non-stationary models more effectively capture meteorological and hydrological drought events than stationary models. The drought and flood events detected by non-stationary indices are compared with historical episodes to assess the robustness of the indices. The results are also compared with drought events obtained from rainfall and streamflow departures. The annual and seasonal departures in rainfall and streamflow show the highest deficiency of rainfall and streamflow in 1987. The probability of different drought classes is calculated, and a higher likelihood of severe to extreme dry conditions is observed compared to very wet and extreme wet conditions in the basin. Investigation has been conducted on the impact of meteorological drought on hydrological drought and a correlation analysis between both types of droughts. A significant correlation is observed between meteorological and hydrological drought at

all analysed time scales. Meteorological drought impacts surface water resources with a one-month lag at all time scales, with the highest response rate obtained at 6-month scale (91.13%). The study also examines the impact of drought on yield loss in Kharif (Bajra) and Rabi (Wheat) crops. Bajra and wheat yield loss rates strongly correlate with non-stationary drought indices, with a more significant effect of drought on bajra yield than wheat during major drought events. The hydrological drought analysis in the humid Netravathi River basin is also conducted using stationary and non-stationary indices.

This drought analysis provides feasible results in both arid and humid regions in a changing environment. This novel dimension of drought studies provides practical insights into semi-arid regions in a changing environment. The findings can be utilized by various sectors, including drought management, agricultural planners, and policymakers, to reduce crop loss due to drought.

Keywords: Drought; Non-stationary analysis; Copula; GAMLSS; Standardized precipitation index (SPI); Crop yield; Return period, Neural Network

TABLE OF CONTENTS

LIST OF FIGURES

LIST OF TABLES

LIST OF ABBREVIATIONS

Abbreviation	Meaning
AD	Anderson Darling
AMO	Atlantic Multidecadal Oscillation
AO	Arctic Oscillation
ARIMA	Autoregressive Integrated Moving Average
CC	Correlation Coefficient
CMI	Crop Moisture Index
GAMLSS	Generalized additive models for location, scale, and shape
EASM	East Asian Summer Monsoon
ENSO	El Niño–Southern Oscillation
FNN	Feed-forward Neural Network
IMD	India Meteorological Department
IOD	Indian Ocean Dipole
ISMR	Indian Summer Monsoon Rainfall
KS	Kolmogorov-Smirnov
MAE	Mean Absolute Error
MEI	Multivariate ENSO Index
ML	Machine learning
MSE	Mean Square Error
MSRRI	Multivariate Standardized Reliability and Resilience Index
NAO	Northern Atlantic Oscillation
NDVI	Normalized Difference Vegetation Index
NOI	Non-stationary Standardized Precipitation Index
NRDI	Non-stationary Reconnaissance Drought Index
NSPI	Non-stationary Standardized Precipitation Index
PDO	Pacific Decadal Oscillation
PDSI	Palmer Drought Severity Index
POT	Peak over Threshold

R^2	R-squared
RAE	Relative Absolute Error
RDI	Reconnaissance Drought Index
RFA	Rainfall Anomaly
RNN	Recurrent Neural Network
SDI	Streamflow Drought Index
SHI	Standardized Hydrological Index
SOI	Southern Oscillation Index
SPA	Standardized Precipitation Anomaly
SPEI	Standardized Precipitation Evapotranspiration Index
SPI	Standardized Precipitation Index
SSI	Standardized Streamflow Drought Index
SST	Sea Surface Temperature
SSWI	Standardized Soil Water Index
NAI	NDVI Anomaly Index
NDVI	Normalized Difference Vegetation Index
VCI	Vegetation Condition Index
WoS	Web of Science

CHAPTER 1

INTRODUCTION

1.1 GENERAL

Drought is an environmental calamity that can have devastating effects on the environment and societal circumstances in all climatic zones, including low and high-rainfall areas (Mishra and Singh 2010). According to several studies (Li et al. 2013; Wang et al. 2015a), drought risks are anticipated to become more common and extensive in the future decades. Since the availability of monsoon rain is crucial to Indian agricultural productivity, deficiency in rainfall harms crop yield and, as a result, the Indian economy (Bacanli 2012). According to Samra (2004), India's 28% geographical area is susceptible to drought. Around 68% of India's net sown land comes under drought-prone areas, and 50% is vulnerable to frequent severe droughts (Dutta et al. 2013). As a result, accurate assessment and understanding of drought events have become paramount (Lambe and Kundapura 2023), necessitating the utilization of sophisticated methodologies that encompass the evolving climate variations (Zhang et al. 2015).

1.2 TYPES OF DROUGHTS

Drought is classified as meteorological, hydrological, agricultural, and socio-economic droughts based on a deficiency in precipitation, streamflow, the productivity of agricultural products, and socio-economic conditions, respectively (Zhang et al. 2017a).

1.2.1 Meteorological drought

Meteorological drought arises from inadequate precipitation, impacting water availability and ecosystems (Sajeev et al. 2021). A severe meteorological drought can progressively impact various water resource sectors, including soil moisture, groundwater, and river discharge, ultimately leading to hydrological drought. Meteorological drought triggers all other kinds of drought and is more frequent (Das et al., 2020a); thus, its analysis is more important. Numerous indicators are being used to monitor the meteorological drought (Shiau, 2006; Kumar et al., 2009). Rainfall

deviation from its long-term mean is observed to monitor the drought condition. Based on the India Meteorological Department (IMD) (https://mausam.imd.gov.in), drought is declared based on this deviation. A meteorological subdivision of India is said to be under drought if the entire seasons' rainfall is below 75% of its long-term mean (Thomas and Prasannakumar 2016). The different areas have different mean rainfall; hence, the rainfall deviation cannot be used uniformly. Thus, several indices were introduced to monitor the drought. Standardized Precipitation Index (SPI) is the most widely used index worldwide (McKee et al.1993; Sasikumar and Nair 2016).

1.2.2 Hydrological drought

Hydrological drought entails decreased surface water and groundwater levels, impacting water sources vital for multiple uses (Lin et al. 2017; Ozkaya and Zerberg 2019). Streamflow data is mainly used for the analysis. There is always a delay between the deficiency of rain and a less measurable amount of water in streams and reservoirs. So, a lag can happen in the hydrological drought indicators compared to meteorological drought indicators (Lin et al. 2017). The theory of runs, Standardized Hydrological Index (SHI)(Sharma and Panu 2014), and Streamflow Drought Index (SDI) (Myronidis et al. 2018) are some indices used to study hydrological drought.

1.2.3 Agricultural drought

Agricultural drought affects crop growth due to insufficient soil moisture and water supply (Duan and Mei 2014). It is the period in which the soil moisture content is insufficient to meet the crop requirements in an area at its various stages of growth. It adversely affects the crop yield and agricultural profitability of a country. The Standardized Soil Water Index (SSWI) (Duan and Mei 2014), Crop Moisture Index (CMI) (Palmer 1968), and Normalized Difference Vegetation Index NDVI (Dutta et al. 2013) are commonly used to define agricultural drought.

1.2.4 Socio-Economic drought

Socioeconomic drought encompasses the broader ramifications of water scarcity, affecting industries, communities, and livelihoods (Huang et al. 2016). It is connected to the water resource system's inability to satisfy different needs and has an impact on the availability and demand for economic commodities. Weather-related deficiency in

the water supply results in an increase in demand compared to supply. It relates to the impact of agricultural, meteorological, and hydrological droughts on society, especially in terms of the supply and demand of commodities and the purchasing power of the people. Severe societal drought may even lead to mass migration in search of food, fodder, water, and work, leading to famine, death, and social unrest. Multivariate Standardized Reliability and Resilience Index (MSRRI) is the main index for Socio-economic drought (Mehran et al. 2015).

1.3 DROUGHT INDICES

Drought indices are the best tool for quantitative drought analysis. Due to the lack of a proper universal definition of drought, several drought indices have been used by various researchers in different regions based on the data availability, and the examples are not limited to Standardized Precipitation Evapotranspiration Index (SPEI) (Wang et al. 2020b), Standardized Precipitation Index (SPI) (McKee et al.1993; Sasikumar and Nair 2016), and Reconnaissance Drought Index (RDI) (Tigkas et al. 2012). For meteorological drought analysis, the Standardized Precipitation Index (SPI) (McKee et al.1993) and Palmer Drought Severity Index (PDSI) (Palmer 1965) are commonly used by researchers. Due to the many limitations associated with PDSI (Kao and Govindaraju 2010), it is suggested that SPI be used as the primary index for meteorological drought studies (Thomas and Prasannakumar 2016). Its simplicity, flexibility to work with various time scales, spatial variance, and probabilistic nature made SPI an appealing index for drought analysis (Guttman 1999). A significant number of studies proved the efficiency of SPI in detecting and monitoring drought events in different climatic regions (Bonaccorso et al. 2015; Hangshing and Dabral 2018; Reddy and Ganguli 2012b; Sajeev et al. 2021; Shiau 2006). Notably, SPI has found utility in assessing drought in Andhra Pradesh, India (Kumar et al. 2009), Ethiopia (Chemeda et al. 2010), Gujarat, India (Ganguli and Reddy 2012), upper Han River basin, China (Chen et al. 2013), north-western Iran (Kazemzadeh and Malekian 2016), Kerala, India (Thomas and Prasannakumar, 2016), Lake Urmia basin, Iran (Amirataee et al. 2018) and Bangladesh (Mortuza et al. 2019). The advantages of the Standardized Precipitation Index (SPI) for drought analysis lie in its capability to

account for its inherent probabilistic nature, and serve as an agricultural drought indicator (Guttman 1999; Patel et al. 2007; Thomas and Prasannakumar 2016).

Drawing from the SPI framework, Vicente-Serrano et al. (2012) introduced the Standardized Streamflow Drought Index (SSI) to assess hydrological drought. The SSI has been applied in various studies globally to assess hydrological drought (Botai et al. 2021; Tijdeman et al. 2020). It can be represented on different time scales (3, 6, 9, 12, and 24) (Borji et al. 2016). The Streamflow Drought Index (SDI) was developed by Nalbantis and Tsakiris (2009) for defining the hydrological drought.

1.4 IMPORTANCE OF NON-STATIONARY INDEX

Traditional analysis done in hydrology was based on the assumption that there is no variation in the statistical characteristics of data with time. Most of the previous drought studies, such as Botai et al. (2021), Ganguli and Reddy (2012), Mishra and Desai (2005a), Sajeev et al. (2021), and Zhao et al. (2014) have done drought studies using only stationary indices. However, it is challenging to proceed with this assumption because of the non-stationarity of hydro-meteorological variables due to climate change and other anthropogenic factors (Griffis and Stedinger 2007; Zhang et al. 2021). A significant connection is observed between climate variations and extreme hydrologic events such as droughts and floods (Himayoun and Roshni 2019; Li et al. 2015). Over the last decade, non-stationary-based tools have been developed in hydrological process studies (Cancelliere 2017). El Niño–Southern Oscillation (ENSO) is the predominant reason behind the variable nature of hydrological variables on a large scale (Agilan and Umamahesh 2018; Zhang et al. 2013). Recent studies revised the Standardized Precipitation Index (SPI) by considering different covariates in non-stationary gamma distributions (Das et al. 2020b; Rashid and Beecham 2019; Wang et al. 2015b), and the revised index is found to be more robust than the normal index. Non-stationary models are appropriate when dealing with dynamic systems where the relationships and behaviour of variables change over time. It can include climate models, environmental systems, and complex socio-economic systems (Wang et al. 2015b). Li et al. (2015b) used climate indices as a covariate in developing non-stationary SPI in the Luanhe River basin in China. In order to develop a non-stationary Standardized Streamflow Drought Index, human-induced non-stationarity is also considered by Wang et al.

(2020b). Bazrafshan and Hejabi (2018) developed a Non-Stationary Reconnaissance Drought Index for Iran using time as a covariate. Significantly fewer researchers (Das et al. 2020b; Das et al. 2021; Masanta and Srinivas 2022) gave attention to the non-stationary analysis of drought in India. Ajayamohan and Rao (2008) observed the significant influence of the Indian Ocean Dipole (IOD) on the central Indian region's extreme rainfall. Agilan and Umamahesh (2018) suggested that the Southern Oscillation Index (SOI) and ENSO index are the best covariates for modeling long-term rainfall in Hyderabad, India. Generalized additive models for location, scale, and shape (GAMLSS) are established to be a flexible tool in non-stationary modeling (Debele et al. 2017a; Stasinopoulos and Rigby 2007; Zhang et al. 2015; Wu et al. 2022).

1.5 COPULA

Drought is stochastic; hence, probability-based studies are more suitable for accurate results (Mishra and Singh 2010). Many studies have proved that drought properties are interdependent; hence, bivariate analysis is more suitable for a comprehensive analysis of drought (Sajeev et al. 2021). However, bivariate distributions such as bivariate exponential and normal distributions apply only to the marginal distributions with the same family (Frees and Valdez 1998). This difficulty can be solved using copula functions as it is independent of the type of marginal distribution. Copulas are functions that are used to join marginal distributions to create multivariate distribution functions and have been used by various studies worldwide (Adarsh et al. 2018; Dodangeh et al. 2017; Hangshing and Dabral 2018; Reddy and Ganguli 2012a; Kao and Govindaraju 2010; Sajeev et al. 2021). There are various copula families, and for this study, elliptical copulas such as normal and t copula, Archimedean copulas such as Gumbel, Clayton, and Frank, and other copulas (Plackett) were considered (Mishra and Singh 2010). Sajeev et al. (2021) used these copulas for bivariate drought analysis in arid regions in India. According to Renard and Lang (2007), the elliptical copulas resemble the multivariate Gaussian distribution. Positive and negative dependence can both be modeled using the elliptical group. This family of copulas offers asymmetric tail dependence.

The student's t copula has both upper and lower tail dependence of the same magnitude (Ganguli and Reddy 2012). Archimedean copulas are more adaptable to modeling data

with various dependencies (Poonia et al. 2021). It can simultaneously capture upper and lower tail dependence (Ganguli and Reddy 2012). The Frank, Gumbel, and Placket copulas are flexible and can model positive and negative dependencies (Zhang and Singh 2007). The Gumbel is applied in risk management, hydrology, and environmental studies to assess the joint behaviour of variables with heavy tails. The Clayton copula is commonly used to model positive tail dependence, significantly when the dependence strength decreases as the variables increase. The t copula is an extension of the normal copula incorporating heavy-tailed distributions. It is used when dealing with non-normal or skewed data and finds applications in risk management and extreme value analysis (Kwak et al. 2012; Zhang et al. 2019).

1.6 SCOPE OF THE RESEARCH

This research aims to enhance the accuracy and relevance of drought prediction by incorporating climate change into drought indices calculations. Specifically, the research focuses on developing non-stationary models for assessing meteorological and hydrological droughts in different climate zones of India: the arid Saurashtra and Kutch, as well as the humid-tropical Coastal Karnataka. The non-stationary drought index developed using climate indices could accurately assess the important aspects of drought, like how severe it was, how long it lasted, and when it reached its peak. By evaluating the return period of a specific drought severity and duration, decision-makers can assess the likelihood of experiencing such an event in a given year or over a specific period. It helps to prioritize resources, plan adaptation measures, and design drought management strategies to mitigate potential impacts. If specific ENSO or IOD conditions are associated with prolonged drought, water resource managers can implement proactive measures like water conservation initiatives, irrigation scheduling, and crop diversification. This research examines the impact of rainfall and drought on major crop yields (bajra in arid regions and rice in humid tropical regions). This knowledge can aid farmers and policymakers in predicting crop losses, optimizing irrigation strategies, and implementing timely interventions to minimize agricultural productivity losses.

Drought forecasting is crucial for effective water resource management and agricultural planning, particularly in regions prone to water scarcity, is another focal point of the

research. The efficiency of various forecasting models, including ARIMA, FNN, RNN, and their hybrid combinations, is rigorously evaluated, demonstrating the superior performance of the FNN-ARIMA hybrid model in predicting drought indices. Another aim of this research is to investigate meteorological and hydrological droughts in the Shetrunji River basin in the Saurashtra region. Correlation, lag, and response rate analysis between these two droughts help to identify the impact of meteorological drought on surface water resources, highlighting the importance of considering integrated drought management plans. In addition, this research analyses streamflow and hydrological drought trends in the Netravathi River basin, emphasizing the importance of studying drought in the humid Netravathi River basin in Coastal Karnataka. Non-stationary indices are developed for the basin, providing a more dynamic and accurate assessment of hydrological drought conditions influenced by changing climatic variables.

Overall, this comprehensive approach to drought analysis integrates climate change considerations, enhancing the predictive capabilities of drought indices and providing practical insights for water resource management and agricultural planning. The findings are expected to aid policymakers and practitioners in developing strategies to mitigate drought impacts in vulnerable regions, ensuring better preparedness and resilience in changing environmental conditions in various climate regions.

1.7 ORGANIZATION OF THE THESIS

The structure of this thesis is comprised of eight chapters.

Chapter 1: This chapter introduces topics such as drought, types of droughts, drought indices, the importance of non-stationary indices in drought studies, copula, and the scope of the research.

Chapter 2: This chapter extensively deals with the literature review to cover the entire research domain.

Chapter 3: This chapter provides a comparative analysis of stationary and non-stationary drought indices in two different climate regions, Saurashtra and Kutch, as

well as Coastal Karnataka. This chapter also delves into an analysis of the impact of meteorological drought on crop yield losses in both areas.

Chapter 4: The focus of this chapter is on the effectiveness of ARIMA, FNN, RNN, and hybrid combinations of ARIMA and Neural Network models in drought prediction in highly drought-prone regions, Saurashtra and Kutch.

Chapter 5: This chapter presents a comparative study of meteorological and hydrological droughts using stationary and non-stationary indices in the Shetrunji River Basin in the Saurashtra region. It also examines the impact of drought on Kharif and Rabi crops in the study area.

Chapter 6: This chapter deals with the trend analysis and forecasting of hydrological drought in the humid Netravathi River basin in Coastal Karnataka.

Chapter 7: This chapter presents a comparative study of stationary and non-stationary hydrological drought in the Netravathi River basin.

Chapter 8: The summary of the findings and conclusions drawn from the study are presented in this last chapter. It also comprises the limitations of the study and future scope.

CHAPTER 2

LITERATURE REVIEW

2.1 GENERAL

India is one of the most vulnerable countries of the world to droughts (Mishra and Singh 2010). In order to plan a water resources project, a proper study of drought characteristics has to be done in the study area. Drought analysis have changed from traditional stationary indices to non-stationary-based indices by including climate changes. The ability to accurately assess and forecast drought conditions is crucial for effective water resource management and agricultural planning.

2.2 DROUGHT ANALYSIS USING STATIONARY INDICES

There are plenty of drought studies using stationary indices. The SPI is used for the assessment of meteorological drought in many regions coming under different climates such as Andhra Pradesh, India (Kumar et al. 2009), Ethiopia (Chemeda et al. 2010), Gujarat, India (Ganguli and Reddy 2012), upper Han River basin, China (Chen et al. 2013), north-western Iran (Kazemzadeh and Malekian 2016), Kerala, India (Thomas and Prasannakumar, 2016), Lake Urmia basin, Iran (Amirataee et al. 2018) and Bangladesh (Mortuza et al. 2019). The analysis done by Li et al. (2008) in southern Amazon observed a decrease in SPI value from 1970 to 1999, indicating an increase in the dry conditions in the region. Kumar et al. (2009) calculated the SPI for two districts of Andhra Pradesh, India. McKee et al. (1993) suggested the various severity levels of drought based on the range of SPI values. Tsakiris (2009) investigated hydrological drought using SDI. It assessed the possibility of analysing hydrological drought with the non-availability of stream flow based on SDI-SPI regression equation in the Greek basin in the West Sterea Hellas. Zamani et al. (2015) analysed extreme hydrological drought events in the Karkheh River basin (51,000 km^2) in Iran. SDI at 3 , 6, 9 and 12 months time scales are used for the study. Kazemzadeh and Malekian (2016) have done a study on the characteristics of hydrological and meteorological drought based on the trend of SPI and SDI indices in north-western Iran. Seasonal correlations between SPI and SDI are compared. The SSI allows accurate spatial and temporal comparisons of the hydrological conditions of a stream; its application on drought analysis can be seen

in various basins, such as, Ebro basin, Spain (Telesca et al. 2012), basins in Europe (Tijdeman et al. 2020), and basins in China (Zhao et al. 2016b). Table 2.1 summarizes some of the findings of the past study on drought analysis using stationary indices.

Table 2.1 Literature on drought analysis using stationary index

Author(s)	Study area	Drought Index	Key Conclusion
		Mereological Drought	
Shiau (2006)	Wushantou (Taiwan)	SPI	Copula based equations are derived for return periods calculation. The drought properties, such as duration and severity, are computed from SPI, which shows the advantage of bivariate drought analysis.
Chemeda et al. (2010)	Awash River Basin (Ethiopia)	SPI, streamflow	Hydrological and meteorological droughts are analysed by considering SPI and streamflow, respectively as drought indices. Meteorological drought affects the hydrological drought at an average of 7 months lags in the basin.
Ganguli (2014)	Maharashtra	Peak over Threshold (POT)	Copulas prove to be a helpful tool for analysing the uncertainty associated with extreme drought events. This capability is valuable for estimating risks in water resources planning in drought-prone regions.
Hangshing and Dabral (2018)	Agartala, India	SPI	Trivariate and bivariate drought analysis is carried out using meta elliptical and Archimedean copulas. The SPI is calculated for four different time

			scales, and drought variables such as length, severity, and duration showed a high positive correlation.
Das et al. (2020a)	Luni River Basin (Rajasthan)	SPI	SPI and GIS are used for detailed drought analysis in the Luni River Basin and observed many severe drought events. The different scales of SPI provided insights into distinctive drought periods and their intensities, which are beneficial for the seasonal analysis of drought. The agriculture in this area is highly prone to drought.
Hydrological Drought			
Kwak et al. (2012)	Namhan river in Korea	Streamflow series	Drought duration and severity are modeled using copula, and the return period is calculated.
Kazemzadehand Malekian (2016)	North-western Iran	SPI, SDI	The characteristics of hydrological and meteorological drought are studied based on the trend of SPI and SDI indices in north-western Iran. KS test is used to determine the best fit for stream flow from selected distributions, namely, exponential, gamma, uniform, and normal distributions.
Dodangeh et al. (2017)	Karkheh River basin	Streamflow	The study highlights the importance of understanding drought severity, frequency, and duration in the planning and management of water

	(southwest Iran)	resources. Frank and Gumbel were the best-fitted copula for the stations considered.

2.2.1 Bibliographic study on drought analysis

A bibliographic analysis is done using the Web of Science (WoS) database to find the number of publications using the keyword "meteorological drought analysis." A total of 130 countries have published 1975 articles on the keyword mentioned above. Figure 2.1 shows the number of publications on the keyword "meteorological drought analysis" each year. From 2000 to 2024, the number of publications on meteorological drought analysis around the world increased. The highest number of publications was in 2022. Figure 2.2 shows the number of publications in the first 10 countries in the database on the keyword "meteorological drought analysis". The highest number of publications are from China. India is in the 3rd position with 169 number of articles.

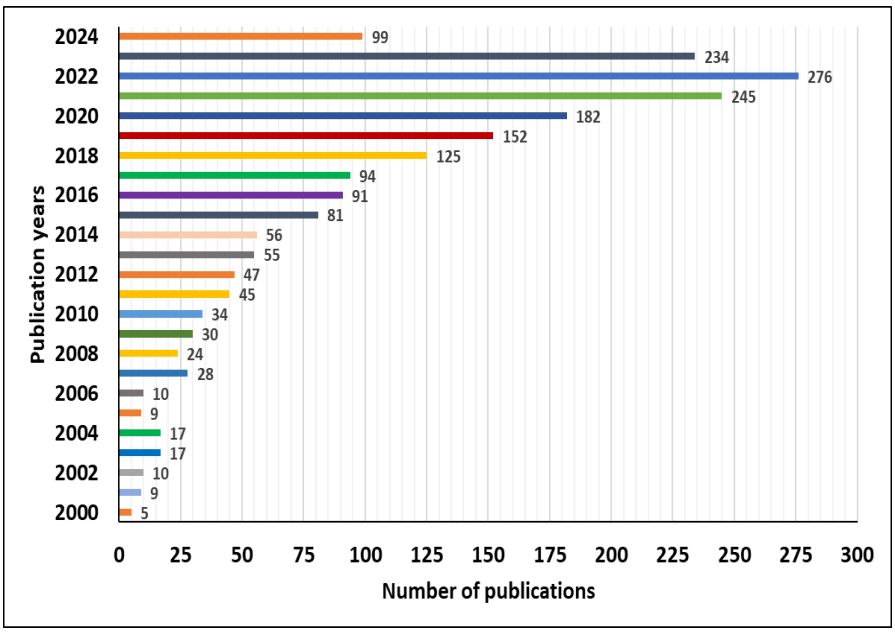

Figure 2.1. Number of publications each year on the keyword "meteorological drought analysis"

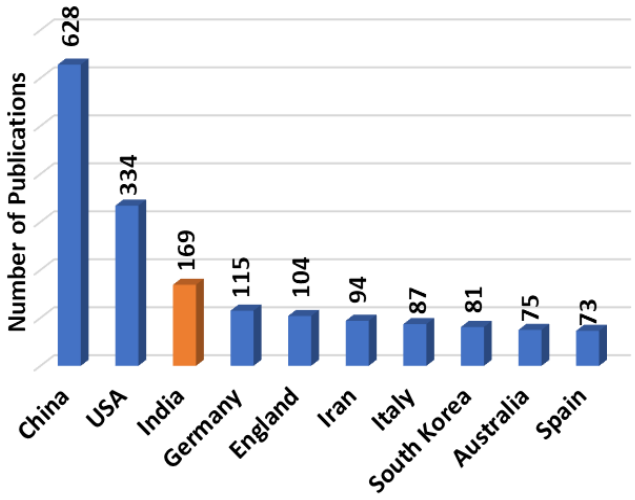

Figure 2.2. Number of publications in the first 10 countries in the database on the keyword "meteorological drought analysis"

The number of publications using the keyword "hydrological drought analysis" shows 498 articles from 2000 to 2024 (Figure 2.3). A total of 70 countries have published those articles. The highest number of publications was in 2020. Figure 2.4 shows the number of publications in the first 10 countries in the database on the keyword "hydrological drought analysis". The highest number of publications (307) are from USA, and India is in the 8th position with 13 publications.

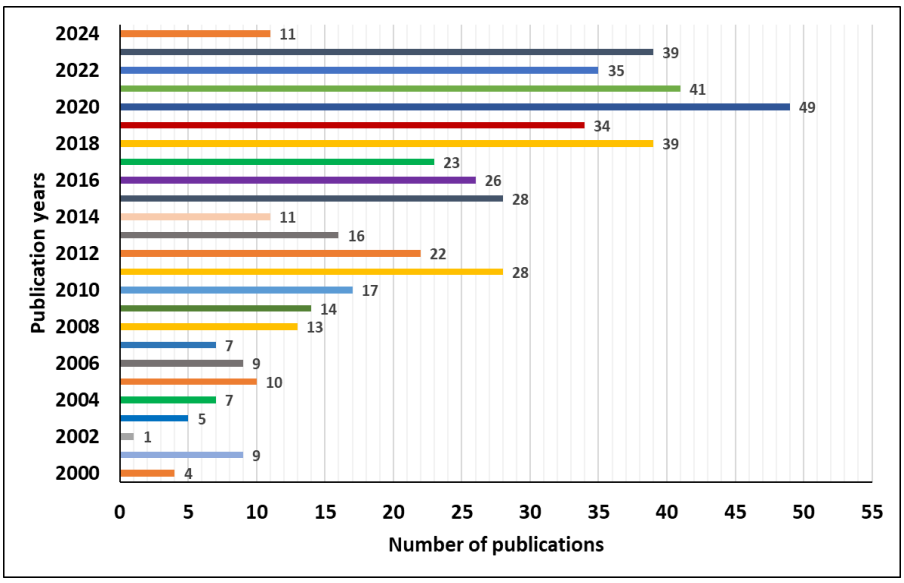

Figure 2.3. Number of publications each year on the keyword "hydrological drought analysis"

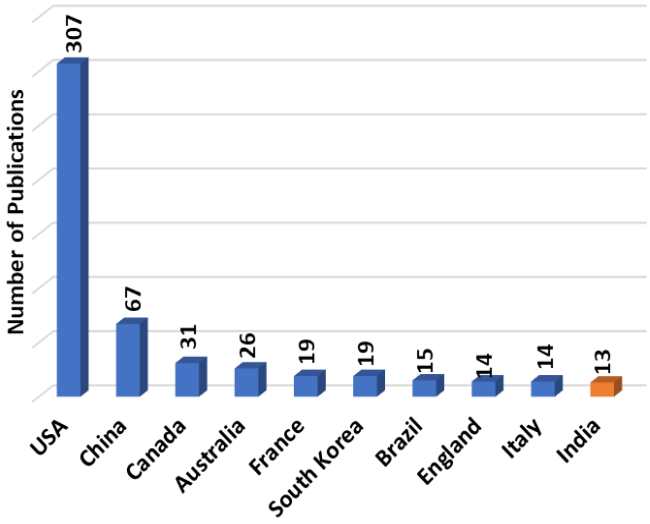

Figure 2.4. Number of publications in the first 10 countries in the database on the keyword "hydrological drought analysis"

2.3 DROUGHT ANALYSIS USING NON-STATIONARY INDICES

The climate patterns in India are subject to the impacts of several significant large-scale climate variables, including the ENSO (Agilan and Umamahesh 2018), IOD (Ajayamohan and Rao 2008), AMO (Zhang and Delworth 2006), PDO (Krishnamurthy and Krishnamurthy 2014), AO (Midhuna and Dimri 2019), and NAO (Dugam et al.1997). Recognizing the substantial impact of climate oscillations on the Indian monsoon, researchers have identified the imperative to integrate climate indices into drought analysis methodologies (Das et al. 2020b; Himayoun and Roshni 2019). Non-stationary SPI has been developed by considering different covariates, such as climate variables (Li et al. 2015) and time (Bazrafshan and Hejabi 2018). Wang et al. (2020b) have developed a non-stationary Standardized Streamflow Drought Index. Fewer researchers (Das et al. 2020b; Das et al. 2021; Masanta and Srinivas 2022) have done drought analysis in India based on the non-stationary concept. Table 2.2 shows the literature on drought analysis using the non-stationary index.

Table 2.2 Literature on Drought Analysis using Non-Stationary Index

Author(s)	Study area	Drought Index	Key Conclusion from the Literature
Li et al. (2015a)	Luanhe River basin China	SPI, NSPI	The study highlights the importance of integrating climate change in drought monitoring and management plans with the non-stationary drought index NSPI. NSPI performs better in assessing drought characteristics than SPI in the Luanhe River Basin.
Rashid and Beecham (2019)	Australia	SPI, NSPI	NSPI is calculated using GAMLSS with DMI, SAM, SOI, Nino3.4, and PDO as covariates. Better performance of NSPI is observed than SPI in the Australian climate.
Das et al. (2020c)	Himalayan states, India	SPI, NSPI	The threshold value considered was -0.8 for the drought index. The non-stationary SPI calculated by incorporating MEI, SOI, IOD, and SST outperformed the stationary index.
Dixit and Jayakumar (2022)	Godavari river basin, India	RDI, NRDI	The non-stationary RDI is developed by considering ENSO indices and IOD. The better performance of the non-stationary index in drought analysis is highlighted by calculating drought characteristics.

2.3.1 Bibliographic Analysis on Non-Stationary Drought Index

A bibliographic analysis of the WoS database using the term "nonstationary drought" shows 91 articles from 2013 to 2024 (Figure 2.5). Notably, since 2019, there has been an increase in the number of published papers on "nonstationary drought," highlighting the relevance and novelty of the topic. The highest number of publications was in 2023. Figure 2.6 shows the number of publications from different countries on the keyword “nonstationary drought”. Only 30 countries have published articles on this topic, and China, USA, and India have published 43, 29, and 9 articles, respectively (Figure 2.6). The results highlight the global attention and research efforts being dedicated to understanding and addressing nonstationary drought in recent years.

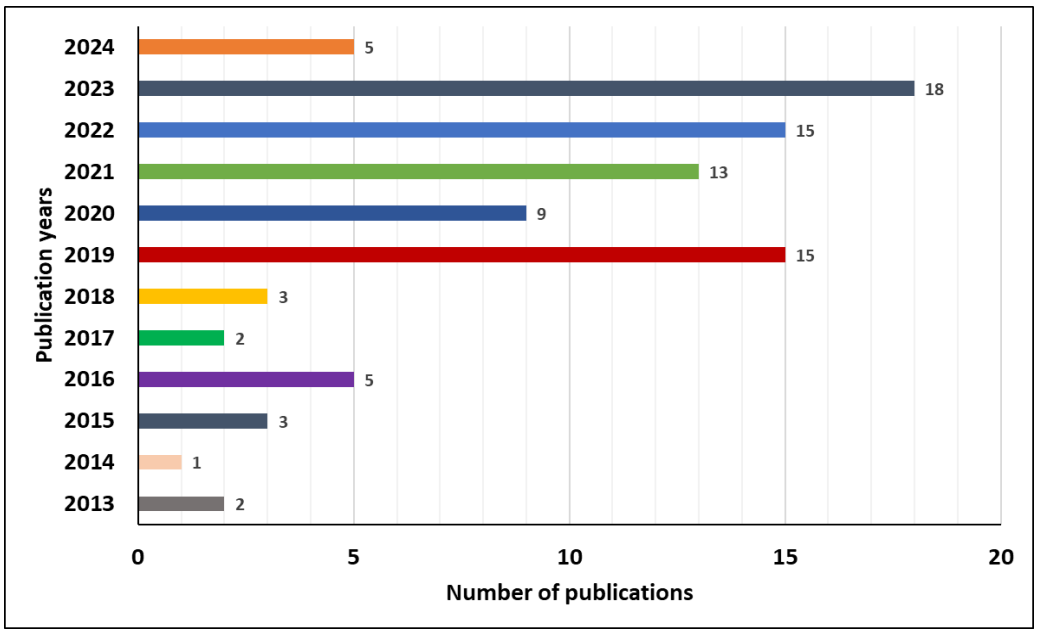

Figure 2.5. Number of publications each year on the keyword “nonstationary drought”

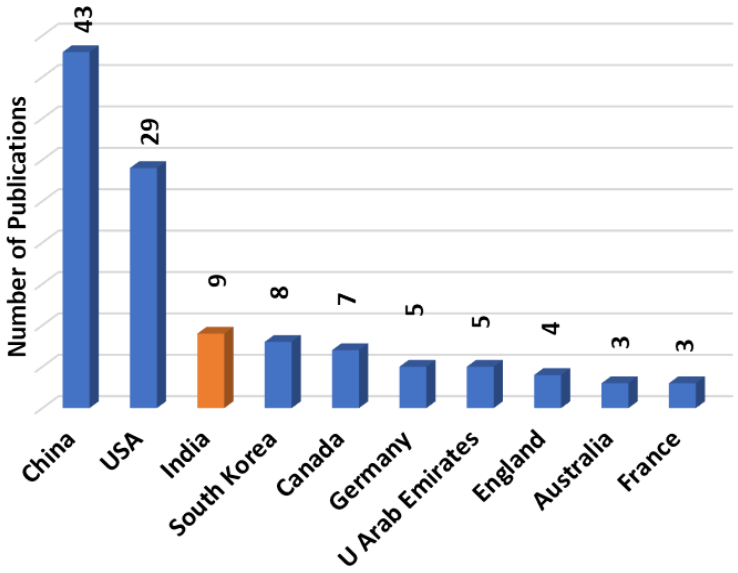

Figure 2.6. Number of publications from different countries on the keyword "nonstationary drought"

2.4 INDIVIDUAL IMPORTANCE OF CLIMATE VARIABLES

2.4.1 Southern Oscillation Index (SOI)

The SOI measures pressure differences between Tahiti and Darwin, Australia, and is the primary indicator of ENSO (Cavazos and Rivas 2004). The negative phase of SOI represents lower-than-normal air pressure in Tahiti and higher-than-normal air pressure in Darwin. El Ni˜no and La Ni˜na events are denoted by negative and positive SOI values, respectively. A significant influence of this index on precipitation variation is observed worldwide (Gu et al. 2007; Trenberth 2011). Todmal (2022) established a relationship between rainfall variability and the ENSO index in semi-arid regions in Maharashtra, India, and observed that below-average rainfall occurred mainly due to the influence of the positive phase of SOI and El Ni˜no events. The SOI is chosen as the best ENSO index for modeling monsoon and non-monsoon rainfall in India by Agilan and Umamahesh (2018). El Niño events are associated with reduced rainfall in many parts of India. On the other hand, La Niña events can lead to increased rainfall in some regions (Kripalani and Kulkarni 1994). By considering the SOI as a covariate in drought studies, researchers can better understand the relationship between ENSO and

drought in India and develop more accurate drought monitoring and prediction models (Das et al. 2021; Li et al. 2015b; Rashid et al. 2016).

2.4.2 Sea Surface Temperature (SST)

The SST has a significant influence on the global climate. In India, many studies, such as Agilan and Umamahesh (2018), Lakshmi Kumar et al. 2014; Mondal and Mujumdar (2015), have reported the strong influence of SST on rainfall. Chattopadhyay et al. (2015) and Yang et al. (2017) have linked Sea Surface Temperature anomaly to precipitation anomaly in India and China, respectively. The SST is used as an ENSO index in finding its relationship with Indian summer monsoon rainfall by Gadgil et al. (2004). Revadekar and Kulkarni (2008) observed a strong connection between SST and extreme rainfall in South India. SST significantly impacts drought occurrence in various regions (Dai 2013; Das et al. 2021b). Ma et al. (2020) demonstrated the strong influence of SST on the occurrence of severe drought in East China. Jena et al. (2020) reported the influence of SST on drought in the Cauvery River basin in India. Hence, SST is selected as one of the covariates.

2.4.3 Multivariate ENSO Index (MEI)

The MEI is a multivariate index that thoroughly assesses ENSO activity by accounting for six important atmospheric and oceanic variables (Wolter and Timlin 1998). The MEI was first developed by Wolter and Timlin (1993) and has been regularly updated. The MEI is calculated on a monthly basis and is used by climate scientists and meteorologists to track and predict ENSO-related climate phenomena, such as changes in temperature (Gonzalez et al. 2009), rainfall (Kiem and Franks 2001), and drought occurrence (Lv et al. 2022). The MEI is also used in climate modeling and weather forecasting, as it provides a useful measure of the overall strength and variability of ENSO. Various studies considered the association of MEI and drought in India (Dixit and Jayakumar 2021; Kumar et al. 2021a). Ganguli and Reddy (2013) investigated the influence of ENSO on drought in Rajasthan, and observed severe drought during El Ni˜no years. Hence, MEI is also an important covariate.

2.4.4 Indian Ocean Dipole (IOD)

It is the difference between the sea surface temperature of the eastern Indian Ocean south of Indonesia and the western Arabian Sea. Similar to ENSO, IOD is also a phenomenon related to ocean and atmosphere, which can affect the climate in regions near to Indian Ocean. Ashok and Saji (2007) and Saji and Yamagata (2003) stressed the significant role of IOD on Indian summer monsoon. Numerous researchers have noted the strong correlation between IOD and droughts around the world (Ummenhofer et al. 2011; Verdon-Kidd and Kiem 2009). Saji et al. (1999) reported the influence of IOD on summer monsoon rainfall of 1961 in India. They found that the positive phase of the IOD was associated with a significant reduction in monsoon rainfall over the Indian subcontinent, leading to drought conditions. The problem of water scarcity in semi-arid regions may become more severe under changing climatic conditions due to a decrease in rainfall and an increase in the IOD (Todmal et al. 2022). These studies provide strong evidence of the impact of the Indian Ocean Dipole on drought occurrence in India. Positive IOD events are consistently associated with decreased rainfall, weakened monsoon winds, and an increased likelihood of drought, with severe droughts occurring during strong positive IOD events. These findings highlight the importance of monitoring IOD events and considering their potential impact on drought management in India.

From the above literature, the influence of ENSO and IOD indices can be observed in arid and humid regions in India. Arid regions in India are already prone to water scarcity and drought conditions (Bandyopadhyay et al. 2016). Monitoring the ENSO index helps predict the occurrence and severity of drought events. By analysing historical ENSO patterns and their relationship with drought occurrences, researchers can develop models and early warning systems to better prepare for and mitigate the impact of droughts. In humid regions, ENSO events can lead to changes in river flow, affecting water availability for various purposes, including drinking water supply, industrial use, and hydropower generation (Ashok and Saji 2007). Hence, the ENSO index is crucial for drought studies in both arid and humid regions of India as it provides valuable insights into rainfall patterns, drought vulnerability, agriculture, water resource management, hydrological systems, and the impacts of climate change.

2.4.5 Atlantic Multidecadal Oscillation (AMO)

The AMO is a climatic phenomenon characterized by prolonged variations in sea surface temperatures (SSTs) within the North Atlantic Ocean (Knight et al. 2006). It exhibits a multidecadal pattern, with periods of warmer and cooler SSTs lasting several decades. This pattern of variability, though not as rapid as oscillations like El Niño or La Niña, holds significant implications for global and regional climates, including the Indian climate (Enfield et al. 2001). The unavoidable influence of AMO is outlined by Wang et al. (2009). Zhang and Delworth (2006) have shown an association with a strengthened Indian summer monsoon during the negative phase of the AMO. It can lead to above-average monsoon rainfall in parts of India, potentially mitigating drought conditions. The positive AMO phases align with increased temperatures in India, hence it is considered in drought studies (Masanta and Srinivas 2022).

2.4.6 Arctic Oscillation (AO)

The AO involves the natural variation of atmospheric pressure patterns in the Northern Hemisphere. It primarily affects the regions around the Arctic and the adjacent mid-latitudes. The Indian monsoon is also influenced by AO (Midhuna and Dimri 2019). Monitoring and understanding the AO's phases are crucial for drought studies, as it can significantly impact weather patterns (Wang et al. 2019; Yang 2011). Masanta and Srinivas (2022) have incorporated this index in the computation of drought indices in India. Hence, AO is also an important index to be considered.

2.4.7 Northern Atlantic Oscillation (NAO)

The NAO is a climate phenomenon that involves variations in atmospheric pressure patterns between two key regions: the subtropical high-pressure system near the Azores in the Atlantic Ocean and the low-pressure system in the vicinity of Iceland and Greenland (Bhatla et al. 2016). The NAO primarily affects weather patterns in the North Atlantic region, including Europe, North America, and adjacent areas (Tsanis and Tapoglou 2019). Dugam et al. (1997) observed a significant correlation of NAO in the Indian summer monsoon. Wu et al. (2012) explained the role of NAO in the interaction between the East Asian Summer Monsoon (EASM) and the ENSO. The significant influence of NAO on drought events in India is found in various studies, such as Masanta and Srinivas (2022).

2.4.8 Pacific Decadal Oscillation (PDO)

The PDO is a climate phenomenon characterized by variations in sea surface temperatures across the North Pacific Ocean. It operates on a longer timescale of multiple decades, and its positive and negative phases are associated with distinct patterns of temperature anomalies in the Pacific Ocean. These temperature anomalies can have far-reaching effects on global climate patterns (Wang et al. 2014). The interplay between the PDO and the ENSO is of paramount importance in shaping the climate patterns in India (Wang et al. 2014). Krishnan and Sugi (2003) studied the connection between these PDO composites and the fluctuations in precipitation across diverse regions within India. They observed that the Indian monsoon is susceptible to drought conditions, particularly when El Niño events coincide with the warm phases of the Pacific interdecadal variability. Further, Krishnamurthy and Krishnamurthy (2014) also observed a similar interrelation of PDO and El Niño in India. Hence, the PDO is also an important climate index to be considered in drought studies.

Table 2.3 shows the review on literature on effect of climate indices on Indian climate

Table 2.3 Literature on effect of climate indices on Indian climate

Author(s)	Study area	Climate Indices	Major Conclusion
Dugam et al. (1997)	India	NAO, ISMR	This comprehensive analysis underscores the complex and region-specific influences of NAO on Indian summer monsoon rainfall. On both climatological and sub-climatological scales, there is a higher correlation between the NAO and rainfall in Northwest India than there is for Peninsular India and the whole of India.
Ashok and Saji (2007)	India	IOD, ENSO	On a monthly scale, both ENSO and IOD events significantly impact various parts of India. The monthly variability of the IOD from July to September significantly affects Indian summer monsoon rainfall variability across different parts of India, confirming that strong IOD events indeed influence the Indian summer monsoon.
Ajayamohan and Rao (2008)	India	IOD	Future high rainfall events and associated risks are expected to be more frequent in central India because to the continuous warming trend of the Indian Ocean and the increased frequency of Indian Ocean Dipole years.
Cherchi and Navarra (2013)		ENSO, IOD	The study underscores the multifaceted influence of external factors, such as El Niño and the IOD, and internal components on Indian summer monsoon variability, offering

			insights into potential predictability and the complex interplay of oceanic and atmospheric phenomena. Correlation between ENO and IOD is also analysed. A lagged relationship between ENSO and IOD is revealed by analysing the summer monsoon characteristics during ENSO and IOD years.
Bhatla et al. (2016)		NAO, ISMR	The research findings indicate that NAO had a stronger impact on ISMR in the later years of the study than in the earlier years. This result implies that there has been an increase in the strength of the association between NAO and ISMR over time.
Guhathakurta et al. (2017)	India	SST	The districts with more drought occurrences were identified using trend analysis of the monthly SPI. The analysis revealed a substantial positive link in the central, northern, and peninsular regions of India and a negative correlation in the eastern districts with NINO 3.4 SST. In order to illustrate how the world climate affects India's drought, it also examined at the temporal association between the SPI for both monsoon seasons and global SSTs.
Himayoun and Roshni (2019)	Jhelum basin, India	ENSO, ENSO-M	The SPEI is calculated for three time scales. The influence of climate index on drought is analysed using wavelet analysis and they observed a significant influence of ENSO-M and ENSO on drought characteristics in the study area.

Gupta and Jain (2020)	India	SOI, NOI, SST	This study investigated the relationships between extreme precipitation and significant global climate phenomena like land elevation, ENSO, and global warming. The association between precipitation extremes and climate indices was found to vary geographically. The SOI and NOI had a large influence on extreme events in Madhya Pradesh, West Bengal, Uttar Pradesh, and Rajasthan.

2.5 DROUGHT PREDICTION

Worldwide, ecosystems, agriculture, water resources, and human communities face severe problems due to drought, defined by extended periods of low precipitation that result in water shortages (Lambe and Kundapura 2023; Sajeev et al. 2021). Developing methods for reducing the effects of drought episodes requires understanding past patterns of drought events (Mishra and Singh 2011). Because the meteorological drought causes other droughts, including hydrological, agricultural, and economic ones, it is essential to predict droughts before their occurrence (Jehanzaib et al., 2023; Zhao et al., 2016). The commonly used method to analyse time series data is the Autoregressive Integrated Moving Average (ARIMA) model (Mishra and Desai 2005b, 2006). This flexible model can extract more detailed information from the data. This linear model performs best when applied to stationary data (Zhang et al. 2017b). Numerous researchers have widely adopted ARIMA for drought analysis in different regions (Karimi et al. 2019; Mishra and Desai 2005b; Mossad and Alazba 2015). Machine learning (ML) models have recently become popular in water resources related studies (Sundar and Kundapura 2023). Also ML proves its great opportunity in drought forecasting with considerable accuracy (Pande et al. 2022). Achite et al. (2023) forecasted SPI using five machine learning models: bagging, random forest, random subspace, additive regression, and support vector machine in the Wadi Mina Basin, Algeria. Morid et al. (2008) have done drought prediction using Artificial Neural Network (ANN) in Iran. Hinge et al. (2022) observed that ANN performed better than multiple linear regression in SPI forecasting in Rajasthan, India. Kumar. et al. (2004) used RNN and FNN to forecast river flow in India and found that RNN performed better than FNN. Feed-forward Neural Network (FNN) (Abarghouei and Kousari 2013; Borji et al. 2016; Keskin et al. 2011) and Recurrent Neural Network (RNN) (Le et al. 2017) are found to be effective in predicting drought.

Because real-world time series data are complicated and lack a single all-encompassing model that can capture all patterns, hybridization approaches have become increasingly popular to improve time series prediction accuracy (Hajirahimi and Khashei 2022). Zhang (2003) suggested that time series have linear and nonlinear components. To handle linear patterns in the data while capturing nonlinear patterns in ARIMA's

residuals, they developed a hybrid model called ARIMA-MLP. Hybridization has been more well-known as a practical technique for more accurately modeling time series data since the publication of this seminal paper. Hybrid ARIMA and ANN models have been used in recent years to process such complex behaviour in prediction (Aladag et al. 2012). In hybrid models, the non-linear and linear components are separately modeled using different individual models to capture the advantages of all models in the prediction. Aladag et al. (2012) used a hybrid model of FNN with autoregressive fractionally integrated moving averages to forecast tourism data in Turkey. Many hybrid models have been developed to deal with mixed data patterns. Mousavi-Mirkalaei and Banihabib, (2019) used the Autoregressive Integrated Moving Average-Nonlinear Auto-Regressive eXogenous (ARIMA-NARX) hybrid model for Urban Water Consumption forecasting in Tehran. The superior performance of ARIMA-ANN over ARIMA and ANN was observed in forecasting Evapotranspiration in South Africa by Phesa et al. (2023). The hybrid models with linear and non-linear models have performed better in every case with good accuracy than individual models. Recent studies such as Moeeni and Bonakdari (2017) and Shafaei et al. (2016) have also attempted to consider hybrid models in forecasting by incorporating linear and non-linear components of time series. In the above studies, the linear model is considered first, followed by a non-linear model. However, Hajirahimi and Khashei (2022) developed MLP-ARIMA and ARIMA-MLP hybrid models for predicting stock prices. They considered a hybrid model with a non-linear followed by a linear model. The literature on drought prediction is given in Table 2.4.

Table 2.4 Literature on drought prediction

Author(s)	Study area	Drought Index	Prediction Model	Key Conclusion
Abarghouei and Kousari (2013)	Ardakan region (Iran)	SPI	ANN	Analysed the ability of ANN models in predicting drought at different time scales by considering different lags of SPI. The correlation coefficient obtained was more than 0.79.
Ali et al. (2017)	Pakistan	SPEI	MLPNN	The neural Network model is applied for drought forecasting and found reasonable accuracy in forecasting SPEI.
Myronidis et al. (2018)	Cyprus, Southeast Mediterranean basin	SDI	ARIMA	The Mann–Kendall (M-K) test indicates a decreasing but statistically insignificant trend in annual and seasonal discharge volumes over time in the basin. ARIMA model is used to forecast streamflow data and thereby computing the future droughts.

Karimi et al. (2019)	Karkheh River Basin, Iran	SPI	ARIMA	The drought is analysed by SPI at different time scales and forecasted SPI3 using ARIMA for the basin. The ARIMA model performed well in forecasting drought in the basin.
Achour et al. (2020)	North-west region (Algeria)	SPI	ANN	ANN models successfully forecasted drought with a 2-month lead time with high accuracy(R^2>0.81). The ANN based forecast can be used for irrigation planning during water stress situations.
Alsumaiei and Alrashidi (2020)	Kuwait	Precipitation Index (PI)	ANN	This paper presents a data-driven approach using an artificial neural network (ANN) algorithm to predict droughts. The approach was tested for forecasting 12- and 24-month droughts. Drought predictions were reliable, with Nash–Sutcliffe values ranging from 0.761 to 0.878 during the validation period. Additionally, the computed R^2 values for model forecasts ranged between 0.784 and 0.883, indicating the high quality of the model predictions.

Xu et al. (2022)	China	SPEI	ARIMA-LSTM	This study demonstrates the effectiveness of hybrid models, particularly ARIMA-LSTM, in improving the accuracy of drought predictions. The hybrid model outperformed single models at different time scales. The ARIMA-LSTM model shows the best prediction accuracy at long term drought prediction.

2.6 PROPAGATION OF METEOROLOGICAL TO HYDROLOGICAL DROUGHT

Some earlier investigations have explored the connection between hydrological and meteorological drought (Liu et al. 2023; Zhao et al. 2016). A good correlation between SSI and SPEI is observed by Salimi et al. (2021) in some basins in Iran. Wu et al. (2017) examined the connections between hydrological and meteorological droughts by utilizing SPI and SSI in the Jinjiang river basin in China, taking into account the influence of a large reservoir. Ozkaya (2023) conducted a drought relation study and observed variation of drought delay with elevation in the upper Tigris river catchments, Turkey. Meresa et al. (2023) investigated how the climate and catchment features in Ethiopia's Awash basin affected the progression of a meteorological to a hydrological drought. Some of the literature on this topic is given in Table 2.5.

Table 2.5 Literature on the propagation of meteorological drought to hydrological drought

Author(s)	Study area	Drought Index	Key Conclusion
Harisuseno (2020)	Pekalen River basin	SPI, RAI, SSI	The annual SPI and RAI indices showed strong correlations, suggesting comparable trends, according to the study. Furthermore, SSI, SPI, and RAI exhibited robust connections. For both monthly and annual estimates of drought characteristics, the SPI outperformed the RAI.
Ding et al. (2021)	China	Self-calibrating PDSI, SPEI, SRI	The findings indicate that, particularly in Northern China, the shift from meteorological to agricultural drought is more noticeable than the transition from agricultural to hydrological drought.
Meresa et al. (2023)	Awash basin in Ethiopia	SPI, SRI, SBI	The research demonstrated the need to study the progression of meteorological drought into hydrological drought. An increase in the propagation of droughts are observed with an increase in aggregation time scales. 4 to 6 months was the average lag time between hydrological and meteorological droughts in the area.

Lin et al. (2023)	Xijiang River basin, China	SPI, SRI	Drought propagation is observed with less than 3 months lag in the study area. It is associated with many factors, such as topography, soil, and groundwater. The research emphasis the importance of early detection of hydrological drought to reduce the drought risks.
Ozkaya (2023)	Tigris River catchment	SPEI, SDI, SPI	A higher correlation is observed between SPEI and SDI than SPI and SDI. This performance difference is more pronounced for time scales below 9. Higher elevation levels exhibited more relation of hydrological to meteorological drought.

2.7 IMPACT OF DROUGHT ON AGRICULTURE

The cultivation of wheat, rice, and maize in Asia has witnessed a decline over recent decades attributed to a decrease in the number of rainy days, a heightened occurrence of El Niño events, and rising temperatures (Bates et al. 2008). As indicated by Ganguli and Reddy (2014), Gujarat experiences water scarcity due to extremely erratic rainfall. Along with irrigation and using fertilizers, rainfall plays a significant role in the agricultural output in this region. The drought has a significant impact on agricultural production (Das et al. 2016). Due to its varying climatic conditions, the Saurashtra region has diverse agricultural practices and a mix of Kharif and Rabi crops. Bajra, groundnuts, green gram, and cotton are the major Kharif crops (summer monsoon season). Wheat, mustard, barley, and sesame are major Rabi crops (winter season). Wheat and bajra have a large impact on Gujarat's agricultural performance (Choudhury 2018). Bajra (pearl millet) is grown mainly in semi-arid and arid places and is better adapted to dry situations. However, prolonged rainfall deficiency severely affects its yields (Singh et al. 2017). Wheat production is more affected by irrigation practices and water availability than rainfall. Table 2.6 shows the Literature on impact of drought on agriculture.

Table 2.6 Literature on impact of drought on agriculture

Author(s)	Study Area	Drought Index	Key Conclusion
(Bandyopadhyay and Saha 2014)	Gujarat	NDVI, RAI	The impact of drought on vegetation is studied in Gujarat, and it was observed that frequent drought events badly affect crop growth in this area. Hence, meteorological and vegetative drought studies are necessary to reduce the impact.
Khatiwada and Pandey (2019)	Karnali River Basin, Western Nepal	RDI, sc-PDSI, SPI, SPEI, SFI, PHDI	SPI could identify the intensityand duration of the drought accurately in the basin. Drought impact on the productivity of crops such as millet, maize, and paddy are observed. Recent years ahd more severe frequent drought in the study area, indicating high risk of water scarcity thereby crop yields.
(Sajeev et al. 2021)	Western Rajasthan, Kerala	SPI	Drought indices were calculated for various time scales for both areas. Drought severity and duration exhibited a good correlation, highlighting the necessity of bivariate analysis of drought. Copula-based return period equations were constructed for the analysis, revealing a high vulnerability of Western Rajasthan to drought. The study also established copula-based non-exceedance conditional distributions for the crop productivity of Bajra

			and rice with rainfall, providing insights into the impact of drought on agricultural productivity.
(Fu et al. 2021)	Corn-Belt, United States	PDSI, SPA	Precipitation is an important factor for crop production. The maize and soybean is found to be affected by drought in the study area.

2.8 DROUGHT STUDIES IN SAURASHTRA AND KUTCH AND COASTAL KARNATAKA

Saurashtra and Kutch and Coastal Karnataka are two meteorological subdivisions in India. The analysis of meteorological drought and flood in all meteorological sub-divisions of India from 1871 to 1984 by Parthasarathy et al. (1987) reported the highest frequency of drought and flood in the Saurashtra and Kutch region. Arid and semi-arid regions are more prone to drought because they are more sensitive to temperature extremes and rainfall deficits (Bandyopadhyay et al. 2016). The state experiences heavy rainfall in shorter periods on fewer days (Hirapara et al. 2020). Gujarat experiences droughts regularly due to delayed monsoons, high temperatures, and a lack of water resources (Bandyopadhyay and Saha 2014). High rainfall variability in coastal areas of Saurashtra close to the Arabian Sea makes them more vulnerable to extreme climatic events like droughts and floods (Pandya et al. 2023). Although Saurashtra represents one of the greatest water-scarce regions of India, it still experiences flooding issues because of the deficient number of rainy days and the high intensity of the precipitation (Kumari and Himanshu 2016). Inconsistent rainfall is the main reason for irregular cycles of drought in Gujarat (Bandyopadhyay and Saha 2014).

Due to climate changes, most Taluks in Karnataka have been exposed to meteorological drought events over the years (Srinivasareddy et al. 2019). According to Pai et al. (2011), a 4% to 35.35% of probability for moderate and above intensity drought in Coastal Karnataka's districts was observed during the period 1901 to 2003. The farmers in the coastal area faced significant challenges as a result of climate-related crises like droughts, floods, and pest infestations, which resulted in crop failures, decreased yields, and higher production costs (Kumar et al. 2017). Cherian et al. (2021) observed a significant influence of ENSO on rainfall and rice yield in various districts of Karnataka. The coastal region of Karnataka is known for high-intensity rainfall. However, due to climate change, the region has also been affected by droughts recently (Shewale and Kumar 2005). According to the study by Das et al. (2014), observation of a decreasing trend in rainfall and rainy days in Coastal Karnataka indicates a higher likelihood of drought. Therefore, research on drought is essential in Coastal Karnataka.

Several drought studies (Bandyopadhyay and Saha 2016b; Chopra 2006; Nathan 2001) were conducted in Gujarat and determined drought years in Gujarat, the worst of which was in 1987. Bandyopadhyay and Saha (2016) analyzed spatial and temporal variation of drought using four drought indices in Gujarat. Zadafiya et al. (2022) predicted drought years and meteorological parameters using GCM data in Gujarat. Table 2.7 shows the literatures on drought studies in Gujarat and Karnataka.

Table 2.7 Review of literature on Drought studies in Gujarat and Karnataka

Author(s)	Study Area	Drought Index	Key Conclusion
Ganguli and Reddy (2012)	Saurashtra and Kutch, Gujarat, India	SPI	Different types of copulas are applied to model the joint dependence of drought characteristics (severity and duration), and better performance of copulas is observed than in traditional bivariate distributions. The threshold value of SPI is taken as -0.8.
Ganguli and Reddy (2014)	Marathwada, Saurashtra and Kutch, western Rajasthan	SPI	From the M-K test, the drought trend is decreased from 1932-1966 in June for Saurashtra region, indicating a greater number of droughts in the region during the season compared to other periods. The univariate and bivariate return periods are also calculated using copula by considering drought peak, severity, and duration. From this study, the highest drought risk is observed in western Rajasthan compared to the other two areas.
Bandyopadhyay and Saha (2016a)	Gujarat	SPI, RFA, VCI, NDVI	This study observed 12 major droughts from 1982 to 2001 in Gujarat. A good correlation exist between meteorological and vegetative drought indices, and RFA and NDVI Anomaly are best among four indices. The north eastern part as well as central part of the study area are highly vulnerable to drought.

Das et al. (2016)	Kutch, Gujarat	SPI	Drought is defined using SPI, and found that, SPI is an efficient index for meteorological drought analysis in Kutch region. Rann of Kutch is found to be highly drought prone and climate change has an impact on agriculture in the study region.
Kumar and Ahmed (2022)	Tumakuru, Karnataka	SPI	The driest years were 1954, 1965, 1968, and 1976. A highly significant correlation has existed between SPI and rainfall in the study area. There is a significant likelihood that a meteorological drought would turn into an agricultural drought.

2.9 RESEARCH GAP

Saurashtra and Kutch are arid regions prone to frequent droughts, whereas Coastal Karnataka is located in the southwestern part of India, and the region is known for its high rainfall and coastal ecosystems. Many studies have considered drought in Gujarat, and only very few are available related to Coastal Karnataka. The non-stationary modeling of drought and evaluation of drought characteristics and properties using the Non-stationary Standardized Precipitation Index (NSPI) with large-scale climate indices as covariates are not yet reported in these specific areas. This research can provide insights into drought characteristics and properties in different climatic contexts by analysing these two distinct regions together. The effect of rainfall and drought on crop productivity has not been analysed in these areas. The primary objective of the present research is to construct non-stationary drought indices with selected covariates to perform a copula-based assessment of meteorological drought properties in Saurashtra and Kutch, and Coastal Karnataka.

The existing literature emphasizes the critical importance of drought prediction methodologies in addressing the complex challenges of drought in Gujarat. Despite high susceptibility to droughts in Gujarat, the state has very little research focused on drought prediction. The literature lacks a lot of comprehensive investigations comparing various modeling techniques for drought prediction in Gujarat. More specifically, no research has been done to compare the effectiveness of Machine Learning models like FNN, RNN and their hybrid combinations with traditional time series models like ARIMA.

There is a limited exploration of non-stationary analysis in hydrological drought assessment. No studies are found on hydrological drought analysis using non-stationary indices in Gujarat. Hence, a river basin (Shetrunji River Basin) from the highly drought-prone region has been selected. Research utilizing non-stationary drought indices in the Shetrunji River basin in Gujarat has not been conducted, particularly incorporating significant large-scale climate covariates such as ENSO, IOD, NAO, AO, PDO, and AMO. No drought studies are found in the highly drought-prone Shetrunji River basin by incorporating climate indices in meteorological and hydrological drought indices. A dearth of investigations involves a comparative analysis of meteorological and

hydrological droughts employing non-stationary indices. Also, the behavioural distinctions of the rabi and kharif seasons crops in response to these two types of droughts within a non-stationary framework have not been previously explored. Very few researchers have attempted drought analysis in Netravathi River basin.

2.10 RESEARCH OBJECTIVES

The objectives of this research are formulated based on a comprehensive review of the existing literature and identification of research gaps. The objectives of this research are:

- Meteorological drought analysis
    - To develop stationary and non-stationary drought indices for two contrasting climate regions, Saurashtra and Kutch, and Coastal Karnataka in India.
    - To study the impact of meteorological drought on crop yields in the two regions.
- Drought forecasting
    - To compare the performance of ARIMA, FNN, RNN, and hybrid combinations of ARIMA and Neural Network models in drought forecasting for semi-arid Saurashtra and Kutch.
- Comparative evaluation of meteorological and hydrological droughts in semi-arid river basin
    - To develop stationary and non-stationary indices for meteorological and hydrological drought in the semi-arid Shetrunji River basin in the Saurashtra region, India.
    - To assess the relationship between hydrological drought and meteorological drought in the basin.
    - To analyse the impact of two droughts on rabi and kharif crop yields in the basin
- Hydrological drought analysis in humid river basin
    - To analyse drought using stationary index in humid Netravathi River basin in Coastal Karnataka region, India.

- To analyse the trend of streamflow and hydrological drought in the basin and forecast drought.
- To analyse hydrological drought under stationary and non-stationary conditions in the Netravathi River basin.

The methodology of the entire research is shown in Figure 2.7. The objective of this research is to develop and evaluate non-stationary drought indices incorporating climate change to assess meteorological and hydrological droughts in diverse climate zones of India. The research aims to compare the performance of stationary and non-stationary models over various time scales and conduct comprehensive drought analysis, including copula-based bivariate analysis, rainfall impact on crop yield, and drought forecasting using hybrid time-series models. The findings seek to enhance drought prediction accuracy and provide valuable insights for water resource management and agricultural planning in drought-prone regions.

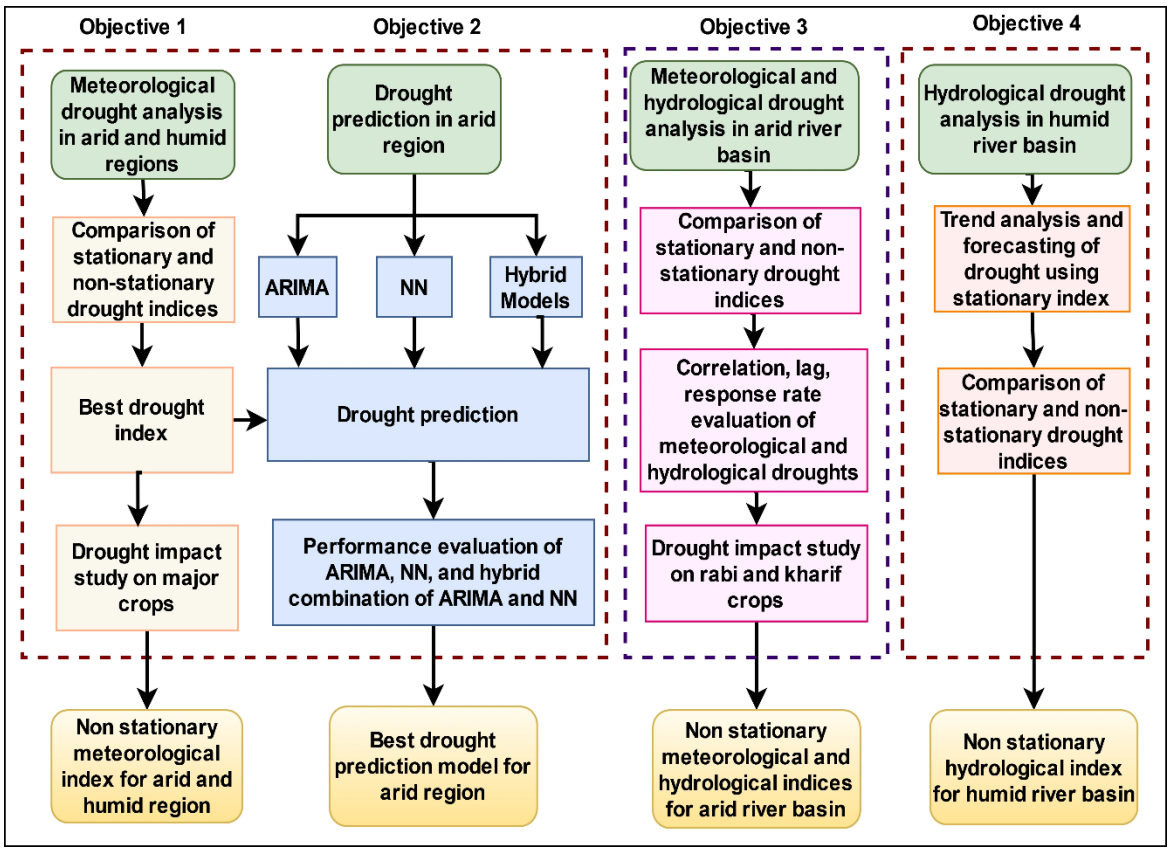

Figure 2.7. Flowchart of Research Methodology

CHAPTER 3

METEOROLOGICAL DROUGHT ANALYSIS USING STATIONARY AND NON-STATIONARY INDICES

3.1 GENERAL

In this chapter, drought analysis is conducted in Saurashtra and Kutch and Coastal Karnataka, India. Here, drought models such as the stationary Gamma model (M0), the non-stationary Gamma model with time as a covariate (M1), and the non-stationary model with climate indices as covariates (M2) were considered to select the best model. The capability of non-stationary drought indices in capturing drought and flood events is checked based on a comparative study with historical drought and flood events. Rainfall excess and deficient years in the study areas are detected from the percentage departure analysis of annual and seasonal rainfall, which is also used to compare the performance of indices. The drought risk is analysed with univariate and bivariate return periods in both areas for all combinations of drought duration, severity, and peak at all time scales (3-,6-,12-, and 24-months). The multivariate distribution functions utilized in this analysis are created using copulas, and it has been used by various studies worldwide (Adarsh et al. 2018; Dodangeh et al. 2017; Hangshing and Dabral 2018; Reddy and Ganguli 2012a; Kao and Govindaraju 2010; Sajeev et al. 2021). Agricultural and associated sectors in a country depend highly on water availability; hence it is necessary to see the significant impacts of extreme events on this sector. Recent literature has pointed out the importance of studies related to the impact of climate variability during various growth stages of crops (Asseng et al. 2015). Hence, another aspect of this research is assessing the correlation between crop yield loss rate and drought indices. The impact of rainfall on crop yield is also analysed through a copula-based non-exceedance conditional probability distribution. The findings from this research contribute to the understanding of drought dynamics, facilitate effective drought management strategies, and provide insights for sectors dependent on water availability and climate conditions.

3.2 STUDY AREA

3.2.1 Overview of Saurashtra and Kutch and Coastal Karnataka

Gujarat is one of India's most drought-prone states on the west coast (Ganguli and Reddy 2014). The region is mainly covered by arid terrain due to its proximity to the Thar Desert in the north (Bandyopadhyay and Saha 2016b). It is situated between 20º 06′ N to 24º 42′ N latitudes and 68º 10′ E to 74º 28′ E longitude, and the study area map is shown in Figure 3.1. Saurashtra and Kutch region of Gujarat is having a geographical area of about 109,950 km^2 (including Kutch, Junagadh, Rajkot, Surendranagar, Porbandar, Jamnagar, Bhavnagar, and Amreli) is taken for investigation. The Indian Meteorological Department divided India into 36 subdivisions based on similar meteorological climates. The history of Meteorological sub-divisions of India is explained in the research article by Kelkar and Sreejith (2020). Saurashtra region receives an annual rainfall of around 400 mm. The northeast part of Kutch is dry, containing the desert called Rann of Kutch. The annual rainfall of the Kutch region is around 300 mm. Rainfall variability and drought badly affect agriculture in the area (Das et al. 2016). Cotton, paddy, wheat, Maize, and Groundnut are the major crops in Gujarat. Gujarat is in the top three in the production of bajra, groundnut, sesame, and mustard. Bajra is the major crop in the Kutch region. Kharif (July to October) and summer (January to April) are the two growing seasons of bajra.

Coastal Karnataka is located on the western side of Karnataka, India, and it is between 12º 27′ N and 15º 32′ N latitudes and between 68º 10′ E and 72º 23′ E longitude. It comprises three districts: Uttara Kannada, Udupi, and Dakshina Kannada, and its total area is around 18441 km^2. It is bounded by the Arabian Sea on the western side and the Western Ghats on the eastern side. So, due to the orographic effects, the western part of the western ghats receives high rainfall, and the eastern part receives low rainfall. The average annual rainfall is around 4000 mm, and 87 % of the rainfall is received during the monsoon season. Some studies noticed a declining trend in the frequency of heavy rainfall in the future along the coastal region of Karnataka (Francis and Gadgil 2006; Revadekar et al. 2011). The temperature of this area ranges from 21º C to 36º C. Rice is the principal crop in Dakshina Kannada and Udupi districts. Agriculture in

Karnataka state is carried out in three seasons; Summer season (January- March), Kharif (April- September), and Rabi (October- December).

According to Köppen's climate classification, the Kutch region comes under the hot desert arid (BWh) region, whereas Saurashtra is a hot semi-arid (BSh) region, and these are water-scarce regions in Gujarat (Ganguli and Reddy 2014). Coastal Karnataka comes under the tropical region, subject to a humid climate. Forest lands are dominant in Coastal Karnataka. Due to fast industrialization and urbanization, the forest area decreases decade by decade (Kumar et al. 2021b). A diverse climate is observed in Saurashtra and Kutch, with arid and semi-arid regions having different annual rainfall, such as 400 mm and 300 mm, respectively (against India's average rainfall value of 1,170 mm). In contrast, Coastal Karnataka receives heavy rainfall with an annual average of 4000 mm during the monsoon season.

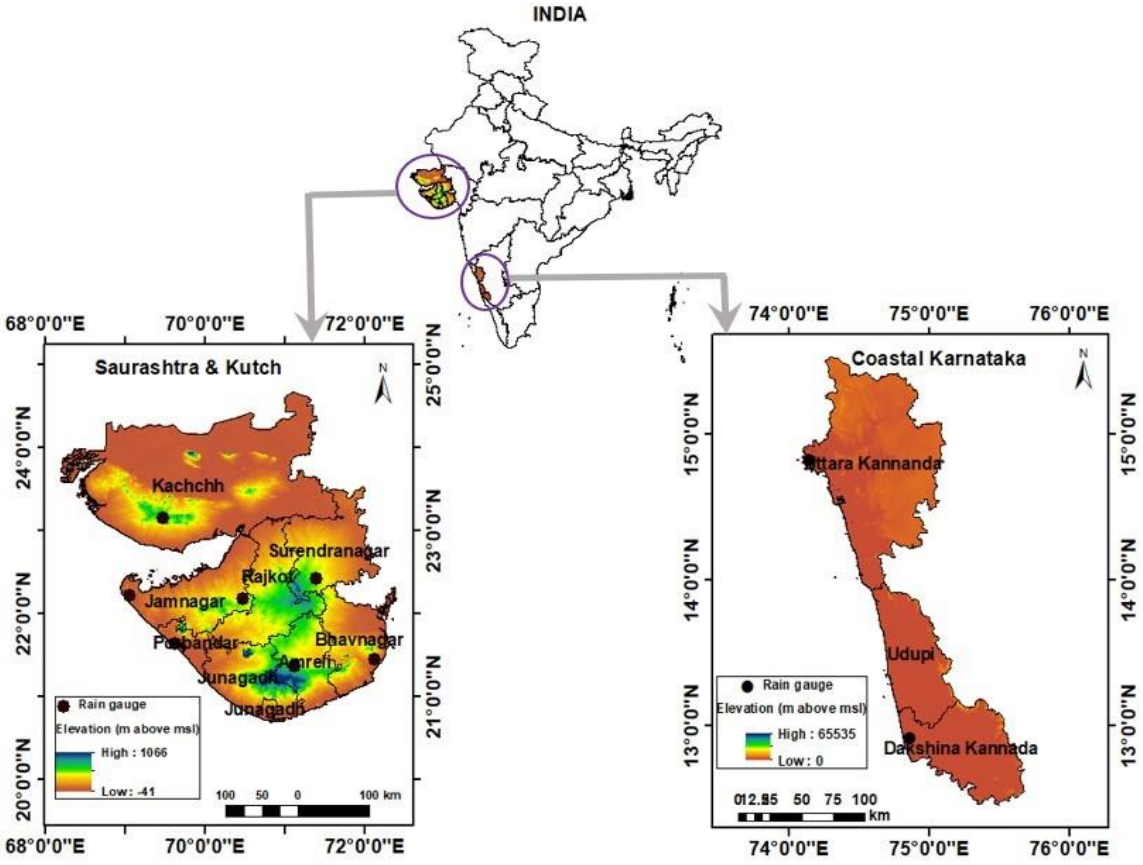

Figure 3.1. Study area

3.2.2 Data Used

The area-weighted monthly rainfall for two study areas was collected from the Indian Institute of Tropical Meteorology, Pune (http://www.tropmet.res.in). These precipitation data are constructed by collecting data from seven stations in Saurashtra and Kutch and two rain gauge stations in the Coastal Karnataka meteorological subdivisions. The data is taken for the period starting from January 1951 to December 2004. The productivity of bajra (1953-2005) and paddy (1966-2005) were obtained from the Directorate of Economics and Statistics of Gujarat and Karnataka, respectively (Kothawale and Rajeevan 2017; Sajeev et al. 2021).

3.3 METHODOLOGY

The methodology flow chart is shown in Figure 3.2. A detailed explanation of each step is given in the following sections.

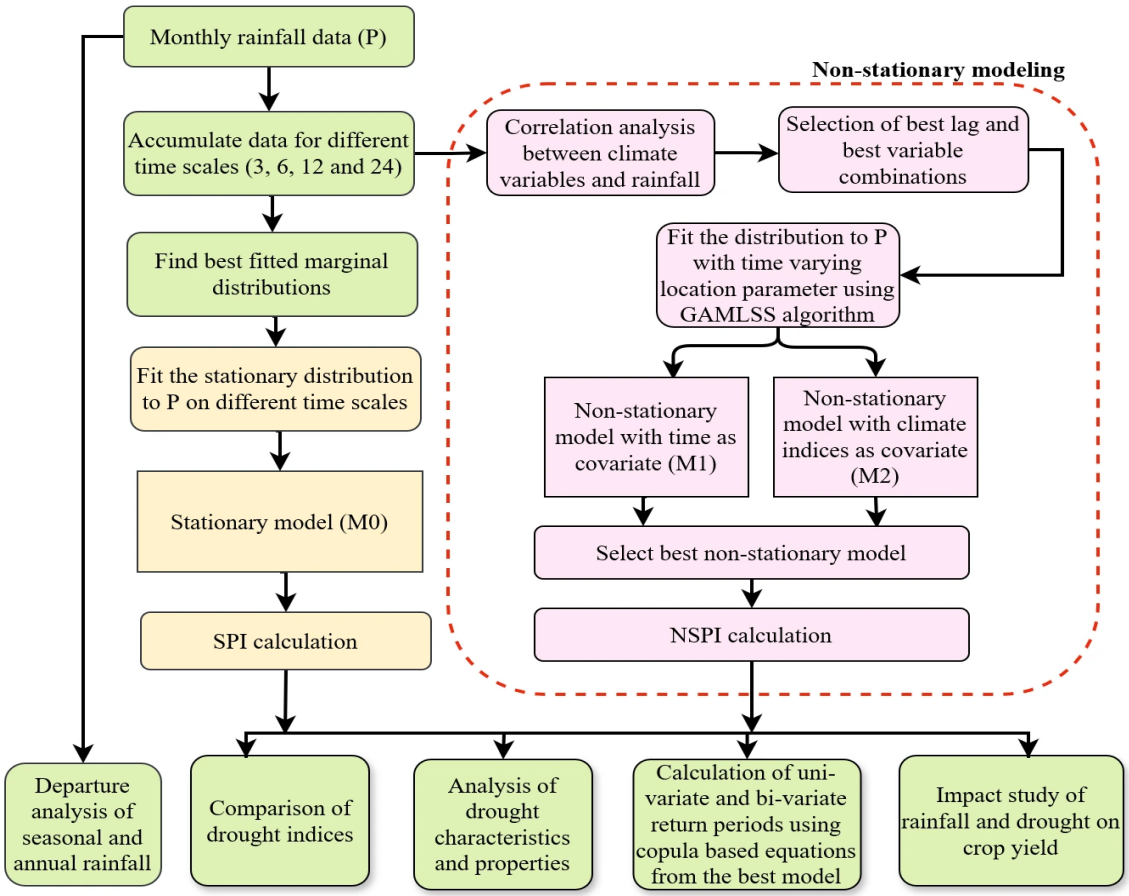

Figure 3.2. Methodology Flowchart

3.3.1 Computation of Standardized Precipitation Index

The Standardized Precipitation Index (SPI) is the most widely used index to analyse mereological droughts, and it is very flexible in defining wet and dry periods (World Meteorological Organization 2012). SPI can be used to monetize drought at various time scales and as an agricultural drought index (McKee et al.1993; Patel et al. 2007). For SPI calculation, cumulative precipitation was calculated from precipitation data for 3, 6, 12, and 24 months time scales in the year j and month i. The best fit for cumulative rainfall was checked from different marginal distributions, and, at all the cases gamma was the best fit in both areas (Table 3.1). The Gamma distribution is found to be the best fit for rainfall in several studies (Das et al. 2020b; McKee et al.1993). The cumulative precipitation is then fitted to a gamma distribution function $g(x)$, having a probability density function as follows:

$$g(x) = \frac{1}{\beta^{\alpha}\,\Gamma(\alpha)}\, x^{\alpha-1}\, e^{\frac{-x}{\beta}} \tag{3.1}$$

where $\alpha =$ shape parameter; β = scale parameter, and $\Gamma(\cdot)$ = ordinary gamma function.

Its Cumulative Distribution Function (CDF), $F(x)$ is shown below:

$$F(x) = q + (1-q)\, G(x) \tag{3.2}$$

where $G(x)$ is the CDF for the non-zero precipitation in month i; and q is the zero-precipitation probability in the month j. The cumulative probability is changed to a standard normal distribution with a mean value equal to zero and a unit standard deviation. The equation for the calculation of SPI is:

$$SPI = \psi^{-1}(F(x)) \tag{3.3}$$

where ψ^{-1} is the inverse cumulative standard normal distribution. The SPI-based drought categorization is given in Table 3.2.

Table 3.1 Marginal distributions for cumulative precipitation

Time Scale	Criteria	Exponential	Gamma	Lognormal	Logistic	Normal	Weibull
Saurashtra and Kutch							
3-months	AIC	8988	**8144**	8262	10059	10155	8171
	BIC	8993	**8153**	8271	10068	10164	8180
6-months	AIC	10053	**9959**	10254	10622	10627	9991
	BIC	10057	**9968**	10263	10631	10636	10001
12-months	AIC	10467	**10435**	10499	10491	10504	10448
	BIC	10471	**10444**	10508	10501	10514	10458
24-months	AIC	11051	**11032**	11069	11047	11058	11064
	BIC	11053	**11042**	11078	11057	11067	11073
Coastal Karnataka							
3-months	AIC	15379	**15017**	15998	15913	16184	15649
	BIC	15383	**15026**	15907	15222	16193	15659
6-months	AIC	16546	**16447**	16687	16597	16924	16837
	BIC	16551	**16456**	16696	16706	16633	16846
12-months	AIC	170513	**17008**	17278	17317	18361	18515
	BIC	170517	**17010**	17287	17326	18370	18524
24-months	AIC	18914	**18804**	18896	18931	18930	19062
	BIC	18919	**18805**	18905	18940	18939	19071

Note: Bold figures indicate best fitted distribution

Table 3.2 SPI-based drought categorization

Index Value	Remarks	Category
>2.00	Extreme wet	W4
1.99 to 1.50	Very wet	W3
1.49 to 1.00	Moderate wet	W2
0.99 to 0.00	Near normal	W1
0.00 to -0.99	Mild drought	C1
-1.00 to -1.49	Moderate drought	C2
-1.50 to -1.99	Severe drought	C3
≤ -2.00	Extreme drought	C4

3.3.2 Selection of Climate Indices

Drought modeling is done non-stationarily by choosing the best covariate from time and large-scale climate oscillation indices like ENSO and IOD. For this study, the approach of Das et al. (2020b) is considered due to regional relevance. ENSO indices such as the Southern Oscillation Index (SOI), Sea Surface Temperature (SST), and Multivariate ENSO Index (MEI) are considered for non-stationary analysis. The SOI is available at http://www.bom.gov.au/climate/current/soihtm1.shtml, and is measured by observing the surface air pressure difference between Darwin and Tahiti. The SST is at http://www.esrl.noaa.gov/psd/gcos_wgsp/Timeseries/Data/nino34.long.anom.data, and it is the monthly data over 17^{o}E-120^{o}W,5^{o}S-5^{o}N (NINO3.4) region. The Multivariate ENSO Index (MEI) obtained from http://www.esrl.noaa.gov/psd/enso/mei.ext/table.ext.html. Dipole Mode Index (DMI) is used to quantify the IOD (Saji et al. 1999). It is available at http://www.jamstec.go.jp/frcgc/research/d1/iod/DATA/dmi.monthly.txt. The data of all indices were collected on 18th May 2020 for 1951-2004.

The monthly rainfall data for 1951-2004 is converted to cumulative rainfall for four time scales (3, 6, 12 and 24 months). As per the previous studies (Agilan and Umamahesh 2018), the monthly data of climate indices are then arranged into different lags (from 0 to 12) to find the best linear association between the indices and precipitation. The Kendall correlation test at a 0.05 significant level is performed to evaluate the correlation between precipitation on a different scale and climate indices at different lags (Das et al. 2020c). The best lag obtained for precipitation at each time scale is further used as a covariate in calculating the non-stationary drought index. The section 2.4 describes the reasons for choosing the above-mentioned climate indices as covariates in this study.

3.3.3 Generalized Additive Models in Location, Scale, And Shape (GAMLSS)

Rigby and Stasinopoulos (2005) proposed Generalized Additive Models in Location, Scale, And Shape (GAMLSS). It is helpful for non-stationary analysis. GAMLSS is a commonly used algorithm for several applications in hydrology, such as rainfall downscaling (Rashid et al. 2016), flood frequency analysis (Debele et al. 2017a), and drought analysis (Shiau 2020; Yu and Kim 2019). Debele et al. (2017b) did a comparative study between Maximum likelihood (ML), two-stage method, and GAMLSS methods to find time-dependent moments under non-stationarity and found that GAMLSS performed better than the other two methods. Non-stationary drought indices are computed similarly to normal indices; hence the drought classification is also the same based on the various ranges of the values (Table 3.2). The GAMLSS relies on a monotonic link function to relate the distribution parameters to the explanatory variables, and it is represented as

$$g_k(\theta_k) = \eta_k = X_k \beta_k + \sum_{j=1}^{m} Z_{jk}(x_{jk}) \tag{3.4}$$

where the monotonic link function is represented as g_k ; θ_k is a vector having the length of n and is the same as the size of the data set; β_k is a parameter vector with length m; X_k is a $n \times m$ matrix of explanatory variables; Z_{jk} is a nonparametric additive function of x_{jk} . For the computation of stationary drought index SPI, the precipitation

is fitted with a gamma distribution. A Gamma distribution with two parameters (scale (σ) and location (μ)) is given as:

$$f(X \mid \mu,\sigma) = \frac{1}{\left(\sigma^2\mu\right)^{\frac{1}{\sigma^2}}} \frac{X^{\frac{1}{\sigma^2}-1} e^{\frac{-X}{\left(\sigma^2\mu\right)}}}{\Gamma\left(\frac{1}{\sigma^2}\right)}; X > 0, \mu > 0, \sigma > 0 \tag{3.5}$$

For each time scale, the cumulative precipitation is modeled with a non-stationary gamma distribution by considering linear combinations of the covariates mentioned above in the location parameter. The best model is chosen using the Akaike Information Criterion (AIC) from the different models constructed from combinations of covariates. The optimal model based on non-stationary analysis is as follows

$$X_t \sim \ gamma\ \left(\mu_t,\ \sigma\right) \tag{3.6}$$

$$\mu_t = c_0 + c_1 I_1(t) + c_2 I_2(t) ..... + c_n I_n(t) \tag{3.7}$$

where, $c_0, c_1, .., c_n$ are constants and, at the time t, $I_1, I_2, .., I_n$ are the covariates. The parameters of models are calculated by maximizing the likelihood based on called Rigby and Stasinopoulos (RS) algorithm, as it is found to be faster in the case of large data sets.

3.3.4 Drought properties

In this research, drought properties are identified based on run analysis by taking the threshold value of -0.8, as suggested by Reddy and Ganguli (2012b) and Sajeev et al. (2021). The classification of the wet and dry periods is listed in Table 3.2, and its occurrence frequencies are compared for stationary and non-stationary analysis. Based on the run analysis, the drought occurrence is assumed to be the sequence of index values below the threshold value. Severity, duration, and peak are the most critical drought properties that can be defined based on the threshold value of the drought index. The definition sketch of drought properties is given in Figure 3.3. Drought duration (Di) is the number of consecutive months when the drought index value falls below the threshold. Drought events are expressed on a monthly scale with a minimum duration

of one month. The cumulative value of the drought index for the drought is defined as severity, and the severity of drought occurrences is provided by Eq. (3.8). The lowest index value during a specific drought duration is called the peak (Pi).

$$S_i = -\sum_{i=1}^{d_i} SPI_i \tag{3.8}$$

where d_i is the duration and S_i is the severity of the drought event i.

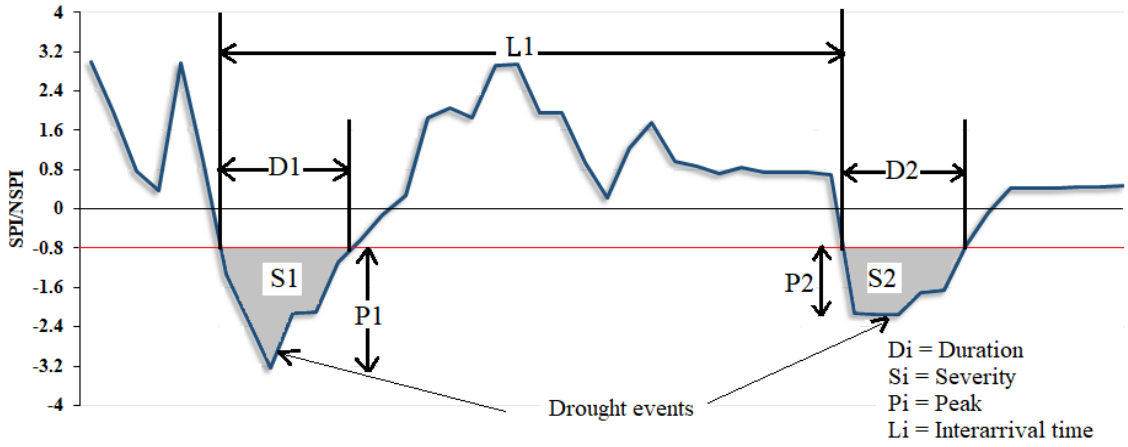

Figure 3.3. Definition sketch of drought properties

3.3.5 Multivariate analysis of drought using copula

Since the drought studies (Das et al. 2020b; Zhang et al. 2021) with non-stationary indices considered stationary distributions for drought properties, gamma, generalized extreme value, weibull, exponential, and lognormal are considered univariate distributions in the present analysis (Sajeev et al. 2021; Shiau 2006). The copula is the most popular tool for multivariate analysis (Amirataee et al. 2018; Muthuvel and Mahesha 2021). In this analysis, the copula function is used to construct bivariate equations to analyse return periods. The main advantage of the copula is that it is more flexible in constructing the multivariate distribution of random variables having different marginal distributions. According to Sklar's theorem, the copula C(.) for two random variables X and Y, and with marginal distributions $F_X(x)$ and $F_Y(y)$ respectively, can be represented in Eq. (3.9).

$$F_{X,Y}(x,y) = C(F_X(x), F_Y(y)) \tag{3.9}$$

where $F_{X,Y}(x,y)$ is the CDF of the joint distribution. If u and v are CDF of X and Y respectively, then the copula $C(u,v)$ satisfies boundary condition and monotonicity on $[0,1]^2$ as follows:

The boundary condition is;

$C(u,0) = 0 = C(0,v)$ and

$$C(u,1) = u;\ C(1,v) = v \tag{3.10}$$

Monotonicity;

For every u_1, v_1, u_2 and v_2 in the interval [0,1], where $u_1 \le u_2$ and $v_1 \le v_2$, then

$$C(u_2,v_2) - C(u_2,v_1) - C(u_1,v_2) + C(u_1,v_1) \ge 0 \tag{3.11}$$

Drought duration, severity, and peak are the correlated random variables considered for the analysis. Different pairs of these properties, such as severity and duration, duration and peak, and severity and peak, were taken for the bivariate analysis of drought using copulas. Normal, t, Gumbel, Clayton, Frank, and Plackett copulas were considered for this research (Mishra and Singh 2010). Bayesian Information Criterion (BIC) and Akaike Information Criteria (AIC) were performed to select the best copula from the various fits. The copula parameters are calculated using the inversion of Kendall's tau approach and the maximum pseudo-likelihood method (Chen et al. 2013; Sajeev et al. 2021).

3.3.6 Univariate return period

The estimated elapsed time between drought events with a specific magnitude or larger is taken as the return period. As per the theoretical expression derived by Shiau and Shen (2001), the return period is a function of the cumulative distribution of the variable and the expected drought interarrival time (*Li*). Here, the return period for drought duration, severity, and peak can be estimated as

$$T_D = \frac{E(L)}{1-F_D(d)};\ T_S = \frac{E(L)}{1-F_S(s)};\ T_P = \frac{E(L)}{1-F_P(p)} \tag{3.12}$$

where L is the interarrival time of drought in months, and it is the period between the starting of a drought event and starting of the next one; $E(L)$ is the expected interarrival time; T_D, T_S and T_P are return period defined solely by duration, severity, and peak of drought respectively; cumulative distribution functions of duration, severity, and peak are represented by $F_D(d), F_S(s)$ and $F_P(p)$ respectively.

3.3.7 Bivariate return period

Here, bivariate distribution is considered for the analysis; hence, the combinations of drought properties obtained from duration, severity, and peak are taken for return period calculations. Shiau (2003) developed two bivariate return periods: the co-occurrence return period (T_{DS}) and the joint return period (T'_{DS}). In the case of the co-occurrence return period (T_{DS}), duration exceeds some specific value, and severity exceeds some other specific value ($D \geq d$ and $S \geq s$). In the joint return period, either duration or severity exceeds some specific values ($D \geq d$ or $S \geq s$). The same definition can be applied to the other two combinations of drought properties. The copula-based equations created for these return periods are defined below:

$$\begin{aligned} T_{DS} &= \frac{E(L)}{P(D \geq d, S \geq s)} = \frac{E(L)}{1-F_D(d)-F_S(\mathrm{s})+F_{DS}(d,s)} \\ &= \frac{E(L)}{1-F_D(d)-F_S(\mathrm{s})+C(F_D(d),F_S(s))} \end{aligned} \tag{3.13}$$

$$T'_{DS} = \frac{E(L)}{P(D \geq d \ or\ S \geq s} = \frac{E(L)}{1-F_{DS}(d,s)} = \frac{E(L)}{1-C(F_D(d),F_S(s))} \tag{3.14}$$

where T_{DS} and T'_{DS} are co-occurrence return period and joint return period, respectively.

3.3.8 Percentage Departure of Rainfall

The departure analysis can account for the years of shortage and surplus rainfall. The departure in the precipitation value with respect to its long-term mean helps to give much information regarding the behaviour of rainfall in each year. The annual and seasonal departure of precipitation can be calculated using Eq. (3.15).

$$\text{Departure}\ (\%) = \frac{x_i - \overline{x}_i}{\overline{x}_i} \times 100 \tag{3.15}$$

where x_i is the rainfall for a year or season i; $\overline{x}_i$ is the long-term mean of rainfall for the considered period.

3.3.9 Copula-Based Conditional Probability to Assess the Impact of Rainfall on Crop Productivity

A copula-based equation for conditional probability is used to study the impact of rainfall on crop productivity. For two cumulative marginal distribution functions $F_U(u), F_V(v)$, the non-exceedance conditional probability equation is shown in Eq.(3.16) (Reddy and Ganguli 2012b; Sajeev et al. 2021).

$$C_{U|V\le v} = C(U \le u \,|\, V \le v) = \frac{C(u,v)}{v} = \frac{C(F_U(u), F_V(v))}{F_V(v)} \tag{3.16}$$

where, $C(F_U(u), F_V(v))$ is the joint distribution function of the copula of the two random variables. Here, the non-exceedance probability of bajra and paddy (annual productivity in kg/ha), given annual average rainfall (in mm), is considered.

3.3.10 Yield Loss Rate

The yield of a crop depends mainly on climate, variety alternation, and proper fertilizer application. Whereas plant diseases, extreme events like drought, heatwaves, and floods are the leading causes of crop yield losses (Ghazaryan et al. 2020; Wang et al. 2020). The rate of yield loss in a particular year with respect to the maximum yield obtained in the previous five years is defined as follows:

$$Y_l = \frac{Y_i - Y_m}{Y_m} \times 100 \tag{3.17}$$

where, Y_l is the rate of yield loss in a given year, Y_i is the yield obtained in the year i, and Y_m is the maximum yield obtained during the last five years.

3.4 RESULTS

3.4.1 Departure analysis of annual and seasonal rainfall

The plot of annual and seasonal rainfall departure with respect to corresponding long-term (56 years) mean values in Saurashtra and Kutch, and Coastal Karnataka are given in Figures 3.4 and 3.5, respectively.

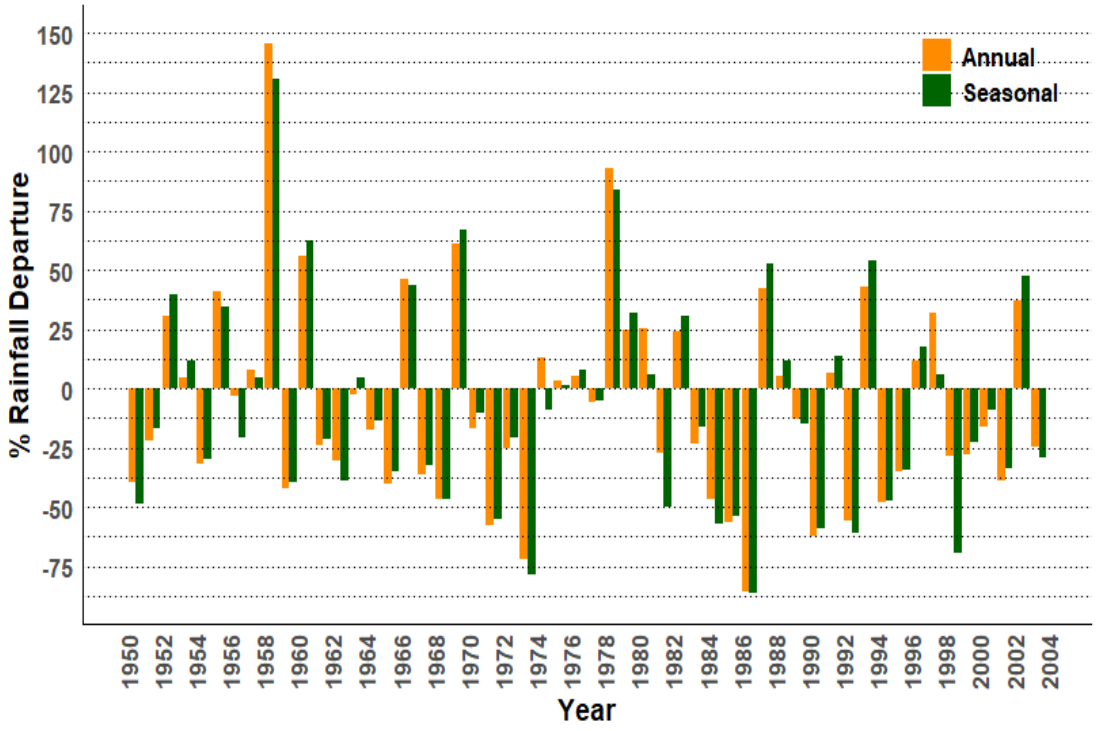

Figure 3.4. Annual and seasonal departure of rainfall with respect to corresponding long term (56 years) mean values in Saurashtra and Kutch

According to the India Meteorological Department (IMD), the area is under meteorological drought if its monsoon rainfall exceeds normal (Thomas and Prasannakumar 2016). Hence, the year with seasonal/ annual deficiency less than or

equal to -25% is considered a drought year in this study. The annual deficiency has almost the same seasonal trend, indicating that the drought events are controlled mainly by monsoon rainfall in both areas. From, Figure 3.4, the maximum deficiencies in Saurashtra and Kutch were observed in 1987 and were -85.39% and -86.24%, respectively, for annual and seasonal. From 1984 to 1987, there was a continuous deficiency in rainfall. The deficiency value was less than -50% from 1985 to 1987, with the average annual and seasonal deficits for these three years being -62.82% and -65.73%, respectively. Similarly, continuous deficiency was noticed from 1971 to 1974 and 1999 to 2002, with annual average deficiencies of -42.90% and -27.56%, respectively. This high deficiency indicates a severe meteorological drought in the region.

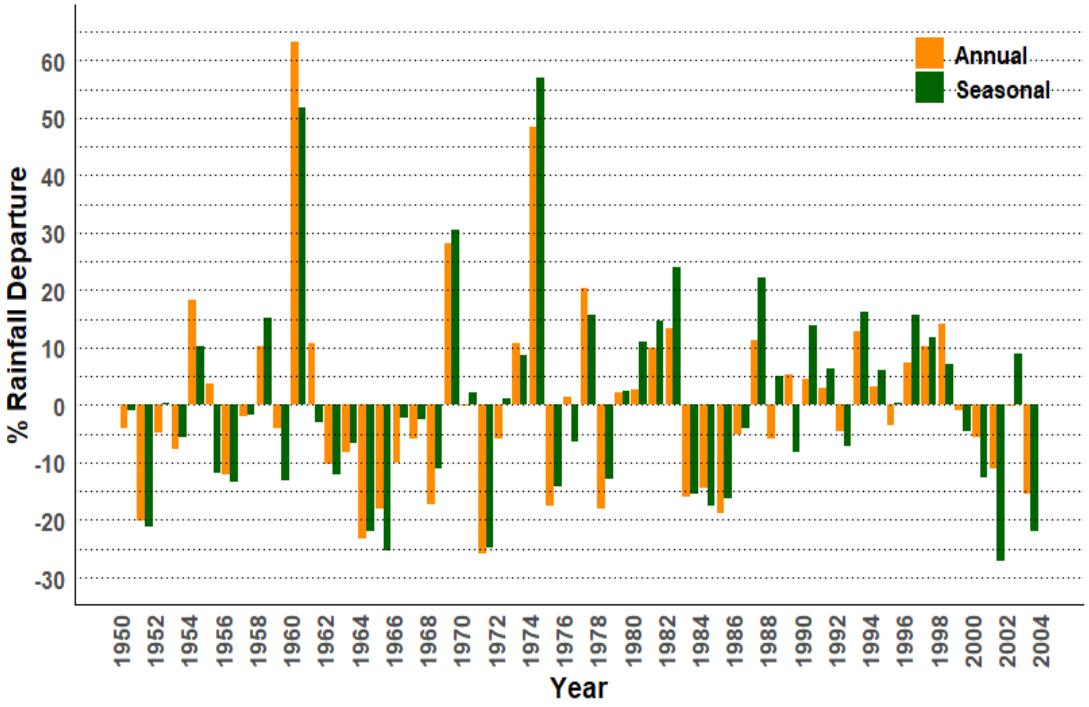

Figure 3.5 Annual and seasonal departure of rainfall with respect to corresponding long-term (56 years) mean values in Coastal Karnataka

In Coastal Karnataka, the highest deficiency in monsoon rainfall (-27.18%) and annual rainfall (-25.92%) occurred in 2002 and 1972, respectively (Figure 3.5). An excess rainfall (greater than 25%) was obtained in 1961, 1970, and 1975. Those rainfall excess values are an indicator of flood conditions in the area. About 21 drought years were

observed in Saurashtra and Kutch region during the period (from 1951 to 2004), and the average return period is three years. In Coastal Karnataka, only three drought years were observed from the departure plot, and the drought frequency was once in 18 years. The deficiency value during drought years varied from -29.24% to -86.24% in Saurashtra and Kutch, indicating mild to extreme drought events, and in Coastal Karnataka, it was -25.42% to -27.18%. The rainfall deficiency values are much higher, and drought events are more frequent in the Saurashtra and Kutch regions than in Coastal Karnataka.

3.4.2 Selection of covariates

In this case study, the area monthly average precipitation data were collected for both the study areas from 1951 to 2004. The ENSO and IOD indices for the same years were downloaded. The best marginal distribution for cumulative rainfall was selected based on AIC and BIC values and are shown in Table 3.1. The minimum AIC and BIC values are obtained for Gamma distribution in every case; hence, it is selected as the best fit for rainfall. By maintaining both parameters constant, the stationary Gamma distribution was modeled. The GAMLSS package was used to create non-stationary gamma distributions for each series of cumulative precipitation data. Only the mean of the distribution is modified as a linear function of covariates in the present work. The first non-stationary model (M1) is constructed by considering time as a covariate, and for the second non-stationary model(M2), climate indices are used as the covariate. The best lag of each climate index is assessed using the Kendall correlation method at a 5% significance level. The significant lag of climate oscillations for various time scales over the study areas is shown in Table 3.3.

Table 3.3 Significant lag of climate oscillations across different time scale in the study areas

Climate Oscillations	SST	SOI	MEI	IOD
Time scale	Saurashtra & Kutch			
3-months	-	-	-	1
6-months	1	0	0	2
12-months	3	4	2	-
24-months	5	5	3	-
Time scale	Coastal Karnataka			
3-months	-	-	-	6
6-months	0	0	0	7
12-months	2	1	1	4
24-months	4	4	3	6

From these results, it is observed that for Saurashtra and Kutch, SST, SOI, and MEI exhibit a substantial influence at different lags in all time scales of precipitation except at the 3 months time scale. For the same study area, IOD has influenced only at the 3 and 6 months time scale, and SOI and MEI have a concurrent (i.e., zero lag) relation with the precipitation at the 6 months time scale. A similar concurrent association of SOI, MEI, and SST can be observed in the case of Coastal Karnataka at the 6 months time scale. The cumulative precipitation of Coastal Karnataka significantly correlates with almost all climate oscillations at different time scales. Out of four indices, only IOD at various lags exhibits significant association with precipitation data at all time scales in Coastal Karnataka. SST, SOI, and MEI have no impact on 3 months cumulative precipitation in the study areas.

3.4.3 Comparison between Stationary and Non-stationary drought indices

The Akaike Information Criteria (AIC) value was checked for different covariate combinations from the selected lags of indices. The one with minimum AIC was selected as the best combination of covariates for the second non-stationary model (M2) and is listed in Table 3.4. The AIC values of the three models are also compared in Table 3.4. Model 0 (M0) is the stationary model. Models 1 and 2 are non-stationary

models with time and climate oscillations as covariates. From Table 3.4, it is observed that the stationary model showed the greatest AIC values for both the study areas at all the time scales of precipitation. A considerable difference in AIC values can be observed between M0 and M2. The AIC value difference between M0 and M1 is lesser than between M0 and M2. Models with minimum AIC values were considered the best, and further calculations were done based on the best model. Both the non-stationary models were found to be having lesser AIC values than the stationary models. Here, the least AIC values belonged to M2, so M2 was the best model in all cases in both study areas. The covariates of the M2 are various combinations of climate oscillations at different lags. In the case of Coastal Karnataka, the best model at the 24 months time scale is the model with all climatic indices. Non-stationary models help to account for changes and trends over time. The equations of Mu and values of sigma of the selected model are listed in Table 3.5. The Maximum Likelihood Estimation (MLE) method is used to estimate the distribution parameter of models as it is flexible in incorporating different forms of non-stationarity.

Table 3.4 AIC values of models fitted to precipitation data and selected covariates

	Model 0 (M0)	Model 1 (M1)	Model 2 (M2)	Selected Covariates for Model 2
Time scale	Saurashtra & Kutch			
3-months	8154.902	8156.35	8133.73	IOD
6-months	8387.926	8388.31	8344.83	SOI, IOD
12-months	8728.09	8655.80	8652.55	SST, MEI
24-months	9014.209	8953.39	8949.96	SST, SOI, MEI
Time scale	Coastal Karnataka			
3-months	14840.23	14842.23	14803.71	IOD
6-months	14082.03	14084.03	14019.65	SOI, IOD
12-months	12979.66	12949.2	12770.50	SST, MEI, IOD
24-months	13299.06	13244.73	13181.88	SST, SOI, MEI, IOD

Table 3.5 Equation of Mu (μ) and Sigma (σ) of non-stationary models

Time scale	Saurashtra & Kutch
3-months	$\mu(t) = 4.78-0.29IOD(t)$
	$\sigma = 1.72$
6-months	$\mu(t) = 5.39+0.01SOI(t)-0.37IOD(t)$
	$\sigma = 1.21$
12-months	$\mu(t) = 6.13-0.17SST(t)+0.04MEI(t)$
	$\sigma = 0.41$
24-months	$\mu(t) = 6.85-0.03SST(t)+0.01SOI(t)+0.01MEI(t)$
	$\sigma = 0.29$
Time scale	**Coastal Karnataka**
3-months	$\mu(t) = 8.99+0.52IOD(t)$
	$\sigma = 1.69$
6-months	$\mu(t) = 9.73+ 0.01SOI(t)+ 0.38IOD(t)$
	$\sigma = 0.94$
12-months	$\mu(t) = 10.44-0.06SST(t) -0.02MEI(t)+0.10IOD(t)$
	$\sigma =0.12$
24-months	$\mu(t) = 11.13-0.04SST(t)+0.01SOI(t)+0.01MEI(t)+0.06IOD(t)$
	$\sigma =0.10$

3.4.4 Analysis of drought characteristics

From the values of SPI and NSPI, drought categorization is done based on the threshold limit and is listed in Table 3.2. As per Table 3.2, drought comes under four classes based on the threshold values: mild (C1), moderate (C2), severe (C3), and extreme (C4) drought. Its occurrence frequencies were compared for stationary and non-stationary approaches in both study areas. Figure 3.6 and Figure 3.7 represent the comparison of drought classification for all the time scales in Saurashtra and Kutch, and Coastal Karnataka, respectively.

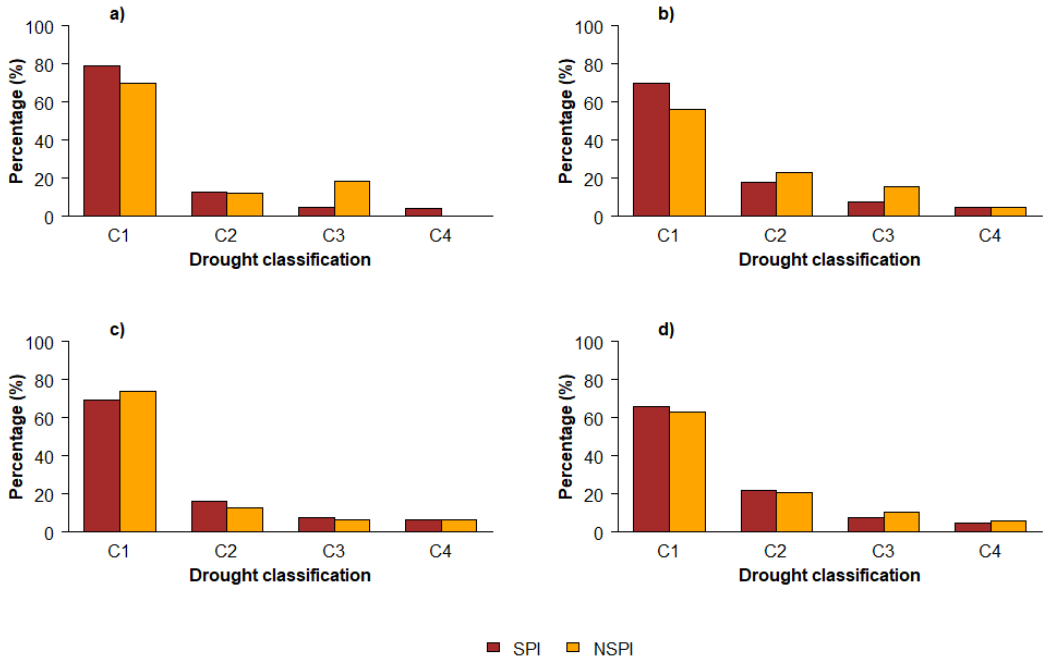

Figure 3.6 Drought classification in Saurashtra and Kutch for (a) 3 months; (b) 6 months; (c) 12 months; and (d) 24 months

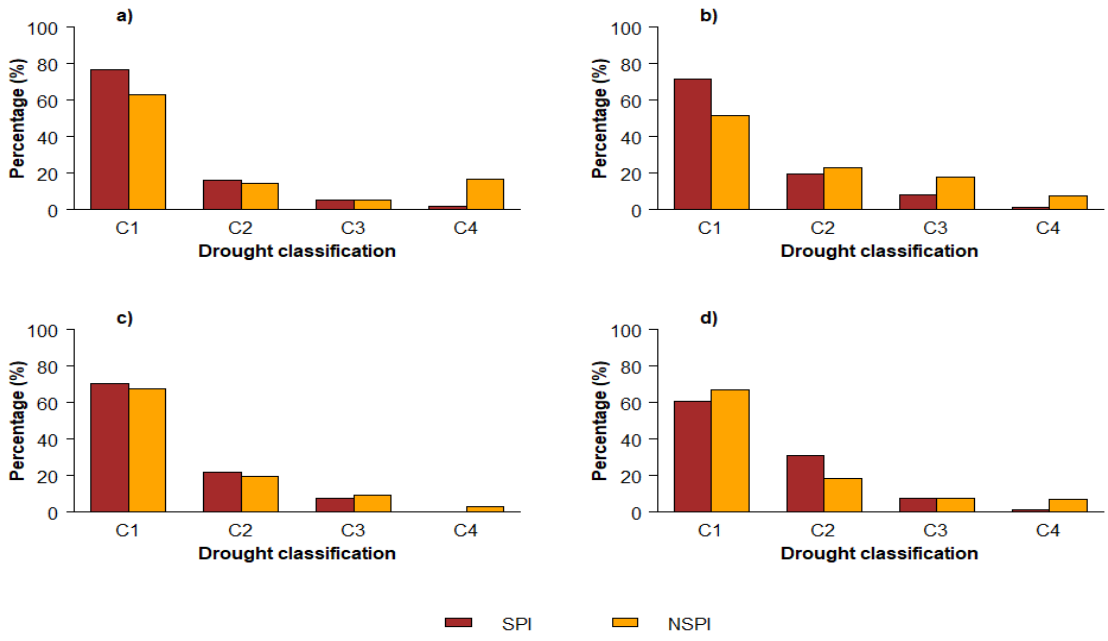

Figure 3.7 Drought classification in Coastal Karnataka for (a) 3 months; (b) 6 months; (c) 12 months; and (d) 24 months

Based on both approaches, the C1 event has a higher percentage of occurrence in both the study area and for all the time scales, but C1 obtained from the non-stationary index has a lower frequency of occurrence than C1 from the stationary index for all time scales except 12 months in Saurashtra and Kutch region and 24 months in Coastal Karnataka. From Figure 3.6, almost the same percentage of C4 can be observed for 6 months and 12 months timescales. A higher percentage of non-stationary-based C4 is noticed in Coastal Karnataka for all-time scales. Based on the non-stationary approach, except for the 24 months scale, a higher frequency of C1 can be observed in Saurashtra and Kutch than in Coastal Karnataka.

3.4.5 Analysis of drought properties

Drought duration, severity, and peak from stationary and non-stationary indices were estimated as drought properties for the present study. The statistics of drought properties at various scales in Saurashtra and Kutch, as well as Coastal Karnataka, are reported in Tables 3.6 and 3.7, respectively. The number of drought events and maximum severity was more in Saurashtra and Kutch than in Coastal Karnataka by both the approaches at 3 months and 24 months scales. Based on NSPI3, the number of droughts and maximum duration are 68 and 7 months for Saurashtra and Kutch and 53 and 4 months for Coastal Karnataka. The maximum peak values of short-term and long-term droughts are greater in Saurashtra and Kutch, and for the same study area, the number of droughts based on the non-stationary approach is more than that obtained from the stationary approach at all scales. Based on NSPI6 and NSPI24, the mean inter-arrival time is longer in Saurashtra and Kutch than in Coastal Karnataka. Based on SPI, short-term drought (SPI3 and SPI6) has a longer inter-arrival time, and long-term drought (SPI12 and SPI24) has a lesser inter-arrival time in Saurashtra and Kutch than in Coastal Karnataka. Both tables show that when the duration is shorter, the corresponding severity and peak value are also lesser; if longer the duration is, the severity and peak are also greater. In order to check the correlations between the three drought variables, the Pearson correlation test is conducted for Saurashtra and Kutch, and the results are shown in Table 3.8. The correlation coefficient value is greater for duration and severity at all time scales than other combinations.

Table 3.6 Descriptive statistics of drought for Saurashtra and Kutch

Climate variables	Statistics	SPI3	NSPI3	SPI6	NSPI6	SPI12	NSPI12	SPI24	NSPI24
		Value							
Drought	Number of drought events	67	68	49	52	21	28	14	18
	Mean inter arrival time (months)	11.70	11.45	13.31	12.38	30.9	23	45.5	35.39
Drought duration	Mean	1.68	2.75	2.71	2.94	6.9	4.07	12.57	7.83
	Standard deviation	1.23	1.61	2.3	1.11	5.82	3.87	11.01	8.07
	Maximum	6	7	9	10	23	20	45	40
	Minimum	1	1	1	1	1	1	1	1
Drought severity	Mean	2.24	3.46	3.76	4.24	10.08	8.20	17.13	11.06
	Standard deviation	2.22	2.38	4.22	2.05	12.32	8.31	20.06	15.24
	Maximum	13.05	9.42	22.15	22.38	53.45	33.51	65.75	56.77
	Minimum	0.82	0.80	0.80	0.82	0.8	0.88	1.01	0.85
Peak	Mean	1.34	1.37	1.46	1.72	1.52	1.42	1.52	1.45
	Standard deviation	0.49	0.40	0.48	0.7	0.62	0.57	0.85	0.8
	Maximum	2.97	2.99	3.15	3.23	3.50	3.64	4.15	4.23
	Minimum	0.82	0.80	0.8	0.82	0.8	0.83	1	0.85

Table 3.7 Descriptive statistics of drought for Coastal Karnataka

Climate variables	Statistics	SPI3	NSPI3	SPI6	NSPI6	SPI12	NSPI12	SPI24	NSPI24
		Value							
Drought	Number of drought events	64	53	58	54	18	26	13	24
	Mean inter arrival time (months)	10.17	12.42	11.17	11.96	35.66	24.69	49	26.54
Drought duration	Mean	1.78	2.39	2.33	2.96	7.3	5.03	11.23	5.45
	Standard deviation	1.16	0.95	1.88	0.93	8.65	6.84	13.86	7.21
	Maximum	7	4	8	4	33	26	42	26
	Minimum	1	1	1	1	1	1	1	1
Drought severity	Mean	2.24	3.98	2.94	4.31	9.28	6.85	14.46	7.64
	Standard deviation	1.66	1.77	2.65	1.61	11.04	10.56	19.26	12.17
	Maximum	8.83	8.31	11.99	8.00	36.70	42.46	58.67	44.76
	Minimum	0.80	0.82	0.82	0.98	0.84	0.8228	0.8	0.83
Peak	Mean	1.38	2.00	1.37	1.84	1.3	1.38	1.40	1.27
	Standard deviation	0.45	0.61	0.45	0.45	0.42	0.52	0.52	0.49
	Maximum	2.78	2.50	2.97	2.85	2.45	2.73	2.47	2.55
	Minimum	0.80	0.82	0.82	0.98	0.81	0.82	0.87	0.83

Table 3.8 Correlation coefficient of drought properties

	Duration-Severity	Duration-peak	Severity-Peak
NSPI3	0.91	0.51	0.63
SPI3	0.94	0.66	0.82
NSPI6	0.80	0.45	0.73
SPI6	0.93	0.77	0.62
NSPI12	0.94	0.79	0.89
SPI12	0.93	0.65	0.84
NSPI24	0.97	0.89	0.97
SPI24	0.94	0.71	0.90

Duration and peak are less correlated to each other when compared to duration-severity and severity-peak combinations. The highest correlation is observed under non-stationary conditions and at a time scale of 24 months, and is 0.97 for duration-severity and also for severity-peak. A high significant correlation is observed between different combinations of the drought variables; hence, it should be modeled together.

The probability density function of drought properties of Saurashtra and Kutch and Coastal Karnataka are also estimated and plotted in Figures 3.8 and 3.9, respectively, for comparison. From both figures (Figures 3.8 and 3.9), it can be observed that in all time scales, there is a noticeable difference in the density plots of all the properties of drought, like severity, duration, and peak obtained from stationary and non-stationary approaches. For all drought properties, the probability density functions on 6 and 12 months time scales appear to have shifted more towards the right for the non-stationary approach. The difference in PDF plots decreases gradually with the time scales in Saurashtra and Kutch. The results are proof of the capability of climate oscillations to change the properties of droughts.

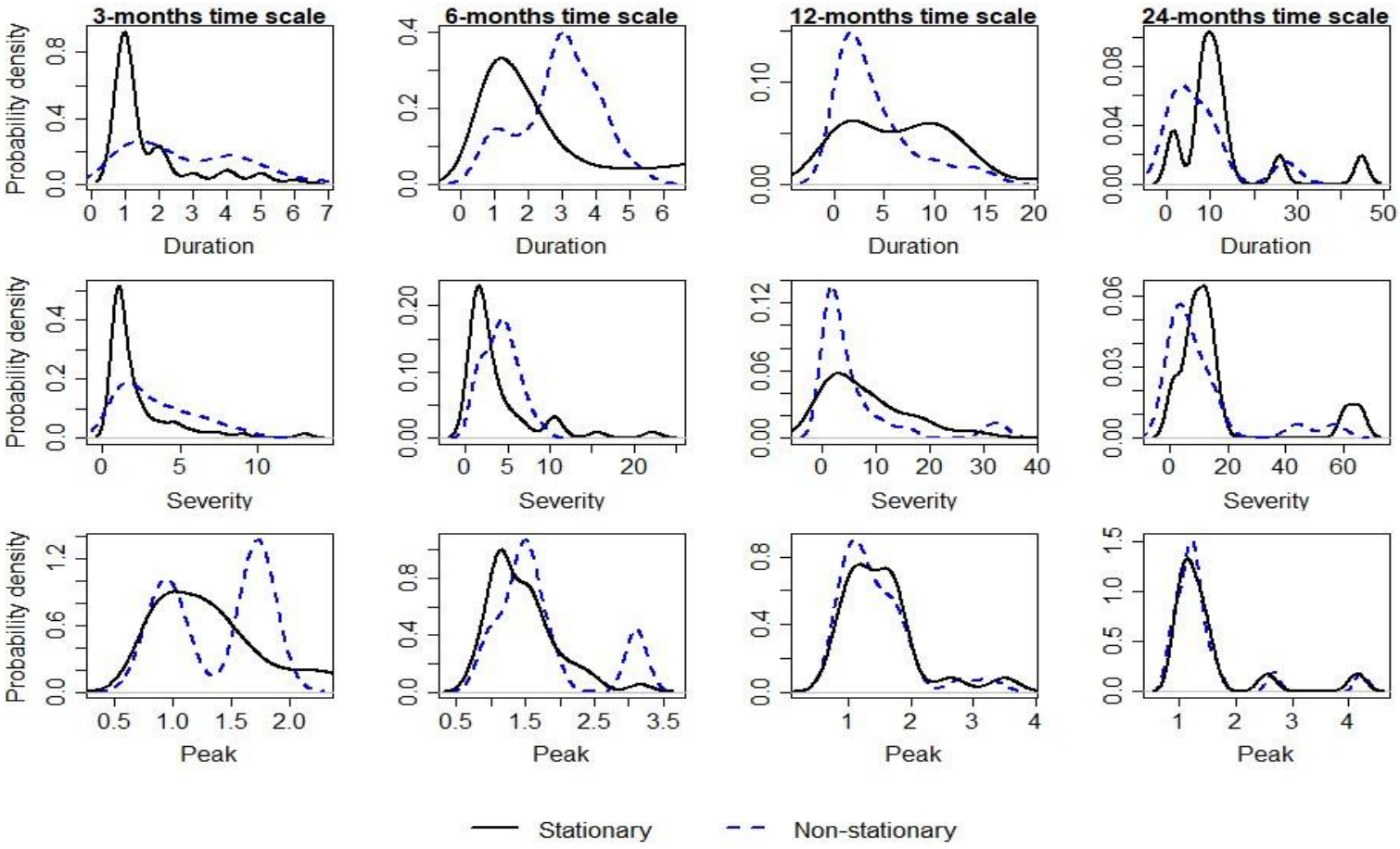

Figure 3.8 Probability density of duration, severity, and peak in Saurashtra and Kutch under stationary and nonstationary conditions for various time scales.

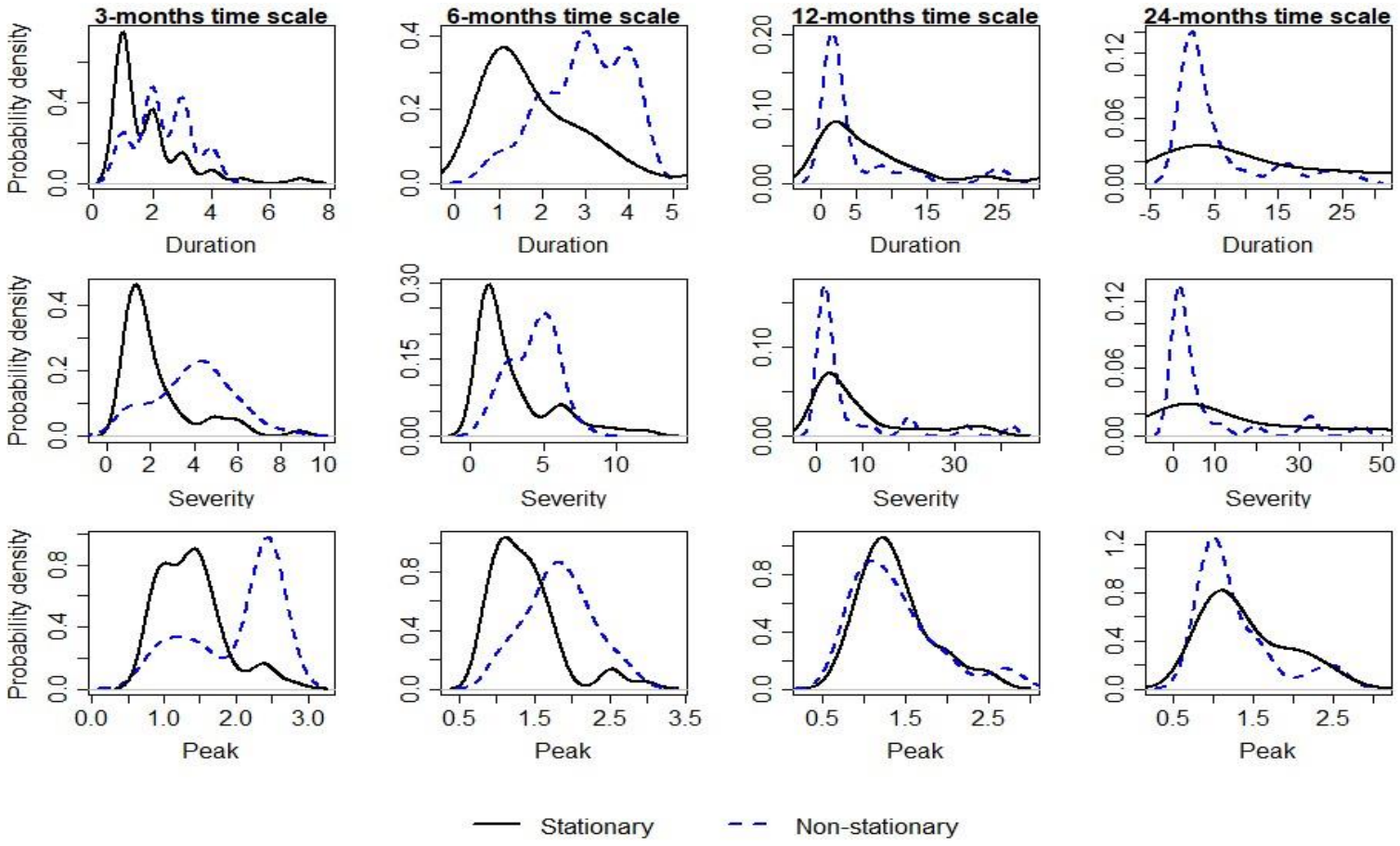

Figure 3.9 Probability density of duration, severity, and peak in Coastal Karnataka under stationary and nonstationary conditions for various time scales.

3.4.6 Bivariate analysis of Droughts using copula

The non-stationary approach was the best in every case, so the drought properties calculated from non-stationary indices were used for bivariate analysis. Different distributions are analysed to determine the suitable fit for each drought property. Gamma, weibull, generalized extreme value, exponential, and lognormal were considered as possible fits for the variables. Parameters of the considered distribution are estimated using the maximum likelihood method. The best marginal distribution is chosen based on Kolmogorov-Smirnov (KS) and Anderson Darling (AD) tests. The parameters of best fits are shown in Table 3.9. From Table 3.9, it can be noticed that all drought properties were best fitted by either weibull or generalized extreme value distributions in most cases except for duration obtained from NSPI6 and NSPI12 in Saurashtra and Kutch, in which the best fit was gamma distribution. Since the distributions are different for duration, severity, and peak, the copula is used for constructing bivariate distributions from the selected marginal distributions. Based on AIC and BIC values, the best-fitted copula was selected for each combination of drought variables at all time scales. The selected copula and its parameters are listed in Table 3.10. All copulas were fitted to the data at different time scales in two study areas except placket and t-copula. Gumbel copula was obtained as the best fit only at 12 and 24 months time scales. In the case of the 3 and 6 months time scale, Clayton copula gave a better fit in most cases.

Table 3.9 Best-fitted marginal distributions and their estimated parameters

Study Area	Index	Duration	Severity	Peak
Saurashtra & Kutch	NSPI3	Weibull	Weibull	Weibull
		1.73	1.52	3.38
		3.09	3.77	1.54
	NSPI6	Gamma	GEV	GEV
		1.39	0.45	0.16
		1.94	1.14	0.43
			2.65	1.38
	NSPI12	Gamma	GEV	GEV
		1.10	0.55	0.20
		3.67	2.18	0.33
			2.15	1.14
	NSPI24	Weibull	Weibull	GEV
		0.98	0.88	0.51
		7.15	8.24	0.22
				1.08
Coastal Karnataka	NSPI3	Weibull	GEV	GEV
		2.45	-0.33	-1.04
		2.70	1.83	0.63
			3.38	2.0161
	NSPI6	Weibull	GEV	Weibull
		2.85	-0.41	4.60
		3.34	1.72	1.98
			3.83	
	NSPI12	GEV	GEV	GEV
		0.58	0.61	0.19
		1.64	2.26	0.32
		1.81	1.99	1.11
	NSPI24	GEV	GEV	GEV
		0.45	0.62	0.35
		2.85	2.63	0.22
		0.22	1.93	1.02

Table 3.10 Selected Copula and their Estimated Parameters

Time scale	Drought properties	Saurashtra & Kutch		Coastal Karnataka	
		Fitted Copula	Parameter	Fitted Copula	Parameter
3-months	Duration-Severity	Frank	16.24	Normal	0.82
	Duration-Peak	Clayton	1.19	Clayton	0.92
	Severity-Peak	Clayton	2.84	Clayton	2.77
6-months	Duration-Severity	Clayton	3.28	Clayton	4.04
	Duration-Peak	Clayton	0.63	Clayton	1.08
	Severity-Peak	Normal	0.77	Normal	0.83
12-months	Duration-Severity	Frank	26.20	Frank	24.52
	Duration-Peak	Gumbel	1.99	Normal	0.81
	Severity-Peak	Gumbel	2.42	Normal	0.91
24-months	Duration-Severity	Frank	39.14	Gumbel	7.22
	Duration-Peak	Normal	0.92	Gumbel	2.98
	Severity-Peak	Gumbel	6.00	Normal	0.94

3.4.7 Analysis of return periods

The return period is an essential factor to be considered in hydraulic designs. Tables 3.11 and 3.12 show the univariate return periods and bivariate return periods (in years) in Saurashtra and Kutch, and Coastal Karnataka, respectively. For univariate return periods of 5, 10, 20, 50, 75, and 100 years, corresponding duration, severity, peak, co-occurrence return period, and joint return periods were calculated. From Table 3.11, considering the 3-month time scale, for a univariate return period of 10 years, the values of duration (D), severity (S), and peak (P) were obtained as 5.05, 6.62, and 1.98 years, respectively. The joint return periods T'_{DS} ($D \geq 5.05$ or $S \geq 6.62$), T'_{DP} ($D \geq 5.05$ or $P \geq 1.98$), and T'_{SP} ($S \geq 6.62$ or $P \geq 1.98$) were 7.27 years, 5.52 years, and 5.84 years respectively. At the same time, the values of co-occurrence return periods such as T_{DS} ($D \geq 5.05$ and $S \geq 6.62$), T_{DP} ($D \geq 5.05$ and $P \geq 1.98$), and T_{SP} ($S \geq 6.62$ or $P \geq 1.98$) were 16, 53.26, and 34.6 years, respectively. For the same time scale and univariate return period, duration, severity, and peak values were 3.78 , 6.26,

and 2.57 years, respectively, in Coastal Karnataka (Table 3.12). Corresponding bivariate joint responses of return periods (in years), i.e., T'_{DS}, T'_{DP}, T'_{SP}, T_{DS}, T_{DP} and T_{SP} were calculated as 6.21, 5.50, 5.91, 25.7, 55.19, and 32.46 years respectively. Compared with a univariate return period of 20 years at the 3 months time scale in Saurashtra and Kutch, the decrease in T'_{DS} ($D \geq 5.86$ or $S \geq 7.85$) was found to be 35.75 %, while the percentage of increase in T_{DS} ($D \geq 5.86$ and $S \geq 7.85$) was observed to be 55.66 %. For the same condition in Coastal Karnataka, the decrease in T'_{DS} ($D \geq 4.22$ or $S \geq 6.83$) and increase in T_{DS} ($D \geq 4.22$ and $S \geq 6.83$) were 43.75 % and 77.82 %, respectively. In most cases, greater values of duration, severity, and peak and lesser return periods were observed in Saurashtra and Kutch compared to the values of the same variables and return periods in Coastal Karnataka under the same conditions. It indicates that the Saurashtra and Kutch region is more vulnerable to drought events than Coastal Karnataka.

At all the time scales in both the study areas, the univariate return periods were greater than the joint return periods and less than the co-occurrence return periods. From this comparative study of return periods, it can be inferred that the drought risk is underestimated by the univariate return period in the 'or' scenario and overestimated in the 'and' criteria. Hence, bivariate analysis is more useful in drought risk studies.

Table 3.11 Comparison of univariate and multivariate return periods (in years) in Saurashtra & Kutch

T (Year)	Duration (months) (D)	Severity (S)	Peak (P)	T'_{DS}	T'_{DP}	T'_{SP}	T_{DS}	T_{DP}	T_{SP}
3-months									
5	4.13	5.26	1.79	4.11	3.01	3.29	6.38	14.67	10.45
10	5.05	6.62	1.98	7.27	5.52	5.84	16	53.26	34.6
20	5.86	7.85	2.14	12.85	10.52	10.88	45.11	202.2	123.84
50	6.82	9.34	2.31	28.37	25.52	25.9	210.35	1223.01	719.02
75	7.21	9.95	2.38	41.02	38.02	38.41	436.94	2731.4	1590.18
100	7.48	10.38	2.43	53.6	50.52	50.91	744.23	4837.71	2802.41
6-months									
5	4.16	5.04	2.11	3.4	2.94	3.65	9.4	16.79	7.93
10	5.69	7.03	2.56	5.99	5.43	6.87	30.15	63.24	18.4
20	7.18	9.69	3.03	11.04	10.42	13.1	105.57	245.13	42.26
50	9.12	14.69	3.74	26.06	25.41	31.22	602.81	1502.56	125.52
75	9.96	17.65	4.09	38.56	37.89	46.02	1327.57	3365.89	202.63
100	10.56	20.09	4.34	51.05	50.38	60.66	2334.48	5970	284.38
12-months									
5	3.98	4.11	1.41	4.68	3.87	4.04	5.37	7.07	6.57
10	6.66	7.49	1.76	8.79	7.37	7.77	11.59	15.56	14.04
20	9.30	12.23	2.14	15.88	14.42	15.26	27.01	32.64	29.01
50	12.77	21.84	2.71	33.59	35.6	37.78	97.8	83.97	73.92
75	14.29	27.87	2.99	47.06	53.25	56.54	184.57	126.77	111.35

100	15.37	33.02	3.21	60.15	70.91	75.31	296.37	169.57	148.78
24-months									
5	3.74	4.02	1.11	4.85	4.53	4.66	5.15	5.57	5.39
10	8.77	10.32	1.4	9.43	8.46	9.09	10.64	12.23	11.11
20	13.85	17.11	1.78	17.86	16.1	17.99	22.73	26.39	22.52
50	20.62	26.55	2.5	37.28	38.28	44.71	75.9	72.05	56.71
75	23.62	30.87	2.94	49.15	56.37	66.98	158.18	112.03	85.2
100	25.76	33.97	3.32	147.46	74.25	89.26	75.65	153.11	113.69

Table 3.12 Comparison of univariate and multivariate return periods (in years) in Coastal Karnataka

T (Year)	Duration (months) (D)	Severity (S)	Peak (P)	T'_{DS}	T'_{DP}	T'_{SP}	T_{DS}	T_{DP}	T_{SP}
3-months									
5	3.26	5.51	2.49	4.5	3	3.34	5.62	15	9.92
10	3.78	6.26	2.57	6.21	5.5	5.91	25.7	55.19	32.46
20	4.22	6.83	2.6	11.25	10.49	10.94	90.19	210.92	115.16
50	4.71	7.38	2.62	26.24	25.53	26	527.95	1287.09	667.2
75	4.9	7.57	2.62	38.89	37.9	38.38	1053.59	2856.24	1462.73
100	5.03	7.7	2.62	51.34	50.57	51.06	1922.23	5103.15	2596.65
6-months									
5	3.96	5.77	2.21	3.48	3.01	3.76	8.88	14.64	7.46
10	4.49	6.37	2.38	6.1	5.52	7.11	27.78	53.36	16.87

20	4.92	6.79	2.52	11.17	10.52	13.6	95.51	203.07	37.82
50	5.41	7.18	2.67	26.22	25.52	32.45	537.73	1230.2	108.86
75	5.6	7.31	2.73	38.73	38.02	47.85	1179.8	2748.45	173.34
100	5.72	7.39	2.77	51.24	50.52	63.09	2071.22	4868.81	240.98
12-months									
5	3.09	3.75	1.34	4.68	4.04	4.3	5.37	6.55	5.98
10	5.66	7.41	1.67	8.8	10	8.08	11.58	10	13.13
20	9.34	12.78	2.02	15.89	14.03	15.41	26.97	34.79	28.48
50	17.05	24.31	2.55	33.61	33.09	36.7	97.56	102.23	78.4
75	22	31.85	2.81	47.1	48.61	54.07	184.04	164.12	122.39
100	26.28	38.46	3.01	60.18	63.94	71.23	295.46	229.38	167.74
24-months									
5	1.96	3.62	1.16	4.66	4.24	4.47	5.39	6.09	5.67
10	5.74	7.73	1.43	9.19	8.18	8.5	10.96	12.87	12.15
20	10.59	13.77	1.76	18.27	16.1	16.34	22.09	26.41	25.77
50	19.59	26.74	2.32	45.52	39.87	39.2	55.45	67.03	69.01
75	24.89	35.24	2.64	68.23	59.69	57.89	83.25	100.87	106.46
100	29.27	42.69	2.88	90.95	79.51	76.39	111.06	134.72	144.72

3.4.8 Effect of rainfall on crop productivity

Crop production is highly controlled by climate change. Here, only major crops in the study area are considered, and it might not be reasonable to compare the productivity of two different crops. Hence, the percentile of precipitation is considered instead of absolute values. In comparison to Saurashtra and Kutch, the 5^{th} percentile rainfall in Coastal Karnataka is almost 129 times higher. Coastal Karnataka's 95^{th} percentile rainfall is 51 times that of the Saurashtra and Kutch region. The ratio of 95^{th} percentile rainfall to the 5^{th} percentile in Coastal Karnataka is 1.5, whereas, in Saurashtra and Kutch, it is 3.8. From the analysis, the best-fitted univariate distribution for bajra productivity and rainfall for Saurashtra and Kutch were Weibull and Lognormal distributions, respectively, and the best-fitted copula was Normal copula. For Coastal Karnataka, the best-fitted distribution for rainfall and rice productivity was the Lognormal distribution, and the Clayton was the fitted copula.

The Normal copula-based non-exceedance conditional probability of bajra productivity was calculated based on Eq. (3.16) for different precipitation values and plotted in Figure 3.10. The productivity of bajra (Figure 3.10(a)) ranges from 100-300 kg/ha to 900-1100 kg/ha. The highest probability value was 63.11% at the 10^{th} percentile of precipitation for the bajra productivity range of 100-300 kg/ha. For 300-500 kg/ha, the highest likelihood value was 40.20% at the 50^{th} percentile of precipitation. The highest probability values for the productivity range 500-700 kg/ha, 700-900 kg/ha, and 900-1100 kg/ha were observed at the 95^{th} percentile, and the values were 26.90%, 10.67%, and 1.99%, respectively. The lowest (22.56%) for the 100-300 kg/ha productivity range was observed at the 95^{th} percentile. However, the lowest probability values for all other ranges, such as 300-500 kg/ha, 500-700 kg/ha, 700-900 kg/ha, and 900-1100 kg/ha, were 9.85%, 0.48%, 0.01%, and 0.00%, respectively at 5^{th} percentile of precipitation. Hence, the higher productivity values of bajra are very sensitive to higher precipitation (95^{th} percentile).

In Coastal Karnataka, rice productivity (Figure 3.10(b)) has the highest probability value of 35.64% at 25^{th} percentile precipitation and 1600-1800 kg/ha productivity range. 1600-1800 kg/ha range is more susceptible to precipitation. Higher productivity ranges such as 2000-2200 kg/ha, 2200-2400 kg/ha, and 2400-2600 kg/ha are more

sensitive to higher precipitation (95th percentile), and the probability values are 15.97%, 4.62%, and 0.88% respectively. For the same productivity ranges, the probabilities at the 5th percentile are 6.03%, 1.56%, and 0.29%, respectively. For the 1800- 2000 kg/ha range, the likelihood value increases from 16.75% (at 5th percentile precipitation) to 32.33% (at 95th percentile). For the lower range of productivity (1400-1600 kg/ha), the probability value decreases (from 33.44% to 12.44%) with the increase in precipitation (5th to 95th percentile).

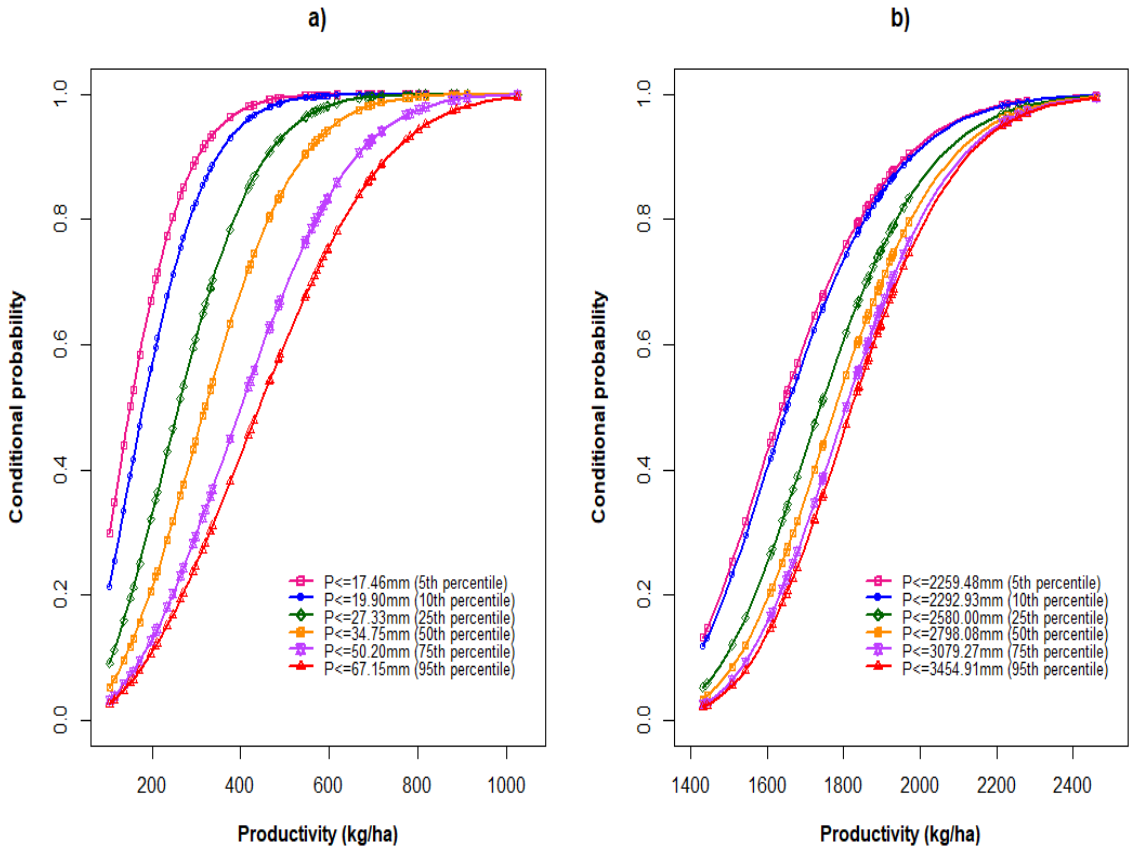

Figure 3.10 Conditional probability of crop productivity for given precipitation in (a) Saurashtra and Kutch; and (b) Coastal Karnataka.

3.4.9 Analysis of crop yield loss rate

Crop production is highly controlled by climate change. The yield loss rate of bajra and rice was calculated based on Eq. (3.17). The Pearson correlation test (Hendrawan et al. 2022) was used to determine the correlation between the crop yield loss rate and

drought index under a non-stationary scenario. The correlation between crop yield loss rate and non-stationary drought index in each month at various time scales was tested for bajra and rice in Saurashtra and Kutch, and Coastal Karnataka, respectively. The results obtained are shown in Table 3.13.

Table 3.13 Pearson correlation between crop yield data and drought index

	Saurashtra & Kutch				**Coastal Karnataka**			
	3-month	6-month	12-month	24-month	3-month	6-month	12-month	24-month
January	**0.32**	0.03	0.02	0.05	0.06	0.20	0.09	0.20
February	0.11	0.00	0.02	0.05	0.22	0.04	0.06	0.17
March	0.22	0.15	0.03	0.06	0.11	0.02	0.04	0.20
April	0.17	**0.32**	0.01	0.06	0.31	0.15	0.00	0.29
May	0.04	0.01	0.02	0.03	0.19	0.17	0.03	0.18
June	**0.32**	**0.33**	0.01	0.11	0.11	0.17	0.05	0.05
July	**0.40**	**0.38**	0.24	0.21	0.04	0.14	0.02	0.07
August	**0.46**	**0.44**	**0.48**	0.27	0.20	0.07	0.13	0.08
September	**0.44**	**0.43**	**0.49**	**0.29**	0.14	0.05	0.18	0.01
October	0.27	**0.46**	**0.42**	**0.28**	0.22	0.12	0.15	0.00
November	0.14	**0.42**	**0.45**	0.26	0.00	0.14	0.16	0.00
December	0.00	**0.31**	**0.45**	**0.28**	0.10	0.02	0.17	0.01

Note: Bold values represent statistically significant at 5% levels of significance

In Saurashtra and Kutch, a significant correlation was obtained between the bajra yield loss rate and drought index at all time scales. The highest significant correlation was found in September on the 12 months time scale. In September, a significant correlation was observed at all the time scales. Since Kharif crops sprout in September, it can be said that September is a crucial month for the bajra output in Saurashtra and Kutch. Drought in September thus has an impact on crop productivity. The graph between the

bajra yield loss rate and NSPI12 is plotted in Figure 3.11. From Figure 3.11, the maximum reduction in bajra yield was 65.19% in 1974. In the same year, NSPI indicated extreme drought in the area. In 1987, Gujarat experienced the worst drought (Bandyopadhyay and Saha 2016; Bhuiyan et al. 2017). According to Nathan (2001), the extreme drought in 1985 affected 75% of the crops in Gujarat. From 1985 to 1987, NSPI showed severe to extreme drought conditions, and the impact of that particular drought event can be seen in the case of bajra yield, with a continuous negative loss rate in those three years with a maximum loss rate (59.04%) in 1987. During all the drought periods shown by NSPI, a more negative value in crop yield loss rate can be observed. It indicates that the drought is one of the main factors affecting bajra's production in Saurashtra and Kutch.

In Coastal Karnataka, there was no significant correlation between rice yield loss rate and drought index at all time scales. As it is an area with high availability of rainfall, the crop production was not affected by the drought as per NSPI-based analysis for the considered period. A greater insignificant correlation was observed in April at the 3 months time scale, and the graph between NSPI3 in April and the rice yield loss rate is given in Figure 3.12. The maximum rice yield loss was -24.49% in 1982. From 1981 to 1987, a continuous loss in yield was observed. During the same period, severe to extreme dry condition was shown by the NSPI.

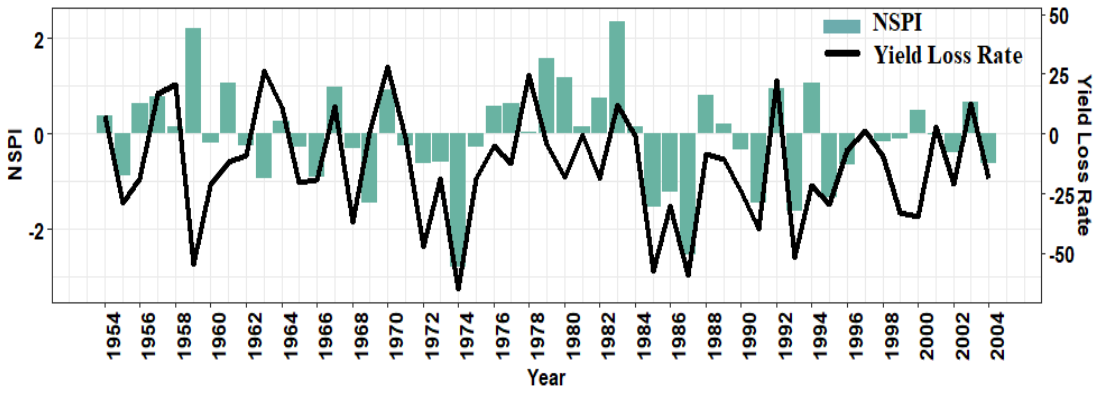

Figure 3.11 NSPI12 versus Bajra Yield Loss rate in Saurashtra and Kutch

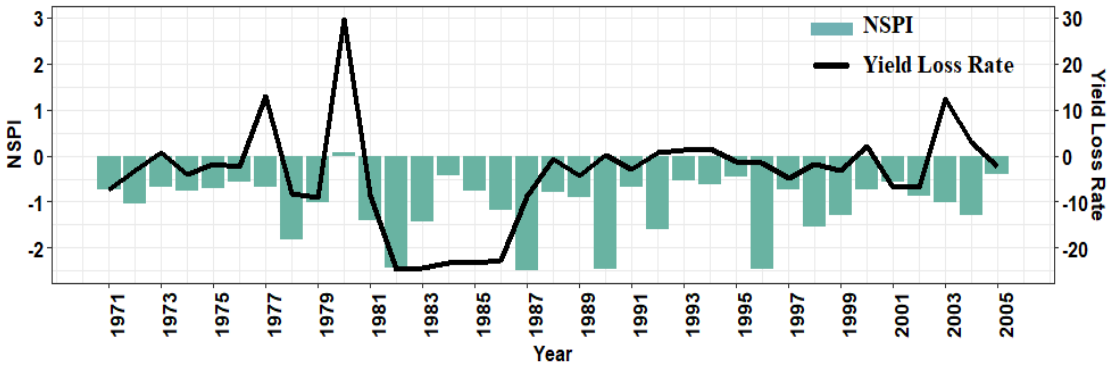

Figure 3.12 NSPI3 versus Rice Yield Loss rate in Coastal Karnataka.

3.5 DISCUSSIONS

The calculated NSPI and SPI of Saurashtra and Kutch and Coastal Karnataka were presented in Figures 3.13 and 3.14. More variability between SPI and NSPI can be observed in 3 months and 6 months time scales plots, whereas, for long-term droughts (12 and 24 months), more consistent plots were noticed. Based on some related literature, the years in which significant drought events and flood events in the areas are also indicated in Figures 3.13 and 3.14. According to the study conducted by Bandyopadhyay et al. (2016) for the three-decade from 1981 to 2010, Gujarat suffered major droughts in 1982, 1985, 1986, 1987, 1990, 1991, 1993, 1995, 1998, 1999, 2000, 2001, 2002, and 2004. Considering the 6 months plots (Figure. 13(b)) for the comparison, both SPI and NSPI showed drought events during the same years. However, in most cases, except in 1982, 1990, 1993, and 1995, the NSPI values were more negative than SPI, indicating severe to extreme drought. So, NSPI is better than SPI in indicating extreme drought events.

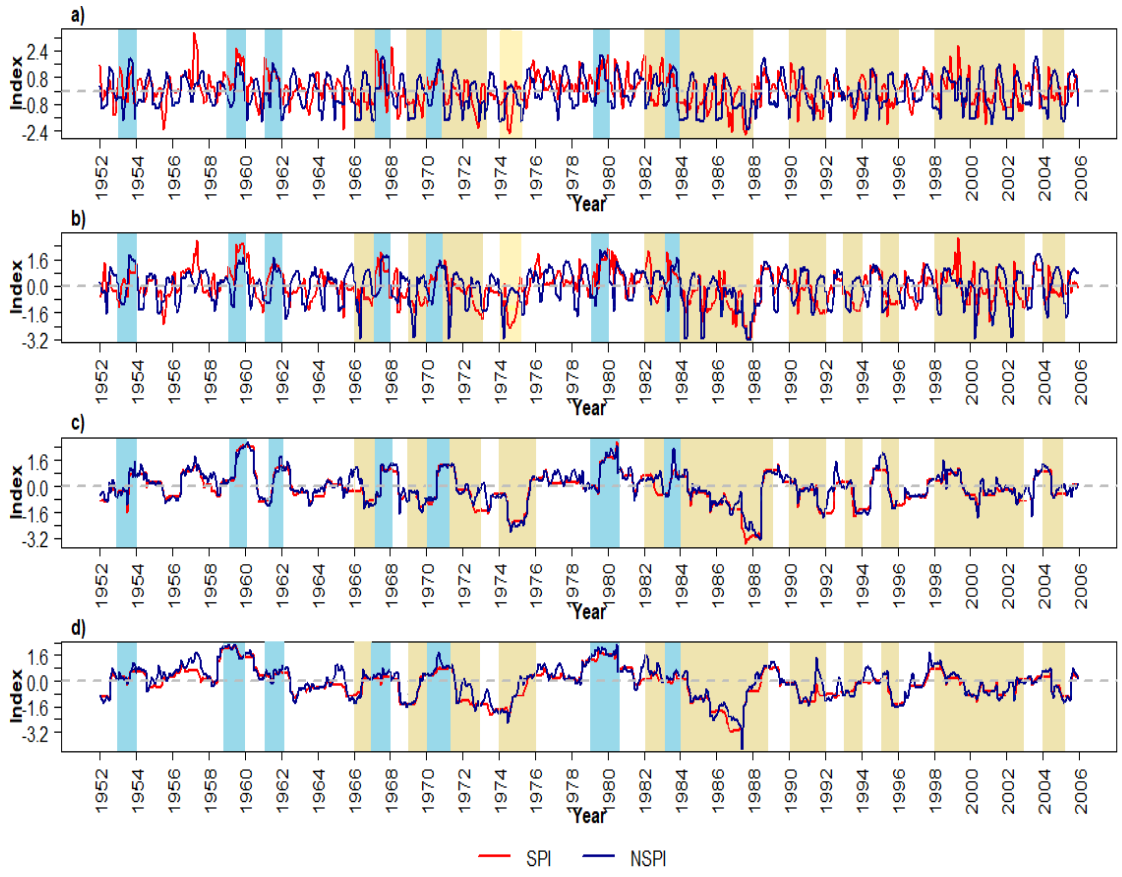

Figure 3.13 SPI versus NSPI in Saurashtra and Kutch for (a) 3 months; (b) 6 months; (c) 12 months; and (d) 24 months. The vertical bars indicate the historic drought and flood events.

Between 1981 and 1990, many regions of Gujarat, especially Kutch, frequently experienced severe drought and water scarcity (Bandyopadhyay et al. 2016). Different areas of the state experienced severe to extreme meteorological droughts in 1985, 1986, and 1987 due to inadequate rainfall during the monsoon seasons, and the worst drought was found in 1987. Surface water was completely absent, with 20 partially dried-out and 40 fully dried-up dams. Five thousand cattle died just in Saurashtra (Nathan 2001). NSPI indicated eight severe and extreme drought events from 1981 to 1990, whereas SPI indicated only four. From this study also, 1987 was the year with the worst drought in Saurashtra and Kutch by both indices. NSPI estimated the worst drought event of 1987 as having a severity of 22.38 and a peak value of 3.23, while SPI reported the same drought event as having a severity of 22.15 and a peak of 3.15. The vegetation was severely affected due to a deficiency in monsoon rainfall during 1990-1991

(Bandyopadhyay and Saha 2016b). A severe bajra crop loss rate (-39.92%) was observed during the period. The western region of Gujarat was severely affected by a drought in 2002 (Bhuiyan et al. 2017). With a severity of 9.02 and a peak value of 3.07, the NSPI classified that drought incident as extreme. SPI classified it as just a moderate drought event with a severity of 6.04 and a peak of 1.49. Here, NSPI is more consistent with the actual situation.

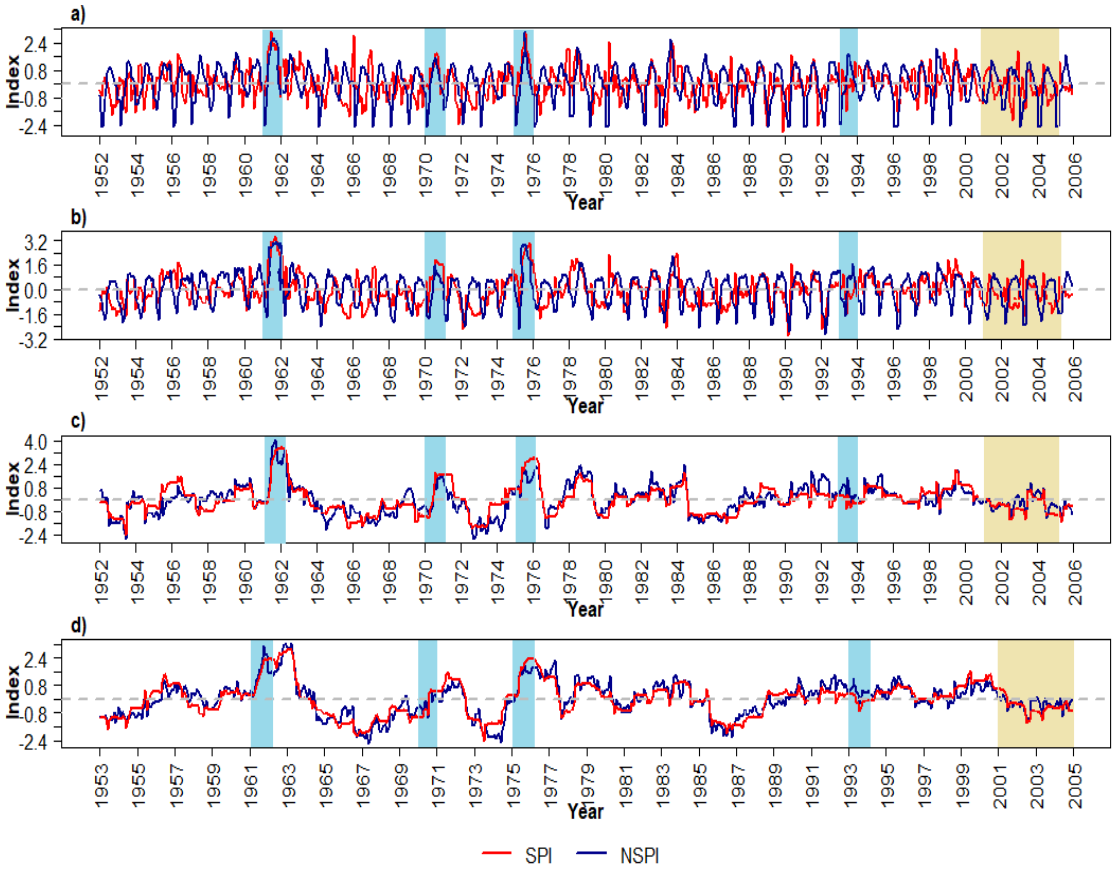

Figure 3.14 SPI versus NSPI in Coastal Karnataka for (a) 3 months; (b) 6 months; (c) 12 months; and (d) 24 months. The vertical bars indicate the historic drought and flood events.

Although Saurashtra has a history of experiencing droughts, a severe drought in 1999 was particularly severe in the districts of Surendranagar, Porbandar, Amreli, Rajkot, Junagadh, Bhavnagar, and Jamnagar. The water table in the regions of Saurashtra and Kutch dropped, and all the water sources dried up, resulting in the non-availability of food (Chopra 2006). NSPI marked that particular drought event in 1999 as severe and

moderate by SPI. According to Chopra (2006), the high deficiency of monsoon rainfall was the reason for this severe drought. From Figure 3.4, the monsoon deficiency value was observed as -69%, which might be the reason for the extreme drought in the summer of 2000, marked by NSPI.

According to Yadav et al. (2021), based on a six-month SPI, Saurashtra and Kutch faced severe drought during 1971-1972 and extreme drought events during 1974-1975, 1984-1985, and 1987-1988. Twelve-month SPI showed extreme drought events in 1974–1975 and 1987–1988. Both NSPI and SPI depicted the extreme drought events in 1974-1975, and both were extreme with a more negative value of NSPI. However, the extreme drought in 1984-1985 was depicted as extreme only by NSPI. According to Ganguli and Reddy (2014), in the 6 months time scale, Saurashtra and Kutch regions experienced drought with high severity in 1974 and 1987, and drought events in this area mainly occurred in the summer season. The summer season drought in 1974 was captured only by NSPI6, whereas SPI indicated it as just a mild drought. Saurashtra and Kutch region experienced severe floods in 1953, 1959, 1961, 1967,1970, 1979, and 1983 (Parthasarathy et al.1987). In 1953, 1967, and 1983, the excess rainfall was greater than 25%, according to Figure 3.4, whereas in 1959, 1961, 1970, and 1979, it was greater than 60%. The NSPI could indicate those flood years with index value of greater than 1.5. The NSPI could match with the historic wet and dry periods of Saurashtra and Kutch.

Almost 75% of the taluks in Karnataka are determined to be highly vulnerable to drought (Srinivasareddy et al. 2019). Coastal Karnataka receives high rainfall in the monsoon season, but drought has been reported in recent years during summer. Only a few researchers attempted drought analysis in the Coastal region of Karnataka. Karnataka faced severe drought from 2001 to 2004, during which enormous economic loss was reported in the state (Jayasree and Venkatesh 2015). During the summer of 2001 to 2004, severe to extreme drought events can be observed from NSPI6, whereas the SPI6 indicated only moderate dry conditions in most cases. According to Srinivasareddy et al. (2019), during the fifteen years from 2001 to 2015, 2003 was the most severe drought in Karnataka, affecting almost all taluks adversely. Also in the year 2002, severe drought was reported. From NSPI6, the extreme drought with a peak

value of 2.26 and a severity of 4.50 can be observed in 2003; however, SPI showed it as a moderate drought with a peak value of 1.4 and a severity of 2.31. According to Jamir et al. (2008), 34 deaths and 11.35 crores of economic damage were reported due to one severe flood that hit Coastal Karnataka in 1993. The NSPI6 indicated this flood event as a severe wet condition with a peak value of 1.61 during the monsoon season; however, the SPI reported the same period as a dry period and failed to identify the specific flood event. According to Parthasarathy et al. (1987), 1961 and 1975 were severe flood years of Coastal Karnataka, and a moderate flood was reported in 1970. Those three flood events were also correctly indicated by the non-stationary index. In Coastal Karnataka also, NSPI has better consistency with historical studies. Murari et al. (2019) observed a rising temperature trend in Karnataka, and there is a likelihood of extreme temperatures in the future; hence, high risk is expected in agricultural production. Also, a long-term negative trend in rainfall is found in Karnataka's coastal region, which points out the importance of more studies in this field to reduce the risk.

Jayasree and Venkatesh (2015) used rainfall data from Directorate of Economics and Statistics, Karnataka, whereas Srinivasareddy et al. (2019) have used Taluk wise rainfall data of Karnataka. Jamir and Gadgil (2008) used meteorological subdivision rainfall data from India Meteorological Department (IMD). Bandyopadhyay and Saha 2016) used rainfall data from the Consultative Group on International Agricultural Research—Consortium for Spatial Information (CGIAR-CSI). Chopra (2006) has used rainfall data for 164 stations in Gujarat collected from the Bhaskaracharya Institute of Satellite and Geoinformation (BISAG), Gandhinagar. Ganguli and Reddy (2014), Parthasarathy et al.(1987), and Yadav et al. (2021) have conducted drought analysis in Saurashtra and Kutch region using the areal-weighted average rainfall obtained from IITM, Pune. The results obtained from this study are found to have better consistency with the above-mentioned studies, indicating that the modeling is robust.

The NSPI-based assessment matched better as far as the historical drought scenario is concerned, than SPI. In most cases, NSPI indicated more severe and extreme drought than SPI, which will help to reduce the risk. From the plots, NSPI was found to be returned from such a severe event to values above average more quickly than SPI. It might be due to the considered climate covariates. The suitability of NSPI in drought

analysis is well established by Das et al. (2021), and Shiau (2020). The implications of using non-stationary models are that they can provide more accurate and meaningful insights into time-series data compared to stationary models.

Significant influence of rainfall and drought on crop yield was observed in both study areas. Panda et al. (2019) observed a significant influence of monsoon rainfall on the productivity of crops in Odisha, India. Madadgar et al. (2017) noticed 45% decrease in the crop yield when the SPI value falls below -0.5. The present large-scale climate variables have a remarkable influence on the future drought conditions; hence drought analysis that takes into account the temporal lags of climate variables and precipitation can bring more reliable results for water management plans (Li et al. 2015a).

3.6 CLOSURE

This chapter has demonstrated the applications and implications of using non-stationary models for assessing meteorological drought in two different climate regions Saurashtra and Kutch, as well as Coastal Karnataka, India. The non-stationary models are developed using GAMLSS from the best combinations of climate indices (SST, MEI, IOD, and SOI). The influence of climate variables on drought characteristics and drought properties are analysed. The non-stationary models outperformed the stationary models in capturing drought properties, indicating the importance of considering time-varying factors in drought analysis. The non-stationary drought index showed better consistency with historical drought and flood events, enhancing its reliability for assessing drought conditions. Additionally, the study employed copula-based bivariate drought analysis as drought variables such as severity, duration, and peak are significantly correlated to each other. This approach allowed for the estimation of joint probabilities of extreme drought events, enabling a more comprehensive understanding of drought risk. The comparison between bivariate and univariate return periods revealed higher drought risk in the arid Saurashtra and Kutch regions compared to Coastal Karnataka.

Furthermore, the study explored the impact of rainfall and drought on crop yield. More crop productivity is depicted in Coastal Karnataka, which has more rainfall availability. Higher productivity of bajra and rice were more sensitive to higher precipitation. The

analysis showed a significant correlation between the Non-stationary Standardized Precipitation Index (NSPI) and bajra yield in Saurashtra and Kutch, emphasizing the influence of drought events on agricultural productivity. This information is crucial for agricultural planners and farmers in making informed decisions regarding crop selection, irrigation practices, and drought-resistant varieties. By incorporating the non-stationary drought index, agricultural planning can be optimized to minimize yield losses and ensure food security.

The results of this research can be used for drought management and agricultural planning in both arid and humid regions. The findings contribute to a better understanding of the changing environment's impact on drought conditions and can guide policymakers and agricultural planners in developing effective strategies to mitigate drought-related risks and support sustainable agricultural practices.

CHAPTER 4

HYBRID MODELS COMBINING ARIMA AND NEURAL NETWORKS FOR DROUGHT PREDICTION IN A SEMI-ARID REGION IN INDIA

4.1 GENERAL

It is crucial to understand the drought patterns in advance for implementing effective mitigation methods. Early detection of meteorological drought is essential because it can lead to other droughts, such as hydrological, agricultural, and socio-economic droughts (Jehanzaib et al., 2023; Zhao et al., 2016). Since it has found a significant effect of various climate oscillations on drought occurrence, researchers have developed non-stationary SPI (Rashid and Beecham, 2019). From Table 3.4, it can be observed that, the non-stationary SPI (NSPI) for Saurashtra and Kutch, in India with climate indices such as Sea Surface Temperature (SST), Extended Multivariate ENSO Index (MEI), Dipole Mode Index (DMI) and Southern Oscillation Index (SOI) as covariates performed much better than SPI. Hence, the same NSPI is used to find a suitable drought prediction model for Saurashtra and Kutch.

Hence, the aim of this chapter is to develop individual models using ARIMA, FNN, and RNN to forecast meteorological drought in Saurashtra and Kutch, which is a highly drought-prone area in India (Parthasarathy et al. 1987). Only a few researchers considered non-linear followed by linear model type hybrid model in time series forecasting. No studies were found in drought prediction using that particular type of hybrid combination. Hence, the efficacy of hybrid models such as ARIMA-FNN, ARIMA-RNN, FNN-ARIMA, and RNN-ARIMA, that combine linear and nonlinear modeling techniques to capture complex dynamics of drought occurrence is also explored in this research. The performance of developed models over 3, 6, 12 and 24 months time scales are analysed to find out best modeling approach for drought prediction in Saurashtra and Kutch. By considering the same, the research aims to provide valuable insights and tools for drought prediction and management in a region highly vulnerable to the impacts of drought.

4.2 STUDY AREA AND DATA

4.2.1 Description of the study region

Gujarat is situated between latitudes 20° 06′ N to 24° 42′ N and longitudes 68° 10′ E to 74° 28′ E. It is an arid terrain and highly drought prone region close to Thar Desert (Bandyopadhyay and Saha 2016; Ganguli and Reddy 2014). The present investigation is conducted on the Saurashtra and Kutch regions, covering an area of approximately 109,950 km^2, encompassing Jamnagar, Porbandar, Kutch, Junagadh, Surendranagar, Bhavnagar, Rajkot, and Amreli. The map of the study area is given in Figure 4.1.

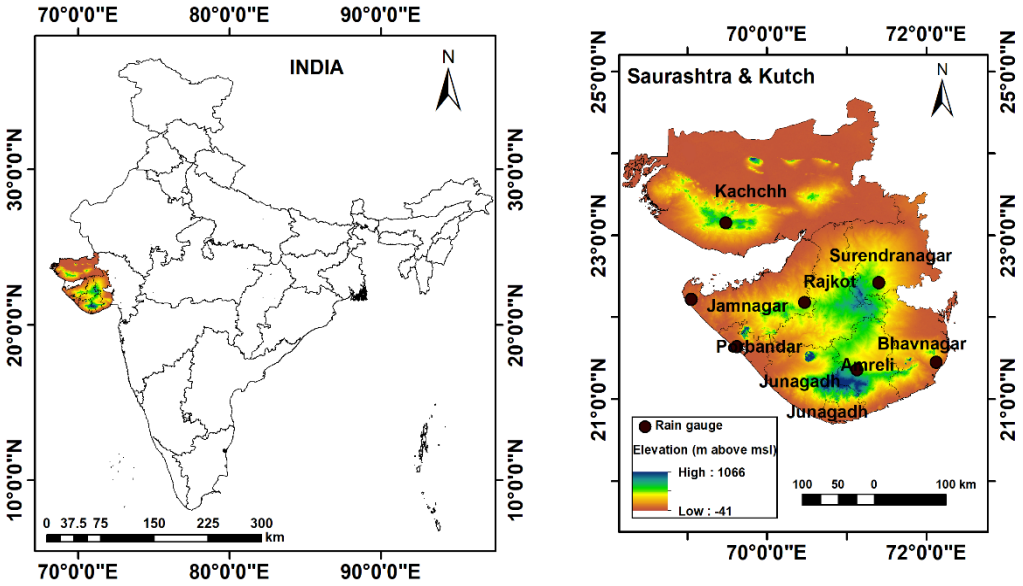

Figure 4.1. Study area

Saurashtra, often referred to as a peninsula, receives an average annual rainfall of about 400 mm. Conversely, the northeastern part of Kutch, characterized by the Rann of Kutch desert, experiences a lower annual rainfall of approximately 300 mm. Kutch is within the hot desert arid (BWh) zone, while Saurashtra is categorized as a hot semi-arid (BSh) area according to the Köppen's climate classification. Variability in rainfall

and drought have a considerable impact on the agriculture of the region (Das et al. 2016). Gujarat ranks among the top three states producing bajra, sesame, groundnut, and mustard.

4.2.2 Data Used

The drought index is computed using area-weighted monthly rainfall data from January 1951 to December 2004 obtained from the Indian Institute of Tropical Meteorology, Pune. The climate indices used for NSPI calculation are the Indian Ocean Dipole (IOD)(DMI 2023), Sea Surface Temperature (SST) (SST 2020), Multivariate ENSO Index (MEI) (MEI 2011), and Southern Oscillation Index (SOI)(SOI 2020). The influence of the selected climate variables on drought is detailed in section 2.4.

4.3 METHODOLOGY

Figure 4.2 displays the flow chart for the methodology for this part of the research. The drought index, NSPI, is calculated using monthly weighted average rainfall data and climate indices. The procedure for calculating NSPI is included in section 3.3. This chapter is focused on identifying an appropriate model for drought prediction in the Saurashtra and Kutch regions. Various models, such as ARIMA, FNN, RNN, and hybrid combinations, are investigated using specific assessment criteria. The subsequent sections provide detailed descriptions of the methodology utilized.

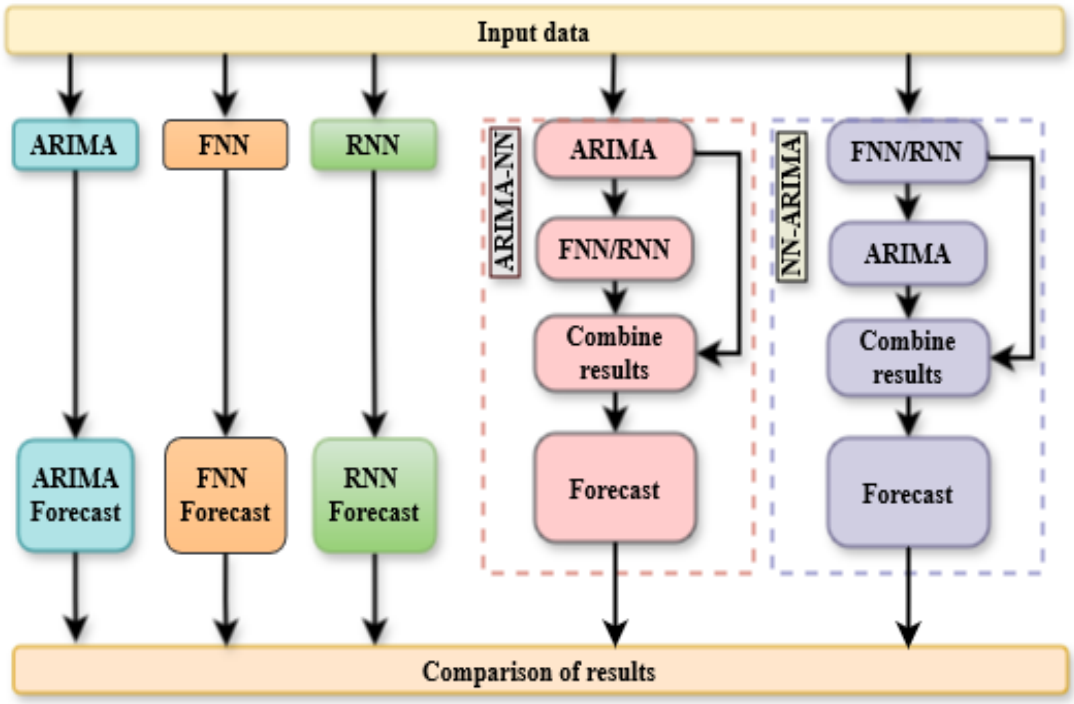

Figure 4.2. Methodology flowchart

4.3.1 Autoregressive Integrated Moving Average (ARIMA) Model

The Autoregressive Integrated Moving Average Model (ARIMA) is a popular statistical technique for forecasting and time series research. It is a powerful tool for identifying and forecasting trends in sequential data, making it useful in various disciplines, including epidemiology, economics, finance, and climate research. The mathematical equation of an ARIMA (p, d, q) model is given as follows;

$$y_{ARIMA_t} = \sum_{i=1}^{p} \phi_i y_{t-i} - \sum_{j=1}^{q} \theta_j \varepsilon_{t-j} \tag{4.1}$$

$\phi_i(1,2,...,\mathrm{p})$, $\theta_j(1,2,....q)$ are polynomials of p and q order. y_t and ε_t are actual value and random error. Seasonal Autoregressive Integrated Moving Average (SARIMA) models address the seasonal patterns inherent in the data. These models can be expressed as ARIMA$\left(p,d,q\right)\left(P,D,Q\right)_L$, where the parameters $p,d,$ and q are non-seasonal autoregressive, differencing, and moving average terms, respectively. $\left(P,D,Q\right)_S$ represents corresponding seasonal components for seasonality' s'. The

parameter selection is based on partial autocorrelation function (PACF), autocorrelation function, and statistical criteria such as the Akaike Information Criterion (AIC) and Bayesian Information Criterion (BIC) (Sajeev et al. 2021).

4.3.2 Neural Network models

ANN model in which information flows in a single direction forward, from the input layer via one or more hidden layers to the output layer is called a Feed-Forward Neural Network (FNN) (Abarghouei and Kousari 2013; Kumar. et al. 2004). A feed-forward network structure is given in Figure 4.3. Neurons in FNNs are arranged in layers, with connections between every neuron in one layer and every other layer. The original data is received in the input layer and processed using weighted connections and activation functions in the hidden layers, reaching in the generation of an output in the final layer.

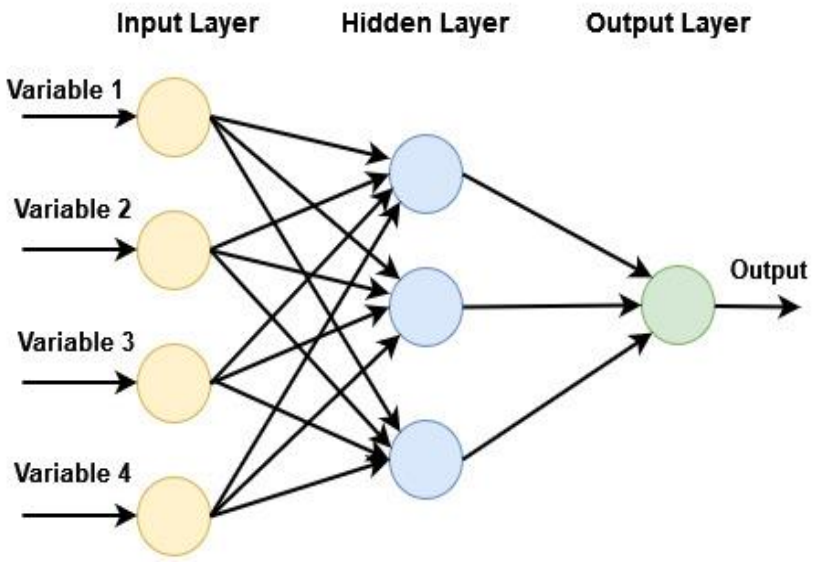

Figure 4.3. Feed Forward Network diagram

Recurrent Neural Networks have a unique design that enables them to store information about prior inputs through internal memory, unlike the feed-forward neural networks, where information travels in a single path from input to output. Recurrent connections facilitate this, establishing a feedback loop in which a neuron's output at one step becomes the neuron's input at the subsequent time step. A typical RNN is shown in Figure 4.4.

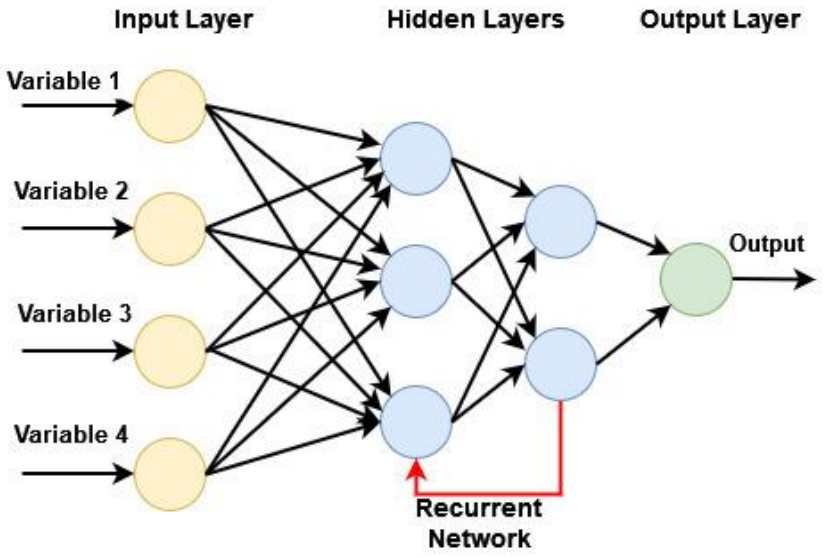

Figure 4.4. Recurrent Neural Network diagram

The mathematical expression for a single hidden layer of FNN model is given below.

$$y_{NN} = \alpha_0 + \sum_{j=1}^{q} \alpha_j g\left(\beta_{0j} \sum_{i=1}^{p} \beta_{ij} y_{t-i} \right) + \varepsilon_t \tag{4.2}$$

$\beta_{ij}(\mathrm{i}=1,2,...,\mathrm{p};\ \mathrm{j}=1,2,...,\mathrm{q})$ and $\alpha_j(\mathrm{j}=1,2,...,\mathrm{q})$ are joining weights. The number of input and hidden nodes are represented by p and q respectively.

4.3.3 Hybrid Models

Based on previous studies (Hajirahimi and Khashei 2022; Singh et al. 2019; Zhang 2003), the time series data is assumed to be a combination of linear and non-linear parts. In the ARIMA-NN hybrid model, the linear and non-linear component is separated as follows:

$$y_t = L_t + N_t \tag{4.3}$$

Where, y_t represents the observation at time t, L_t and N_t are linear ARIMA part and non-linear Neural Network part, respectively. From the ARIMA model, the residual at time t is calculated as follows:

$$e_{ARIMA,t} = y_t - L_{ARIMA,t} \tag{4.4}$$

Where $L_{ARIMA,t} = \phi_1 y_{t-1} + \phi_2 y_{t-2} + ... + \phi_p y_{t-p} + \theta_1 \varepsilon_{t-1} + \theta_2 \varepsilon_{t-2} + ... + \theta_q \varepsilon_{t-q}$ (4.5)

Then, the non-linear part is expressed as follows.

$$N_{NN,t} = \alpha_0 + \sum_{j=1}^{q} \alpha_j g\left(\beta_{0j} \sum_{i=1}^{p} \beta_{ij} e_{ARIMA,t-i} \right) + \varepsilon_t \tag{4.6}$$

The hybrid forecast result is the summation of results from the ARIMA and NN model as below:

$$y_{ARIMA-NN,t} = L_{ARIMA,t} + N_{NN,t} \tag{4.7}$$

In contrast to the ARIMA-NN model, the NN-ARIMA model is developed by fitting the NN model to the data first, and then the residual is fitted by ARIMA. The NN equation will be as follows.

$$N'_{NN,t} = \alpha_0 + \sum_{j=1}^{q} \alpha_j g\left(\beta_{0j} \sum_{i=1}^{p} \beta_{ij} y'_{t-i} \right) + \varepsilon_t \tag{4.8}$$

The residual obtained from the above model is then modeled by ARIMA as follows:

$$L'_{ARIMA,t} = \phi_1 e_{NN,t-1} + \phi_2 e_{NN,t-2} + ... + \phi_p e_{NN,t-p} + \theta_1 \varepsilon_{t-1} + \theta_2 \varepsilon_{t-2} + ... + \theta_q \varepsilon_{t-q} \tag{4.9}$$

Then, the final result is the combined results of NN and ARIMA.

$$y'_{NN-ARIMA,t} = N'_{NN,t} + L'_{ARIMA,t} \tag{4.10}$$

4.3.4 Model Evaluation Indicators

Several statistical indices such as Correlation Coefficient (CC) (Harisuseno 2020), R-squared (R^2) (Surakhi et al. 2021), Mean Square Error (MSE) (Demirel et al. 2009), Mean Absolute Error (MAE), Relative Absolute Error (RAE) (Pande et al. 2023) were

used to evaluate the model performance. The formula of the accuracy indices are given in Table 4.1.

Table 4.1 Formula of the accuracy indices

Index	Formula	Range
Correlation Coefficient	$CC = \frac{\sum_{i=1}^{N}[(O_i - \overline{O_i})(P_i - \overline{P_i})]}{\sqrt{\sum_{i=1}^{N}(O_i - \overline{O_i})^2}\sqrt{\sum_{i=1}^{N}(P_i - \overline{P_i})^2}}$	(-1 to +1)
R-squared	$R^2 = 1 - \frac{\sum_{i=1}^{N}(O_i - P_i)^2}{\sum_{i=1}^{N}(O_i - \overline{O_i})^2}$	(0 to +1)
Mean Square Error	$MSE = \frac{1}{N}\sum_{i=1}^{N}(P_i - O_i)^2$	(0 to ∞)
Mean Absolute Error	$MAE = \frac{1}{N}\sum_{i=1}^{N}\lvert P_i - O_i \rvert$	(0 to ∞)
Relative Absolute Error	$RAE = \sum_{i=1}^{N}\lvert P_i - O_i \rvert / \sum_{i=1}^{N}\lvert \overline{O_i} - O_i \rvert$	(0 to ∞)

Where, $\overline{P_i}$ and $\overline{O_i}$ are sample mean of random variables P_i and Q_i, respectively.

The linear relationship between two variables (P_i and Q_i), both in strength and direction, is measured by CC. A perfect positive linear relationship is represented by a value of 1, a perfect negative linear relationship by a value of -1, and no linear relationship by a value of 0. The percentage of the dependent variable's variance that the independent variables in a regression model account for are expressed as R-squared, sometimes referred to as the coefficient of determination. It is a binary variable with 1 denoting a perfect fit and 0 denoting no explanatory power. The average of the squared differences between the expected and actual values is determined by the mean square error, where higher values indicating a more significant prediction error. The mean

absolute error calculates the average of the absolute differences between predicted and actual values (Karimi et al. 2019). It measures the average magnitude of the errors, regardless of their direction, with higher values indicating more significant prediction errors. The relative absolute error measures the average absolute percentage difference between the predicted and actual values relative to the actual values. These evaluation metrics are commonly used to assess the performance of predictive models across various domains, providing insights into the accuracy of the model, reliability, and goodness of fit.

4.4 RESULTS

The NSPI is computed across different time scales, and an in-depth analysis of its performance is provided in section 3.4. Following this, the NSPI data is divided into training (70%) and testing (30%) sets for subsequent analysis. ARIMA, FNN, and RNN are standalone models, while combinations of ARIMA and Neural Networks are utilized as hybrid models.

4.4.1 Selection of Input Variables

The utilization of Autocorrelation Function (ACF) and Partial Autocorrelation Function (PACF) diagrams aids in determining the optimal lags within the data, thereby facilitating the selection of input variables. These diagrams, depicting the ACF and PACF graphs for NSPI across various time scales, are illustrated in Figure 4.5. The chosen inputs comprised lag values corresponding to a 95% confidence limit. From the PACF diagram, it is observed that lag-1 has the highest correlation at all time scales. For a 3 months time scale, lag-1, 2, 3, 4, 5, 6, 10, 11, and 12 have significant partial autocorrelation. Similarly, for a 6 months scale, significant correlation was observed for lag-1, 2, 3, 4, 5, 6, 9, 10, and 11. Lags-1, 11, and 13 were significant for 12 months, whereas only lags-1 and 3 exhibited significance for 24 months. Feed-forward and backward selection methods were employed to determine the optimal lag combination.

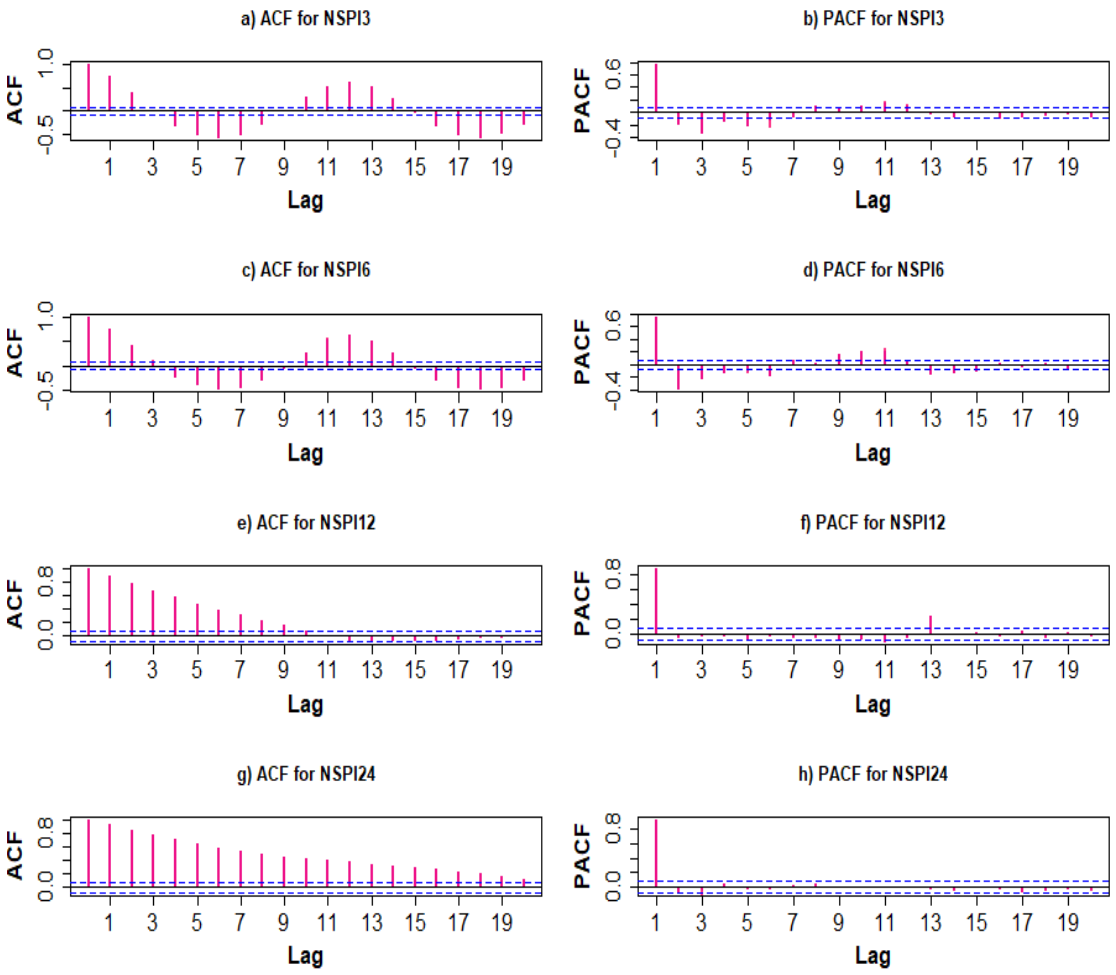

Figure 4.5. ACF and PACF diagram of NSPI at various time scales

The selection summary in Table 4.2 outlines the best lag combinations of each NSPI. For instance, for NSPI3, the optimal lag combination was determined to be Lag-1, 3, 6, 11, and 12, which aligns with the significant correlations observed in the PACF diagram. Similarly, Lag-1, 2, 3, 5, 6, and 11 were identified as the best combination for NSPI6. NSPI12 and NSPI24 exhibited simpler lag combinations, with only Lag-1 and 11 selected for NSPI12 and Lag-1 and 3 selected for NSPI24. Thus, based on these methods, the selected input variables and corresponding targets are summarized in Table 4.3.

Table 4.2 Selection summary of the best lag combinations using Feed forward and backward method

Data	Best Lag combinations	R^2	AIC
NSPI3	Lag.1	0.572	1253.715
	Lag.3	0.677	1076.411
	Lag.11	0.715	999.503
	Lag.6	0.721	987.872
	Lag.12	0.724	983.584
NSPI6	Lag.1	0.583	1302.598
	Lag.11	0.695	1105.163
	Lag.3	0.717	1060.695
	Lag.6	0.722	1050.249
	Lag.2	0.726	1043.882
	Lag.5	0.728	1041.237
NSPI12	Lag.1	0.780	856.578
	Lag.11	0.785	842.762
NSPI24	Lag.1	0.863	546.58
	Lag.3	0.864	544.358

Table 4.3 Selected inputs

Inputs	Target
NSPI3(t-1), NSPI3(t-3), NSPI3(t-6), NSPI3(t-11), NSPI3(t-12)	NSPI3
NSPI6(t-1), NSPI6(t-2), NSPI6(t-3), NSPI6(t-5), NSPI6(t-6), NSPI6(t-11)	NSPI6
NSPI12(t-1), NSPI12(t-11)	NSPI12
NSPI24(t-1), NSPI24(t-3)	NSPI24

4.4.2 Comparative analysis of Model performance

The structure of the ARIMA model is developed with different combinations of p, q, and d values by examining the ACF and PACF diagram, and the best one is selected based on the evaluation indicators. The auto. arima package in R is also used to find the best ARIMA model for each case. The ARIMA models performed best for long-term droughts during training but failed during testing. However, ARIMA demonstrated good performance in short-term droughts in both the training and testing phases. After selecting the suitable input combinations for FNN and RNN models, the number of hidden layers is chosen based on the evaluation indices. The selected network architecture of ARIMA, FNN, RNN, and hybrid models are given in Table 4.4.

Table 4.4 The selected network architecture of the model

Time Scale	Models	Network architecture considered
3-months	ARIMA	(2,0,2) (1,1,0)
	FNN	5-2-1
	RNN	5-6-1
	ARIMA-FNN	ARIMA (1,0,2) (2,1,0)-FNN (2-10-1)
	ARIMA-RNN	ARIMA (1,0,2) (2,1,0)-RNN (2-10-1)
	FNN-ARIMA	FNN (5-2-1)- ARIMA (1,0,0) (0,0,1)
	RNN-ARIMA	RNN (5,2,1) – ARIMA (1,0,1) (2,0,0)
6-months	ARIMA	(1,0,2) (2,1,0)
	FNN	6-2-1
	RNN	6-5-1
	ARIMA-FNN	ARIMA (1,0,0) (2,1,0)-FNN (2-2-1)
	ARIMA-RNN	ARIMA (1,0,0) (2,1,0)- RNN (2-10-1)
	FNN-ARIMA	FNN (6-2-1)- ARIMA (2,0,2) (1,1,1)

	RNN-ARIMA	RNN (6-5-1)-ARIMA (2,0,2) (1,1,1)
12-months	ARIMA	(1,0,0) (2,0,0)
	FNN	2-2-1
	RNN	2-7-1
	ARIMA-FNN	ARIMA (1,0,0) (2,0,0) – FNN (2-2-1)
	ARIMA-RNN	ARIMA (1,0,0) (2,0,0) – RNN (2-10-1)
	FNN-ARIMA	FNN (2-2-1)-ARIMA (0,0,0) (0,0,1)
	RNN-ARIMA	RNN (2-5-1) – ARIMA (5,1,0) (0,0,1)
24-months	ARIMA	(0,1,0) (1,0,2)
	FNN	2-9-1
	RNN	2-3-1
	ARIMA-FNN	ARIMA (2,1,0) (2,0,0)- FNN (2-2-1)
	ARIMA-RNN	ARIMA (2,1,0) (2,0,0)-RNN (2-10-1)
	FNN-ARIMA	FNN (2-9-1) – ARIMA (0,0,0)
	RNN-ARIMA	RNN (2-3-1) – ARIMA (1,0,1)

The NSPI is predicted for four different time scales using seven models: ARIMA, FNN, RNN, ARIMA-FNN, ARIMA-RNN, FNN-ARIMA, and RNN-ARIMA. The training and testing outcomes from the models were evaluated using various evaluation indicators, which are displayed in Table 4.5. Among the individual models, during both training and testing phases, FNN performed best at all the time scales, and the NSPI24 was the best-performing scale. Among the short-term drought index, NSPI6 and NSPI24 showed better performance for long-term drought. The ARIMA model performed better for short-term droughts than long-term droughts. The correlation coefficient of ARIMA during the test phase was 0.771 and 0.754 for 3 and 6 months scales. The correlation values were only 0.078 and 0.238 for 12 and 24 months scales.

Table 4.5 Evaluation indices obtained for each model at different time scales

Models	Training					Testing				
	CC	**R^2**	**MSE**	**MAE**	**RAE**	**CC**	**R^2**	**MSE**	**MAE**	**RAE**
					NSPI3					
ARIMA	0.843	0.701	0.292	0.408	0.486	0.771	0.532	0.446	0.490	0.578
FNN	***0.878***	***0.773***	***0.222***	***0.357***	***0.425***	***0.829***	***0.689***	***0.297***	***0.385***	***0.454***
RNN	0.866	0.746	0.223	0.384	0.451	0.834	0.646	0.301	0.391	0.462
ARIMA-FNN	0.867	0.744	0.250	0.378	0.450	0.756	0.410	0.562	0.574	0.677
ARIMA-RNN	0.850	0.836	0.253	0.401	0.481	0.752	0.550	0.601	0.647	0.681
FNN-ARIMA	**0.879**	**0.774**	**0.221**	**0.350**	**0.416**	**0.835**	**0.699**	**0.290**	**0.383**	**0.453**
RNN-ARIMA	0.855	0.729	0.265	0.387	0.460	0.815	0.663	0.320	0.424	0.500
					NSPI6					
ARIMA	0.857	0.729	0.292	0.385	0.459	0.754	0.509	0.517	0.555	0.644
FNN	***0.873***	***0.764***	***0.258***	***0.365***	***0.431***	***0.873***	***0.763***	***0.252***	***0.344***	***0.399***
RNN	0.861	0.739	0.299	0.371	0.456	0.867	0.739	0.292	0.379	0.443
ARIMA-FNN	0.867	0.749	0.272	0.381	0.452	0.792	0.588	0.434	0.500	0.580
ARIMA-RNN	0.870	0.754	0.268	0.374	0.444	0.791	0.600	0.421	0.492	0.570
FNN-ARIMA	**0.873**	**0.763**	**0.257**	**0.364**	**0.431**	0.873	0.761	0.252	0.343	0.397
RNN-ARIMA	0.862	0.744	0.285	0.3883	0.460	**0.894**	**0.789**	**0.210**	**0.336**	**0.389**
					NSPI12					
ARIMA	0.901	0.812	0.212	0.316	0.377	0.078	0.029	0.697	0.652	1.031
FNN	***0.903***	***0.828***	***0.206***	***0.316***	***0.375***	***0.838***	**0.*845***	***0.209***	***0.315***	***0.500***
RNN	0.894	0.797	0.211	0.355	0.394	0.832	0.797	0.214	0.320	0.508
ARIMA-FNN	0.903	0.808	0.217	0.316	0.376	0.236	0.232	0.836	0.745	1.170
ARIMA-RNN	0.901	0.805	0.221	0.320	0.381	0.192	0.250	0.549	0.750	1.187
FNN-ARIMA	**0.908**	**0.835**	**0.200**	**0.312**	**0.371**	**0.848**	0.715	**0.193**	**0.308**	**0.490**
RNN-ARIMA	0.890	0.789	0.241	0.348	0.413	0.821	0.645	0.241	0.346	0.549
					NSPI24					
ARIMA	0.942	0.885	0.136	0.263	0.308	0.238	0.406	0.436	0.847	0.678
FNN	***0.953***	***0.911***	***0.105***	***0.242***	***0.283***	***0.874***	***0.911***	***0.123***	***0.266***	***0.449***
RNN	0.929	0.857	0.106	0.245	0.354	0.850	0.857	0.152	0.327	0.455
ARIMA-FNN	0.941	0.884	0.136	0.252	0.299	0.147	0.402	0.442	0.540	0.487
ARIMA-RNN	0.942	0.884	0.139	0.269	0.310	0.213	0.224	0.402	0.785	0.489
FNN-ARIMA	**0.954**	**0.912**	**0.104**	**0.241**	**0.284**	**0.884**	0.758	**0.122**	**0.264**	**0.441**
RNN-ARIMA	0.934	0.868	0.155	0.290	0.342	0.851	0.719	0.138	0.260	0.457

Note: Bold and italics: best values among non-hybrid model; bold and shaded: best value among all models.

Considering all seven models, FNN-ARIMA was the best at 3 months (CC= 0.835, R^2 = 0.695, MSE = 0.290, MAE = 0.383, RAE = 0.453), 12 months (CC= 0.848, R^2 = 0.715, MSE = 0.193, MAE = 0.308, RAE = 0.490) and 24 months (CC= 0.864, R^2 = 0.758, MSE = 0.122, MAE = 0.264, RAE = 0.441) time scales during testing phase. Similarly, during the testing phase, the hybrid model RNN-ARIMA performed best only at 6 months (CC= 0.894, R^2 = 0.800, MSE = 0.210, MAE = 0.336, RAE = 0.389). The performance of hybrid models is observed to be better than non-hybrid models in most cases.

The observed and predicted index plots of the best standalone and hybrid models during the training and testing phases are shown in Figures 4.6 and 4.7. A better agreement between the predicted index and the observed index at all time scales can be achieved by the best-selected models during both phases. The best non-hybrid model was FNN at all time scales, whereas the best hybrid model was FNN-ARIMA for all time scales except for 6 months. The best hybrid model obtained at 6 months scale was RNN-ARIMA. The scatterplot for the training and testing phases of the best non-hybrid and hybrid models is depicted in Figure 4.8. The positive quadrant indicates the wet period, and the negative quadrant indicates the dry period. The R^2 value is greater than 0.6 in all cases, indicating a high precision in prediction. The scatterplot indicates a high degree of precision by the non-hybrid model (FNN) at the 24 months scale during training and testing, whereas the hybrid model performed best at the 6 and 24 months scales in the testing and training phases, respectively. At 3 and 6 months scales, the degree of correlation was higher for hybrid models than non-hybrid models during the testing phase. In every case, long-term droughts showed more precision in prediction than short-term droughts.

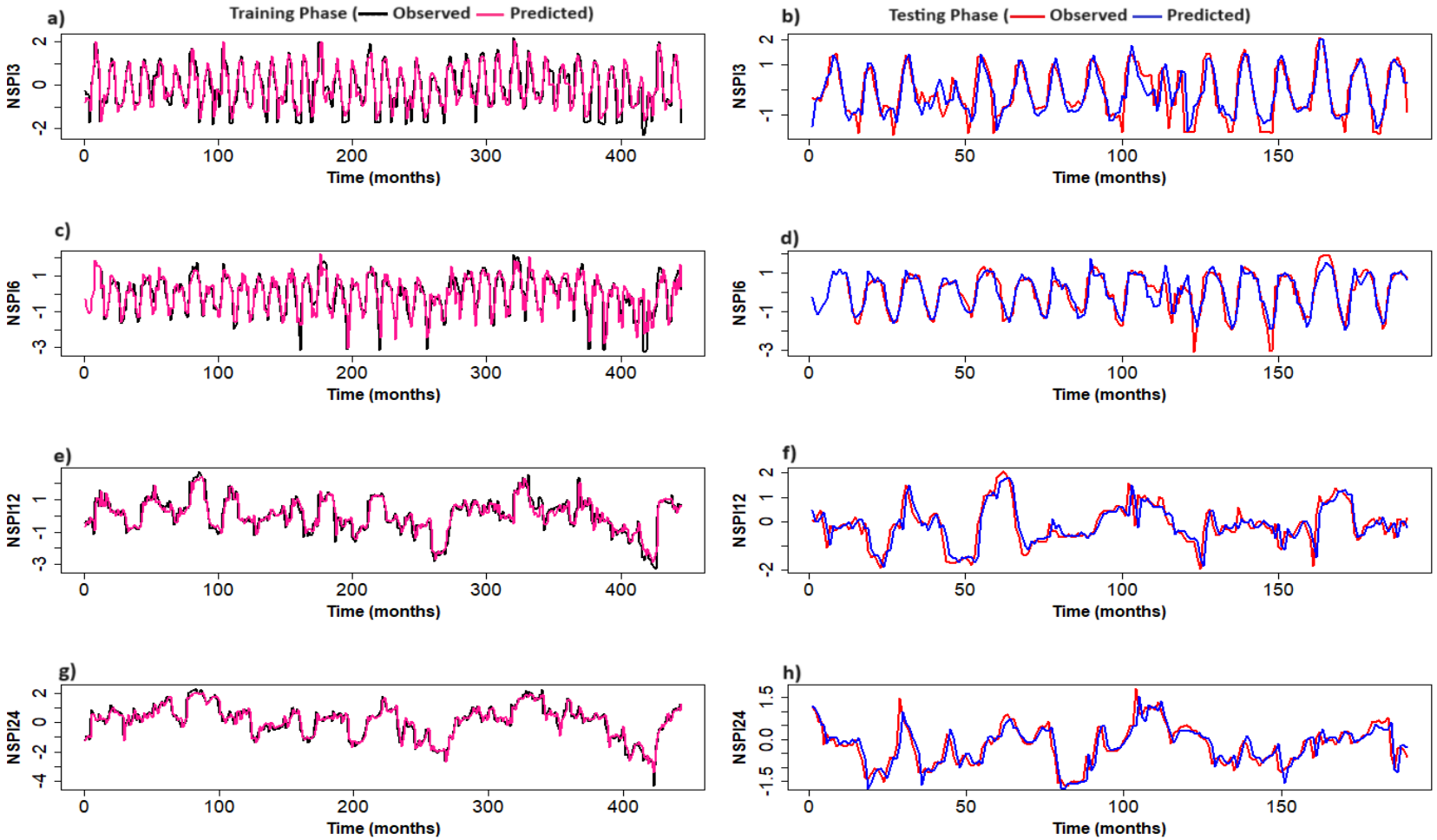

Figure 4.6. Observed and predicted Index using best standalone models

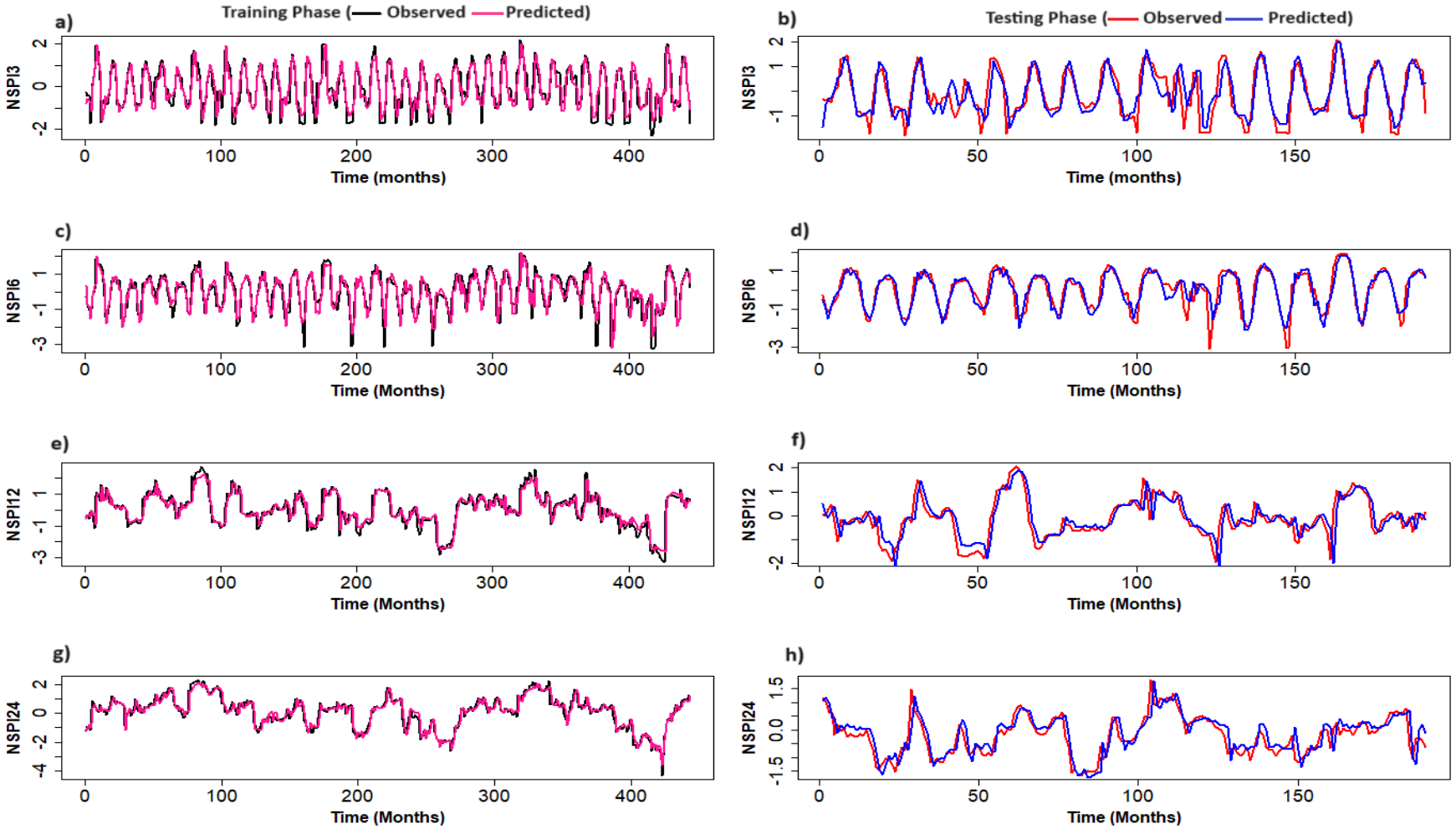

Figure 4.7. Observed and predicted Index using best hybrid models

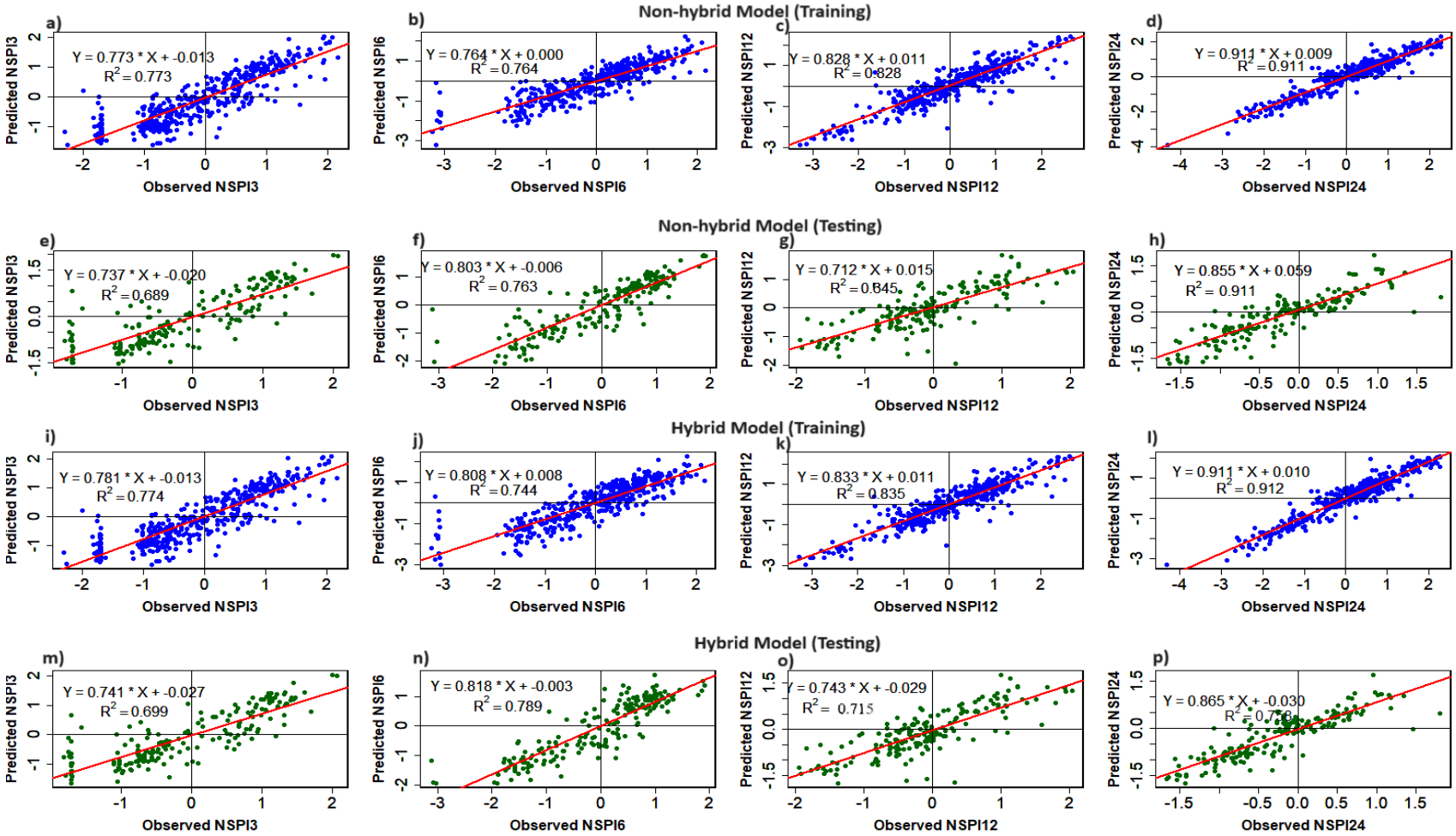

Figure 4.8. Scatterplot of best models

4.5 DISCUSSION

Appropriate model inputs are essential for improving the performance of neural network models. Significantly, little attention is given to this area by most Neural Network application problems (Maier and Dandy 2000). As per Bowden et al. (2005), input selection based on prior knowledge (Thirumalaiah and Deo 2000), linear cross-correlation (Silverman and Dracup 2000), stepwise selection methods (Tokar and Johnson 1999), sensitivity analysis (Schleiter et al. 1999) and combinations of different methods are commonly used approaches for input selection for ANN models. This research uses PACF, feed-forward, and backward methods to find optimum input lags. The results from PACF diagrams and stepwise methods are almost similar at every case. The lag 1 showed the most significant correlation at all the time scales. A similar observation can be found in Achite et al. (2023). One of the main limitations of the ARIMA model is the pre-assumption of the linear form of the data and its modeling (Aladag et al. 2012). Sometimes, real-world time series data are non-linear, so the accuracy of the results of ARIMA is questionable. There comes the importance of hybrid models. Time series prediction by hybrid ARIMA and Neural Network models outperformed the standalone models in various studies (Kaytez, 2020; Moeeni and Bonakdari, 2017; Mousavi-Mirkalaei and Banihabib, 2019; Phesa et al. 2023; Singh et al. 2019). In this research also, the best-selected model is the hybrid model. The result in Table 4.5 is represented graphically in Figures 4.9 and 4.10 for the training and testing phases, respectively. A superior performance of the FNN-ARIMA model is observed at all time scales for training and testing data sets except at a 6 months time scale. At 6 months, FNN-ARIMA was best at only the training phase, and for the testing phase, RNN-ARIMA was superior with a slight variation from FNN-ARIMA. MAE, MSE, and RAE are prediction errors. From Figures 4.9 and 4.10, the slope of prediction errors varies almost similarly in every case, ensuring that the model's predictions are reliable and consistent across diverse scenarios. For the training data set, the R^2 and CC values did not fall below 0.6 at all scales, which suggests that the models are robust and reliable in their predictive capabilities during the training phase. However, for the testing data set, CC and R^2 values of only NN and NN-ARIMA models did not fall below 0.6 at all scales.

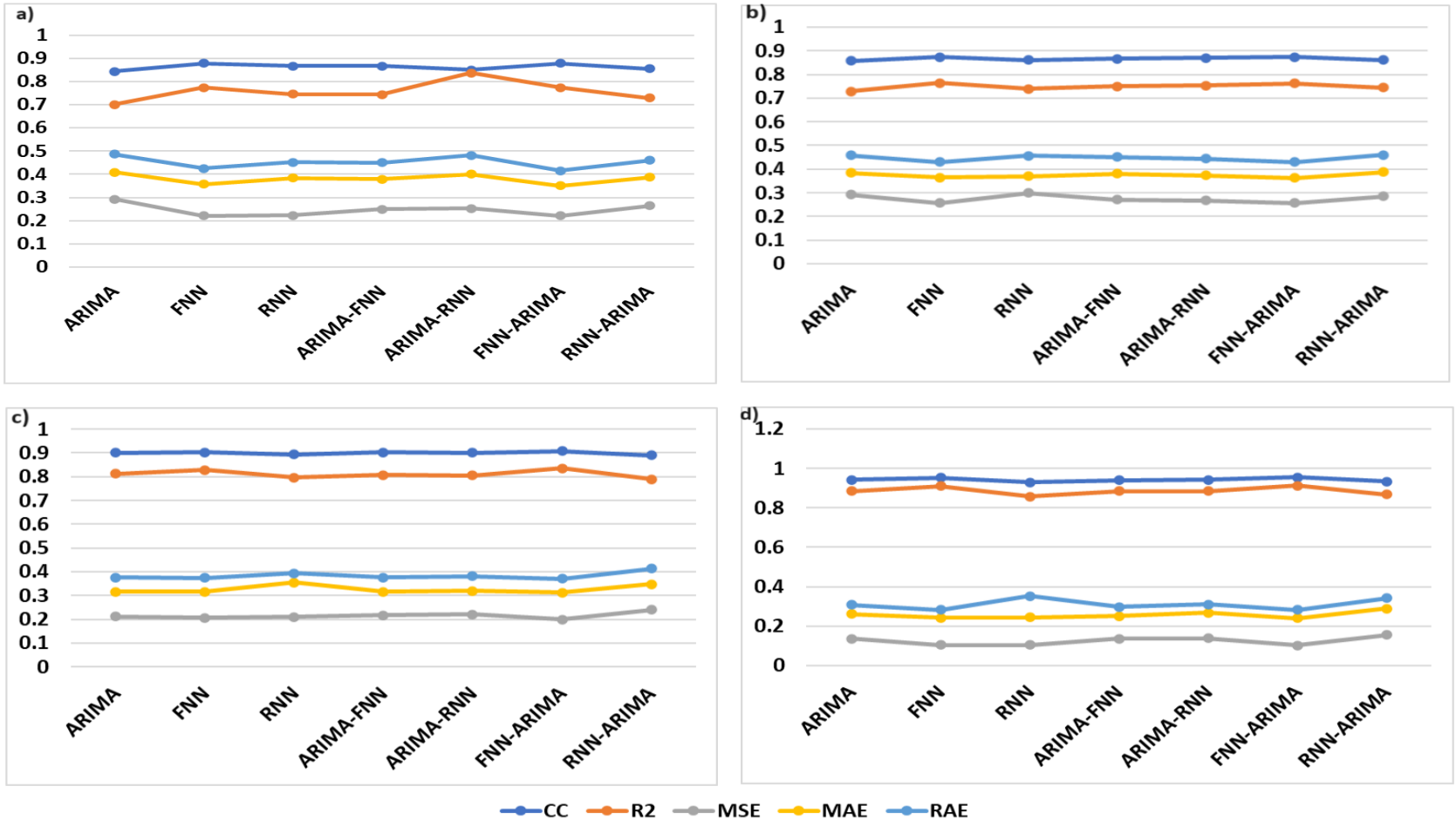

Figure 4.9. Comparison of evaluation indicators in training phase

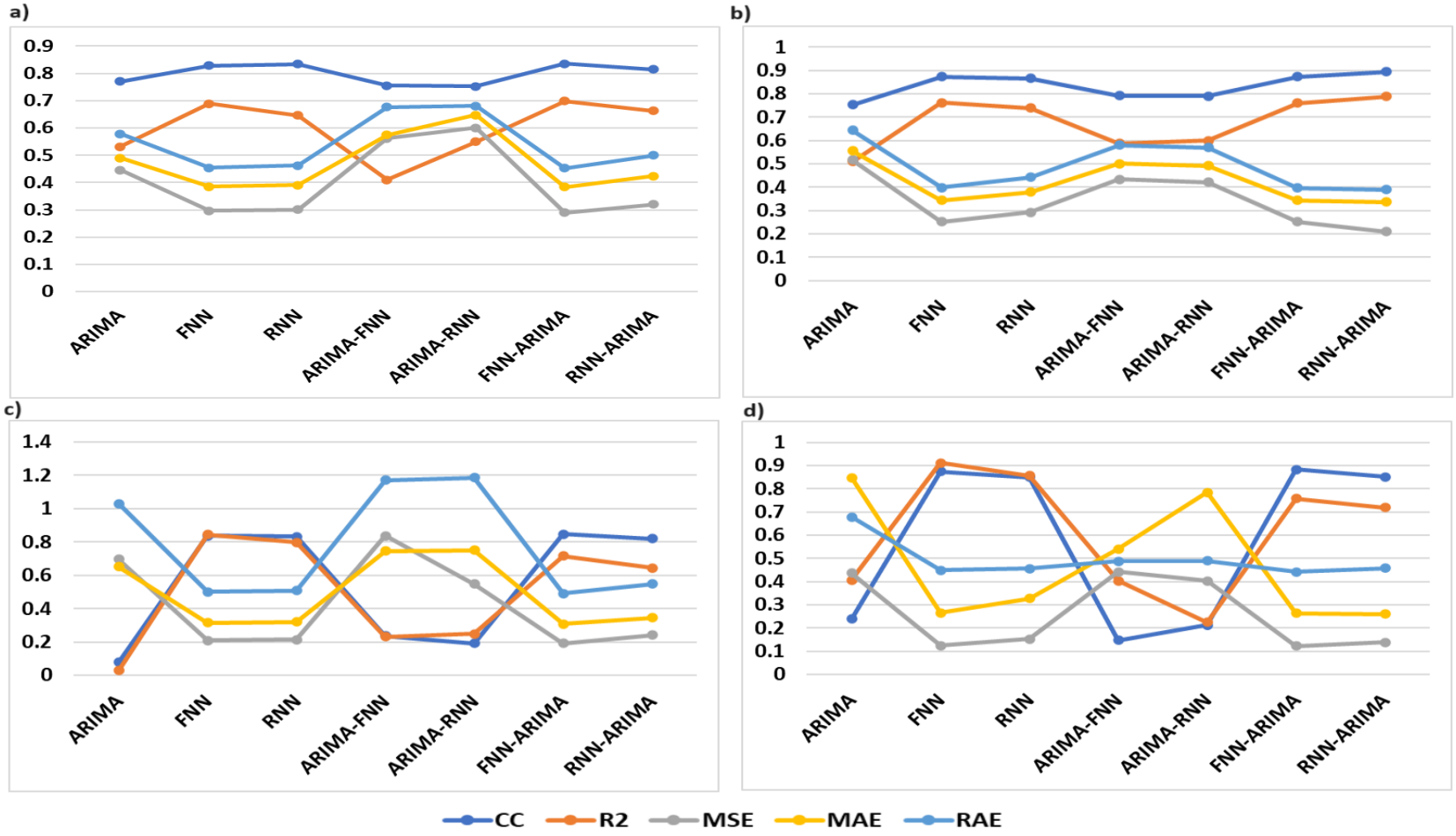

Figure 4.10. Comparison of evaluation indicators in testing phase

Considering standalone models, FNN is superior to other models, such as RNN and ARIMA. It was obvious that the NN model could perform better than statistical models. Prybutok et al. (2000) also observed superior performance of neural network models over ARIMA and regression in ozone forecasting problems. Paing et al. (2023) observed that FNN and RNN could perform well at time series forecasting. In this research, the performance of FNN and RNN was better than that of the ARIMA model in all cases. The superior performance of FNN-ARIMA models reveals that it can effectively leverage the strengths of both linear and nonlinear modeling approaches.

4.6 CLOSURE

Three standalone models, such as the statistical model ARIMA, and Neural Network models, such as FNN and RNN, are used to predict the drought index in Saurashtra and Kutch, in India, at different time scales (3, 6, 12, and 24 months). FNN produced more accurate results than the other two models at all the scales. The performance of the hybrid combination of ARIMA with FNN and RNN in drought prediction is also examined with the same data due to the strong ability of the hybrid model to deal with mixed patterns, which exhibited outstanding performance in prediction compared to standalone models in most cases. The findings from this research suggest that FNN-ARIMA can be used to forecast the drought index in semi-arid regions. Among the seven models considered, FNN-ARIMA performed best at all the time scales except at 6 months. Machine Learning models like FNN and RNN are more effective in drought forecasting than statistical models like ARIMA. The hybrid models outperformed the non-hybrid models in most cases. Hence, the nonlinear-linear hybrid models can be used as reliable models to obtain accurate results for drought prediction in semi-arid regions. The findings from this study will be helpful for disaster management and agriculture departments in the early prediction of drought in order to plan necessary actions to reduce the effect of drought in various fields.

CHAPTER 5

COMPARATIVE STUDY OF METEOROLOGICAL AND HYDROLOGICAL DROUGHTS

5.1 GENERAL

Droughts are recurring natural phenomena with profound societal, ecological, and economic impacts (Mishra and Singh 2010). Studies indicate that in the coming decades, there will be a likely increase in both the severity and frequency of drought risks (Li et al. 2013; Wang et al. 2015a). Diverse indices such as Palmer Drought Severity Index (PDSI) (Palmer 1965), Reconnaissance Drought Index (RDI) (Tigkas et al. 2012), Standardized Precipitation Evapotranspiration Index (SPEI) (Wang et al. 2020b), Standardized Precipitation Index (SPI) (McKee et al.1993) have been used based on study area and data availability. The present research uses the Standardized Precipitation Index (SPI) and Standardized Streamflow Drought Index (SSI) to distinguish meteorological and hydrological droughts, respectively.

Assessing and understanding drought patterns hold critical importance in regions facing water scarcity, such as semi-arid basins (Ganguli and Reddy 2012; Sajeev et al. 2021). In this context, the evaluation of drought indices, both stationary and non-stationary, emerges as a vital component of effective drought monitoring and management strategies. Hence, the main goal of this research is to assess non-stationary drought indices in the Shetrunji River basin, Gujarat, considering the influence of large-scale climate covariates, including ENSO, IOD, NAO, AO, PDO, and AMO. Limited drought studies explored the nonstationary scale and location parameters of the distribution. The models under consideration consist of three types: the stationary model, denoted as M0; the non-stationary model, which includes a changing location parameter referred to as M1; and the non-stationary model with both changing location and scale parameters (M2). It provides a comprehensive understanding of interactions between climate oscillations and two types of droughts, meteorological and hydrological, over a multi-decadal time frame from 1971 to 2015. The results are compared with historical drought and flood events. The excessive and deficient rainfall and streamflow are

identified within the study area by analysing the percentage departure of annual and seasonal data. These identified rainfall patterns will also serve as a basis for evaluating and comparing the performance of the non-stationary drought indices in capturing meteorological anomalies associated with droughts and floods. Most of the previous researchers considered only Gamma distribution for the non-stationary drought index calculation (Li et al. 2015; Das et al. 2020). Therefore, this research considers various marginal distributions, including exponential, gamma, lognormal, logistic, normal, and weibull distributions. The best-fitted distributions to rainfall and streamflow values at different time scales are taken for index calculation.

Another objective is to compare meteorological and hydrological droughts using non-stationary indices to better understand the dynamic relationships between these two droughts within a changing climate based on correlation, lag, and response rate analysis. Furthermore, this research aims to investigate the distinct responses of the rabi and kharif crops to meteorological and hydrological droughts within a non-stationary scenario. This research aims to improve the comprehension of drought patterns within the Shetrunji River basin and contribute valuable insights into the complex interactions between climate indices, meteorological and hydrological droughts, and agricultural seasons in a changing climate context. Results can be used by various sectors, such as disaster management and agricultural departments, to monitor the drought and mitigate its adverse impact on crop yields across seasons.

5.2 STUDY AREA AND DATA

5.2.1 Overview of Shetrunji River Basin

The study area is the Shetrunji River basin in the Saurashtra region of Gujarat. It is located between 21º 10′ N to 21º 52′ N latitudes and 70º 49′ E to 71º 37′ E longitudes. Figure 5.1 shows the map of the study area.

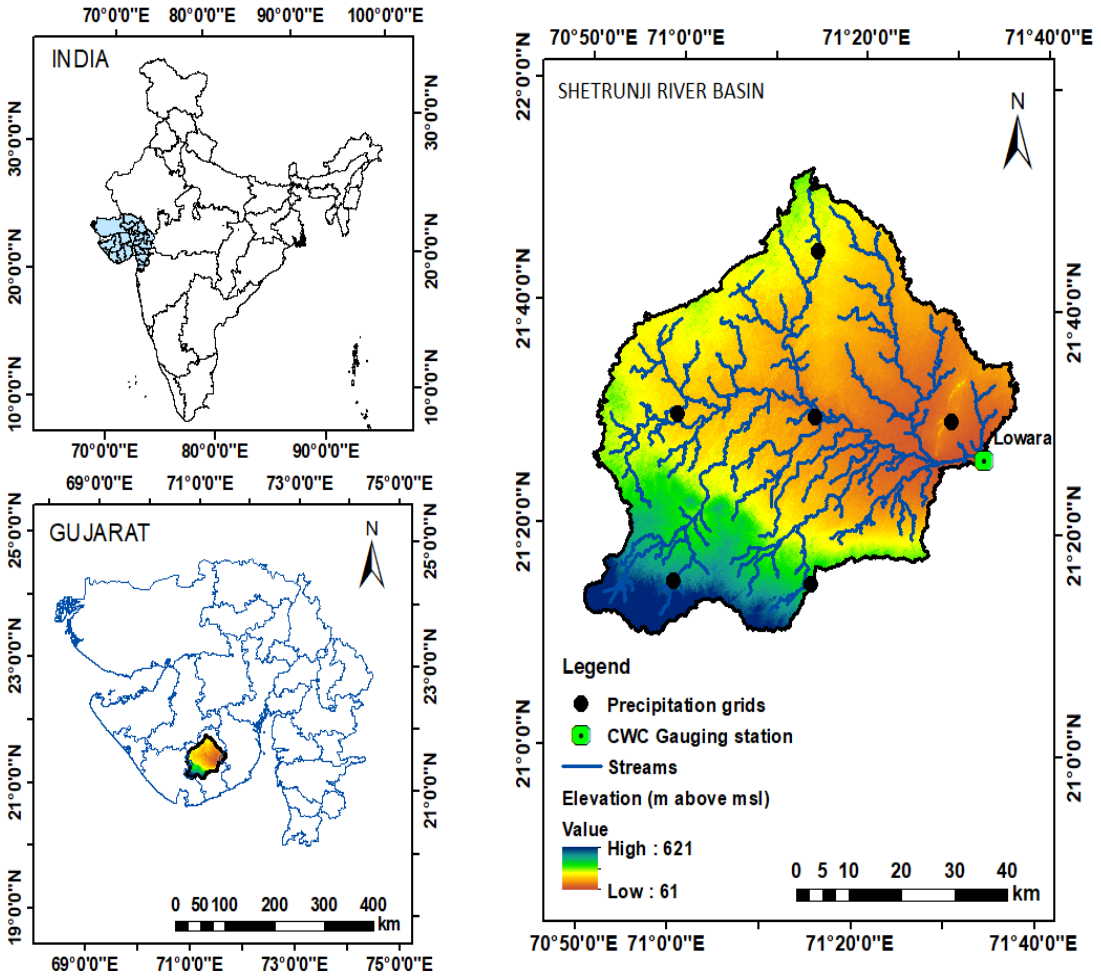

Figure 5.1. Study area

This area receives an average rainfall of 604.52mm, and 90 percent of total rainfall is received in July and August. The month of May is the warmest, with maximum monthly temperatures ranging from 30°C to 44°C, and January is the coldest, with mean monthly temperatures between 14.5°C and 20°C. The study region under consideration spans an area of approximately 3678.33 km^2 and extends until the CWC (Central Water Commission, India) gauging station in Lowara. Shetrunji originates about 380 meters above sea level in the Chchai Hills, Gir Forest in Junagadh District. It then runs eastward until it meets the Gulf of Khambhat near Santrampur Port. Köppen climate classification, developed by German botanist-climatologist Wladimir Köppen, is a widely used classification system in numerous studies (Muthuvel and Mahesha 2021; Sajeev et al. 2021). As per Köppen's categorization of climatic zones, the Kutch region

is classified as a hot desert arid (BWh) zone, and the Saurashtra region is a hot semi-arid (BSh) zone (Beck et al. 2018). Hence, the Shetrunji River basin is situated in a hot semi-arid zone. For the present drought impact study, bajra and wheat crops are considered.

5.2.2 Data Used

Daily gridded rainfall data with a spatial resolution of $0.25° \times 0.25°$ (6 grid points) covering the period from 1971 to 2015 were obtained from the India Meteorological Department (IMD), Pune (Pai et al. 2014). Monthly streamflow data for the Shetrunji River basin were sourced from the Water Resources Information System, India. This data pertains to the Lowara River gauging station observations from 1971 to 2015. Information regarding the productivity of bajra and wheat from 1971 to 2015 was sourced from the Directorate of Economics and Statistics of Gujarat (Kothawale and Rajeevan 2017). The drought index computation is carried out by using climate indices such as Indian Ocean Dipole (IOD)(DMI 2023), Southern Oscillation Index (SOI)(SOI 2020), Multivariate ENSO Index (MEI)(MEI 2018), Sea Surface Temperature (SST) (SST 2020), Atlantic Multi-decadal Oscillation (AMO)(AMO. 2023), Arctic Oscillation (AO)(AO 2023), Northern Atlantic Oscillation (NAO) (NAO 2023) and Pacific Decadal Oscillation (PDO)(PDO 2023). All the climate indices were collected from 1971 to 2015.

5.3 METHODOLOGY

The flow chart of the methodology is shown in Figure 5.2. In the current research, the meteorological drought analysis employs the Standardized Precipitation Index (SPI), while hydrological drought is assessed using the Standardized Streamflow Index (SSI). A drought episode is a consecutive month during which the values of the drought indices remain consistently below a threshold of -1 (McKee et al.1993).

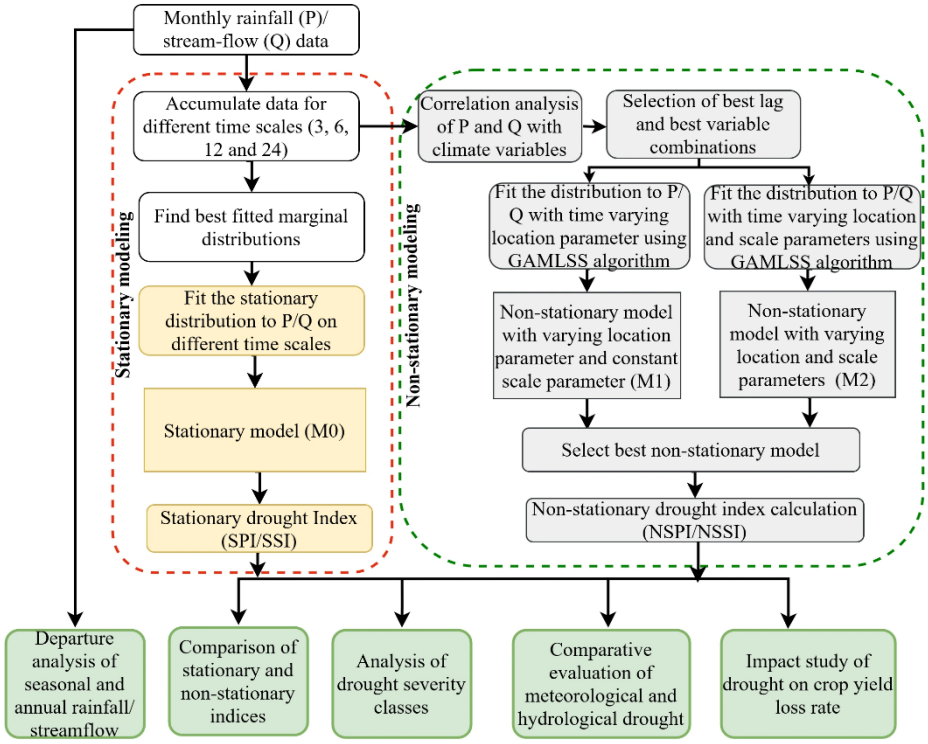

Figure 5.2. Methodology flowchart

5.3.1 Percentage Departure of Rainfall and Streamflow

Years characterized by deficient or excessive rainfall and streamflow can be assessed using departure analysis. This approach examines the deviation of precipitation and streamflow values from their long-term averages. Analysing departures from the long-term mean provides valuable insights into the behaviour of these variables compared to their historical averages. The yearly and seasonal deviations of precipitation and streamflow can be computed using equation (5.1).

$$\text{Departure}\ (\%) = \frac{x_i - \overline{x}_i}{\overline{x}_i} \times 100 \tag{5.1}$$

Here x_i represents the precipitation or streamflow value for a specific year or season. $\overline{x}_i$ is the average precipitation or streamflow over the considered time.

5.3.2 Computation of drought Index

This research defines meteorological drought using SPI, while SSI characterizes hydrological drought. Drought indices are calculated for 3, 6, 12, and 24 months time scales. The SPI is a widely used meteorological drought index developed by McKee et al. (1993). It gives a standardized measure of precipitation anomalies over different time scales, allowing for the assessment of dry and wet periods. The index is particularly useful because it accounts for short-term and long-term precipitation deficits. Using different time scales, the SPI can provide insights into different aspects of drought, ranging from rapidly evolving short-term droughts to more prolonged and slowly developing drought events (McKee et al.1993; Patel et al. 2007). The computation of SPI is given below, considering the Gamma distribution as the best fit. It involves fitting a two-parameter gamma distribution to the cumulative precipitation data over different time intervals. The PDF of the gamma distribution is expressed as follows, relying on the shape and scale parameters:

$$g(x) = \frac{1}{\beta^{\alpha}\,\Gamma(\alpha)}\, x^{\alpha-1}\, \mathrm{e}^{\frac{-x}{\beta}} \tag{5.2}$$

In this formula, $g(x)$ stands for the PDF of the distribution at the value x, with shape parameter α and scale parameter β. Construct the cumulative distribution function (CDF) based on the PDF obtained in the previous step. The cumulative distribution values obtained from the gamma distribution are converted to values following a standard normal distribution with zero mean and unit standard deviation. This transformation involves using the inverse cumulative distribution function of the standard normal distribution. The transformed values are the SPI values, and the equation is given as:

$$SPI = \psi^{-1}(F(x)) \tag{5.3}$$

where ψ^{-1} is the inverse of cumulative standard normal distribution.

Positive SPI values indicate drier conditions (below-average precipitation), while negative SPI values indicate wetter conditions (above-average precipitation). The

researchers derived an index for hydrological drought similar to meteorological ones. This research employed the Standardized Streamflow Index (SSI) as a hydrological drought indicator. The SSI is computed using a process similar to the Standardized Precipitation Index (SPI). The key distinction is that stream flow data is utilized as the input instead of precipitation data. The classification of the dry and wet conditions based on indices (SPI, NSPI, SSI, and NSSI) is outlined in Table 3.2.

5.3.3 Non-stationary modeling using GAMLSS

Large-scale climate oscillations such as Southern Oscillation Index (SOI), Sea Surface Temperature (SST), Multivariate ENSO Index (MEI), Indian Ocean Dipole (IOD), Atlantic Multi-decadal Oscillation (AMO), Arctic Oscillation (AO), Northern Atlantic Oscillation (NAO) and Pacific Decadal Oscillation (PDO) are considered for this research. For non-stationary modeling, Generalized Additive Models for Location, Scale, and Shape (GAMLSS) are used and developed by Rigby and Stasinopoulos (2005). GAMLSS has gained widespread adoption across a range of hydrological applications. Notable examples include its utilization in tasks like rainfall downscaling (Rashid et al. 2016), assessment of frequency of flood, and drought assessment (Bazrafshan and Hejabi 2018; Garcia Galiano et al. 2015; Yu and Kim 2019). In a study by Debele et al. (2017b), a comparative investigation was carried out involving the two-stage method, the Maximum Likelihood (ML) approach, and the Generalized Additive Models in Location, Scale, and Shape (GAMLSS) methodology. The aim was to identify time-dependent moments within a non-stationary framework. The study concluded that GAMLSS performed better than the other two methods. In the context of GAMLSS analysis, the response variables of datasets, denoted as y_i for i varies from 1 to n are assumed to be independent. These response variables are then fitted using a distribution function $F_y(y_i;\ \theta_i)$, where $\theta_i = (\theta_{1i}, \theta_{2i}, \theta_{3i}, \theta_{4i})$ represents distinct statistical parameters. These parameters encompass properties such as location, scale, shape, and kurtosis. To achieve this, a set of monotonic link functions, denoted as $g_k(.)$, is employed. Here, k signifies the various distribution parameters to the design matrix of the covariate. These monotonic link functions are used in the GAMLSS approach to efficiently link the explanatory variables and distribution parameters. This relationship can be succinctly represented as follows:

$$g_k(\theta_k) = \eta_k = X_k \beta_k + \sum_{j=1}^{m} Z_{jk}(x_{jk}) \tag{5.4}$$

Where, θ_k is a vector with the same size of the data set, and the length equal to n; β_k is a parameter having length m; X_k is the matrix of explanatory variables; Z_{jk} is a nonparametric additive function. The non-stationary distribution (for example, non-stationary gamma) is fitted to cumulative rainfall or streamflow. This modeling involves incorporating linear combinations of the previously mentioned covariates into the distribution parameters. Among the various models constructed using different combinations of covariates, the model that best fits the data is determined using the Akaike Information Criterion (AIC). The optimal model with only varying location parameters derived from the non-stationary analysis takes the form as outlined below:

$$X_t \sim \ gamma \ (\mu_t, \ \sigma) \tag{5.5}$$

$$\mu_t = c_0 + c_1 I_1(t) + c_2 I_2(t) ..... + c_n I_n(t) \tag{5.6}$$

where, $c_0, c_1, .., c_n$ are constants and, at the time t, $I_1, I_2, .., I_n$ are the covariates. A similar equation can also be derived for scale parameters for model 2. The model parameters are computed by maximizing the likelihood using a method known as the Rigby and Stasinopoulos (RS) algorithm. This algorithm has been identified as particularly efficient, especially when dealing with extensive datasets.

5.3.4 Evaluation criteria for indices comparison

In this research, the evaluation indices were conducted using the Pearson correlation coefficient and the crossover correlation function, as detailed in the work by Salimi et al. (2021). The coefficient of determination was also employed to assess the effectiveness of mathematical relationships between these indices. The equations of the accuracy indices are presented in Table 5.1.

Table 5.1 Equations of the accuracy indices

Index	Equations	Range
Pearson correlation coefficient	$R=\frac{\left(\sum_{i=1}^{t}\left(x_i y_i\right)\right)-\left(\sum_{i=1}^{t} x_i\right)\left(\sum_{i=1}^{t} y_i\right)}{\sqrt{\left[n\left(\sum_{i=1}^{t}\left(x_i^2\right)\right)-\left(\sum_{i=1}^{t} x_i\right)^2\right]\left[n\left(\sum_{i=1}^{t} y_i^2\right)-\left(\sum_{i=1}^{t} y_i\right)^2\right]}}$	$-1 \le R \le +1$
Crossover correlation function	$R=\frac{\sum_{i}^{n=1}\left(x_i-\bar{x}\right)\left(y_{(i-d)}-\bar{y}\right)}{\sqrt{\sum_{i}^{n=1}\left(x_i-\bar{x}\right)}\sqrt{\sum_{i}^{n=1}\left(x_i-\bar{x}\right)}\sqrt{\sum_{i}^{n=1}\left(y_{(i-d)}-\bar{y}\right)^2}}$	$-1 \le R \le +1$
R^2	$R^2=\left[\frac{\sum_{N}^{I=1}\left(x_i-\bar{x}\right)\left(y_i-\bar{y}\right)}{\sqrt{\sum_{N}^{I=1}\left(x_i-\bar{x}\right)^2\left(\sum_{N}^{I=1}\left(y_i-\bar{y}\right)\right)^2}}\right]^2$	$0 \le R^2 \le +1$

Where, x_i and y_i are two variables. $\bar{x}$ and $\bar{y}$ are corresponding mean of sample size N.

5.3.5 The Response Rate of Hydrological to Meteorological Drought

In this research, the response rate (R_r) was employed to quantify the proportion of instances when hydrological dry and wet periods coincide with meteorological dry and wet events. This metric serves as an indicator of how streamflow reacts to varying time scales of meteorological drought (Zhao et al. 2016b). A higher value of R_r implies a higher proportion of times when hydrological drought conditions align with meteorological drought conditions. It suggests a stronger or more sensitive response of

hydrological drought to changes in precipitation deficits. Conversely, a lower value indicates a lower proportion of alignment between meteorological and hydrological drought conditions, implying a less sensitive response.

The specific procedure for calculating R_r is provided by equation (5.7):

$$R_r = \frac{n}{m} \times 100\% \tag{5.7}$$

Where m denotes the frequency of occurrences of dry periods identified by the meteorological drought index (SPI < 0) between 1971 and 2015. n denotes the frequency of occurrences of dry periods according to the streamflow drought index (SSI < 0) under the condition that SPI is less than 0. Each instance of n signifies a concurrent occurrence of meteorological and hydrological drought. Similarly, for wet periods, instances where indices are above zero are considered. This indicator gives valuable insights into the interconnected nature of these phenomena and their implications for water resource management and drought monitoring.

5.3.6 Yield Loss Rate

Several factors influence crop yield, including climate, variety choice, and appropriate fertilizer use. However, extreme weather conditions, like heatwaves, droughts, and floods, contribute significantly to a decrease in yield (Ghazaryan et al. 2020; Wang et al. 2020). This rate is measured by comparing the rate of yield loss in a particular year to the greatest yield recorded in the five years prior, and it is given below:

$$Y_l = \frac{Y_i - Y_m}{Y_m} \times 100 \tag{5.8}$$

Here Y_i is the yield achieved in the year i. Y_m is the highest yield achieved among the last five years and Y_l is the yield loss rate in the given year.

5.4 RESULTS

5.4.1 Departure analysis of streamflow and rainfall

Figure 5.3 displays the annual and seasonal departure of streamflow, while Figure 5.4 illustrates the same for rainfall. As per the India Meteorological Department (IMD), a region is classified as being in a meteorological drought when its monsoon rainfall deficit surpasses the standard level (Thomas and Prasannakumar 2016). Therefore, this study defines a year as experiencing drought if its seasonal or annual deficit is equal to or greater than -25%. The yearly deficit follows a nearly identical seasonal pattern, suggesting that monsoon rainfall primarily influences drought occurrences. This same pattern is noticeable in the trend of annual streamflow as well. According to Figure 5.3, the maximum deficit values in annual and seasonal streamflow occurred in 1972, 1987, 1999, 2000, 2001, and 2003, reaching as low as -99.90%. A sustained deficit exceeding -25% for multiple years in the streamflow data indicates prolonged and severe drought conditions within the basin. Based on the streamflow departure analysis, the drought years are identified as follows: 1972-1978, 1981-1993, 1995-1997, 1999-2004, 2008-2009, 2012-2013, and 2015. The highest deficits in annual and seasonal rainfall departure were recorded in 1971 (-73.25%) and 1987 (-72.39%), respectively. The years characterized by drought, as determined from the analysis of rainfall departure, include 1971, 1974-1975, 1978, 1984-1987, 1991, 1995-1996, 1999-2000, 2004, and 2012. From the Kendall correlation analysis at a 5% significance level, a significant correlation of 0.27 is identified between the annual departure of streamflow and rainfall within the basin. In this case, the positive value of 0.27 suggests a moderate positive correlation between annual streamflow departure and annual rainfall departure in the basin. It means that as one of these variables increases (or decreases), the other tends to increase (or decrease), although the correlation is not very strong. The significance level of 5% suggests that the observed correlation is statistically significant, indicating that it is unlikely to have occurred due to random chance. However, the strength of the correlation being moderate means that while there is an association, other factors might also contribute to the variability observed in these two variables.

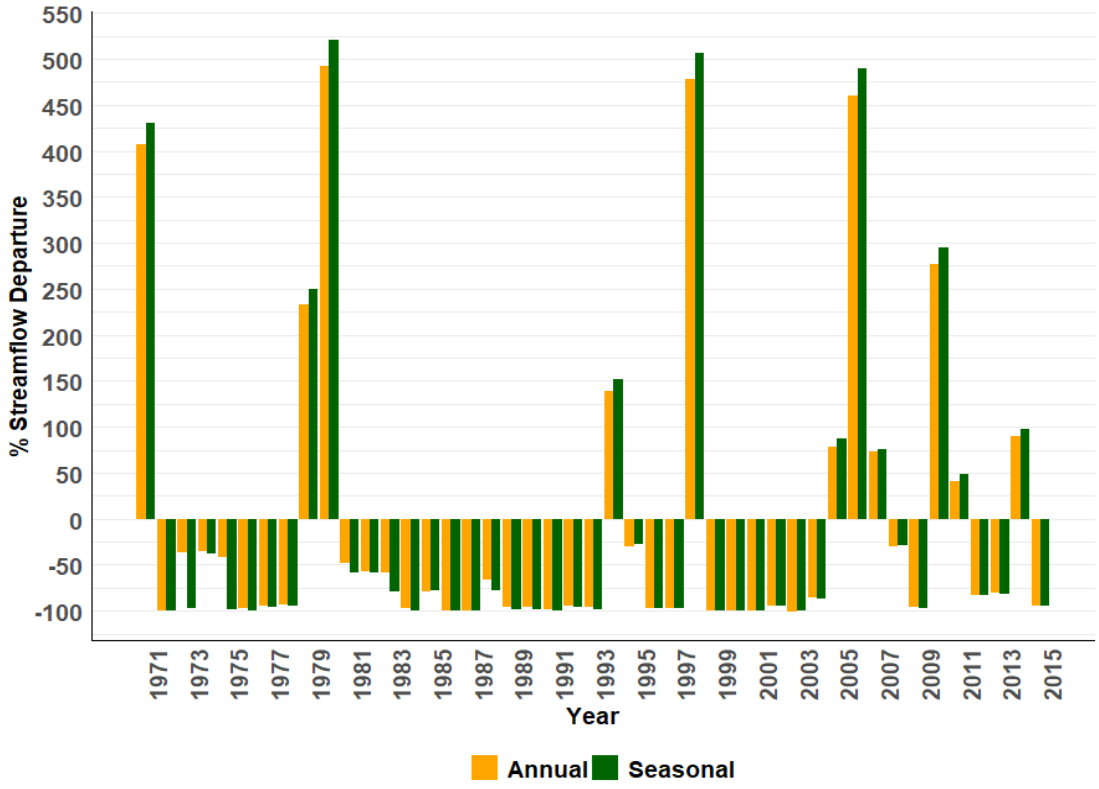

Figure 5.3. Annual and seasonal departure of streamflow

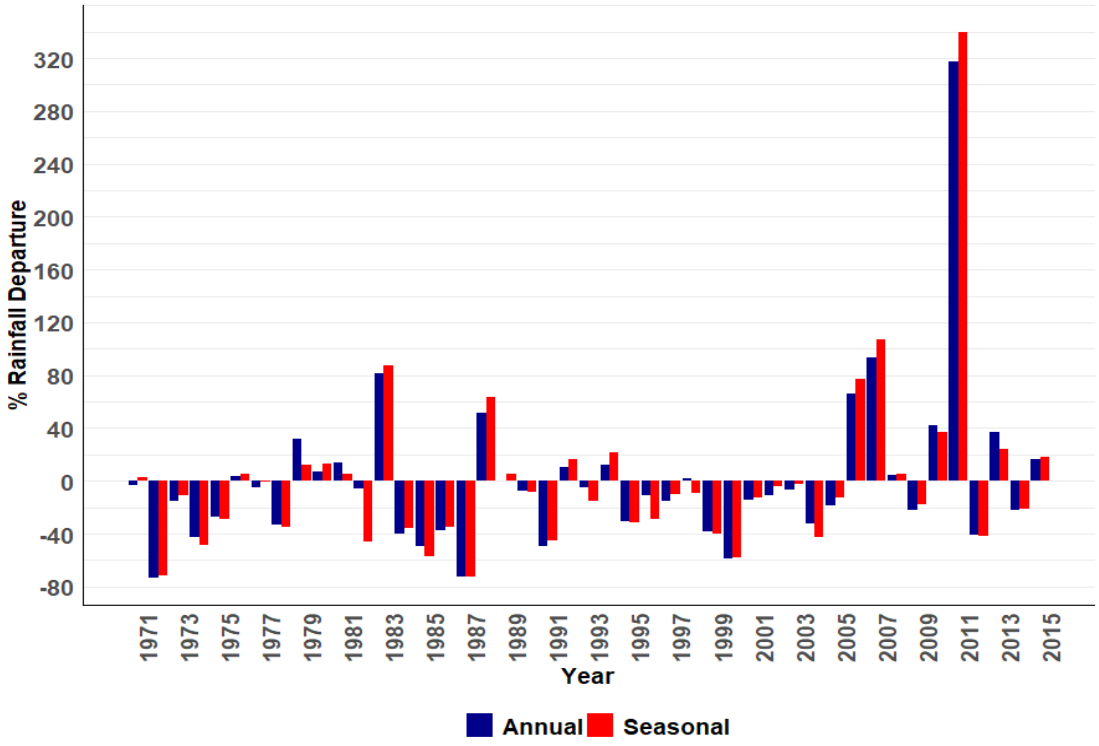

Figure 5.4. Annual and seasonal departure of rainfall

5.4.2 Fitting to the marginal distribution

Cumulative streamflow and rainfall data were subjected to fitting with various marginal distributions, including exponential, gamma, lognormal, logistic, normal, and weibull distributions. The selection of the most suitable distributions at each time scale is determined using the AIC (Akaike Information Criterion) and BIC (Bayesian Information Criterion) criteria, widely used statistical measures for model selection. The AIC and BIC values for streamflow and rainfall are visually represented in Figures 5.5 and 5.6, respectively.

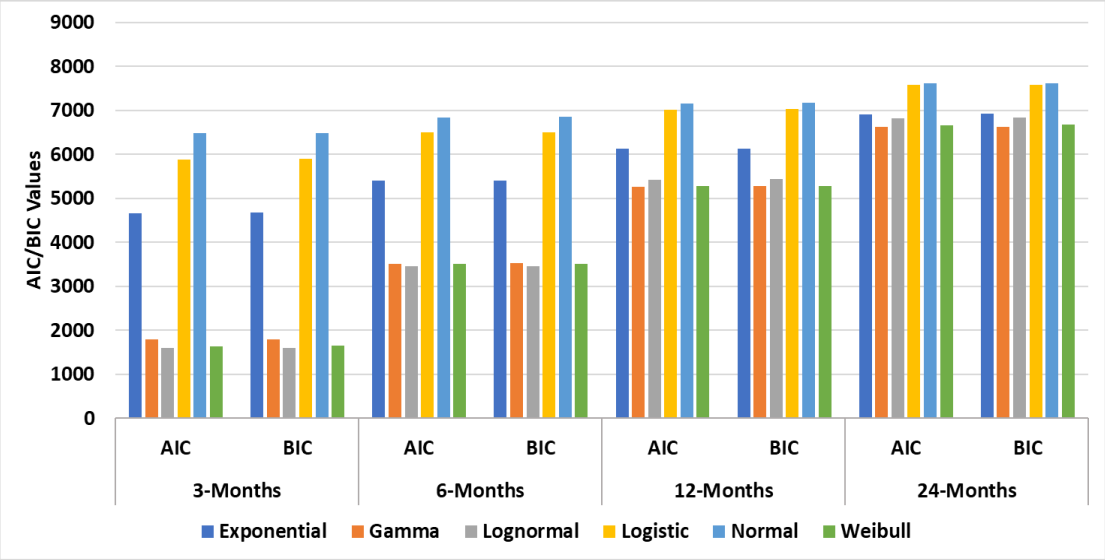

Figure 5.5. AIC and BIC values of marginal distribution for streamflow

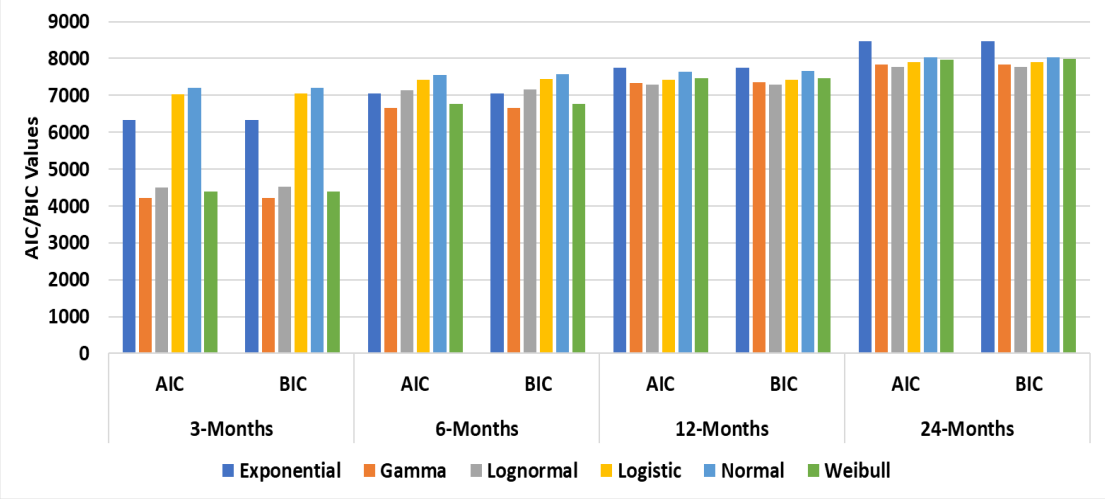

Figure 5.6. AIC and BIC values of marginal distribution for rainfall

In the case of streamflow data, the lognormal distribution was found to be the most suitable fit for the 3 and 6 months time scales. On the other hand, the gamma distribution was chosen as the best-fit model for streamflow at the 12 and 24 months time scales. The gamma distribution was selected for precipitation data as the optimal fit for the 3 and 6 months time scales. However, the lognormal distribution was identified as the most appropriate fit when considering precipitation at the 12 and 24 months time scales. These findings suggest that different distribution models are required to accurately describe the behavior of streamflow and rainfall data at varying time scales, emphasizing the significance of considering the appropriate distribution for each context.

5.4.3 Covariates selection

In this research, the areal monthly average rainfall data were derived from the India Meteorological Department (IMD) dataset using the Thiessen polygon method. From the accumulated monthly streamflow and rainfall data, cumulative values were then calculated for various periods (3, 6, 12, and 24 months). For the analysis of climate indices, they were arranged in a sequence with lags ranging from 0 to 12 months. The goal was to determine the most suitable lag for each climate index using the Kendall correlation method. This method helps in assessing the strength and significance of the relationship between variables. The lag value that exhibited a significant correlation with the precipitation and streamflow series was identified as the best lag for each climate index. The findings are shown in Table 5.2.

Table 5.2 Significant lag of climate indices for different time scale

Climate Indices	SST	SOI	MEI	IOD	AMO	AO	NAO	PDO
Time scale	Streamflow							
3-months	12	11	12	1	1	7	2	4
6-months	12	0	0	4	3	8	3	0
12-months	4	4	3	12	6	11	8	1
24-months	1	1	0	8	12	8	8	0
Time scale	Rainfall							
3-months	12	12	12	0	1	-	12	3
6-months	12	12	0	2	3	-	2	5
12-months	3	4	12	0	12	3	12	12
24-months	-	-	-	0	12	-	-	-

The results highlight that all the indices have a notable impact at various time lags across different time scales for streamflow data. At the 6 months time scale, the SOI, MEI, and PDO exhibit concurrent relationships (zero lag) with streamflow. A similar association of MEI and PDO with streamflow is observed at the 24 months scale. The Arctic Oscillation (AO) demonstrates a significant correlation with precipitation solely at the 12 months time scale. At the 24 months time scale, only the Indian Ocean Dipole (IOD) and Atlantic Multi-decadal Oscillation (AMO) show significant correlations with precipitation. This information is valuable in understanding the complex interactions between climate indices and hydrological variables.

5.4.4 Comparative analysis of Stationary and Non-stationary drought indices

The Akaike Information Criterion (AIC) values were examined for various combinations of covariates derived from the chosen lag values of climate indices. The combination of covariates yielding the lowest AIC was designated as the optimal choice for the non-stationary models (M1 and M2), and these selected combinations are detailed in Table 5.3.

Table 5.3 Best combination of covariates for Streamflow and Rainfall

Time Scale	Stream flow	
	For Mu	**For Sigma**
3-months	SST, MEI, IOD, NAO, PDO	SST, AMO
6-months	SST, SOI, MEI, IOD, AMO, NAO, PDO	SST, SOI, IOD, AMO, AO
12-months	SST, AMO, NAO, PDO	MEI, AMO, PDO
24-months	MEI, IOD, AMO, AO, PDO	MEI, AMO, AO
Time scale	**Rainfall**	
3-months	AMO, NAO	IOD, AMO, NAO, PDO
6-months	MEI, AMO	MEI, IOD, AMO, NAO, PDO
12-months	SST, IOD, AMO, AO, PDO	SST, IOD, NAO, PDO
24-months	IOD, AMO	AMO

This approach prevents overfitting of the model and gauges the relative effectiveness of the models based on the provided parameters. For streamflow, the optimal combinations for the Mu parameter typically consisted of at least four climate indices. The Atlantic Multi-decadal Oscillation (AMO) exhibited a notable influence on both Mu and Sigma parameters across all time scales, except for Mu at the scale of 3 months. In the case of the precipitation, the Mu parameter had optimal combinations involving only two climate indices, except for the 12 months time scale, where more indices were involved. Similarly, the AMO significantly impacted both Mu and Sigma parameters across all time scales in the context of precipitation as well. These observations indicate the significant role of the AMO in influencing the Mu and Sigma parameters for both streamflow and precipitation models across various time scales, which emphasizes its importance in understanding hydrological and climatic patterns. The AIC values of all models are included in Table 5.4.

Table 5.4 AIC values of different models

	Model 0 (M0)	Model 1 (M1)	Model 2 (M2)	Absolute difference between M0 and M1	Absolute difference between M1 and M2
Time scale			**Streamflow**		
3-months	1593.963	1585.45	**1553.96**	8.51	31.49
6-months	3451.153	3422.66	**3373.34**	28.49	49.32
12-months	5379.15	5347.91	**5261.31**	31.24	86.6
24-months	6624.15	6588.14	**6583.28**	36.01	4.86
Time scale			**Rainfall**		
3-months	4346.51	4354.72	**4324.81**	8.21	29.91
6-months	6,654.90	6647.54	**6633.20**	7.36	14.34
12-months	7364.13	7343.65	**7286.82**	20.48	56.83
24-months	**7689.60**	7772.24	7704.41	82.64	67.83

The stationary model is represented by Model 0 (M0). Models 1 and 2 correspond to non-stationary models, with Model 1 varying only the location parameter and Model 2 varying both the location and scale parameters. These variations are achieved through the incorporation of climate oscillations as covariates. According to Burnham and Anderson (2004), if the difference in AIC values between two models is equal to or greater than 2, then there is substantial evidence indicating their differences. This criterion is also considered when selecting the best model from the available options. It is evident from the data in Table 5.4 that the stationary model consistently exhibits the highest AIC values across all time scales for streamflow. The AIC value of the stationary model is highest in the case of precipitation at all the time scales except at 24 months. For streamflow and precipitation, the model with varying Mu and varying Sigma exhibited better performance than the M0 and M1. The absolute difference of AIC value between models is larger than 2 in all the cases, and an increase in absolute difference value with time scale was also observed. Thus, based on the information in Table 5.4, models with variable parameters were selected as the optimal choice in all situations except for 24 months precipitation, where the stationary model fits best. The

subsequent calculations were carried out using the best-fit model. Table 5.5 provides the equations for Mu and Sigma for the selected model.

Table 5.5 Equations of Mu and Sigma of non-stationary models

Time scale	Shetrunji River Basin
3-months	$\mu(t) = -1.2043+1.7054$ SST(t)-0.7586 MEI(t)-2.0794 IOD(t)-0.4904 NAO(t)$+0.2600$ PDO(t)
	$\sigma(t) = 1.314-0.1924$ SST(t)$+0.7903$ AMO(t)
6-months	$\mu(t) = 2.485+0.4942$ SST(t)-0.1186 SOI(t)-0.7027 MEI(t)-0.3600 IOD(t)$+1.3686$ AMO(t) -0.2444 NAO(t) -0.3458 PDO(t)
	$\sigma(t) = -1.09635 +0.30793$ SST(t)$+ 0.06089$ SOI(t)-0.22406 IOD(t) -0.77588 AMO(t) $+0.08726$ AO(t)
12-months	$\mu(t) = 4.8056-0.1653$ SST(t)$+1.3878$ AMO(t)-0.1916 NAO(t)-0.1657 PDO(t)
	$\sigma(t) = 0.53342+0.13629$ MEI(t)$+0.23079$ AMO(t)-0.07573 PDO(t)
24-months	$\mu(t) = 5.59074 -0.19015$ MEI(t)$+0.49842$ IOD(t)$+1.54978$ AMO(t)-0.16096 AO(t)-0.09891 PDO(t)
	$\sigma(t) = 0.31351+0.08622$ MEI(t)$+0.24230$ AMO(t)-0.04032 AO(t)
Time scale	Shetrunji River Basin -Rainfall
3-months	$\mu(t) = 5.1548 +1.1061$ AMO(t) -0.1587NAO(t)
	$\sigma = 0.73260+ 0.21250$ IOD(t)-0.36454 AMO(t)$+0.08634$ NAO(t)-0.07229 PDO(t)
6-months	$\mu(t) = 5.8859-0.1670$ MEI(t)$+0.9494$ AMO(t)
	$\sigma(t) = 0.32201+0.11007$ MEI(t)$+ 0.23036$ IOD(t) -0.75153 AMO(t) $+ 0.06121$ NAO(t)-0.08769 PDO(t)
12-months	$\mu(t) = 6.41830 -0.10822$ SST(t) $+0.16845$ IOD(t)$+0.55536$ AMO(t)$+0.06328$ AO(t)$+ \quad 0.01651$ PDO(t)
	$\sigma(t) = -0.85312+0.05619$ SST(t)$+0.24462$ IOD(t)$+0.05451$ NAO(t) -0.12365 PDO(t)
24-months	$\mu(t) = 7.15600+0.09539$ IOD(t)$+0.58392$ AMO(t)
	$\sigma(t) =-1.0721+0.5998$ AMO(t)

Due to its adaptability to diverse types of non-stationarity, the Maximum Likelihood Estimation (MLE) approach was utilized in the estimation of distribution parameters of the models.

5.4.5 Analysis of drought classes

The categorization of droughts based on SPI, NSPI, SSI, and NSSI values is detailed in Table 3.2. According to Table 3.2, drought is categorized into four classes: mild (C1), moderate (C2), severe (C3), and extreme (C4), depending on the severity indicated by the threshold values. Similarly, the wet period is also classified into near normal(W1), moderate wet (W2), very wet (W3,) and extreme wet (W4). A comparison was made for the frequency of occurrence of drought classes from non-stationary and stationary models in the case of both types of droughts from 1971 to 2015. Figures 5.7a and b depict the drought classification across all time scales within the basin for meteorological and hydrological droughts, respectively.

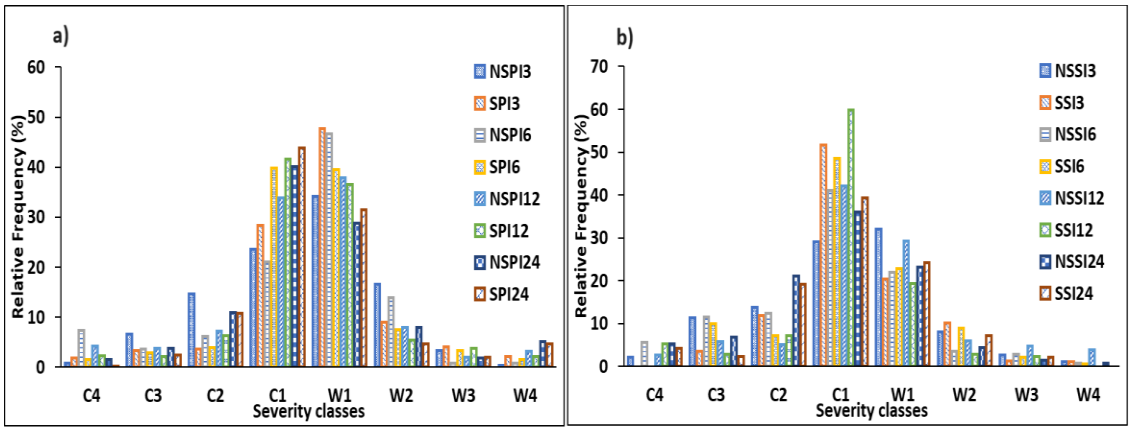

Figure 5.7. Drought classification for a) meteorological drought b) hydrological drought

Shorter time scales (3 and 6 months) exhibited a higher percentage of total wet periods than dry periods in meteorological drought. The non-stationary indices showed a greater likelihood for the C3 and C4 categories compared to the W3 and W4 categories across all time scales. When examining Figure 5.7 (a and b), it becomes apparent that both stationary and non-stationary approaches reveal that either C1 or W1 holds a higher frequency across all time scales. However, it is notable that the occurrence frequency of C1, calculated from the non-stationary index, is consistently lesser than

that of C1 derived from the stationary index at all scales. Non-stationary indices consistently exhibited improved identification of severe to extreme drought classes across all time scales. Considering the 6 months time scale, when NSPI6 showed 3.55% and 7.31% frequency for severe and extreme drought, respectively, SPI6 exhibited a 2.82% to 1.21% chance of occurrence. However, the chance of occurrence of W3 and W4 were 0.74% and 0.73%, respectively, as indicated by NSPI6. Based on SPI6, the values are 3.28% and 1.54%, respectively, for W3 and W4. For the same time scale, the hydrological drought index, when NSSI6 showed 11.55% and 5.68% for C3 and C4, respectively, SSI6 indicated 9.94% and 0% for C3 and C4. The lowest frequencies for C1, C2, C3, and C4 were indicated by NSPI3 (20.97%), SPI6 (3.55%), SPI12 (2.09%), and SPI24 (0.19%). Whereas the highest frequency of C1, C2, C3, and C4 were shown by SPI24 (43%), NSPI6 (14.63%), NSPI6 (6.56%), and NSPI3 (7.30%). When considering hydrological drought indices, the overall percentage of dry periods was greater than that of wet periods. As per the non-stationary index, there is a higher likelihood of severe to extreme dry conditions occurring compared to very wet and extreme wet conditions within the basin.

From 1984 to 1990, the Saurashtra region faced a prolonged sequence of severe to extreme drought conditions, with the most severe drought occurring in 1987 (Bandyopadhyay et al. 2016; Nathan 2001). Consequently, the performance of each index in indicating drought classification for the period 1984 to 1990 was also examined and visualized in Figure 5.8 (a-b).

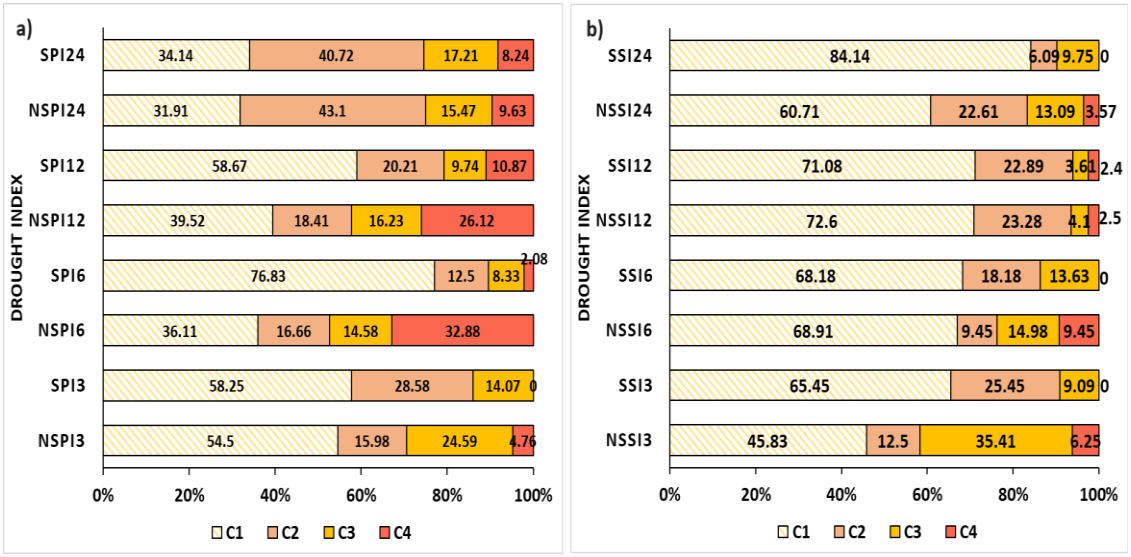

Figure 5.8. Drought classification for the period 1984 to 1990 for a) Meteorological drought, b) Hydrological drought

A higher percentage of severe and extreme meteorological drought was indicated by NSPI3 and NSPI6, respectively. NSPI6 showed 14.58% and 32.88% as a severe and extreme drought during the period, whereas SPI6 indicated 76.83% as a mild condition. Non-stationary hydrological drought indices also marked a higher frequency of occurrence of C3 and C4 than stationary indices at all the time scales. SSI3, SSI6, and SSI24 indicated 0% of extreme dry conditions. Saurashtra has a history of experiencing severe to extreme droughts (Chopra 2006). Non-stationary indices are more suitable for capturing severe to extreme drought events of the basin than stationary indices.

5.4.6 Comparative evaluation of the meteorological and hydrological droughts

Table 5.6 displays the Pearson correlation coefficients between stationary and non-stationary indices for both droughts at various time scales.

Table 5.6 Pearson correlation coefficients between stationary and non-stationary indices

Drought index	Pearson correlation coefficient
NSPI3-NSSI3	0.48
NSPI6-NSSI6	0.48
NSPI12-NSSI12	0.41
NSPI24-NSSI24	0.39
SPI3-SSI3	0.13
SPI6-SSI6	0.26
SPI12-SSI12	0.44
SPI24-SSI24	0.46

In every case, a significant positive correlation was detected between the droughts. A significant positive correlation implies that a reduction in rainfall corresponds to a decrease in streamflow. The highest correlation is evident for the 3 and 6 months time scales of NSPI and NSSI. Conversely, the lowest correlation is observed between SPI3 and SSI3. Notably, stationary drought indices displayed a lower correlation between the two types of droughts in short-term time scales. However, non-stationary indices exhibited higher correlations in the same short-term time scales.

Cross-correlation analysis was performed across lags ranging from zero to 24 months, revealing that the highest correlation values were consistently obtained within the range of zero to 4 months lags across all cases. Hence, Figure 5.9 illustrates the cross-correlation between NSPI-NSSI and SPI-SSI, focusing on the 0 to 4 months lag range.

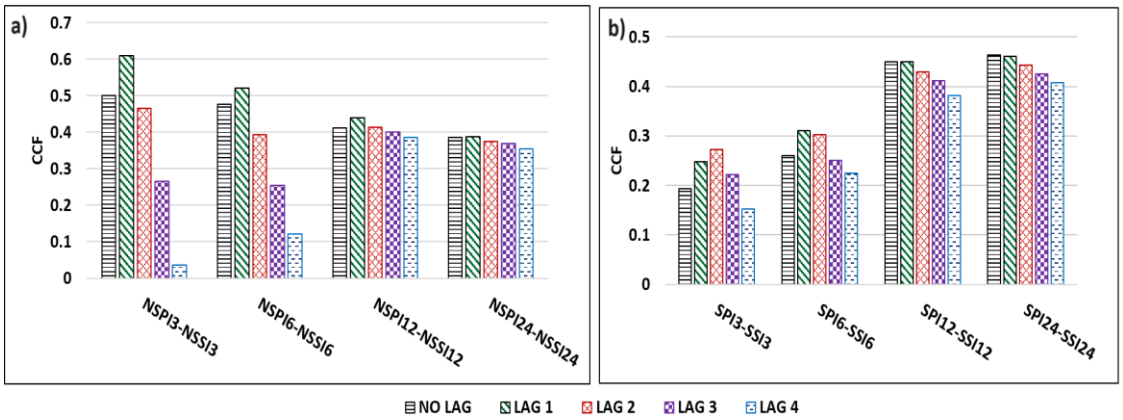

Figure 5.9. Crossover correlation between a) non-stationary indices (NSPI-NSSI), b) stationary indices (SPI-SSI)

The peak correlation of 0.61 was identified at the 3 months scales for NSPI-NSSI, specifically at a one-month lag. The highest correlation between non-stationary meteorological and hydrological drought indices occurred at a one-month lag across all time scales. The maximum correlation at a one-month lag implies a delayed effect of meteorological drought on hydrological drought. It implies that meteorological drought in the region appears to impact surface water resources with a one-month delay. For stationary drought indices, the maximum correlation with a lag of one month was identified only at the 6 and 12 months time scales. The cross-correlation analysis between meteorological and hydrological droughts, based on the best-selected model, was visualized and presented in Figure 5.10. The correlations between meteorological and hydrological drought derived from the best models consistently exhibited their highest values at a one-month lag across all cases. Figure 5.11 illustrates time series plot of indices with high cross-correlation coefficients for the meteorological and hydrological droughts, focusing on a one-month lag. The plot highlights a consistent positive correlation between these indices, underscoring that alterations in meteorological drought conditions closely connect with subsequent shifts in hydrological drought conditions.

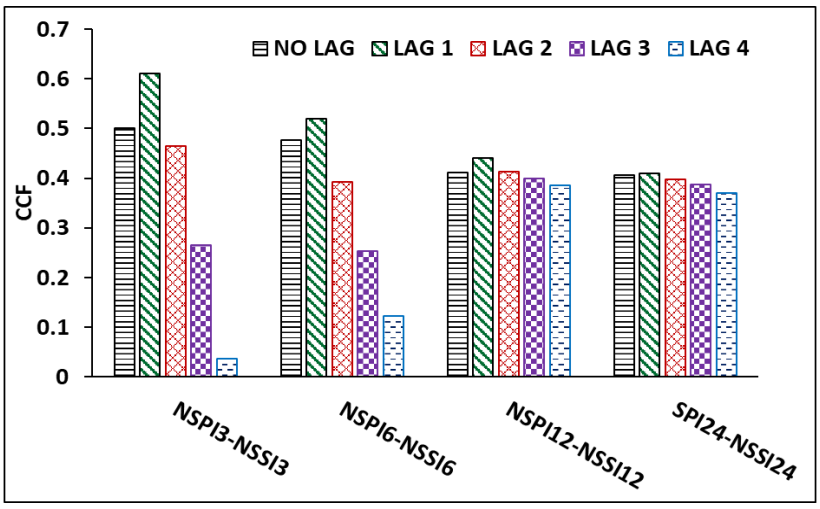

Figure 5.10. Crossover correlation between best models

Although with a one-month delay, this correlation emphasizes the interdependency and temporal relationship between meteorological and hydrological droughts within the studied region. To provide a clear visualization of the relationship between two types of droughts, the Pearson correlation coefficient was calculated between each month of indices at different time scales, and the results are presented as a heat map in Figure 5.12. On a monthly basis, September of NSPI3 and October of NSSI3 had the strongest positive association (0.62). For NSPI6 and NSSI6, the greatest significant association was obtained between December of NSPI and November of NSSI. The highest correlation (0.59) was observed between August of NSPI and September of NSSI at the 12 months scale. Additionally, between SPI24 and NSPI24, the strongest correlation was noted between November and December. Remarkably, at all-time scales, the most robust correlation was consistently observed at a lag of one month.

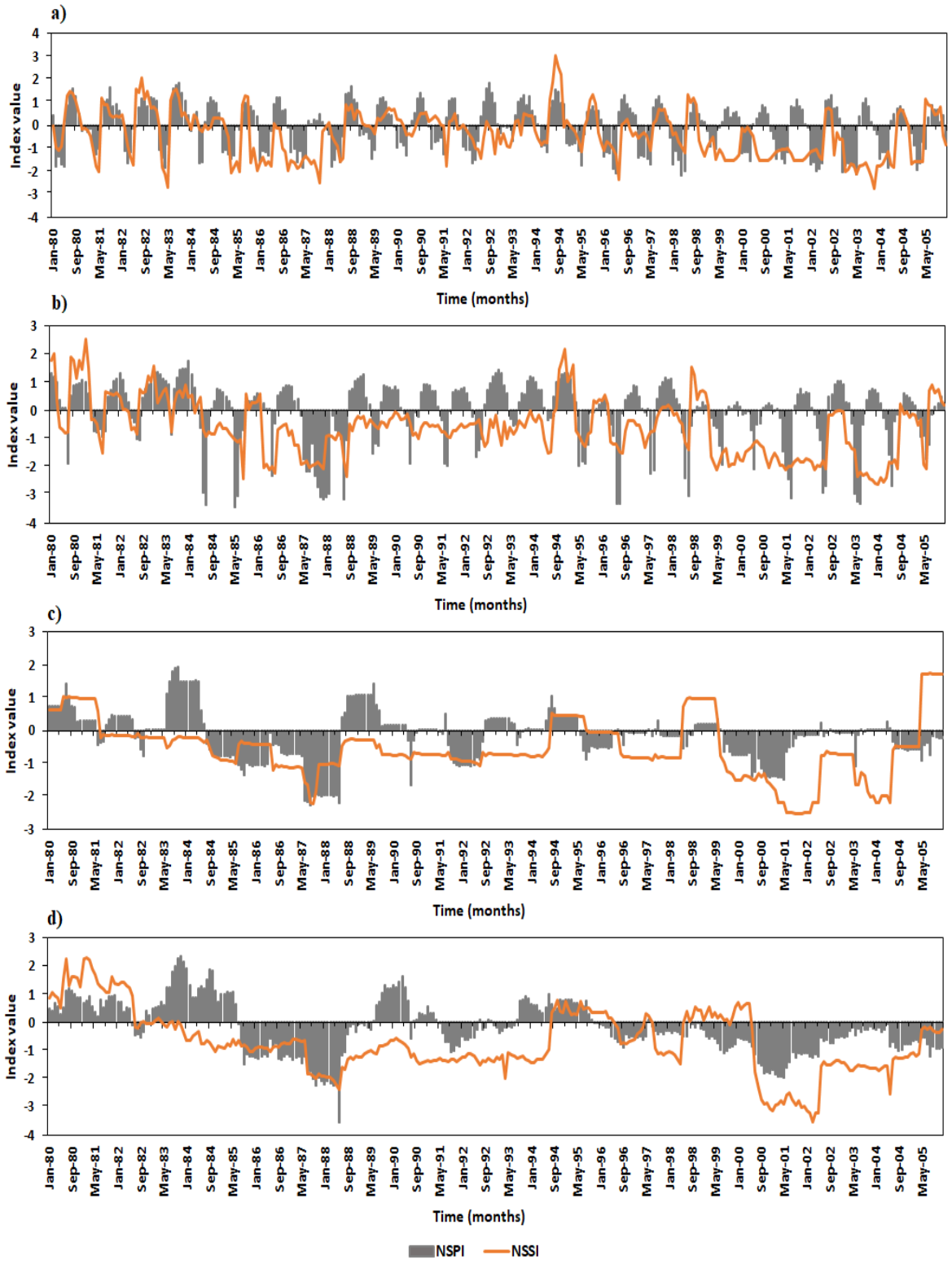

Figure 5.11. Time series plot of indices with high cross-correlation coefficient for a) 3-months; b) 6-months; c) 12-months; d) 24-months

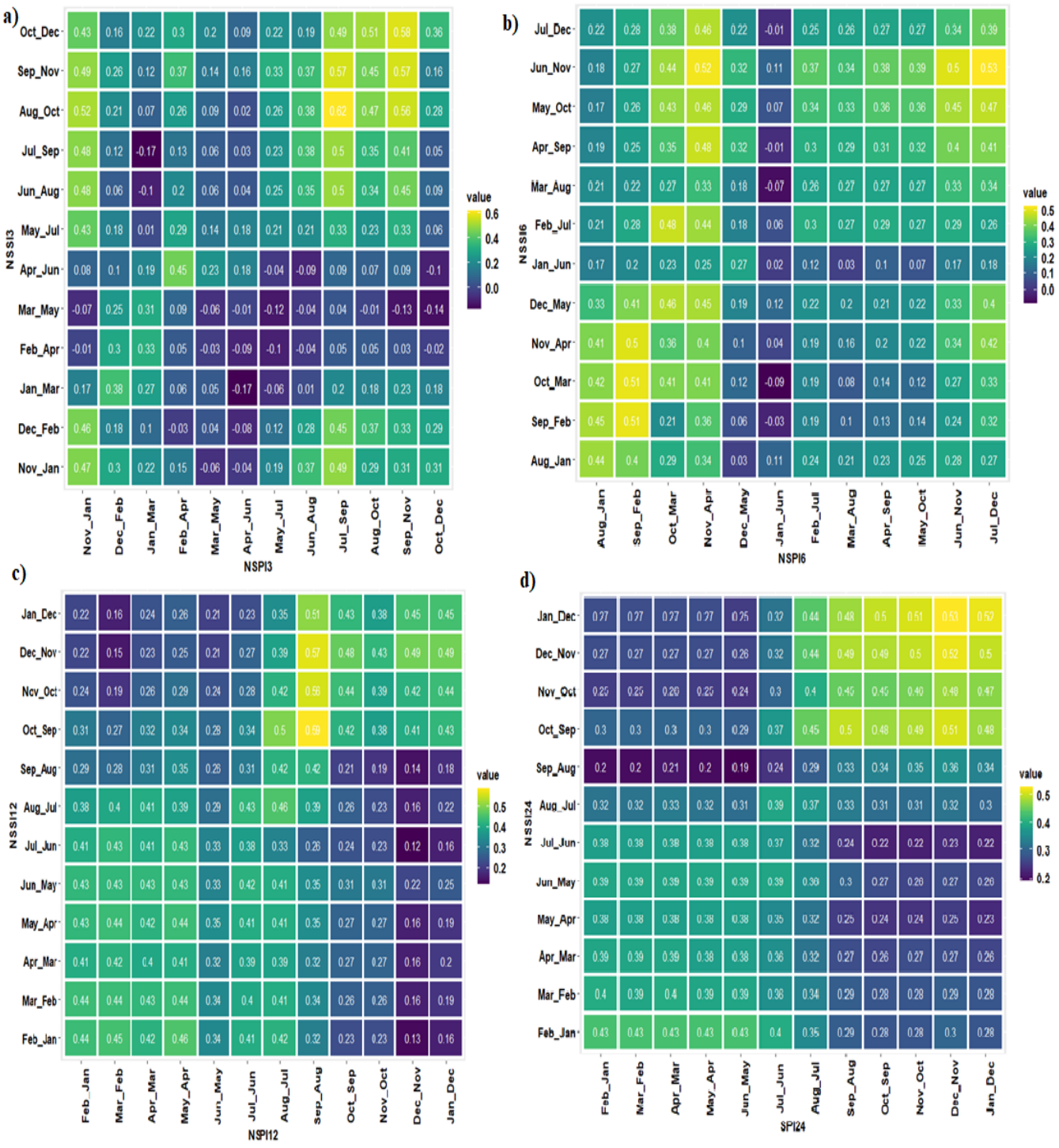

Figure 5.12. Heat map of the Pearson correlation coefficients between NSPI and NSSI for a) 3-months; b) 6-months; c) 12-months; d) 24-months

5.4.7 Association between meteorological and hydrological drought indices

Figure 5.13 visually represents the response rate of hydrological drought to meteorological drought across various time scales. The figure also displays the response rate of wet periods, as indicated by the hydrological drought index, to the meteorological drought index. Notably, a strong response rate relationship was observed between both indices.

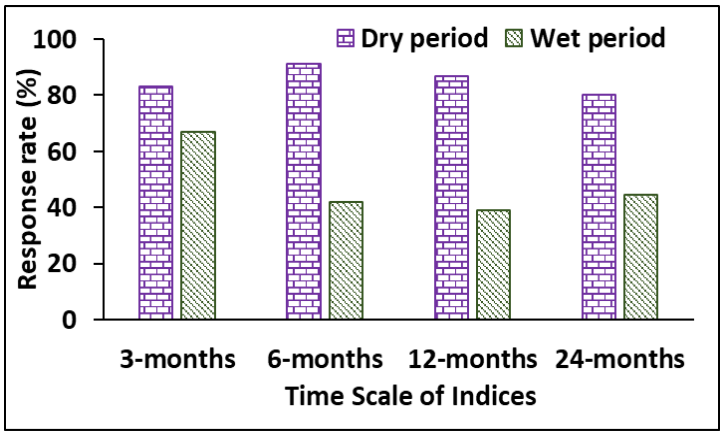

Figure 5.13. Response rate of hydrological to meteorological drought index

The response rate during drought periods is significantly higher than in wet periods. This observation suggests that the hydrological drought index strongly reacts to dry conditions over wet conditions. The result indicated that, at a 6 months scale, the hydrological drought in the region responded to meteorological drought very well, with a response rate of 91.13%. The wet period response rate (66.78%) is higher at a 3 months time scale. Furthermore, across all time scales, the response rate during drought periods exceeds 80%. This finding underscores the heightened sensitivity of hydrological drought to meteorological drought conditions within the studied basin. Particularly, this heightened sensitivity is most pronounced at the 6 months scale.

In this research, various regression models, including linear, quadratic, and cubic polynomial models, were applied to pairs of indices to establish statistical relationships. The hydrological indices were considered as dependent variables, while the meteorological variables were treated as independent variables. The analysis of R^2 values indicated that the cubic polynomial regression model yielded the highest R^2 values among the tested models. Subsequently, the quadratic model showed better R^2

values compared to the linear models. The statistical relations between indices are presented in Table 5.7.

Table 5.7 Statistical relations between indices

Time scale	Equation	R^2
3-months	NSSI = -0.23 + 0.48 NSPI	0.23
	NSSI = -0.39 + 0.51 NSPI + 0.16 $NSPI^2$	0.35
	NSSI = -0.39 + 0.45 NSPI + 0.17 $NSPI^2$ + 0.02 $NSPI^3$	0.45
6-months	NSSI = -0.49 + 0.43 NSPI	0.25
	NSSI = -0.54 + 0.46 NSPI + 0.03 $NSPI^2$	0.36
	NSSI = -0.57 + 0.62 NSPI + 0.03 $NSPI^2$ - 0.02 $NSPI^3$	0.38
12-months	NSSI = -0.34 + 0.41 NSPI	0.20
	NSSI = -0.28 + 0.46 NSPI + 0.06 $NSPI^2$	0.32
	NSSI = -0.30 + 0.53 NSPI - 0.02 $NSPI^2$ - 0.01 $NSPI^3$	0.33
24-months	NSSI = -0.49 + 0.42 NSPI	0.16
	NSSI = -0.36 + 0.57 NSPI - 0.14 $NSPI^2$	0.32
	NSSI = -0.37 + 0.58 NSPI - 0.13 $NSPI^2$ - 0.01$NSPI^3$	0.32

Notably, the highest R^2 value was achieved with the cubic model, particularly at the 3 months time scale. It is interesting to observe that the R^2 values tend to decrease as the time scale increases. Furthermore, the establishment of statistical relationships between the hydrometeorological indices serves as a valuable tool for anticipating hydrological drought events in the study area. By analysing these relationships, predicting the occurrence of hydrological drought in advance is possible based on meteorological drought conditions.

5.4.8 Analysis of Crop Yield Reduction

Changes in climatic patterns have a significant impact on agricultural productivity. This study specifically examined the impact of drought on agriculture by analysing two major crops: Bajra (a kharif crop) and wheat (a rabi crop). Wheat is a winter cereal crop, and its growing season in Gujarat is during the Rabi season. The Rabi season typically starts in October and extends until March. Wheat is planted during the cooler months of October and November, allowing it to take advantage of the available soil

moisture and moderate temperatures. Bajra is typically sown during the monsoon months of June and July when the region receives rainfall. These crops benefit from the moisture provided by the monsoon rains and are harvested in the autumn. Rabi crops require relatively cooler temperatures and less water than Kharif crops (Patel et al. 2015).

The Pearson correlation method (Hendrawan et al. 2022) is employed to ascertain the correlation between the rate of yield reduction and the most suitable index of drought chosen for various time scales. This correlation was examined for both crops, with each month being considered at different time scales. Pearson correlation between drought index and crop yield loss rate of bajra and wheat are presented in Tables 5.8 and 5.9, respectively.

Table 5.8 Pearson correlation between drought index and crop yield loss rate of Bajra

Months	Meteorological drought				Hydrological drought			
	3-month	6-month	12-month	24-month	3-month	6-month	12-month	24-month
January	0.04	0.17	0.20	0.16	0.12	0.06	0.07	0.22
February	0.11	0.24	0.19	0.16	0.04	0.03	0.06	0.23
March	0.13	0.04	0.13	0.16	0.01	0.06	0.04	0.23
April	0.02	0.05	0.18	0.16	0.09	0.05	0.06	0.25
May	0.12	0.07	0.15	0.17	0.02	0.09	0.04	0.20
June	**0.32**	**0.34**	0.01	0.09	0.04	0.01	0.09	0.26
July	**0.41**	**0.40**	0.15	0.02	0.07	0.18	0.03	0.24
August	**0.45**	**0.39**	**0.35**	0.01	0.16	0.21	0.04	0.02
September	**0.27**	**0.42**	**0.51**	0.03	0.19	**0.29**	0.17	0.06
October	0.18	**0.41**	**0.45**	0.03	0.22	0.27	0.14	0.07
November	0.12	**0.47**	**0.47**	0.05	0.24	0.21	0.17	0.08
December	0.16	**0.39**	**0.49**	0.09	0.03	0.13	0.12	0.01

Note: Bold numbers indicate statistically significant correlation at 5% levels of significance

Table 5.9 Pearson correlation between drought index and crop yield loss rate of Wheat

Months	Meteorological drought				Hydrological drought			
	3-month	6-month	12-month	24-month	3-month	6-month	12-month	24-month
January	0.19	0.20	0.02	0.02	0.13	0.06	0.15	0.15
February	0.09	0.24	0.01	0.02	0.07	0.11	0.20	0.20
March	**0.32**	0.01	0.03	0.02	0.10	0.06	0.18	0.17
April	0.09	0.23	0.02	0.02	0.14	0.00	0.16	0.13
May	0.08	0.04	0.02	0.02	0.18	0.11	0.20	0.12
June	0.06	0.04	0.15	0.07	0.03	0.00	0.12	0.05
July	0.22	0.27	0.07	0.08	**0.29**	0.20	0.13	0.11
August	**0.31**	**0.33**	0.28	0.09	**0.39**	0.27	**0.21**	0.24
September	**0.41**	**0.36**	**0.40**	0.16	**0.38**	**0.29**	**0.36**	0.29
October	0.12	**0.36**	**0.36**	0.16	**0.35**	**0.33**	**0.43**	**0.32**
November	0.20	**0.43**	**0.46**	0.20	**0.39**	**0.34**	**0.40**	**0.34**
December	0.08	**0.45**	**0.42**	0.19	0.14	0.29	**0.33**	**0.34**

Note: Bold numbers indicate statistically significant correlation at 5% levels of significance

Except for the 24 months scale, a significant association between the loss rate of bajra and the meteorological drought index was found in the research region. The most significant correlation (0.51) was obtained in September, corresponding to the 12 months scale. Except for the 24 months, a significant association was visible in September across all time scales. This observation aligns with the flowering phase of Kharif crops, highlighting the impact of drought conditions in September on crop production. The significant correlation with the hydrological drought index was observed only in September at a 6 months time scale. However, a considerable impact of hydrological drought spanning from the monsoon to the winter season was discernible for wheat. On a 24 months scale, no correlation was observed between the rate of wheat loss and the meteorological drought index. However, a significant

association was witnessed between the hydrological drought index and the loss rate of wheat at the 24 months time scale. The most robust correlations were identified at the 12 months time scale, specifically reaching 0.46 in November and 0.43 in October for wheat when correlated with the NSPI and NSSI, respectively.

Interestingly, the impact of drought on bajra yield was more pronounced during the monsoon season than in the winter season. In contrast, the influence of drought on wheat was more substantial during the winter season compared to the monsoon season. This differential effect underscores how varying crop types respond differently to seasonal drought conditions, indicating the complexity of their sensitivities to environmental factors. Figures 5.14a and b show the plot between yield loss rate and best-correlated drought indices NSPI and NSSI.

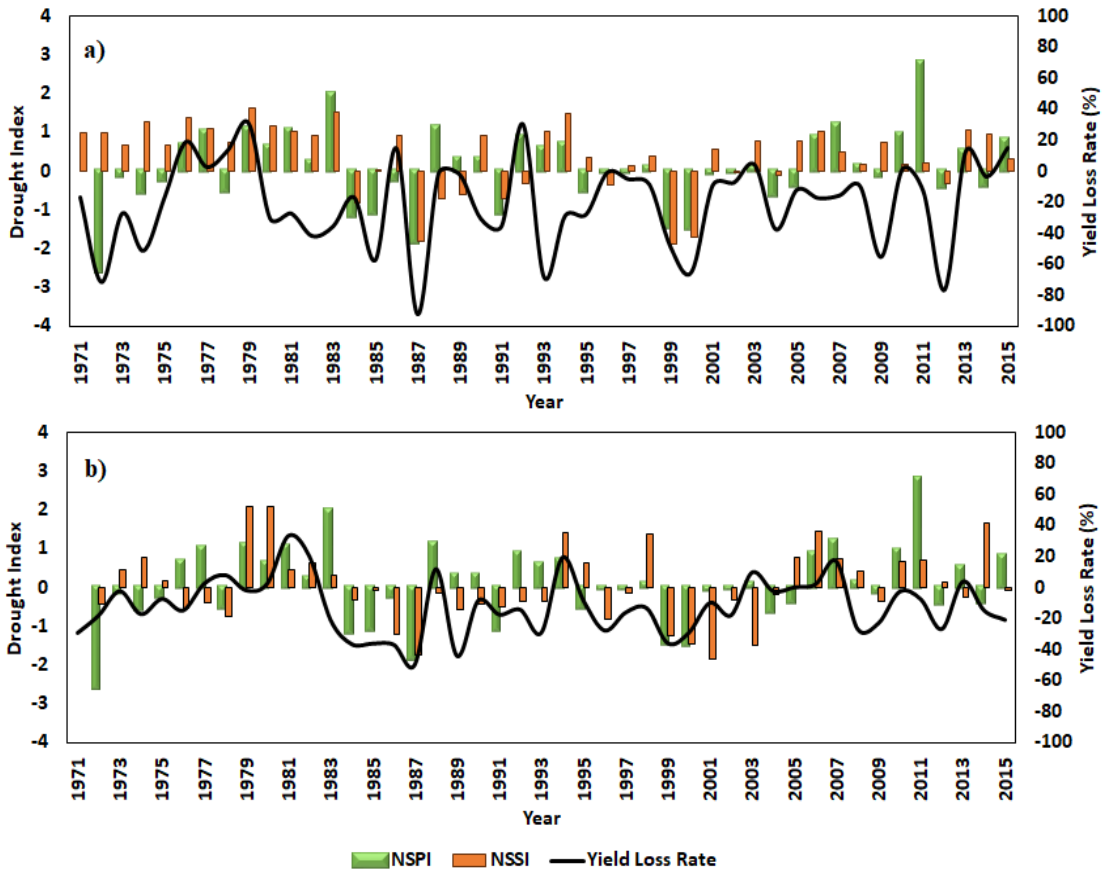

Figure 5.14. Drought indices vs yield loss rate of a) bajra, b) wheat

The highest departure of rainfall and streamflow occurred in 1987 (Figures 5.3 and 5.4). As depicted in Figure 5.14a, the most substantial loss rate of -92.55% in bajra productivity was observed in 1987, which is considered the worst drought year. Similarly, wheat also experienced a notable loss rate of -49.47% during the same year (Figure 5.14b). This indicates that the most severe drought year had a more pronounced impact on bajra production than wheat.

5.5 DISCUSSIONS

The climatic index can influence atmospheric circulation patterns to distant places through teleconnections. The variation in ocean conditions can affect the atmospheric pressure, wind cycles, and moisture transport, which take time to impact weather systems in nearby land areas (Zhang et al. 2013). ENSO indices are strongly associated with the Indian monsoon (Agilan and Umamahesh 2017; Pervez and Henebry 2015). According to Agilan and Umamahesh (2018), the SOI is the most suitable ENSO index for modeling monsoon and non-monsoon rainfall in India. However, the effect can vary depending on the locations within India. According to this research, IOD exhibited a strong concurrent relation with rainfall among all the climate variables considered, indicating a shorter response time between IOD phases and Indian rainfall variability. The reason can be that the IOD represents the variation in SST between the eastern and the western Indian Ocean, with a closer influence on Indian regions. Other Indices showed impacts with lags of more than one month. A significant influence of AMO is also observed compared to AO and NAO. This finding is compatible with a study by Nagaraj and Srivastav (2022), which concluded that the dominant influence of AMO is in the Northwest region, whereas NAO/AO is in the Northeast region of India. In this research, AO showed the least impact on rainfall compared to other indices. The significant lags of Arctic and Atlantic climate indices were higher than the Pacific and Indian Ocean indices. Geographical distance may be the reason for this variation. Further research can be extended to an analysis of the feedback mechanism between the indices (Kug and Kang 2006).

A non-stationary marginal distribution, characterized by varying Mu and sigma parameters, is employed to compute non-stationary drought indices. These indices are evaluated using a common threshold value of -1 to identify drought events. Specifically,

the Standardized Precipitation Index (SPI) and Standardized Streamflow Index (SSI) are calculated using the M0 model, while the Non-Stationary SPI (NSPI) and Non-Stationary SSI (NSSI) are computed using the M2 model. The resulting SPI and NSPI values are illustrated in Figure 5.15 (a-d), and the SSI and NSSI values are depicted in Figure 5.16 (a-d). Greater variability between the stationary and non-stationary models becomes evident in the plots for shorter time scales, particularly in the 3 months and 6 months intervals. Conversely, for longer-term drought assessments (12 and 24 months), the plots appear more consistent between the two models.

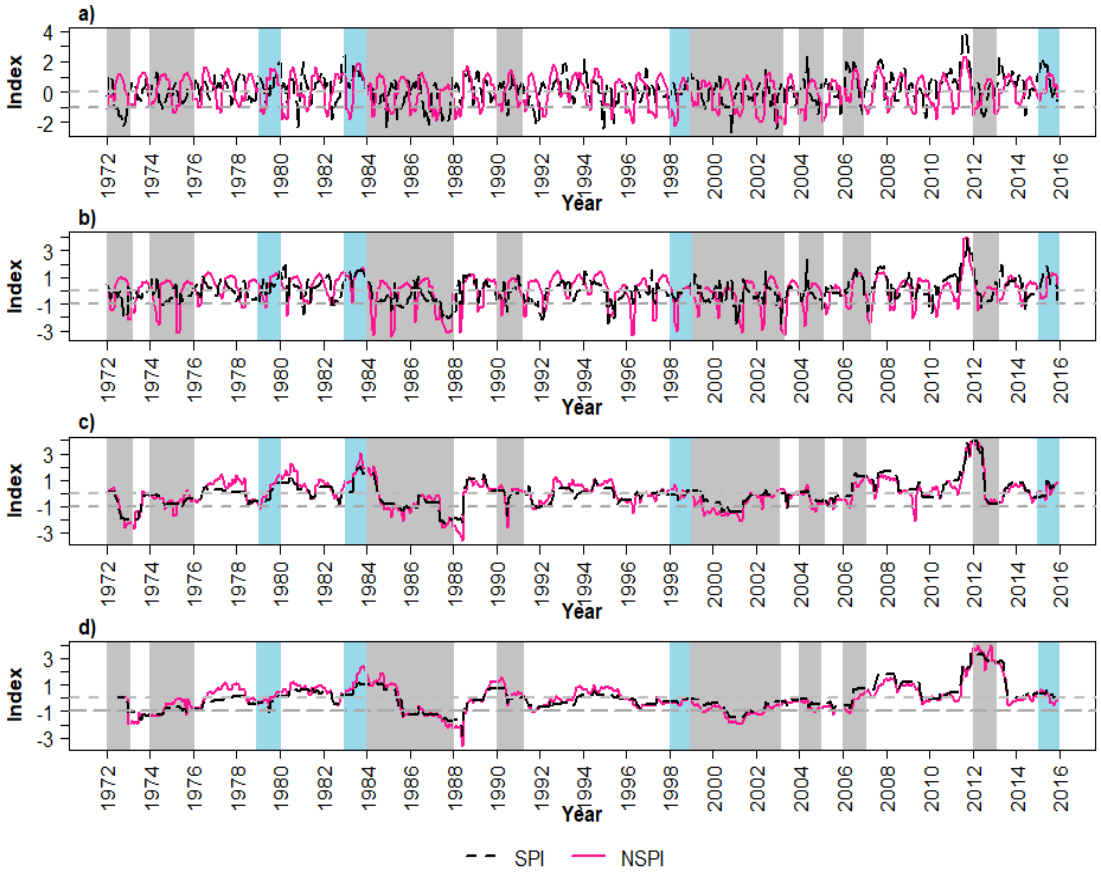

Figure 5.15. SPI vs NSPI for a) 3-months; b) 6-months; c) 12-months; d) 24-months, and Vertical blue and grey bars represent historical flood and drought events respectively.

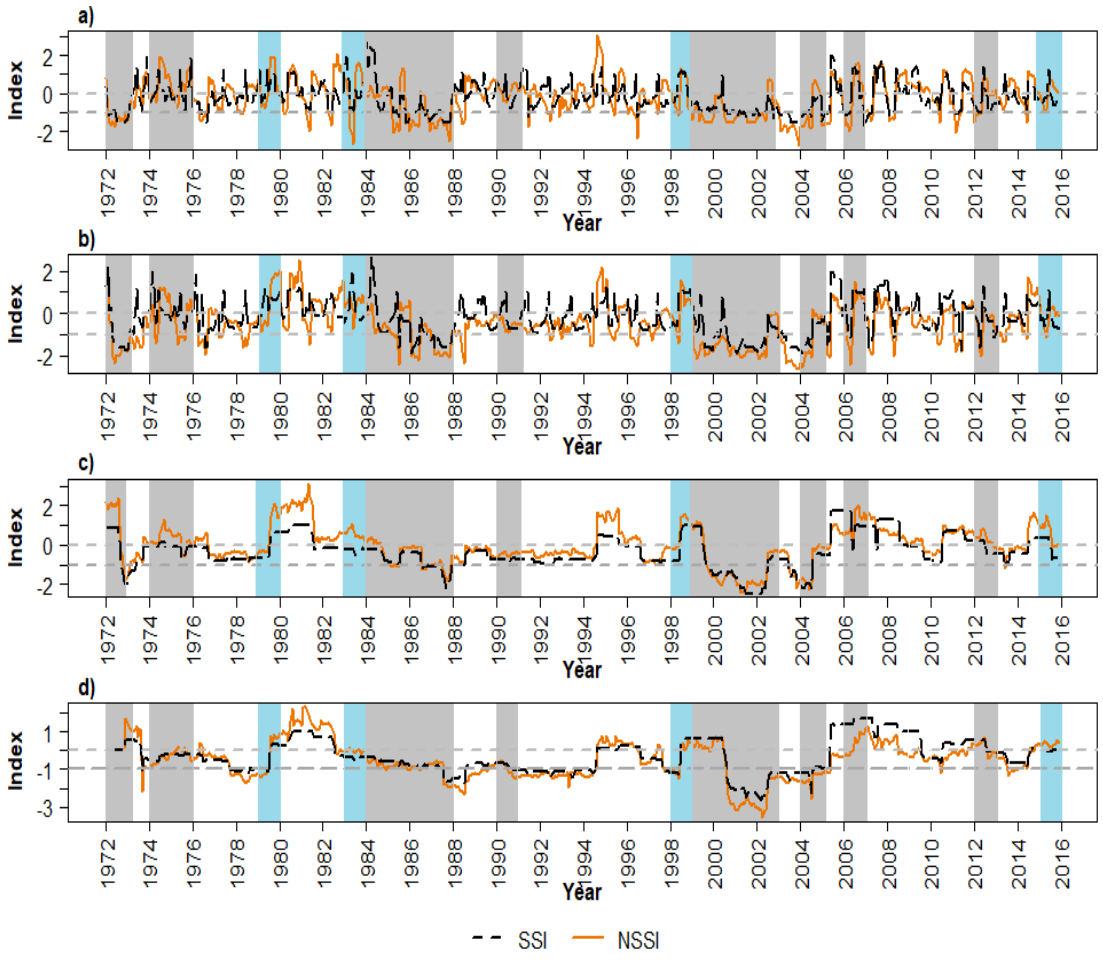

Figure 5.16. SSI vs NSSI for a) 3-months; b) 6-months; c) 12-months; d) 24-months, and Vertical blue and grey bars represent historical flood and drought events, respectively.

From relevant literature, the figures also incorporate severe historical drought and flood events within the specific region. Saurashtra has a historical track record of enduring droughts, and a particularly severe occurrence took place in 1999, affecting districts such as Bhavnagar, Porbandar, Surendranagar, Rajkot, Amreli, Jamnagar, and Junagadh (Chopra 2006). This event resulted in a significant reduction in the water table in the area, causing the depletion of all water sources. While examining a 6 months time scale for comparison, the drought that occurred in 1999 is identified solely by the Non-Stationary SPI (NSPI), with a severity and peak of 3.18 and 1.93, respectively. Similarly, during the same year, the hydrological drought is characterized by the Non-

Stationary SSI (NSSI), reaching a peak of 2.11. In contrast, the Standardized Streamflow Index (SSI) exhibits a peak value of 1.74 for that particular year.

According to Ganguli and Reddy (2014), on a 6 months scale, 1974 and 1987 had particularly severe droughts in the Saurashtra and Kutch areas. Notably, drought incidents were primarily recorded in this region during the summer. The Non-Stationary SPI (NSPI) identified the drought in 1974 as an extreme drought during the summer season. In contrast, the Standardized Precipitation Index (SPI) classified the same event as only a moderate drought in the monsoon season. The years 1985, 1986, and 1987 witnessed severe to extreme meteorological droughts across different regions of the state. These droughts were primarily a result of insufficient rainfall during the monsoon seasons, with the most severe occurrence recorded in 1987. This year, the absence of surface water was particularly dire, resulting in the partial drying out of 20 dams and the complete drying up of 40 dams. The devastating impact was also reflected in the significant loss of cattle, with 5,000 deaths reported in Saurashtra alone (Bandyopadhyay et al. 2016; Nathan 2001). The most severe drought, which occurred in 1987, was classified as an extreme event according to the NSPI, with a severity value of 24.49 and a peak of 3.15. Meanwhile, the SPI indicated a lower severity of 13.75 with a peak of 2.04 for the same drought event. Additionally, during 1987, indications of hydrological drought were also evident. NSSI and the SSI depicted this drought with severity values of 19.73 and 17.11, respectively.

From 1971 to 1972, there was a severe drought in the Saurashtra and Kutch areas. There were also extreme drought occurrences in 1974–1975, 1984–1985, and 1987–1988 (Yadav et al. 2021). In 1972, both the NSPI and the SPI indicated a meteorological drought. Furthermore, an extreme hydrological drought was also observed during the same period. In 1974 and 1975, the NSPI indicated an extreme drought, whereas the SPI categorized it as a moderate drought. Interestingly, within these drought years, the SSI6 failed to signal the drought occurrence. However, the NSSI indicated events ranging from moderate to severe drought during the same periods. The western region of Gujarat faced a significant drought in 2002 (Bhuiyan et al. 2017). During this period, both NSPI and the NSSI indicated the severity of the drought, with NSPI categorizing it as severe and NSSI classifying it as extreme.

The Saurashtra and Kutch regions encountered severe floods in 1979, 1983, 1998, and 2015 (Parthasarathy et al.1987). In 1979, the NSPI identified a period of moderate wetness, while the SPI indicated a near-normal condition. The NSSI signified an extreme situation with a peak of 2.02 during the monsoon season. The SSI could not indicate the wet period in this case. During the flood event in 1983, the NSPI and SPI identified a condition ranging from moderate to very wet. In 1998, neither the NSPI nor the SPI indicated any wet period. Only the NSSI and SSI marked very wet and moderate wet conditions, respectively. The non-stationary drought indices demonstrated a notable ability to align with historical wet and dry periods in a majority of instances. Sometimes, the opposite time series patterns are observed between stationary and non-stationary indices at shorter time scales. The reason for this can be the influence of climate variables. The above comparison of current results with historical drought and flood events shows that non-stationary indices correctly indicate climate situations during extreme events.

Analysis of the probability of occurrence of drought and wet classes showed a higher probability for severe and extreme drought classes as indicated by NSPI and NSSI at all time scales compared to mild and moderate droughts. Also, the C3 and C4 classes marked a higher probability than W3 and W4. This trend can be explained by the deficient annual average rainfall in Saurashtra and Kutch, which is only 604.52mm. According to several studies (Bandyopadhyay and Saha 2014; Bhuiyan et al. 2017; Ganguli and Reddy 2012; Nathan 2001), the study area is highly prone to severe to extreme droughts rather than extreme wet conditions. The number of historical drought events is more frequent than flood events. This observation is evident from the figures 5.15 and 5.16.

Understanding the propagation of meteorological drought to hydrological drought is important in drought and water resources management studies. From the correlation analysis between meteorological and hydrological drought indices, the stationary indices exhibited a lower correlation than non-stationary indices at short-term time scales. A similar significant correlation between these two types of droughts is observed in literature such as Salimi et al. (2021) and Zhao et al. (2016) in semi-arid basins in Iran and China, respectively. From the response rate analysis of hydrological

drought to meteorological drought, a higher response rate is observed during the dry than the wet period. Meresa et al. (2023) observed higher drought frequency propagation during summer in the Awash basin in Ethiopia. Findings from correlation analysis at different lags, such as the impact of meteorological drought on water resources in Saurashtra and Kutch, are observed with a one-month delay. However, the response time of hydrological drought to meteorological drought depends on various factors such as slopes, catchment features, climate properties, elevation, and many other factors (Lin et al. 2023; Meresa et al. 2023; Ozkaya 2023). The significant correlation between two droughts underscores the importance of integrated drought management in the basin to enhance sustainable water use.

According to Panda et al. (2019), there is a significant correlation between monsoon rainfall and crop productivity in Odisha, India. Several studies proved a good correlation between the drought index and crop yield (Hendrawan et al. 2022). In 1999, the Saurashtra and Kutch experienced a severe drought, as mentioned by Chopra (2006). During this period, this research indicated that the loss rates for bajra and wheat were -48.85% and -35.93%, respectively. Nathan (2001) reported that the extreme drought of 1985 impacted 75% of the crops in Gujarat. This particular drought led to a significant loss rate of -57.51% in bajra production and -36.03% for wheat in the same year. Both crops exhibited positive correlations with drought indices. However, the major drought had a more substantial adverse impact on bajra production within the region. In contrast, wheat production appeared to be less affected by these major drought events. The findings from this research exhibit a stronger coherence with the outcomes reported in the previously mentioned studies, thereby underlining the robustness of the modeling approach employed.

5.6 CLOSURE

Based on a case study in the Shetrunji river basin in the semi-arid Saurashtra region of India, this research has shown the usefulness and relevance of utilizing non-stationary indices to assess meteorological and hydrological droughts. The GAMLSS framework was used to build the non-stationary models, and the best combinations of climatic indicators (IOD, SOI, SST, MEI, AMO, NAO, AO, and PDO) were used. The impact of these climatic factors on the various drought classes is examined in the research.

Notably, the non-stationary models exhibited superior performance compared to stationary models in effectively capturing significant severe drought events, highlighting the necessity of incorporating climatic factors for more accurate assessments. The non-stationary drought index exhibited higher agreement with previous flooding and drought conditions, enhancing its reliability for evaluating prevailing drought situations. A comparative analysis between meteorological and hydrological drought under stationary and non-stationary conditions shows the maximum significant correlation for 3 and 6 months of NSPI-NSSI. Longer time scales demonstrated weaker correlations than short scales. From the cross-correlation method, the effect of meteorological drought on the surface water resources was observed more at a month lag at all the time scales. The response rate analysis indicates that the hydrological drought in the basin responded to meteorological drought at a 6 months time scale very well, with a response rate of 91.13%. The better statistical relation between the droughts is obtained at 3 months time scales than other time scales with cubic models. Given the limited variance explained by the equations, it is reasonable to conclude that for accurate prediction of hydrological drought in the Shetrunji River basin, relying solely on meteorological indices and polynomial regression models might not yield sufficiently reliable results. Instead, incorporating streamflow data-based calculations and other relevant factors may lead to more accurate predictions of hydrological drought events.

This research also investigated how drought affected the rate of agricultural yield loss in the kharif (bajra) and rabi (wheat) harvests. In the basin, the research demonstrates a substantial relationship between the Non-stationary Standardized Precipitation Index and bajra production, highlighting the impact of meteorological drought episodes on agricultural output. The hydrological drought effect is observed more in wheat production than in bajra. However, the loss rate comparison at major drought events reveals that bajra production is more affected by severe droughts than wheat production in the study area. These findings underscore the sensitivity of different crops to varying types and intensities of drought. The correlation with the NSPI emphasizes the significance of meteorological factors, while the varying impacts of hydrological and severe droughts on different crops underscore the need for tailored adaptation strategies

in agricultural planning. Decision-makers, agricultural planners, and farmers need this knowledge to make wise decisions to increase crop resilience and reduce production losses in changing climatic circumstances.

CHAPTER 6

HYDROLOGICAL DROUGHT TREND ANALYSIS AND FORECASTING IN HUMID RIVER BASIN IN INDIA USING STATIONARY INDEX

6.1 GENERAL

Drought is a natural hazard that badly affects many sectors of a country (Bacanli 2012). A large population in India depends on the agricultural sector, and its production associated with monsoon rainfall availability. Monsoon (June-September), post-monsoon (October –November), winter (December-February), and summer (March-May) are the principal seasons in India (MoEF 2004). More than 80% of the rainfall is received during the monsoon season. Hence, some parts of the country sometimes face water scarcity during other seasons. Drought often leads to the worst impact on Indian water security (Mishra 2020). Drought is classified into four categories: meteorological, hydrological, agricultural, and socioeconomic drought (Wilhite and Glantz 2019), based on the type of water scarcity, such as periods with a deficiency in rainfall, streamflow or groundwater, soil moisture, and supply and demand power of community, respectively (Wilhite and Glantz 2019). This chapter deals only on hydrological drought analysis. Most of the human activities are dependent on water resources like either groundwater or surface water. So, it is necessary to assess the hydrological drought (Hasan et al. 2019).

The drought is defined based on different indices over the years (Shiau 2006; Nazir et al. 2016; Ganguli and Reddy. 2012; Swetalina and Thomas 2016). SPI is the most popular index to measure meteorological drought across the world developed by McKee et al. (1993). SDI has been used by many researchers in different parts of the world (Chemeda et al. 2010; Tigkas et al. 2012; Hong et al. 2015). Kazemzadeh and Malekian (2016) analysed the trend of hydrological and meteorological droughts defined based on the SPI and SDI, respectively, using the non-parametric approach in northwestern Iran. SPI-based drought study is done in the Tone river basin in India by Meshram et al. (2019), and the annual departure of rainfall during drought years is found to be varying from -26% to -60% in 1976 and 1973 respectively in the basin.

Understanding the streamflow pattern would help to know the problems associated with drought and flood. Mann-Kendall (MK) test method is a non-parametric test that is the most widely accepted trend detection method (Kumar and Jain 2011). It is beneficial in finding out the exact variation in rainfall patterns and streamflow patterns. The results have high importance in the planning of different projects related to water resources. But, limited studies are present in analysing the trend of drought indices using the M-K test and Sen's slope estimator (Mahajan and Dodamani. 2015; Myronidis et al. 2018). Forecasting future conditions is also of great importance in water management and planning. Especially for irrigation practices and reservoir operations, medium to long-term forecasting of streamflow and drought conditions is very useful. Many models have been developed to do streamflow forecasting, including low flow recession models, rainfall-runoff models, time series models, and artificial neural network models (Abudu et al. 2010). Time series models like Auto-Regressive Integrated Moving Average (ARIMA) methods are widely used for forecasting streamflow because of its systematic way of running the model and including more information (Zhou et al. 2008).

The Netravathi River basin is a dominant agricultural basin in the Western Ghats region of Karnataka, India. It plays a crucial role in serving the population in Dakshina Kannada District. With rapid population increase due to urbanization, the water demand is also increasing (Madhavi and Gowda 2014). Many industries and agricultural practices in the district mainly depend on this river. Hence, proper and systematic water management is necessary to meet the demands of the water for various purposes. Studies on trend analysis of streamflow and hydrological drought have not yet been reported in the Netravathi River basin. This part of the research aims to analyse the trend of streamflow and hydrological drought in the Netravathi River basin. Only hydrological drought is considered and defined using SDI at different time scales (SDI-3, SDI-6, SDI-9, and SDI-12). ARIMA model is used to forecast the streamflow to determine the drought conditions in future years. The results of this research could give some basic idea about the streamflow trend and hydrological drought trend.

6.2 STUDY AREA

6.2.1 Overview of the basin

The location of the study area is presented in Figure 6.1. The Netravathi is a west-flowing river that originates in the tropical forest of the Western Ghats of India in Karnataka and lies between 12°30´N and 13°10´N latitudes and 74°50´E-75°50´E longitudes. The basin has an area of approximately 3401.85 km^2. The river gauging station, Bantwal, is 25 km upstream of the river mouth. The average annual precipitation of the basin is 3076 mm, and around 80% of the annual rainfall is obtained during the monsoon season (June to September). The temperature ranges from 20℃ to 26℃. The upper portion is covered with dense forest, whereas the lower regions have agricultural lands and urban areas. The water of this river is mainly used for agricultural purposes, industrial uses, and drinking. Paddy is the main crop in this area. Sandy clay loam and clay loam are the main categories of soil found in the basin (Kumar and Eldho 2018).

6.2.2 Data used

The monthly streamflow data in the Netravathi River basin is used in this part of the research to analyse hydrological drought. The observed streamflow data at the river gauging station (Bantwal) is obtained from the Water Resources Information System, India, database (http://www.india.wris.nrsc.gov.in). The data obtained is from 1971 to 2016 (45 years of data), and the obtained seasonal and non-seasonal streamflow values are shown in Figure 6.2.

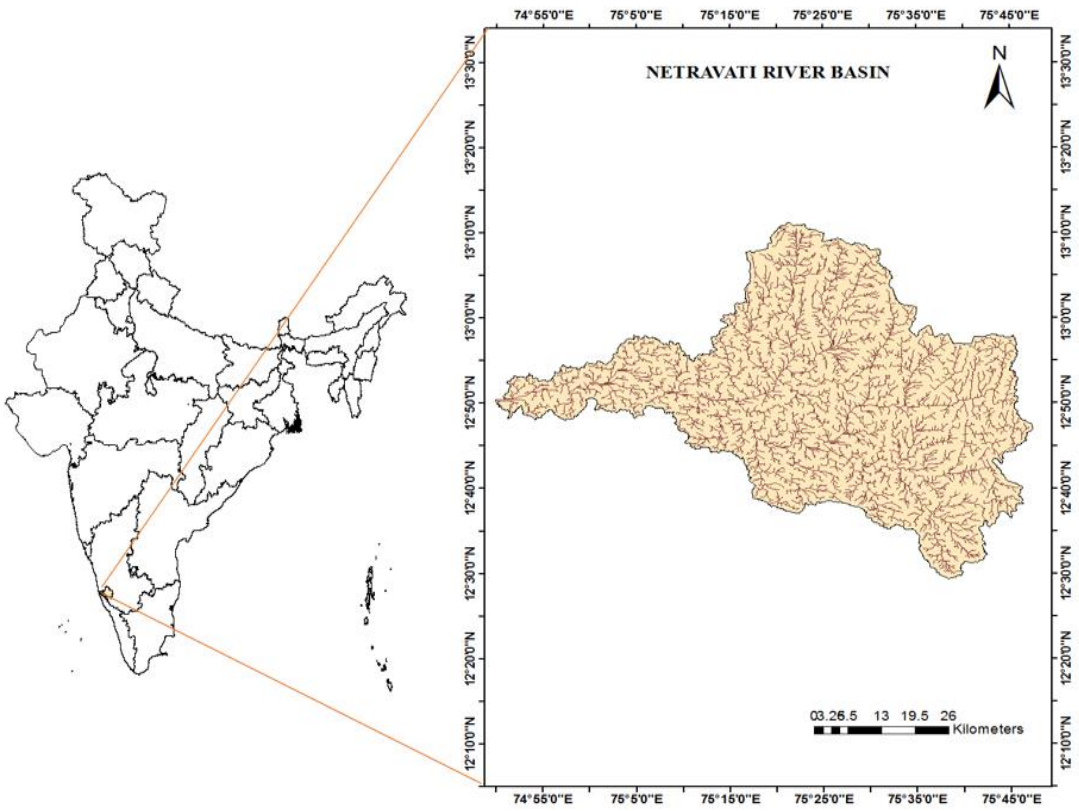

Figure 6.1. Location of Study Area

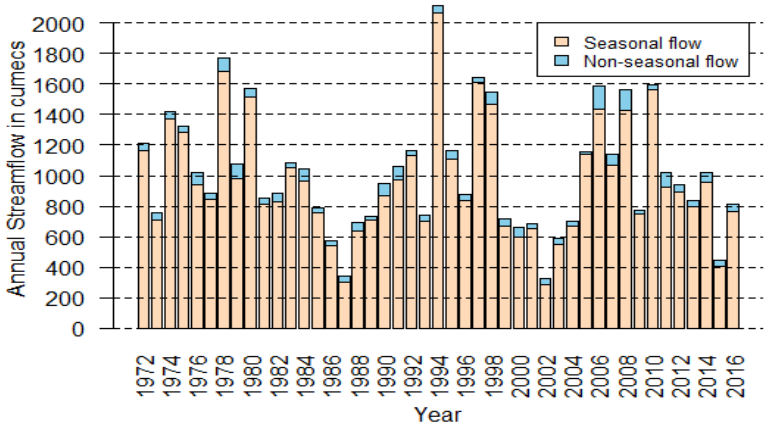

Figure 6.2. Seasonal and non-seasonal streamflow

6.3 METHODOLOGY

6.3.1 Departure analysis of streamflow

The departure of streamflow with respect to their long term mean can give much information for the analysis. Eq. (6.1) can be used to compute the annual and seasonal streamflow departure with respect to the mean values.

$$Departure(\%) = \frac{y_i - \bar{y}_i}{\bar{y}_i} \times 100 \tag{6.1}$$

Where, y_i is streamflow for a year or season i; and $\bar{y}_i$ is long term mean for the considered period.

6.3.2 Streamflow Drought Index

Nalbantis and Tsakiris (2009) developed the SDI based on monthly streamflow values (Q_{ij}) to characterize the hydrological drought, where the i indicates the hydrological year and j is the considered month within the hydrological year. SDI value is calculated based on the cumulative volume (V_{ik}) of the flow, and it is calculated based on the Eq. (6.2).

$$V_{ik} = \sum_{i=0}^{k} Q_{ij} \; ; \; i = 1,2,3,\ldots \; j = 1,2,3,\ldots 12 \; k = 1,2,\ldots \tag{6.2}$$

where V_{ik} is the cumulative volume of the streamflow for hydrological year i, k is the month base period and the k values 1,2,3 and 4 indicate 3 months, 6 months, 9 months, and 12 months SDI, respectively. The SDI value for i^{th} hydrological year is defined as below;

$$SDI_{ik} = \frac{V_{ik} - \bar{V}_k}{S_k} \tag{6.3}$$

$\bar{V}_k$ and S_k are mean of the discharge and standard deviation of the cumulative volume for k^{th} period.

Tsakiris (2008) categorized the hydrological drought into mild, moderate, severe and extreme when the SDI values are in the interval of $-1 \le SDI < 0$, $-1.5 \le SDI < -1$, $-2 \le SDI < -1.5$ and $-2 > SDI$ respectively.

6.3.3 Trend Analysis

The entire streamflow data is divided into four seasons: namely, monsoon, post-monsoon, winter, and summer. Sen's slope estimator is used to get the magnitude of the trend in the time series data. In this method, the slopes of all the pairs of ordinal time points are computed using the median of those slopes as the overall slope (Sen 1968; Gilbert 1987). Slopes of data pairs are calculated based on Eq. (6.4).

$$T_i = \frac{x_j - x_k}{j - k} \quad \text{for } i = 1, 2, ..., \text{N} \tag{6.4}$$

where x_j and x_k are data values at times j and k ($j > k$), respectively. The median of N values of T_i is taken as Sen's slope estimator of a slope and is given as;

$$Q_{med} = T_{\frac{N+1}{2}} \text{ if N is odd} \tag{6.5}$$

$$Q_{med} = \frac{1}{2}\left(T_{\frac{N}{2}} + T_{\frac{N+2}{2}} \right) \text{ if N is even.} \tag{6.6}$$

The negative values of Q represent the decreasing trend, and a positive value indicates the increasing trend of the given time series data.

6.3.4 Significance of Trend

To determine the presence of a statistically significant trend, the Mann-Kendall (MK) technique is widely used in the research. Both hypotheses, namely, the null hypothesis (no trend) and the alternative hypothesis (increasing or decreasing trend), are checked using this method. The MK test statistic(S) is given as

$$S = \sum_{i=1}^{n-1} \sum_{j=i+1}^{n} \text{sgn}(x_j - x_i) \tag{6.7}$$

Where x is data points at time j and i ($i > j$) and n is the number of data. The sign function is given as

$$\text{sgn}(x_j - x_i) = \begin{cases} +1 \text{ if } (x_j - x_i) > 1 \\ 0 \quad \text{if } (x_j - x_i) = 0 \\ -1 \quad \text{if } (x_j - x_i) < 1 \end{cases} \tag{6.8}$$

The S statistic is assumed to be approximately normal when the sample size is greater than 8 ($n \geq 8$), with

$$E(S) = 0 \tag{6.9}$$

$$Var(S) = \frac{n(n-1)(2n+5) - \sum_t t(t-1)(2t+5)}{18} \tag{6.10}$$

where t is the extent of any given tie. A tie is the sample of data with the same values and $\sum_t$ is the overall summation ties. Statistical significance is evaluated based on the Z value and is calculated using the Eq. (6.11)

$$Z = \begin{cases} \frac{S-1}{\sqrt{Var(S)}} & \text{if S>0} \\ 0 & \text{if S=0} \\ \frac{S+1}{\sqrt{Var(S)}} & \text{if S<1} \end{cases} \tag{6.11}$$

The probability p of Z statistic is estimated as given below

$$p = 0.5 - \frac{1}{\sqrt{2\pi}} \int_0^{|Z|} e^{\frac{-t^2}{2}} dt \tag{6.12}$$

In this part of the research, the null hypothesis is tested at a 95% confidence level. Hence the null hypothesis H_0 (ie., there is no trend in the tie series data) is rejected, and the alternative hypothesis H_A (i.e., presence of a trend in the series) is accepted if the p-value is less than or equal to the chosen significance level ($\alpha = 0.05$). The trend of streamflow is evaluated by considering the hydrological year comprising of 12 months starting from June. The trend analysis for streamflow was done for annual, monsoon, post-monsoon, winter, and summer seasons. The trend of SDI values at different time scales, namely SDI-3, SDI-6, SDI-9, and SDI-12, were also investigated.

6.3.5 Future discharge

ARIMA model is the generalization of the Autoregressive Moving Average (ARMA) model. An ARIMA (p, d, q) is given by the Eq. (6.13)

$$\Phi_p(\beta)_p \Delta^d Z_t = \theta_q + \theta(B) a_t \tag{6.13}$$

Φ_p, θ_q are polynomials for p and q order, B is backward shift operator, and a_t is the independent variable.

Seasonal ARIMA (SARIMA) models are used to deal with the seasonality associated with the data. It can be represented as ARIMA$\left(p,d,q\right)\left(P,D,Q\right)_L$, where *p, d,* and *q* are non-seasonal autoregressive, differencing, and moving average terms, respectively. $\left(P,D,Q\right)_S$ represents corresponding seasonal components for seasonality 's'. SARIMA model is defined in Eq. (6.14).

$$\Phi(B^S)\varphi(B)(1-B^S)^D(1-B)^d\, yt = \Theta(B^S)\theta(B)\varepsilon_t \tag{6.14}$$

where ϕ and φ are autoregressive parameters of seasonal and non-seasonal components, respectively; Θ and θ are moving average parameters of seasonal and non-seasonal components respectively; ε_t is independently distributed random variable; $B =$ backward operator, $B(y_t) = y_{t-1}; (1-B^S)^D =$ D$^{\text{th}}$ seasonal difference of season s.

The model initial parameters (*p, q, P, Q*) are determined based on an ACF diagram and PACF diagram. Ljung-Box Q test is used to test the autocorrelation of forecasts. By using the auto-ARIMA model, it is easy to find out the best model for the data. The main advantage of using the auto ARIMA model is that the model directly fits the best model by trying different combinations of *p, d,* and *q* values based on AIC criteria. Kwiatkowski-Phillips-Schmidt-Shin (KPSS) test is used by auto ARIMA to determine the number of differences (d) in the Hyndman-Khandakar algorithm.

6.4 RESULTS AND DISCUSSION

6.4.1 Basic statistics and Departure analysis of streamflow

The basic statistical parameters like mean, standard deviation, and variance of different seasonal and annual streamflow are presented in Table 6.1. The annual cycle of

streamflow is shown in Figure 6.3. From 1971 to 2016, the mean annual streamflow value is 359.14 cumecs with a standard deviation (sd) of 135.75. Monsoon occurs from June to September, and the higher flow occurs during this season. The mean streamflow during monsoon is 964.87 cumecs, with a standard deviation of 381.83 cumecs. Least flow is observed during the winter and summer seasons for the considered period. The highest variance is observed in monsoon. In Figure 6.3, the flow of the river increases from May onwards, attains its peak in July, and then decreases. The lowest value is observed in March.

Table 6.1 Statistical Parameters of streamflow

Statistical Parameters	Monsoon	Post monsoon	Winter	Summer	Annual
min	289.4054	44.385	0	0	128.7868
max	2068	558.85	49.33333	270.4275	726.5173
mean	964.8707	170.7326	13.05353	15.37449	359.1371
sd	381.8385	92.03083	10.88222	42.20175	135.7556
variance	145800.6	8469.674	118.4227	1780.988	18429.58

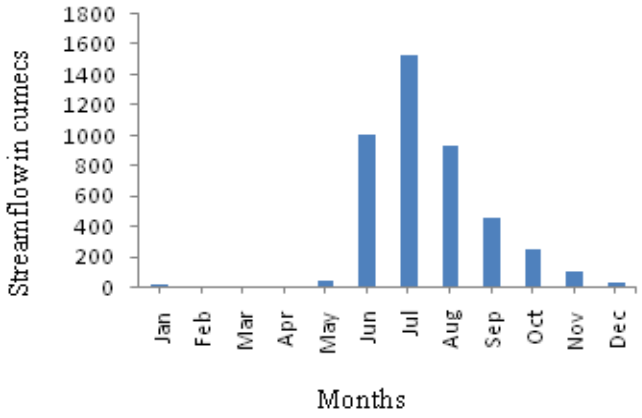

Figure 6.3. The annual cycle of streamflow

The annual and seasonal departure of streamflow from the long-term (1971-2016) mean has been computed using Eq. (6.1) for the basin. Results are demonstrated in Figure 6.4. It is observed that the streamflow is above normal in the beginning for some consecutive years, followed by below normal values for the next few years, following a nearly cyclic behaviour.

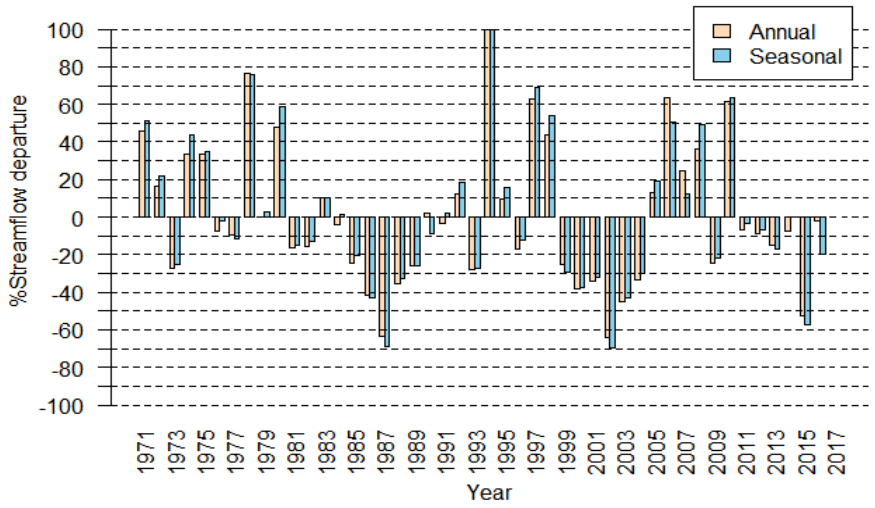

Figure 6.4. Annual and seasonal departure of streamflow

From 1999 to 2004, a continuous deficiency can be observed in both the annual and seasonal streamflow. The maximum deficiencies are observed in the year 2002 and are 64.37% and 69.68%, respectively for annual and seasonal. Similarly, from 1984 to 1989 and from 2011 to 2016, continuous deficiency has occurred in the annual flow. According to the India Meteorological Department, in 1994, India witnessed the highest seasonal rainfall of around 110% of the long-period average. In the same year (1994), the highest excess annual and seasonal flows were observed in the basin, which is above the normal.

6.4.2 Hydrological Drought Assessment

The SDI values calculated for the four-reference period are illustrated in Figure 6.5 for the period from 6/1971 to 5/2016. The reference period considered for SDI-3 is from June to August, which covers the three months of monsoon (Jun-Sep).

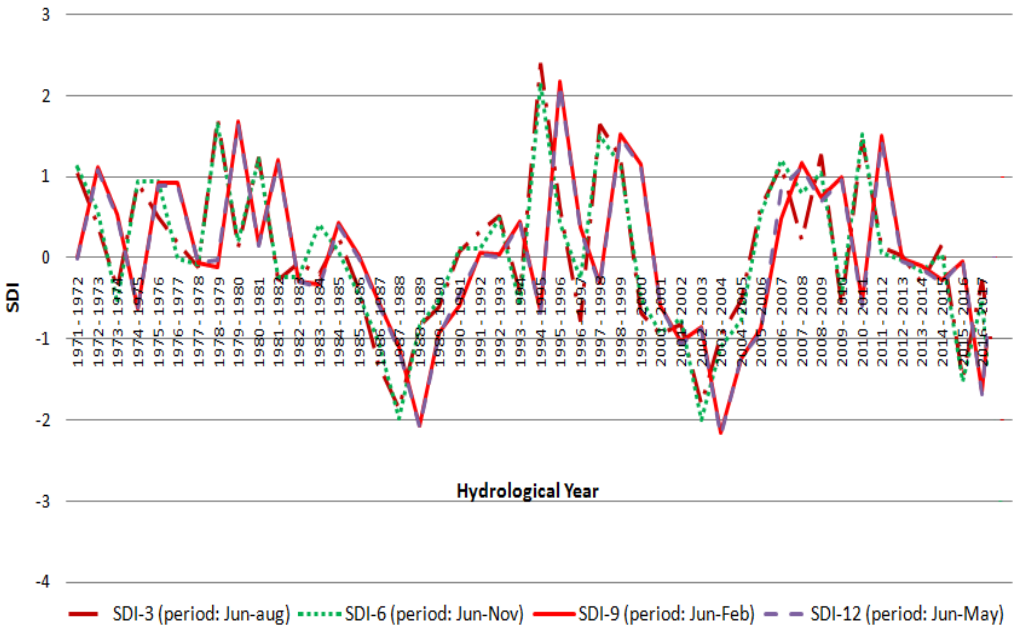

Figure 6.5. SDI value for all the reference period

From Figure 6.5, it is observed that SDI-9 and SDI-12 are showing almost similar values for the considered periods. Here, SDI-9 is for February, and SD-12 is for May. Both months have the least flow values. Severe droughts observed from SDI-3 and SDI-6 have occurred in 1987-1988, 2003-2004, and 2015-2016 hydrological years and only 2017-2018 is the hydrological year with extreme drought. Based on SDI-9 and SDI-12, only 2016-2017 was the hydrological year with severe drought, while in 1988-1989 and 2003-2004 hydrological years, extreme droughts were observed. The first three reference periods converged more with the SDI-12. Comparing Figure 6.5 with Figure 6.4, the streamflow deficiency can be observed during the drought-detected years. So there exists a matching between the deficit in the flow and drought conditions.

6.4.3 Trend Analysis

The streamflow trend for annual and four seasons has been analysed from 1971 to 2016 using the M-K test and Sen's slope estimator tests (Table 6.2) at a 95% confidence interval. Monsoon, winter, summer, and annual streamflow showed a negative trend, and the Sen's slope values are -9.4557, -1.697, -0.37, and -0.970, respectively. Post-monsoon showed an increasing trend. But except for winter and summer, all other

seasons have no statistical significance. Winter and summer are showing a statistically significant decreasing trend. The M-K test and Sen's slope test results for SDI are shown in Table 6.3. Decreasing trends can be observed for all SDIs (SDI-3, SDI-6, SDI-9, and SDI-12). M-K test statistics revealed that these observed trends for SDI are significant. The decreasing trend in the SDIs is indicating the increasing drought conditions in the basin.

Table 6.2 Results of the M-K test for streamflow

Parameters	Monsoon	Post monsoon	Winter	Summer	Annual
Kendall's tau (τ)	-0.145	0.025	-0.543	-0.275	-0.057
S	-32.00	24.00	-145.00	-74.00	-54.00
p value	0.228	0.816	**<0.0001**	**0.021**	0.592
Sen's slope	-9.4557	0.203	-1.697	-0.37	-0.970

Note: Bold figures indicate significant trend

Table 6.3 Results of the M-K test for SDI

Parameters	SDI-3	SDI-6	SDI-9	SDI-12
Kendall's tau (τ)	-0.175	-0.127	-0.099	-0.099
S	-9132.00	-3253.00	-15173.00	-15094.00
p value	**<0.0001**	**<0.0001**	**0.001**	**0.00**
Sen's slope	-0.004	-0.005	-0.001	-0.001

6.4.4 Streamflow forecast and future drought

Monthly streamflow data from 1971 to 2016 was used for forecasting the streamflow till 2024. The stationarity of monthly streamflow was checked using the augmented Dickey-Fuller test (ADF), and it was found that the p-value is less than 0.05; hence it is stationary. Periodic peaks and lows in the graph indicated seasonality in the data, and it was proved in the trend analysis using the M-K test at $\alpha = 0.05$. In order to find out the best ARIMA model, auto.arima from the forecast package of R is used, and the obtained best fit as ARIMA $(1, 0, 1)(1, 1, 0)_{12}$ with -0.0276 and -0.4770 as autoregressive parameters of non-seasonal and seasonal components, respectively. Using the best fit model, the streamflow is forecasted until December 2024. The observed, predicted and forecasted streamflow values together are plotted (Figure 6.6). From Figure 6.6, it is observed that the model is unable to capture the very high flow and very low flow values. The forecasted flow for two years (Jan 2015 to Dec 2016) was compared with the observed value, as shown in Figure 6.7. During this validation period, the R^2 value obtained is 0.85. The model is found to be useful to forecast high streamflow values during monsoon.

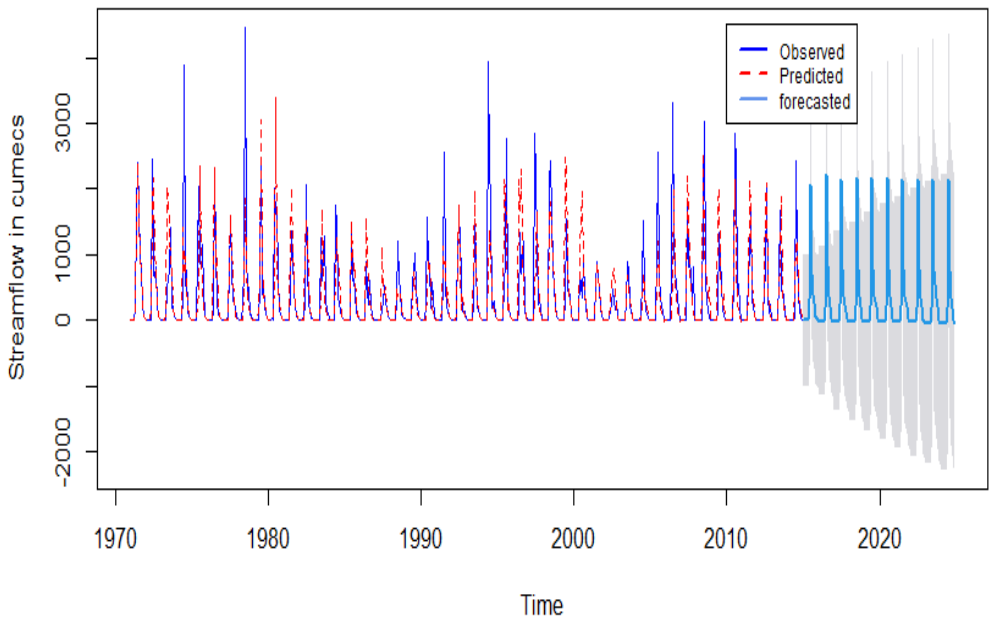

Figure 6.6. Observed, predicted and forecasted streamflows

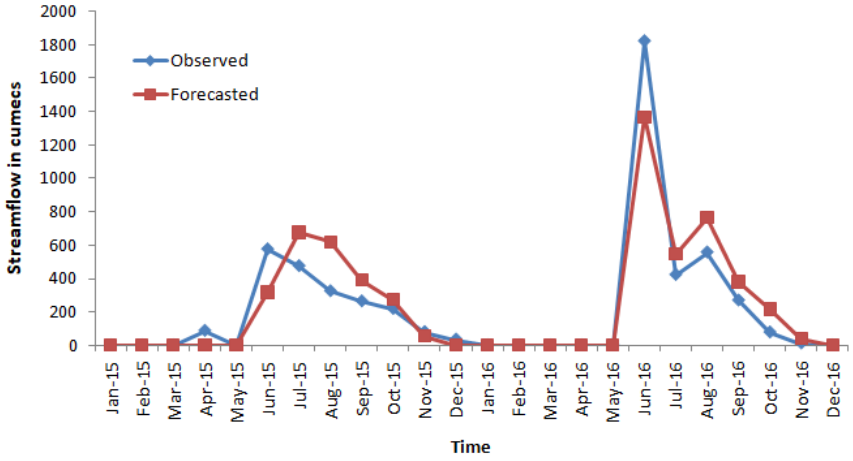

Figure 6.7. Observed data and forecasted flow values from January 2015 to December 2016

The annual cycle of streamflow obtained for the period from 2021 to 2024 is shown in Figure 6.8. During this period, more streamflow is expected in July. Except during the monsoon season, the flow values reach zero. SDI-3 for the reference period Jun-Aug is calculated from the forecasted flow values from 2017 to 2024 (Figure 6.9). All values of SDI-3 are between 0 and -0.1; hence, only mild drought conditions are expected in the future. From 2020 to 2024, the SDI value is becoming more negative, indicating the increased trend of risk of drought in the basin.

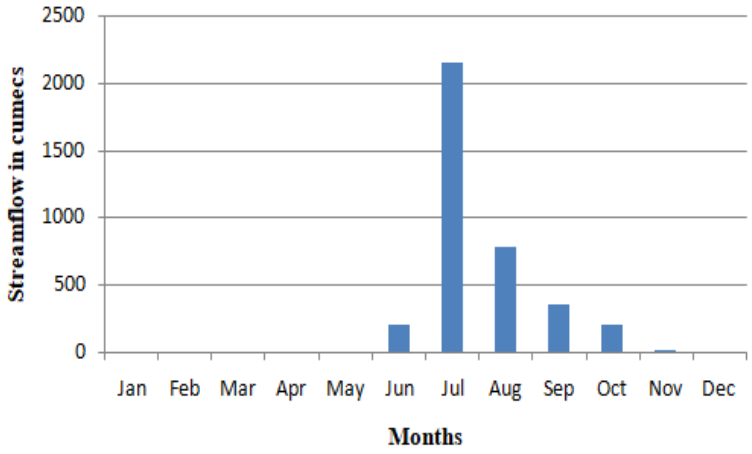

Figure 6.8. Annual cycle of streamflow for the forecasted period

Figure 6.9. SDI-3 (Period: Jun-Aug)

6.5 CLOSURE

This part of the research used 45 years of streamflow data for the trend analysis and the future prediction of streamflow and drought. Analysing the historical data, cyclic up and down behaviour was observed in the percentage departure of streamflow. SDI at different time scales successfully captured the drought conditions based on streamflow patterns. SDI-3 and SDI-6 showed severe drought conditions in the basin during the hydrological year 2003-2004. A maximum deficiency in the streamflow was observed around the same period for both annual and seasonal flows. The trend analysis test of streamflow by the M-K method showed a significant decreasing trend during winter and summer. The seasonal ARIMA model was the best fit for the data, and the model forecasted the discharge until 2024. SDI-3 calculated for the forecasted streamflow estimated mild drought over the forecasted period. The above results indicate that SDI is a useful drought index for the hydrological drought analysis.

CHAPTER 7

A NON-STATIONARY HYDROLOGIC DROUGHT INDEX IN HUMID RIVER BASIN IN INDIA

7.1 GENERAL

Hydrological drought is related to a deficiency of streamflow (Chemeda et al. 2010). It is represented by using various drought indices such as Streamflow Drought Index (SDI) (Myronidis et al. 2018), the Standardized Streamflow index (SSI) (Shamshirband et al. 2020), Standardized Terrestrial Water Storage Index (SWSI) (Zhu et al. 2021). The calculation of these indices is based on the stationary assumption, but in the changing climate, non-stationarities in the streamflow cannot be ignored, and stationary indices lead to inaccurate results (Jehanzaib et al. 2020). Previous research has established the impact of large-scale climate variables on the rainfall pattern in India (Agilan and Umamahesh, 2018).

Recent research has mostly focused on drought studies using non-stationary indices, like the Non-stationary Standardized Precipitation Index (NSPI) (Li et al. 2015a), time-dependent Standardized Precipitation Index (SPIt) (Wang et al. 2015b), and non-stationary Reconnaissance Drought Index (RDI_N) (Das et al. 2021). These indices were developed for the analysis of meteorological drought. The hydrological drought is associated with streamflow deficiency, so it is also essential to consider climate change in the hydrological drought index. Because of its simplicity, the Standardized Streamflow Index (SSI) has been used by various researchers globally for drought studies (Botai et al., 2021; Harisuseno 2020; Shamshirband et al., (2020). Various researchers examined the influence of the SOI and ENSO index on the Indian climate (Agilan and Umamahesh 2018; Ajayamohan and Rao 2008; Zhang et al. 2013). In non-stationary modeling, the generalized additive model for location, scale, and shape (GAMLSS) is a widely used algorithm (Das et al. 2020; Shiau 2020; Yu and Kim 2019).

In terms of the geographical area experiencing drought, Rajasthan is first, with Karnataka coming in second in India (Reddy and Prabhu, 2017). Most of the droughts in Karnataka were reported in arid regions. Although Dakshina Kannada experiences

heavy rain during the monsoon, recent years have reported drought situations throughout the summer (Gowda et al. 2015). Water scarcity exists due to the extensive expansion of industries during the past two decades. Revadekar et al. (2011) examined a declining trend in heavy rainfall along the coastal region of Karnataka in the future. Economic development of Dakshina Kannada is significantly influenced by the Netravathi River. There is very less research found in the literature on the drought conditions of Netravathi River basin. So, it is necessary to study the drought situations in the river basin and to implement necessary water management programs to reduce the water scarcity problems. The primary goal of part of this research is to create a non-stationary standardized streamflow drought index using climate indices for the Netravathi River basin. It is compared with the traditional hydrological drought index. Drought severity, peak, and duration are also calculated and compared under both scenarios.

7.2 STUDY AREA

7.2.1 Overview of the basin

The Netravathi River basin covers 3401 km2 and has been chosen as the study area. It originates in the Indian state of Karnataka, in the Western Ghats, and flows westward. The basin is situated between 12°30'N and 13°10'N latitudes and 74°50'E and 75°50'E longitudes. The river gauging station is located in Bantwal. The annual average rainfall is 3076 mm, and the temperature is 20℃ to 26℃. The monsoon season begins in June and lasts until September. The water from the river is mainly used for agricultural purposes, and the main crop in the region is paddy. Sandy clay loam and clay loam are the main types of soil found in the region (Kumar and Eldho. 2018). This river is the primary water source for nearby cities such as Mangalore, Bantwal, Dharmasthala, and Puttur. The study area map is shown in Figure 7.1.

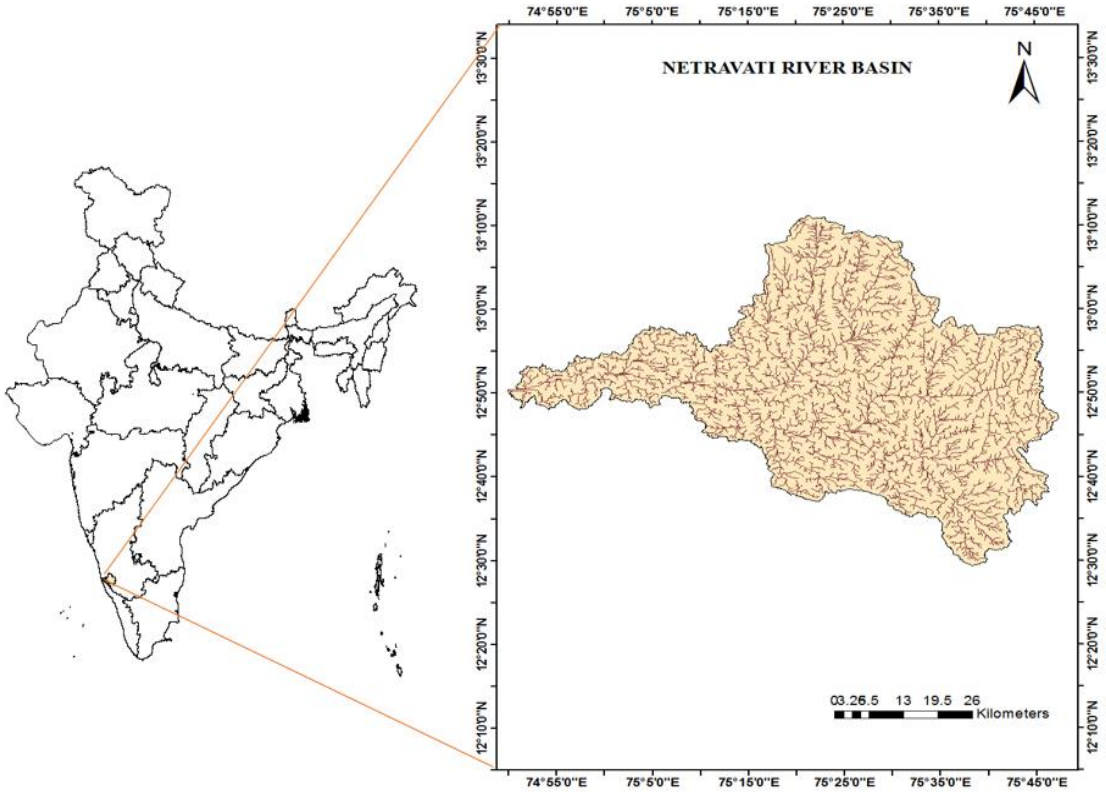

Figure 7.1. Study Area

7.2.2 Data used

The monthly streamflow data of the Netravathi River is obtained from the Water Resources Information System, India, database (http://www.india.wris.nrsc.gov.in). It is the observed data at the Bantwal River gauging station from 1971 to 2016. The climate indices such as SST, SOI, and IOD are obtained for the same period from www.esrl.noaa.gov.

7.3 METHODOLOGY

7.3.1 Climate Indices

In this research, three climate variables, IOD, SOI, and SST, are taken as covariates for constructing non-stationary models. The streamflow data are arranged to 3, 6, 12, and 24 months time scales. The monthly data of climate indices are arranged to 0 to 12

months lags. The Kendall correlation test is performed at a 5% significance level to find the best lag of climate data correlated with the streamflow data arranged on different time scales. Different combinations of selected climate indices are also checked to find the best combination for non-stationary modeling.

7.3.2 Hydrologic Drought Index

This study defines the hydrological drought using the streamflow-based Standardized Streamflow Index, and a new drought index based on climate variables is developed. The SSI is calculated based on the SPI concept. The first step is to identify the marginal distribution that fits the data the best. For instance, the gamma distribution is selected as the best-fitted probability distribution (Botai et al. 2021). The probability density function of a Gamma distribution shape parameter α and scale parameter β are given as:

$$g(x) = \frac{1}{\beta^{\alpha}\,\Gamma(\alpha)}\, x^{\alpha-1}\, \mathrm{e}^{\frac{-x}{\beta}} \tag{7.2}$$

Its cumulative probability density is given below:

$$F(x) = q + (1-q)G(x) \tag{7.3}$$

where $G(x)$ is the cumulative distribution function for the non-zero streamflow q is the probability of zero values. The cumulative distribution is then changed to a normal distribution with zero mean value and unit standard deviation to get SSI values. The drought is classified into different categories and is given in Table 7.1 (Tsakiris, 2009).

Table 7.1 Classification of drought

Index values	Class	Category
-1 ≤ SSI<0	Mild drought	C1
-1 .5 ≤ SSI<-1	Moderate drought	C2
-2 ≤ SSI<-1.5	Severe drought	C3
SSI< -2	Extreme drought	C4

7.3.3 Calculation of the non-stationary index

The GAMLSS is used for non-stationary modeling (Rigby and Stasinopoulos 2005). The non-stationary gamma distribution with linearly varying location parameters is used to calculate the non-stationary Standardized Streamflow Index (NSSI), and it is given as follows:

$$X_t \sim gamma\ (\mu_t,\ \sigma) \tag{7.4}$$

$$\mu_t = c_0 + c_1 I_1(t) + c_2 I_2(t) ..... + c_n I_n(t) \tag{7.5}$$

where, constants are $c_0, c_1, .., c_n$, and the covariates are $I_1, I_2, .., I_n$ at time t. The parameters are computed using the maximum likelihood approach. NSSI is classified similarly to SSI (Table 7.1) and can monitor drought events on various time scales.

The stationary and non-stationary indices based on drought properties are calculated. The duration is defined by the number of consecutive months with an index value below the threshold, where the threshold value is typically -1. The severity is the total of those index values for that duration. Peak is the lowest value of the index for that specific period.

7.4 RESULTS AND DISCUSSIONS

7.4.1 Significant lag of climate indices

For the time scales of 3, 6, 12, and 24 months, the cumulative streamflow data are calculated. The lag of the climate oscillations ranges from 0 to 12 months. The correlation between streamflow on various time scales and climate oscillation on 0 to 12 lags was tested using the Kendall correlation method at a significance level of 5%. The significant lag obtained is listed in Table 7.2. At all time scales, only SOI exhibited a significant influence on streamflow. SST had no significant correlation on streamflow at 3 and 6 months time scales. Except for the 6 months time scale, IOD showed a significant correlation at all other time scales, and at the 12 months time scale, there was a concurrent association between IOD and streamflow. There was a concurrent association of SST and SOI with the flow at 24 and 6 months time scales, respectively. So, the climate oscillations with significant lag are taken as a covariate for developing a non-stationary index.

Table 7.2 Significant lag of climate indices

Climate oscillations	SST	SOI	IOD
Time scale			
3-months	-	9	11
6-months	-	0	-
12-months	2	1	0
24-months	0	1	2

7.4.2 Non-stationary drought index

The gamma distribution is identified to be the best fit for streamflow data in this research (Botai et al. 2021). The stationary model is made using gamma distribution with both parameters as constant. For the non-stationary model, the location parameter of the distribution is considered to be varied linearly with the selected covariates. Various combinations of climate oscillations at significant lags are tested to find the best model based on AIC values. The selected covariates and AIC values of models are tabulated in Table 7.3. Combination of SST and IOD was the best for non-stationary models at 12 and 24 months time scales. At all time scales, the AIC values of non-stationary models were less than the stationary models. The non-stationary model is selected since the same is better than the stationary model at all time scales based on the statistical measure.

Table 7.3 Selected covariates and AIC values of models

Time scale	Selected covariates and lag	AIC value of non-stationary	AIC value of stationary
3-months	IOD_{11}	8053.60	8230.86
6-months	SOI_0	9486.72	9592.23
12-months	SST_2, IOD_0	9445.99	9482.70
24-months	SST_0, IOD_2	9774.04	9813.20

The non-stationary gamma with constant sigma and linearly varying Mu is taken for calculating the non-stationary hydrologic drought index NSSI. The equation of Mu and Sigma are given in Table 7.4. The distribution parameters are computed using the Maximum Likelihood Estimation (MLE) approach.

Table 7.4 Equations of μ and σ values

Time scale	Equations
3-months	$\mu(t) = 6.92615-0.29054\ IOD_{11}(t)$
	$\sigma = 1.701114$
6-months	$\mu(t) = 7.692151+0.007906\ SOI_0(t)$
	$\sigma = 1.121142$
12-months	$\mu(t) = 8.36594-0.07928\ SST_2(t)+0.18086\ IOD_0(t)$
	$\sigma = 0.3568845$
24-months	$\mu(t) = 9.06111-0.09120\ SST_0(t)+0.18638\ IOD_2(t)$
	$\sigma = 0.2914951$

7.4.3 Comparison of drought classes

The drought classes, based on the index values based on Table 7.1, are mild (C1), moderate (C2), severe (C3), and extreme (C4) droughts. Figure 7.2 illustrates the percentage occurrence of drought classes under stationary and non-stationary conditions. Based on both approaches, C1 has a higher percentage of occurrence at all time scales. C2 has a higher frequency based on non-stationary than stationary index at all scales except 24 months. At all time scales, the occurrence frequency of all types of drought classes for stationary and non-stationary indices varies; hence it can be postulated that climate oscillations influence the drought class in the basin.

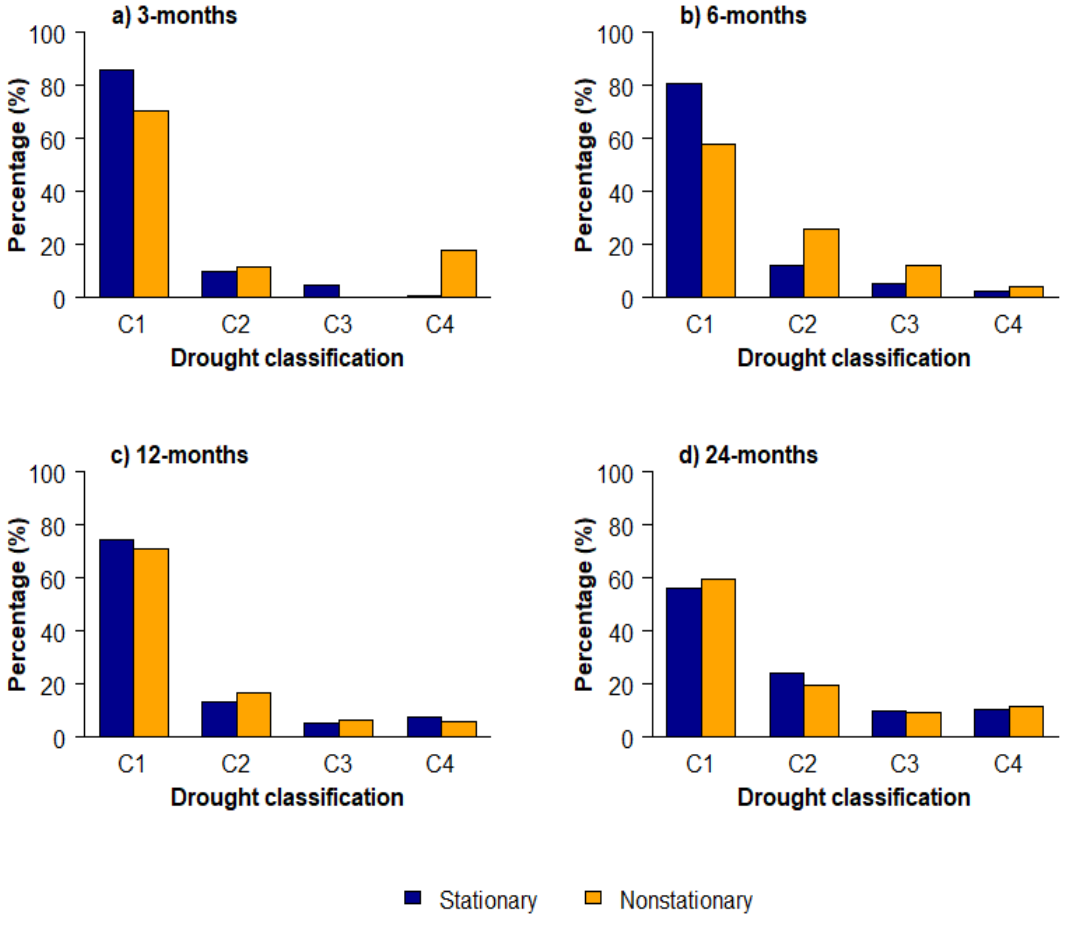

Figure 7.2. Percentage occurrence of drought classes

7.4.4 Comparison of drought properties

The peak, severity, and duration of drought events are calculated from SSI and NSSI values, and its statistical characteristics are given in Table 7.5. The mean duration, severity, and peak values obtained from NSSI are higher than those obtained from SSI at all the time scales except at 12 months. In every case, drought properties under stationary conditions differ from non-stationary conditions. For the comparative study, the probability density of drought duration is also plotted in Figure 7.3. At all the time scales, a noticeable difference is observed in the density plots of duration. The density plot for non-stationary is shifted towards the right of the stationary plot at the time scales of 6 and 12 months. This variation shows the association of climate indices to drought properties.

Table 7.5 Statistical characteristics of drought properties

	SSI			**NSSI**		
	Duration (in months)	**Severity**	**Peak**	**Duration (in months)**	**Severity**	**Peak**
3-months						
Mean	1.71	2.35	1.33	2.38	4.17	1.57
Maximum	4.00	6.85	2.13	4.00	8.80	2.24
Minimum	1.00	1.01	1.01	1.00	1.00	1.00
6-months						
Mean	2.16	3.09	1.35	2.22	3.46	1.88
Maximum	7.00	13.47	2.29	4.00	7.55	3.89
Minimum	1.00	1.00	1.00	1.00	1.00	1.00
12-months						
Mean	9.25	14.17	1.49	5.92	9.12	1.46
Maximum	26.00	41.61	2.30	24.00	40.70	2.50
Minimum	1.00	1.00	1.00	1.00	1.01	1.01

24-months						
Mean	13.62	21.42	1.44	16.00	26.27	1.72
Maximum	48.00	80.31	2.52	49.00	79.13	2.68
Minimum	1.00	1.02	1.02	1.00	1.22	1.17

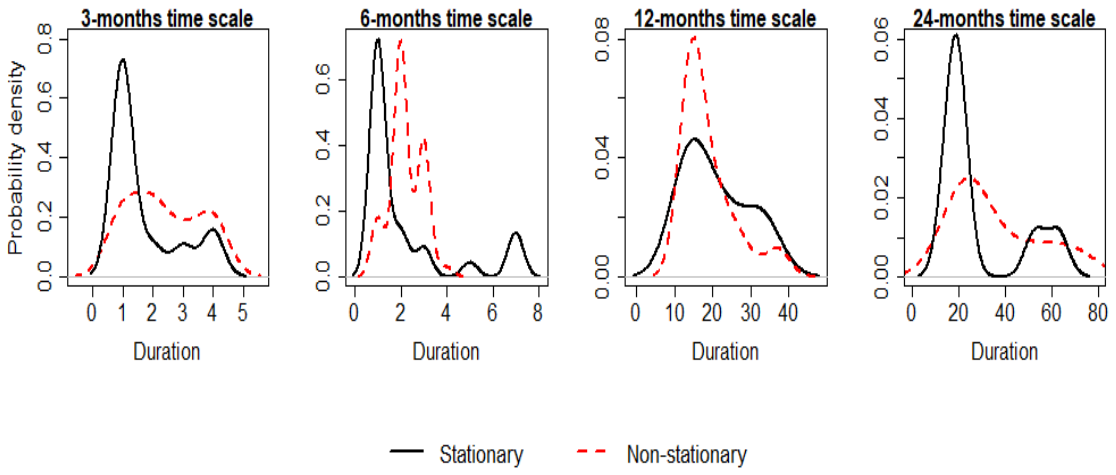

Figure 7.3 Probability density of duration

7.4.5 Departure analysis of streamflow and comparison with historical droughts

The annual and seasonal departure of streamflow of the Netravathi basin is computed using eq. (6.1), and plotted in Figure 7.4. Cyclic up and down behavior can be observed in the graph. The maximum deficiency observed in seasonal and annual rainfall was 69.68% and 64.37%, respectively, in 2002. In 1987, the deficiency was also more than 60%. A continuous deficiency was observed in the annual and seasonal flow from 1984 to 1989, 1999 to 2004, and 2011 to 2016. According to the India Meteorological Department, 110% of long-period average seasonal rainfall was obtained in India in 1994; hence, excess flow can be observed in the river in the same year. Both stationary and non-stationary indices were plotted and depicted in Figure 7.5. The deficiency in the streamflow is the primary reason for hydrological drought in a basin. From Figure 7.5, the drought events can be observed during the streamflow deficiency years.

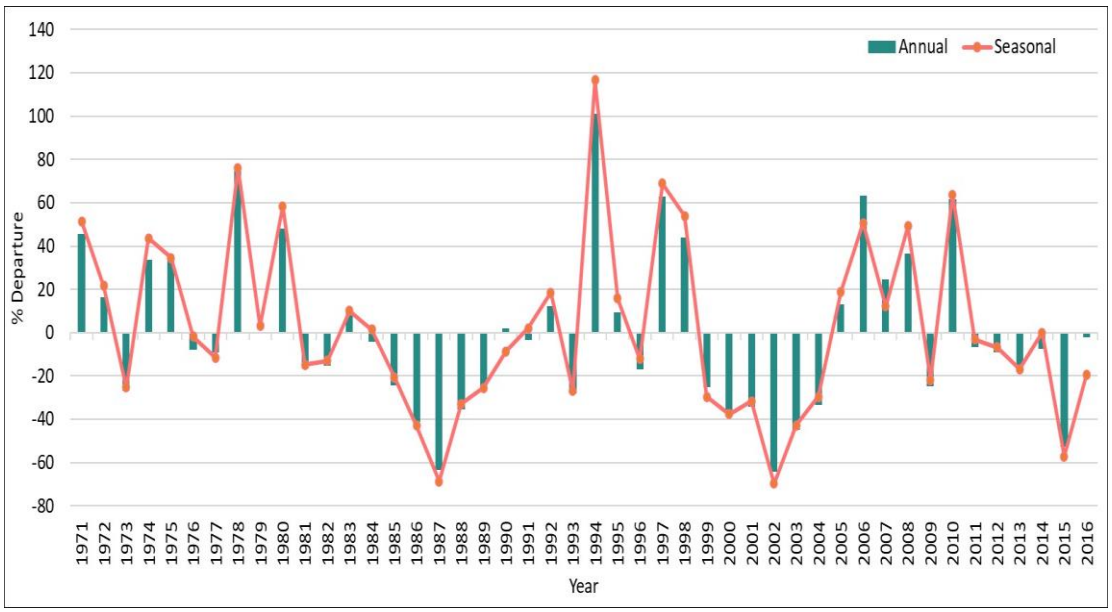

Figure 7.4. Annual and seasonal departure of streamflow

India experienced the worst drought situations in 1917, 1918, 1965, 1966, 1986,1987, 2002, 2009, and 2012 during the last century (Manual for drought management 2016). According to previous studies, Karnataka faced severe drought from 2001 to 2004, 2009, and 2012 (Jayasree and Venkatesh 2015; Srinivasareddy et al. 2019). In the same years, the deficiency in the streamflow of Netravathi can be observed. NSSI also clearly showed the drought conditions during the same period (Figure 7.5). The numbers of drought events are higher under short-term compared to longer-duration drought in the basin. Even though Dakshina Kannada receives much rain during the monsoon, recent years have been noted as drought conditions throughout the summer (Gowda et al. 2015). After 2000, the severity of drought is observed to be increased in the basin, and this is well captured by NSSI than SSI.

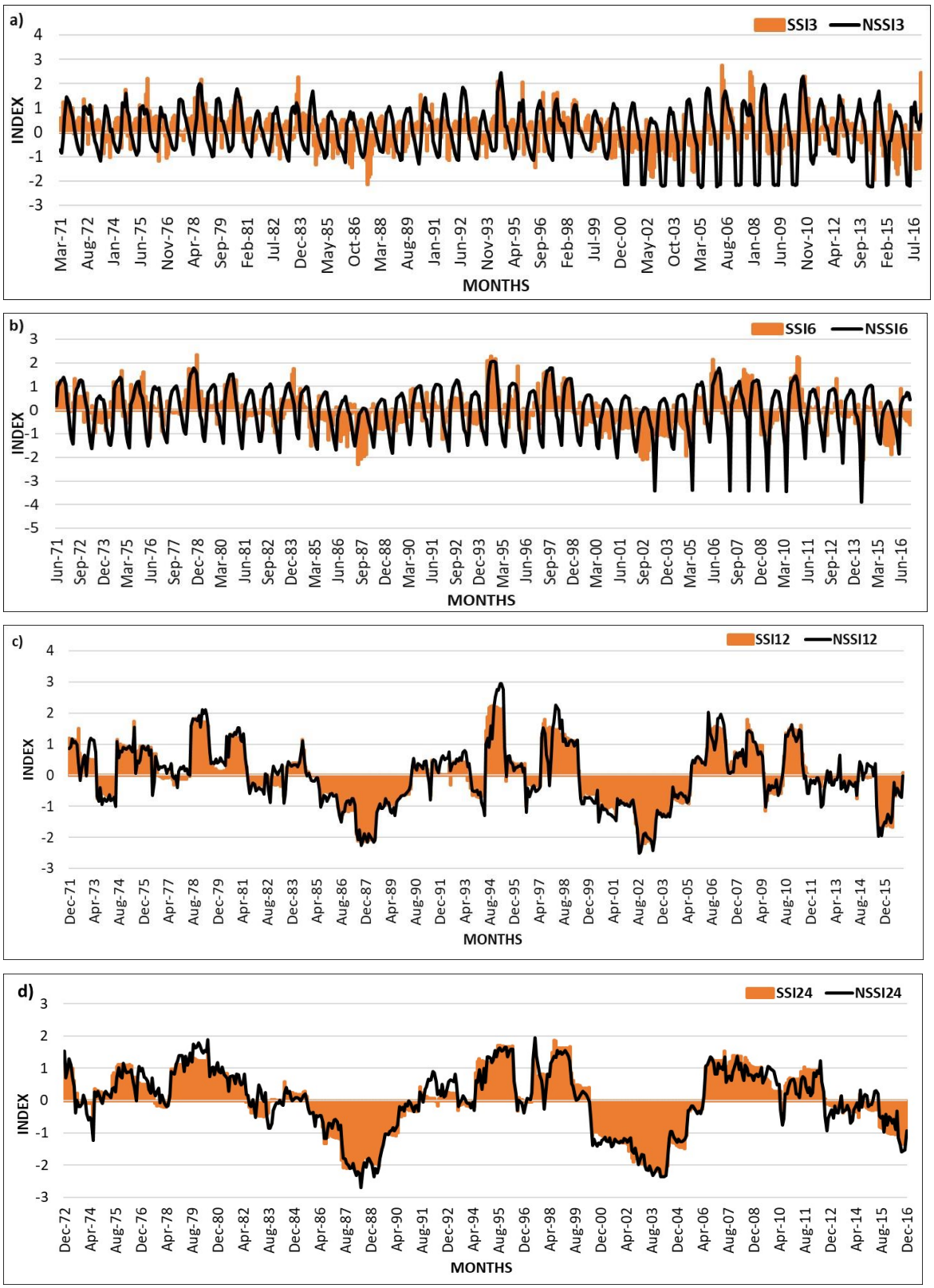

Figure 7.5. Stationary and non-stationary indices; a) 3 months, b) 6 months, c) 12 months, d) 24 months

7.5 CLOSURE

The streamflow at various time scales significantly correlated with various climate indices with different lags. Hence, the non-stationary models were constructed with the GAMLSS algorithm and compared with the traditional stationary models. From statistical measures, non-stationary models were the best at all the time scales. The influence of climate variables on drought classes, drought properties, and probability density plots was observed. From the comparison of NSSI with streamflow departure and historical drought events, it was found that the NSSI is better than SSI at detecting more severe drought events at short-term scales. The hydrological drought in the basin was the main focus of this part of the research.

CHAPTER 8

SUMMARY AND CONCLUSIONS

This research highlights the critical importance of assessing droughts in a changing climate using non-stationary models. These models offer a more accurate and reliable assessment of drought conditions, capturing the influence of time-varying climatic factors. Two meteorological subdivisions in India (Saurashtra and Kutch and Coastal Karnataka) with contrasting climates are taken for drought analysis. Four climate indices, such as SOI, SST, MEI, and IOD, are considered for developing non-stationary meteorological drought index in these study areas. For analyzing hydrological drought, the Shetrunji river basin in Saurashtra and the Netravathi River basin in Coastal Karnataka were selected. The non-stationary drought indices were calculated using SOI, SST, MEI, IOD, AMO, AO, NAO, and PDO as covariates in the Shetrunji river basin. Whereas only IOD, SOI, and SST were considered for the Netravathi River basin.

Interestingly, in every case, climate indices showed a significant influence on drought characteristics. The non-stationary drought indices outperformed stationary indices in all study areas, underscoring the necessity of incorporating non-stationary models in drought studies to accurately capture the complex and dynamic nature of climatic influences on drought. Additionally, the accuracy of drought predictions could be significantly enhanced using hybrid forecasting models, particularly those combining Neural Networks with conventional time-series models like ARIMA.

8.1 METEOROLOGICAL DROUGHT ANALYSIS IN ARID AND HUMID REGIONS

Stationary and nonstationary meteorological drought indices are developed for Saurashtra and Kutch and Coastal Karnataka. The gamma distribution is obtained as the best fitted marginal distributions to rainfall data across various time scales (3, 6, 12, and 24 months). Only the location parameter is considered as varying with covariates. Best combination of climate indices is taken from the selected lags of indices based on AIC criteria. Drought characteristics and drought properties are analysed. Additionally, the impact of rainfall on agricultural productivity is examined, showing that bajra (pearl

millet) and rice yields in Saurashtra and Kutch and Coastal Karnataka, respectively, are influenced by rainfall availability. Major conclusions from this part of the research are given below.

- SST, SOI, MEI, and IOD significantly correlate with rainfall at all time scales at different lags. This underlines the intricate relationship between these climatic factors and regional rainfall patterns.
- The superior performance of the non-stationary model with climate oscillations as a covariate is observed at all time scales in both study areas.
- A significantly large correlation is observed between drought properties such as peak, severity, and duration, with the highest correlation of 0.97 between duration-severity and severity-peak for NSPI24. The results indicate the necessity of bivariate analysis. Hence, copula is considered for bivariate analysis, and return period analysis shows a higher drought risk in Saurashtra and Kutch than in Coastal Karnataka.
- The drought risk is underestimated by the univariate return period in the 'or' scenario and overestimated in the 'and' criteria. Hence, bivariate analysis is more useful in drought risk studies.
- Coastal Karnataka experiences much higher rainfall than Saurashtra and Kutch. The 5^{th} percentile rainfall in Coastal Karnataka is 129 times higher than in Saurashtra and Kutch, and the 95^{th} percentile rainfall is 51 times higher. This indicates a substantial contrast in precipitation patterns between the two regions.
- The copula-based non-exceedance conditional probability analysis shows that the higher productivity values of bajra are sensitive to higher precipitation levels. The highest probability for low productivity (100-300 kg/ha) is at lower precipitation (10^{th} percentile), while the highest productivity ranges (900-1100 kg/ha) are less likely and occur at high precipitation (95^{th} percentile).
- Rice productivity is also influenced by precipitation, with the highest probability for moderate productivity (1600-1800 kg/ha) at the 25^{th} percentile precipitation. Higher productivity ranges (2000-2600 kg/ha) are more sensitive to higher precipitation levels.

- There is a significant correlation between the bajra yield loss rate and the drought index at all time scales, with the highest correlation (0.49) in September on the 12-month time scale. Hence, September is a critical month for bajra productivity.
- Historical data indicate severe yield reductions during drought years, such as a 65.19% reduction in 1974 and a 59.04% reduction in 1987, aligning with periods of extreme drought as shown by the NSPI.
- There is no significant correlation between the rice yield loss rate and the drought index at any time scale, reflecting the region's high rainfall and its mitigating effect on drought impacts. The maximum rice yield loss was -24.49% in 1982, with a continuous yield loss from 1981 to 1987, a period also marked by severe to extreme dry conditions, according to the NSPI.

The results provide valuable insights into the behavior of meteorological droughts in these regions, the associated risks, and the implications for agricultural productivity under changing climate scenarios. The findings can aid in better drought preparedness and management strategies, ensuring more resilient agricultural practices in climatic uncertainties.

8.2 DROUGHT PREDICTION

The Saurashtra and Kutch is a highly drought-prone regions in India. Hence, identifying the drought patterns in advance is crucial for implementing effective mitigation methods to reduce risk. To address this, hybrid models combining ARIMA and Neural Network models such as FNN and RNN, are developed and investigated. Linear-nonlinear (ARIMA-FNN and ARIMA-RNN) and nonlinear-linear (FNN-ARIMA and RNN-ARIMA) combinations are examined to identify the most suitable drought prediction model. The key findings from this analysis are:

- The input variable selected through feed forward and backward selection methods shows a similar result to those obtained from PACF methods, ensuring the robustness of the selection process. Lag-1 has the highest correlation at all time scales.

- Among individual models, FNN performed best at all time scales during both training (with CC values 0.878, 0.873, 0.903, and 0.953 at 3, 6, 12, and 24 months, respectively) and testing phases (with CC values 0.829, 0.873, 0.838, and 0.874 at 3, 6, 12, and 24 months, respectively).
- NSPI6 was the best-performing index for short-term droughts (with CC= 0.894, R^2 = 0.800, MSE = 0.210, MAE = 0.336, RAE = 0.389 during testing phase by RNN-ARIMA), while NSPI24 was best for long-term droughts (with CC= 0.864, R^2 = 0.758, MSE = 0.122, MAE = 0.264, RAE = 0.441 during testing phase by FNN-ARIMA).
- ARIMA model demonstrated good results at short time scales (with CC values 0.771 and 0.754 for 3 and 6 months scales during testing), but was less effective at longer time scales (with CC values 0.078 and 0.238 for 12 and 24 months scales during testing).
- The superior performance of FNN-ARIMA during training (with CC values 0.879, 0.873, 0.908, and 0.954, at 3, 6, 12, and 24 months, respectively) and testing stages is observed at all time scales except at 6 months (with CC values 0.835, 0.873, 0.848, and 0.884, at 3, 6, 12, and 24 months, respectively), where RNN-ARIMA was the best during testing (with CC values 0.815, 0.894, 0.821, and 0.851, at 3, 6, 12, and 24 months, respectively).
- NN and NN-ARIMA models performed well at all time scales with CC and R^2 greater than 0.6 in the testing and training phases.

The hybrid models, particularly FNN-ARIMA and RNN-ARIMA, provided more accurate and reliable predictions, especially for long-term drought indices. These findings underscore the potential of hybrid modeling approaches in enhancing drought prediction accuracy, thereby enabling better preparedness and response strategies in drought-prone regions like Saurashtra and Kutch. The use of advanced hybrid models can significantly contribute to more effective drought risk management and mitigation efforts, ultimately supporting the resilience of agricultural and water resource management in these areas.

8.3 HYDROLOGICAL AND METEOROLOGICAL DROUGHTS IN ARID RIVER BASIN

Nonstationary models with varying location parameters and models with varying location and scale parameters were developed to assess hydrological and meteorological droughts in the arid Shetrunji River basin in Saurashtra, India. These models utilized ENSO, IOD, NAO, AO, PDO, and AMO as covariates and were compared to stationary models. Understanding the propagation of meteorological drought to hydrological drought is crucial for effective drought and water resources management. Hence, a comparative analysis is conducted between two types of droughts. Additionally, the drought impact on rabi and kharif crops is also analysed. The conclusions are given below:

- Nonstationary indices (NSPI and NSSI) with varying Mu and Sigma were more effective in indicating extreme drought events compared to stationary indices, making them more suitable for capturing severe to extreme drought events in the basin.
- A significant correlation between meteorological and hydrological drought indices was observed at all time scales under both stationary and nonstationary conditions, indicating the impact of meteorological drought on hydrological drought. The highest correlation of 0.48 is obtained for NSPI and NSSI at 3 and 6 months time scales.
- From cross-correlation analysis, a consistent positive correlation was found at a one-month lag. Specifically, September NSPI3 and October NSSI3 showed the strongest positive association (0.61). This finding indicates a strong linkage between meteorological conditions in September and subsequent hydrological responses in October.
- At a 6 month scale, hydrological drought in the region responded well to meteorological drought, with a response rate of 91.13%. This highlights the heightened sensitivity of hydrological drought to meteorological drought conditions in the Shetrunji River basin.

- The cubic model proved to be the best fit between NSPI and NSSI at all time scales, and the best at 3 months scale with R^2 of 0.45. The statistical relationships between the hydrometeorological indices are valuable tools for predicting hydrological drought periods in the research area in advance from meteorological drought index.
- Bajra experienced the highest loss rate of -92.55% in productivity during the worst drought year, 1987. Wheat also suffered a notable loss rate of -49.47% in productivity during 1987.
- The bajra yields were more adversely affected by drought during the monsoon season (with the highest correlation of 0.51 with NSPI12 in September) than in the winter season (with the highest correlation of 0.49 with NSPI12 in December). Conversely, wheat showed a more substantial yield reduction during the winter season (with the highest correlation of 0.46 with NSPI12 in November) compared to the monsoon season (with the highest correlation of 0.41 with NSP3 in September).

This differential impact highlights the varied responses of crop types to seasonal drought conditions, emphasizing the complexity of their sensitivities to environmental factors. Understanding these variations can guide agricultural planning and crop management, ensuring better adaptation strategies to mitigate drought impacts on different crops throughout the year.

8.4 HYDROLOGICAL DROUGHT IN HUMID RIVER BASIN

The Netravathi River basin, located in the humid coastal region of Karnataka, India, has recently experienced severe water scarcity during the summer, highlighting the need for comprehensive drought studies. Initially, the stationary hydrological drought index SDI is calculated. Additionally, the suitability of non-stationary SSI is evaluated for drought analysis in the Netravathi river basin by considering SST, SOI, and IOD as covariates.

- The Mann-Kendall (M-K) test revealed a statistically significant decreasing trend in streamflow during winter and summer (Sen's slope of -1.697 and -0.37,

respectively), along with a decreasing trend in SDI at all time scales (Sen's slope of -0.004, -0.005, -0.001, and -0.001 at 3, 6, 9, and 12 months) indicating increasing drought conditions in the basin.

- Using the ARIMA model for drought forecasting, it is anticipated that the region may face mild drought conditions in the future.
- The non-stationary model with a varying location parameter outperformed the stationary model across all time scales. The influence of climate indices is observed on drought properties and drought classes.

The findings from these non-stationary models provide a deeper understanding of the drought dynamics in the Netravathi River basin. Incorporating these climate indices into drought prediction models offers valuable insights that can enhance the accuracy of drought forecasts.

8.5 LIMITATIONS

- This research is specific to regions, focusing on the Saurashtra and Kutch, Coastal Karnataka. The findings and models developed may not be directly applicable to other regions with different climatic and hydrological conditions.
- This research analysed only the temporal difference of drought, which may limit our understanding of the spatial correlation between the indices.
- The geographical distances and response times between ocean and land are not analysed in detail, which is also a limitation of this research.
- The impact analysis of drought on crop yields, such as bajra and wheat, focuses on specific crops and seasons. Other crops and agricultural practices within the regions were not analysed, which could provide a more complete picture of the agricultural impacts of drought.

8.6 SCOPE OF FUTURE WORK

- It is worth noting that future research should expand the analysis to include other types of droughts, such as agricultural and socio-economic droughts, and consider additional climate variables. Additionally, exploring the non-stationarity of other distribution parameters and drought properties could further

enhance the understanding of drought dynamics. Also, the study should be expanded to include other drought-prone regions in India and globally, allowing for comparative analysis and validation of models in diverse climatic and hydrological conditions.

- Investigating the suitability of a wider range of prediction models could enhance the accuracy of prediction and reliable forecasts. Hence, future research should consider performance analysis of other Machine Learning models and forecasting each drought type separately to understand diverse challenges by drought events.
- In future drought studies, spatial analysis is also recommended in addition to temporal analysis. It would be even more interesting if such research could also conduct a comparative analysis with other drought indices, including temperature, socioeconomic factors, and anthropogenic activities.

REFERENCES

Abarghouei, H. B., and Kousari, M. R. (2013). "Prediction of drought in dry lands through feedforward artificial neural network abilities." *Arab J Geosci*, 1417–1433.

Abudu, S., Cui, C. L., King, J. P., and Abudukadeer, K. (2010). "Comparison of performance of statistical models in forecasting monthly streamflow of Kizil River, China." *Water Sci. Eng.*, 3(3), 269–281.

Achite, M., Elshaboury, N., Jehanzaib, M., Vishwakarma, D. K., Pham, Q. B., Anh, D. T., Abdelkader, E. M., and Elbeltagi, A. (2023). "Performance of Machine Learning Techniques for Meteorological Drought Forecasting in the Wadi Mina Basin, Algeria." *Water (Switzerland)*, 15(4).

Achour, K., Meddi, M., Zeroual, A., Bouabdelli, S., Maccioni, P., and Moramarco, T. (2020). "Spatio-temporal analysis and forecasting of drought in the plains of northwestern Algeria using the standardized precipitation index." *J. Earth Syst. Sci.*, 129(1).

Adarsh, S., Karthik, S., Shyma, M., Prem, G. Das, Shirin Parveen, A. T., and Sruthi, N. (2018). "Developing Short Term Drought Severity-Duration-Frequency Curves for Kerala Meteorological Subdivision, India Using Bivariate Copulas." *KSCE J. Civ. Eng.*, 22(3), 962–973.

Agilan, V., and Umamahesh, N. V. (2017). "What are the best covariates for developing non-stationary rainfall Intensity-Duration-Frequency relationship ?" *Adv. Water Resour.*, 101, 11–22.

Agilan, V., and Umamahesh, N. V. (2018). "El Niño Southern Oscillation cycle indicator for modeling extreme rainfall intensity over India." *Ecol. Indic.*, 84(Jan), 450–458.

Ajayamohan, R. S., and Rao, S. A. (2008). "Indian ocean dipole modulates the number of extreme rainfall events over India in a warming environment." *J. Meteorol. Soc. Japan*, 86(1), 245–252.

Aladag, H. ., Egrioglu, E., and Kadilar, C. (2012). "Improvement in Forecasting Accuracy Using the Hybrid Model of ARFIMA and Feed Forward Neural Network." *Am. J. Intell. Syst.*, 2(2), 12–17.

Ali, Z., Hussain, I., Faisal, M., Nazir, H. M., Hussain, T., Shad, M. Y., Shoukry, A. M.,

and Gani, S. H. (2017). “Forecasting Drought Using Multilayer Perceptron Artificial Neural Network Model Zulifqar.” *Adv. Meteorol.*, 2017.

Alsumaiei, A. A., and Alrashidi, M. S. (2020). “Hydrometeorological drought forecasting in hyper-arid climates using nonlinear autoregressive neural networks.” *Water (Switzerland)*, 12(9).

Amirataee, B., Montaseri, M., and Rezaie, H. (2018). “Regional analysis and derivation of copula-based drought Severity-Area-Frequency curve in Lake Urmia basin, Iran.” *J. Environ. Manage.*, 206, 134–144.

AMO. (2023). “Atlantic Multidecadal Oscillation (AMO) Index Time Series Data.” *Boulder, CO NOAA Phys. Sci. Lab.*, <https://psl.noaa.gov/data/timeseries/AMO/>.

AO. (2023). “Arctic Oscillation (AO) Index Monthly Data.” *Boulder, CO NOAA Clim. Predict. Cent.*

Ashok, K., and Saji, N. H. (2007). “On the impacts of ENSO and Indian Ocean dipole events on sub-regional Indian summer monsoon rainfall.” *Nat. Hazards*, 42(2), 273–285.

Asseng, S., Ewert, F., Martre, P., Rötter, R. P., Lobell, D. B., Cammarano, D., Kimball, B. A., Ottman, M. J., Wall, G. W., White, J. W., Reynolds, M. P., Alderman, P. D., Prasad, P. V. V., Aggarwal, P. K., Anothai, J., Basso, B., Biernath, C., Challinor, A. J., Sanctis, G. De, Doltra, J., Fereres, E., Garcia-Vila, M., Gayler, S., Hoogenboom, G., Hunt, L. A., Izaurralde, R. C., Jabloun, M., Jones, C. D., Kersebaum, K. C., Koehler, A. K., Müller, C., Naresh Kumar, S., Nendel, C., O’leary, G., Olesen, J. E., Palosuo, T., Priesack, E., Eyshi Rezaei, E., Ruane, A. C., Semenov, M. A., Shcherbak, I., Stöckle, C., Stratonovitch, P., Streck, T., Supit, I., Tao, F., Thorburn, P. J., Waha, K., Wang, E., Wallach, D., Wolf, J., Zhao, Z., and Zhu, Y. (2015). “Rising temperatures reduce global wheat production.” *Nat. Clim. Chang.*, 5(2), 143–147.

Bacanli, Ü. G. (2012). “Entropy based assessment and palmer drought severity index of drought analysis.” *Sci. Res. Essays*, 7(44), 3823–3833.

Bandyopadhyay, N., Bhuiyan, C., and Saha, A. K. (2016). “Heat waves, temperature extremes and their impacts on monsoon rainfall and meteorological drought in Gujarat, India.” *Nat. Hazards*, 82(1), 367–388.

Bandyopadhyay, N., and Saha, A. K. (2014). “Analysing Meteorological and Vegetative Drought in Gujarat.” Springer Japan, 61–71.

Bandyopadhyay, N., and Saha, A. K. (2016a). “A comparative analysis of four drought indices using geospatial data in Gujarat, India.” *Arab. J. Geosci.*, 9(5), 1–11.

Bandyopadhyay, N., and Saha, A. K. (2016b). “A comparative analysis of four drought indices using geospatial data in Gujarat, India.” *Arab. J. Geosci.*, 9(5), 341.

Bates, Bryson, Zbigniew Kundzewicz, and S. W., and Vi, P. (2008). *Climate change and water*. Intergovernmental Panel on Climate Change Secretariat.

Bazrafshan, J., and Hejabi, S. (2018). “A Non-Stationary Reconnaissance Drought Index (NRDI) for Drought Monitoring in a Changing Climate.” *Water Resour. Manag.*, 32(8), 2611–2624.

Beck, H. E., Zimmermann, N. E., Mcvicar, T. R., Vergopolan, N., Berg, A., and Wood, E. F. (2018). “Data Descriptor : Present and future Köppen-Geiger climate classi fi cation maps at 1 -km resolution.” *Nat. Publ. Gr.*, 1–12.

Bhatla, R., Singh, A. K., Mandal, B., Ghosh, S., Pandey, S. N., and Sarkar, A. (2016). “Influence of North Atlantic Oscillation on Indian Summer Monsoon Rainfall in Relation to Quasi-Binneal Oscillation.” *Pure Appl. Geophys.*, 173(8), 2959–2970.

Bhuiyan, C., Saha, A. K., Bandyopadhyay, N., and Kogan, F. N. (2017). “Analyzing the impact of thermal stress on vegetation health and agricultural drought–a case study from Gujarat, India.” *GIScience Remote Sens.*, 54(5), 678–699.

Bonaccorso, B., Peres, D. J., Castano, A., and Cancelliere, A. (2015). “SPI-Based Probabilistic Analysis of Drought Areal Extent in Sicily.” *Water Resour Manag.*, 29, 459–470.

Borji, M., Malekian, A., Salajegheh, A., and Ghadimi, M. (2016). “Multi-time-scale analysis of hydrological drought forecasting using support vector regression (SVR) and artificial neural networks (ANN).” *Arab J Geosci*, 9(725).

Botai, C. M., Botai, J. O., Wit, J. P. De, Ncongwane, K. P., Murambadoro, M., Barasa, P. M., and Adeola, A. M. (2021). “Hydrological Drought Assessment Based on the Standardized Streamflow Index : A Case Study of the Three Cape Provinces of South Africa.” *water*, 13(24), 3498.

Bowden, G. J., Dandy, G. C., and Maier, H. R. (2005). “Input determination for neural network models in water resources applications. Part 1 - Background and methodology.” *J. Hydrol.*, 301(1–4), 75–92.

Burnham, K. P., and Anderson, D. R. (2004). “Multimodel inference: Understanding

AIC and BIC in model selection." *Sociol. Methods Res.*, 33(2), 261–304.

Cancelliere, A. (2017). "Non Stationary Analysis of Extreme Events." *Water Resour. Manag.*, 31(10), 3097–3110.

Cavazos, T., and Rivas, D. (2004). "Variability of extreme precipitation events in Tijuana, Mexico." *Clim. Res.*, 25(3), 229–243.

Chattopadhyay, R., Phani, R., Sabeerali, C. T., Dhakate, A. R., Salunke, K. D., Mahapatra, S., Rao, A. S., and Goswami, B. N. (2015). "Influence of extratropical sea-surface temperature on the Indian summer monsoon: An unexplored source of seasonal predictability." *Q. J. R. Meteorol. Soc.*, 141(692), 2760–2775.

Chemeda, D., Mukand, E., and Babel, S. (2010). "Drought Analysis in the Awash River Basin , Ethiopia." *Water Resour Manag.*, 24, 1441–1460.

Chen, L., Singh, V. P., Guo, S., Mishra, A. K., and Guo, J. (2013). "Drought Analysis Using Copulas." *J. Hydrol. Eng.*, 18(7), 797–808.

Cherchi, A., and Navarra, A. (2013). "Influence of ENSO and of the Indian Ocean Dipole on the Indian summer monsoon variability." *Clim. Dyn.*, 41(1), 81–103.

Cherian, S., Sridhara, S., Manoj, K. N., Gopakkali, P., Ramesh, N., Alrajhi, A. A., Dewidar, A. Z., and Mattar, M. A. (2021). "Impact of el niño southern oscillation on rainfall and rice production: A micro-level analysis." *Agronomy*, 11(6).

Chopra, P. (2006). "Drought Risk Assessment Using Remote Sensing and GIS: A Case Study of Gujarat." *Enschede, Netherlands ITC.*, 67.

Choudhury, S. (2018). "Agricultural development and inclusive growth in India." *Int. J. Adv. Res.*, 5(1), 41–52.

Dai, A. (2013). "Increasing drought under global warming in observations and models." *Nat. Clim. Chang.*, 3(1), 52–58.

Das, J., Gayen, A., Saha, P., and Bhattacharya, S. K. (2020a). "Meteorological drought analysis using Standardized Precipitation Index over Luni River Basin in Rajasthan, India." *SN Appl. Sci.*, 2(9), 1–17.

Das, J., Jha, S., and Goyal, M. K. (2020b). "On the relationship of climatic and monsoon teleconnections with monthly precipitation over meteorologically homogenous regions in India: Wavelet & global coherence approaches." *Atmos. Res.*, 238, 104889.

Das, J., Jha, S., and Goyal, M. K. (2020c). "Non-stationary and copula-based approach to assess the drought characteristics encompassing climate indices over the Himalayan

states in India." *J. Hydrol.*, 580.

Das, P. K., Chakraborty, A., and Seshasai, M. V. R. (2014). "Spatial analysis of temporal trend of rainfall and rainy days during the indian summer monsoon season using daily gridded (0.5° × 0.5°) rainfall data for the period of 1971-2005." *Meteorol. Appl.*, 21(3), 481–493.

Das, S., Choudhury, M. R., Gandhi, S., and Joshi, V. (2016). "Application of Earth Observation Data and Standardized Precipitation Index Based Approach for Meteorological Drought Monitoring, Assessment and Prediction Over Kutch, Gujarat, India." *Int. J. Environ. Geoinformatics*, 3(2), 24–37.

Das, S., Das, J., and Umamahesh, N. V. (2021). "Nonstationary Modeling of Meteorological Droughts: Application to a Region in India." *J. Hydrol. Eng.*, 26(2), 05020048.

Debele, S. E., Bogdanowicz, E., and Strupczewski, W. G. (2017a). "Around and about an application of the GAMLSS package to non-stationary flood frequency analysis." *Acta Geophys.*, 65(4), 885–892.

Debele, S. E., Strupczewski, W. G., and Bogdanowicz, E. (2017b). "A comparison of three approaches to non-stationary flood frequency analysis." *Acta Geophys.*, 65(4), 863–883.

Demirel, M. C., Venancio, A., and Kahya, E. (2009). "Flow forecast by SWAT model and ANN in Pracana basin, Portugal." *Adv. Eng. Softw.*, 40(7), 467–473.

Ding, Y., Gong, X., Xing, Z., Cai, H., Zhou, Z., Zhang, D., Sun, P., and Shi, H. (2021). "Attribution of meteorological, hydrological and agricultural drought propagation in different climatic regions of China." *Agric. Water Manag.*, 255(May), 106996.

Dixit, S., and Jayakumar, K. V. (2021). "A study on copula-based bivariate and trivariate drought assessment in Godavari River basin and the teleconnection of drought with large-scale climate indices." *Theor. Appl. Climatol.*, 146(3–4), 1335–1353.

Dixit, S., and Jayakumar, K. V. (2022). "A Non-stationary and Probabilistic Approach for Drought Characterization Using Trivariate and Pairwise Copula Construction (PCC) Model." *Water Resour. Manag.*, 36(4), 1217–1236.

DMI. (2023). "Dipole Mode Index (DMI) Monthly Time Series Data." *Boulder, CO NOAA Phys. Sci. Lab. Glob. Clim. Obs. Syst. Gr. Surf. Press.*, <https://psl.noaa/gov/data/timeseries/DMI>.

Dodangeh, E., Shahedi, K., Shiau, J. T., and Mirakbari, M. (2017). “Spatial hydrological drought characteristics in Karkheh river Basin, Southwest Iran using copulas.” *J. Earth Syst. Sci.*, 126(6), 1–20.

Duan, K., and Mei, Y. (2014). “Comparison of Meteorological , Hydrological and Agricultural Drought Responses to Climate Change and Uncertainty Assessment.” *Water Resour Manag.*, 5039–5054.

Dugam, S. S., Kakade, S. B., and Verma, R. K. (1997). “Interannual and long-term variability in the North Atlantic Oscillation and Indian Summer monsoon rainfall.” *Theor. Appl. Climatol.*, 58(1–2), 21–29.

Dutta, D., Kundu, A., and Patel, N. R. (2013). “Predicting agricultural drought in eastern Rajasthan of India using NDVI and standardized precipitation index.” *Geocarto Int.*, 28(3), 192–209.

Enfield, D. B., Mestas-Nunez, A. M., and Trimble, P. J. (2001). “The Atlantic Multidecadal Oscillation and its relation to rainfall and river flows in the continental U.S.” *Geophys. Res. Lett.*, 28(10), 2077–2080.

Francis, P. A., and Gadgil, S. (2006). “Intense rainfall events over the west coast of India.” *Meteorol. Atmos. Phys.*, 94(1–4), 27–42.

Frees, E. W., and Valdez, E. A. (1998). “Understanding Relationships Using Copulas.” *North Am. Actuar. J.*, 2(1), 1–25.

Fu, P., Jaiswal, D., McGrath, J. M., Wang, S., Long, S. P., and Bernacchi, C. J. (2021). “Drought imprints on crops can reduce yield loss: Nature’s insights for food security.” *Food Energy Secur.*

Gadgil, S., Vinayachandran, P. N., Francis, P. A., and Gadgil, S. (2004). “Extremes of the Indian summer monsoon rainfall, ENSO and equatorial Indian Ocean oscillation.” *Geophys. Res. Lett.*, 31(12), 2–5.

Ganguli, P. (2014). “Probabilistic analysis of extreme droughts in Southern Maharashtra using bivariate copulas.” *ISH J. Hydraul. Eng.*, 20(1), 90–101.

Ganguli, P., and Janga Reddy, M. (2013). “Analysis of ENSO-based climate variability in modulating drought risks over western Rajasthan in India.” *J. Earth Syst. Sci.*, 122(1), 253–269.

Ganguli, P., and Reddy, M. J. (2012). “Risk Assessment of Droughts in Gujarat Using Bivariate Copulas.” *Water Resour. Manag.*, 26(11), 3301–3327.

Ganguli, P., and Reddy, M. J. (2014). “Evaluation of trends and multivariate frequency analysis of droughts in three meteorological subdivisions of western India.” *Int. J. Climatol.*, 34(3), 911–928.

Garcia Galiano, S. G., Gimenez, P. O., and Giraldo-Osorio, J. D. (2015). “Assessing nonstationary spatial patterns of extreme droughts from long-term high-resolution observational dataset on a semiarid basin (Spain).” *Water (Switzerland)*, 7(10), 5458–5473.

Ghazaryan, G., König, S., Rezaei, E. E., Siebert, S., and Dubovyk, O. (2020). “Analysis of drought impact on croplands from global to regional scale: A remote sensing approach.” *Remote Sens.*, 12(24), 1–17.

GOI. (2016). “Drought Management Manual.” (1), 154.

Gonzalez, J. M., Rodriguez, H. G., Treviño, E. G., Ybarra, E. J., Moreno, M. P., and Perez, T. C. (2009). “Spatial and temporal tele-connections of the Multivariate Enso Index (MEI) to rainfall, maximum and minimum temperature anomalies in Mexico.” *IOP Conf. Ser. Earth Environ. Sci.*, 6(29), 292033.

Gowda, H. C. C., Girisha, K., and Gowda, C. C. (2015). “Nethravathi River - Water Supply Scheme in Dakshina Kannada District - A Case Study.” *Aquat. Procedia*, 4(Icwrcoe), 625–632.

Griffis, V. W., and Stedinger, J. R. (2007). “Incorporating Climate Change and Variability into Bulletin 17B LP3 Model.” *Proc., World Environmentaland Water Resources Congress*.

Gu, G., Adler, R. F., Huffman, G. J., and Curtis, S. (2007). “Tropical rainfall variability on interannual-to-interdecadal and longer time scales derived from the GPCP monthly product.” *J. Clim.*, 20(15), 4033–4046.

Guhathakurta, P., Menon, P., Inkane, P. M., Krishnan, U., and Sable, S. T. (2017). “Trends and variability of meteorological drought over the districts of India using standardized precipitation index.” *J. Earth Syst. Sci.*, 126(8), 1–18.

Gupta, V., and Jain, M. K. (2020). “Impact of ENSO, Global Warming, and Land Surface Elevation on Extreme Precipitation in India.” *J. Hydrol. Eng.*, 25(1), 05019032.

Guttman, N. B. (1999). “Accepting the standardized precipitation index: a calculation algorithm.” *J. Am. Water Resour. Assoc.*, 35(2), 311–322.

Hajirahimi, Z., and Khashei, M. (2022). “A Novel Parallel Hybrid Model Based on

Series Hybrid Models of ARIMA and ANN Models." *Neural Process. Lett.*, 54(3), 2319–2337.

Hangshing, L., and Dabral, P. P. (2018). "Multivariate Frequency Analysis of Meteorological Drought Using Copula." *Water Resour. Manag.*, 32(5), 1741–1758.

Harisuseno, D. (2020). "Comparative study of meteorological and hydrological drought characteristics in the Pekalen River basin, East Java, Indonesia." *J. Water L. Dev.*, 45, 19–41.

Hasan, H. H., Fatin, S., Razali, M., Muhammad, N. S., and Ahmad, A. (2019). "Research Trends of Hydrological Drought :A Systematic Review." *water*, 11, 1–19.

Hendrawan, V. S. A., Kim, W., Touge, Y., Ke, S., and Komori, D. (2022). "A global-scale relationship between crop yield anomaly and multiscalar drought index based on multiple precipitation data." *Environ. Res. Lett.*, 17(1), 014037.

Himayoun, D., and Roshni, T. (2019). "Spatio-temporal variation of drought characteristics, water resource availability and the relation of drought with large scale climate indices: A case study of Jhelum basin, India." *Quat. Int.*, 525(July), 140–150.

Hinge, G., Piplodiya, J., Sharma, A., and Mohamed, M. M. (2022). "Evaluation of Hybrid Wavelet Models for Regional Drought Forecasting." *Remote Sens.*, 14, 6381.

Hirapara, J., Patel, P. K. S., Singh, M., and Patel, C. . (2020). "Analysis of Rainfall Characteristics for Crop Planning in North and South Saurashtra Region of Gujarat." *J. Agric. Eng.*, 57(2), 162–171.

Hong, X., Guo, S., and Zhou, Y. (2015). "Uncertainties in assessing hydrological drought using streamflow drought index for the upper Yangtze River basin." *Stoch. Environ. Res. Risk Assess.*, 29, 1235–1247.

Huang, S., Huang, Q., Leng, G., and Liu, S. (2016). "A nonparametric multivariate standardized drought index for characterizing socioeconomic drought : A case study in the Heihe River Basin." *J. Hydrol.*, 542, 875–883.

Jamir, T., Gadgil, A. S., and De, U. . (2008). "Recent floods related natural hazards over West coast and Northeast India." *J. Ind. Geophys. Union*, 12(4), 179–182.

Jayasree, V., and Venkatesh, B. (2015). "Analysis of Rainfall in Assessing the Drought in Semi-arid Region of Karnataka State, India." *Water Resour. Manag.*, 29(15), 5613–5630.

Jehanzaib, M., Shah, S. A., Kim, J. E., and Kim, T. W. (2023). "Exploring spatio-

temporal variation of drought characteristics and propagation under climate change using multi-model ensemble projections." *Nat. Hazards*, 115(3), 2483–2503.

Jehanzaib, M., Shah, S. A., Yoo, J., and Kim, T. W. (2020). "Investigating the impacts of climate change and human activities on hydrological drought using non-stationary approaches." *J. Hydrol.*, 588(March), 125052.

Jena, P., Kasiviswanathan, K. S., and Azad, S. (2020). "Spatiotemporal characteristics of extreme droughts and their association with sea surface temperature over the Cauvery River basin, India." *Nat. Hazards*, 104(3), 2239–2259.

Kao, S.-C., and Govindaraju, R. S. (2010a). "A copula-based joint deficit index for droughts." *J. Hydrol.*, 380(1–2), 121–134.

Kao, S. C., and Govindaraju, R. S. (2010b). "A copula-based joint deficit index for droughts." *J. Hydrol.*, 380(1–2), 121–134.

Karimi, M., Melesse, A. M., Khosravi, K., Mamuye, M., and Zhang, J. (2019). "Analysis and prediction of meteorological drought using SPI index and ARIMA model in the Karkheh River Basin, Iran." *Extrem. Hydrol. Clim. Var. Monit. Model. Adapt. Mitig.*, (July), 343–353.

Kaytez, F. (2020). "A hybrid approach based on autoregressive integrated moving average and least-square support vector machine for long-term forecasting of net electricity consumption." *Energy*, 197, 117200.

Kazemzadeh, M., and Malekian, A. (2016). "of meteorological and hydrological droughts in northwestern Iran." *Nat. Hazards*, 80(1), 191–210.

Kelkar, R. R., and Sreejith, O. P. (2020). "Meteorological sub-divisions of india and their geopolitical evolution from 1875 to 2020." *Mausam*, 71(4), 571–584.

Keskin, M. E., Terzi, Ö., Taylan, E. D., and Küçükyaman, D. (2011). "Meteorological drought analysis using artificial neural networks." 6(21), 4469–4477.

Khatiwada, K. R., and Pandey, V. P. (2019). "Characterization of hydro-meteorological drought in Nepal Himalaya: A case of Karnali River Basin." *Weather Clim. Extrem.*, 26(November 2018), 100239.

Kiem, A. S., and Franks, S. W. (2001). "De l'identification de la variabilité des pluies et des écoulements causée par l'ENSO: Comparaison de méthodes et d'indices." *Hydrol. Sci. J.*, 46(5), 715–727.

Knight, J. R., Folland, C. K., and Scaife, A. A. (2006). "Climate impacts of the Atlantic

multidecadal oscillation.” *Geophys. Res. Lett.*, 33(17), 2–5.

Kothawale, D. R., and Rajeevan, M. (2017). *Monthly, Seasonal and Annual Rainfall Time Series for All-India, Homogeneous Regions and Meteorological Subdivisions: 1871-2016*. IITM Research Rep. No. RR-138. Pune, India: Indian Institute of Tropical Meteorology.

Kripalani, R. H., and Kulkarni, A. (1994). “Climatic impact of El NiAo / La Niiia on the Indian monsoon :” *R. Meteorol. Soc.*, (1976), 205–209.

Krishnamurthy, L., and Krishnamurthy, V. (2014). “Decadal scale oscillations and trend in the Indian monsoon rainfall.” *Clim. Dyn.*, 43(1–2), 319–331.

Krishnan, R., and Sugi, M. (2003). “Pacific decadal oscillation and variability of the Indian summer monsoon rainfall.” *Clim. Dyn.*, 21(3–4), 233–242.

Kug, J.-S., and Kang, I.-S. (2006). “Interactive Feedback between ENSO and the Indian Ocean.” *J. Clim.*, 19, 1784–1801.

Kulithalai, Shiyam, Sundar, P., and Kundapura, S. (2023). “Spatial Mapping of Flood Susceptibility Using Decision Tree–Based Machine Learning Models for the Vembanad Lake System in Kerala, India.” *J. Water Resour. Plan. Manag.*, 149(10), 1–21.

Kumar., D. N., RAJU., K. S., and SATHISH., T. (2004). “River flow forecasting using artificial neural networks.” *Water Resour. Manag.*, 9(18), 143–161.

Kumar, K. S., Anandraj, P., Sreelatha, K., Bisht, D. S., and Sridhar, V. (2021a). “Monthly and seasonal drought characterization using grace-based groundwater drought index and its link to teleconnections across south indian river basins.” *Climate*, 9(4).

Kumar, M. N., Murthy, C. S., Sesha, M. V. R., and Roy, P. S. (2009). “On the use of Standardized Precipitation Index (SPI) for drought intensity assessment.” *Meteorol. Appl. 16*, 389(April), 381–389.

Kumar, M. S., Kolluru, V., Gowthami, S. B., Anjita, N. A., Nayana, N., Regi, L., and Dwarakish, G. S. (2021b). “Monitoring land use and land cover changes in coastal karnataka.” *Trends Civ. Eng. Challenges Sustain.*, 99, 785–795.

Kumar, R., and Eldho, S. T. I. (2018). “Effects of historical and projected land use / cover change on runoff and sediment yield in the Netravati river basin , Western Ghats , India.” *Environ. Earth Sci.*, 77(3), 1–19.

Kumar, S., and Ahmed, S. A. (2022). “Spatial and Temporal Pattern Assessment of Meteorological Drought in Tumakuru District of Karnataka during 1951-2019 using Standardized Precipitation Index.” 98, 822–830.

Kumar, V. H. M., Shivamurthy, M., Govinda Gowda, V., and Biradar, G. S. (2017). “Assessing decision-making and economic performance of farmers to manage climate-induced crisis in Coastal Karnataka (India).” *Clim. Change*, 142(1–2), 143–153.

Kumari, P., and Himanshu, S. K. (2016). “Estimation of Design Flood for Rivers of Saurashtra Region Contributing into the Gulf of Khambhat.” 11(3), 869–882.

Kwak, J., Soo, Y., So, J., and Soo, H. (2012). “Drought Severity-Duration-Frequency Analysis of Hydrological Drought Based on Copula Theory 2 . Drought Identification using streamflow series 3 . Analysis of Existing Drought Characteristics in Study Area.” *Dep. Civ. Eng. Inha Univ.*, 82–89.

Lakshmi Kumar, T. V., Koteswara Rao, K., Barbosa, H., and Uma, R. (2014). “Trends and extreme value analysis of rainfall pattern over homogeneous monsoon regions of India.” *Nat. Hazards*, 73(2), 1003–1017.

Lambe, B. T., and Kundapura, S. (2023). “Recent Changes in Hydrometeorological Extremes in the Bilate River Basin of Rift Valley, Ethiopia.” *J. Hydrol. Eng.*, 28(7), 1–17.

Le, J. A., El-Askary, H. M., Allali, M., and Struppa, D. C. (2017). “Application of recurrent neural networks for drought projections in California.” *Atmos. Res.*, 188, 100–106.

Li, C., Singh, V., and Mishra, A. (2013). “A bivariate mixed distribution with a heavy-tailed component and its application to single-site daily rainfall simulation.” *Water Resour. Res.*, 49, 767–789.

Li, J. Z., Wang, Y. X., Li, S. F., and Hu, R. (2015a). “A Nonstationary Standardized Precipitation Index incorporating climate indices as covariates.” *J. Geophys. Res.*, 120(23), 12082–12095.

Li, J. Z., Wang, Y. X., Li, S. F., and Hu, R. (2015b). “A Nonstationary Standardized Precipitation Index incorporating climate indices as covariates.” *J. Geophys. Res. Atmos.*, 82–95.

Li, W., Fu, R., Juárez, R. I. N., and Fernandes, K. (2008). “Observed change of the standardized precipitation index, its potential cause and implications to future climate

change in the Amazon region." *Philos. Trans. R. Soc. B Biol. Sci.*, 363(1498), 1767–1772.

Lin, Q., Wu, Z., Singh, V. P., Sadeghi, S. H. R., He, H., and Lu, G. (2017). "Correlation between hydrological drought, climatic factors, reservoir operation, and vegetation cover in the Xijiang Basin, South China." *J. Hydrol.*, 549, 512–524.

Lin, Q., Wu, Z., Zhang, Y., Peng, T., Chang, W., and Guo, J. (2023). "Propagation from meteorological to hydrological drought and its application to drought prediction in the Xijiang River basin, South China." *J. Hydrol.*, 617(PB), 128889.

Liu, Q., Yang, Y., Liang, L., Jun, H., Yan, D., Wang, X., Li, C., and Sun, T. (2023). "Thresholds for triggering the propagation of meteorological drought to hydrological drought in water-limited regions of China." *Sci. Total Environ.*, 876, 162771.

Lv, A., Fan, L., and Zhang, W. (2022). "Impact of ENSO Events on Droughts in China." *Atmosphere (Basel).*, 13(11).

Ma, S., Zhu, C., and Liu, J. (2020). "Combined Impacts of Warm Central Equatorial Pacific Sea Surface Temperatures and Anthropogenic Warming on the 2019 Severe Drought in East China." *Adv. Atmos. Sci.*, 37(11), 1149–1163.

Madadgar, S., AghaKouchak, A., Farahmand, A., and Davis, S. J. (2017). "Probabilistic estimates of drought impacts on agricultural production." *Geophys. Res. Lett.*, 44(15), 7799–7807.

Madhavi, K., and Gowda, G. (2014). "HYDROLOGICAL STUDY OF COASTAL WATERS OF MANGALORE :" 5(4), 23–35.

Mahajan, D. R., and Dodamani, B. M. (2015). "Trend Analysis of Drought Events Over Upper Krishna Basin in Maharashtra." *Aquat. Procedia*, 4(Icwrcoe), 1250–1257.

Maier, H. R., and Dandy, G. C. (2000). "Neural networks for the prediction and forecasting of water resources variables : a review of modelling issues and applications." 15, 101–124.

Masanta, S. K., and Srinivas, V. V. (2022). "Proposal and evaluation of nonstationary versions of SPEI and SDDI based on climate covariates for regional drought analysis." *J. Hydrol.*, 610(November 2021).

McKee, T. B., Doesken, N. J., and Kliest, J. (1993). "The relationship of drought frequency and duration to time scales." *In Proc., 8th Conf.*, 179–184.

Mehran, N., Moutzouros, V. (Bill), and Bedi, A. (2015). "A Review of Current Graft

Options for Anterior Cruciate Ligament Reconstruction." *JBJS Rev.*, 3(11).

MEI. (2011). "Extended multivariate ENSO index (MEI.ext)." *Boulder, CO Phys. Sci. Lab.*

MEI. (2018). "MEI updated 2018(1950-18." *Boulder, CO NOAA Phys. Sci. Lab.*

Meresa, H., Zhang, Y., Tian, J., and Abrar Faiz, M. (2023). "Understanding the role of catchment and climate characteristics in the propagation of meteorological to hydrological drought." *J. Hydrol.*, 617(PB), 128967.

Meshram, S. G., Ghorbani, M. A., Shamshirband, S., Karimi, V., and Meshram, C. (2019). "River flow prediction using hybrid PSOGSA algorithm based on feed-forward neural network." *Soft Comput.*, 23(20), 10429–10438.

Midhuna, T. M., and Dimri, A. P. (2019). "Impact of arctic oscillation on Indian winter monsoon." *Meteorol. Atmos. Phys.*, 131(4), 1157–1167.

Ministry of Environment and Forests, G. of I. (2004). *India's initian nation communication to the United Nations Framework Convention on Climate Change*.

Mishra, A. K., and Desai, V. R. (2005a). "Spatial and temporal drought analysis in the kansabati river basin, india." *Int. J. River Basin Manag.*, 3(1), 43–52.

Mishra, A. K., and Desai, V. R. (2005b). "Drought forecasting using stochastic models." *Stoch. Environ. Res. Risk Assess.*, 19(5), 326–339.

Mishra, A. K., and Desai, V. R. (2006). "Drought forecasting using feed-forward recursive neural network." *Ecol. Modell.*, 198(1–2), 127–138.

Mishra, A. K., and Singh, V. P. (2010). "A review of drought concepts." *J. Hydrol.*, 391(1–2), 202–216.

Mishra, A. K., and Singh, V. P. (2011). "Drought modeling - A review." *J. Hydrol.*, 403(1–2), 157–175.

Mishra, V. (2020). "Long-term (1870 – 2018) drought reconstruction in context of surface water security in India." *J. Hydrol.*, 580(October 2019), 124228.

Moeeni, H., and Bonakdari, H. (2017). "Forecasting monthly inflow with extreme seasonal variation using the hybrid SARIMA-ANN model." *Stoch. Environ. Res. Risk Assess.*, 31(8), 1997–2010.

Mondal, A., and Mujumdar, P. P. (2015). "Modeling non-stationarity in intensity, duration and frequency of extreme rainfall over India." *J. Hydrol.*, 521, 217–231.

Morid, S., And, V. S., and Bagherzadehc, K. (2008). "Drought forecasting using

artificial neural networks and time series of drought indices." *Int. J. Climatol.*, 2029(March 2008), 2011–2029.

Mortuza, R., Moges, E., Demissie, Y., and Li, H. (2019). "Historical and future drought in Bangladesh using copula-based bivariate regional frequency analysis." *Theor. Appl. Climatol.*, 135(3), 855–871.

Mossad, A., and Alazba, A. A. (2015). "Drought forecasting using stochastic models in a hyper-arid climate." *Atmosphere (Basel).*, 6(4), 410–430.

Mousavi-Mirkalaei, Pezhman, and Banihabib, M. E. (2019). "An ARIMA-NARX hybrid model for forecasting urban water consumption (case study: Tehran metropolis)." *Urban Water J.*, 16(5), 365–376.

Murari, K.K., Mahato, S., Jayaraman, T. and Swaminathan, M. (2018). *Extreme Temperatures and Crop Yields in Karnataka, India*. *Review of Agrarian Studies*.

Muthuvel, D., and Mahesha, A. (2021). "Spatiotemporal Analysis of Compound Agrometeorological Drought and Hot Events in India Using a Standardized Index." *J. Hydrol. Eng.*, 26(7), 04021022.

Myronidis, D., Ioannou, K., Fotakis, D., and Dörflinger, G. (2018). "Streamflow and Hydrological Drought Trend Analysis and Forecasting in Cyprus." *Water Resour. Manag.*, 32(5), 1759–1776.

Nagaraj, M., and Srivastav, R. (2022). "Spatial multivariate selection of climate indices for precipitation over India." *Environ. Res. Lett.*, 17(9), 0–11.

NAO. (2023). "Northern Atlantic Ocillation NAO." *NOAA Natl. Centers Environ. Inf.*, <https://www.ncei.noaa.gov/access/monitoring/nao/>.

Nathan, K. K. (2001). *Poor Water Resources and Drought in the Gujarat/Saurashtra Poor Water Resources and Drought in the Gujarat/Saurashtra Regions of India Regions of India*. Drought Network News (1994-2001).

Nazir. M., Pandiyarajhan, G. K., and Ravikumar, G. (2016). "DROUGHT ANALYSING TECHNIQUES USING VARIOUS DROUGHT INDICESNo Title." 126–137.

Ozkaya, A. (2023). "Evaluating the relation between meteorological drought and hydrological drought, and the precipitation distribution for drought classes and return periods over the upper Tigris River catchment." *Theor. Appl. Climatol.*, 153(1–2), 727–753.

Ozkaya, A., and Zerberg, Y. (2019). “A 40-year analysis of the hydrological drought index for the Tigris Basin, Turkey.” *Water (Switzerland)*, 11(4).

Pai, D. S., Sridhar, L., Guhathakurta, P., and Hatwar, H. R. (2011). “District-wide drought climatology of the southwest monsoon season over India based on standardized precipitation index (SPI).” *Nat. Hazards*, 59(3), 1797–1813.

Pai, D. S., Sridhar, L., Rajeevan, M., Sreejith, O. P., Satbhai, N. S., and Mukhopadhyay, B. (2014). “Development of a new high spatial resolution (0.25° × 0.25°) long period (1901-2010) daily gridded rainfall data set over India and its comparison with existing data sets over the region.” *Mausam*, 1(January), 1–18.

Paing, K. H., Li, Y., Mie, Z., and Sein, M. (2023). “Temperature (maximum) and Rainfall Prediction Us- ing FNN and RNN Models over Kaba Aye Station , Yangon Region , Myanmar.” 6(3), 1–13.

Palmer, W. (1965). *Meteorological Drought*. Research Paper No. 45. Washington, DC: US Weather Bureau.

Palmer, W. C. (1968). “Keeping Track of Crop Moisture Conditions, Nationwide: The New Crop Moisture Index.” *Weatherwise*, 21(4), 156–161.

Panda, A., Sahu, N., Behera, S., Sayama, T., Sahu, L., Avtar, R., Singh, R. B., and Yamada, M. (2019). “Impact of climate variability on crop yield in Kalahandi, Bolangir, and Koraput districts of Odisha, India.” *Climate*, 7(11), 126.

Pande, C. B., Al-Ansari, N., Kushwaha, N. L., Srivastava, A., Noor, R., Kumar, M., Moharir, K. N., and Elbeltagi, A. (2022). “Forecasting of SPI and Meteorological Drought Based on the Artificial Neural Network and M5P Model Tree.” *Land*, 11(11), 1–24.

Pande, C. B., Kushwaha, N. L., Orimoloye, I. R., Kumar, R., Abdo, H. G., Tolche, A. D., and Elbeltagi, A. (2023). *Comparative Assessment of Improved SVM Method under Different Kernel Functions for Predicting Multi-scale Drought Index*. *Water Resour. Manag.*, Springer Netherlands.

Pandya, P. A., H., P. S., V., P. G., D., G. G., and D., V. D. (2023). “Rainfall Variability Analysis of Saurashtra Region of Gujarat.” *Int. J. Adv. Res. Biol. Sci*, 10(6), 131–140.

Parthasarathy, B., Sontakke, N. A., Monot, A. A., and Kothawale, D. R. (1987). “Droughts/floods in the summer monsoon season over different meteorological subdivisions of India for the period 1871-1984.” *J. Climatol.*, 7, 57–70.

Patel, H. R., Lunagaria, M. M., Karande, B. I., Yadav, S. B., Shah, A. V., Sood, V. K., and Pandey, V. (2015). “Climate change and its impact on major crops in Gujarat.” *J. Agrometeorol.*, 17(2), 190–193.

Patel, N. R., Chopra, P., and Dadhwal, V. K. (2007). “Analyzing spatial patterns of meteorological drought using standardized precipitation index.” *Meteorol. Appl.*, 14(4), 329–336.

PDO. (2023). “Pacific Decadal Oscillation (PDO) Monthly Data.” *Japan Meteorol. Agency*, <https://ds.data.jma.go.jp/tcc/tcc/products/elnino/decadal/pdo_month.html>.

Pervez, M. S., and Henebry, G. M. (2015). “Spatial and seasonal responses of precipitation in the Ganges and Brahmaputra river basins to ENSO and Indian Ocean dipole modes : implications for flooding and drought.” 147–162.

Phesa, M., Woyessa, Y., and Mbatha, N. (2023). “Evapotranspiration Prediction Using ARIMA, ANN and Hybrid Models for Optimum Water Use in Agriculture: A Case Study of Keiskammahoek Irrigation Scheme, Eastern Cape, South Africa.” (Iswee 2022), 276–286.

Poonia, V., Jha, S., and Goyal, M. K. (2021). “Copula based analysis of meteorological, hydrological and agricultural drought characteristics across Indian river basins.” *Int. J. Climatol.*, 41(9), 4637–4652.

Prybutok, V. R., Yi, J., and Mitchell, D. (2000). “Comparison of neural network models with ARIMA and regression models for prediction of Houston’s daily maximum ozone concentrations.” *Eur. J. Oper. Res.*, 122(1), 31–40.

Publishing, I. W. A. (2011). “Trends in rainfall amount and number of rainy days in river basins of India (1951 – 2004) Vijay Kumar and Sharad K . Jain.” 290–306.

Rashid, M., and Beecham, S. (2019). “Science of the Total Environment Development of a non-stationary Standardized Precipitation Index and its application to a South Australian climate.” *Sci. Total Environ.*, 657, 882–892.

Rashid, M. M., Beecham, S., and Chowdhury, R. K. (2016). “Statistical downscaling of rainfall: a non-stationary and multi-resolution approach.” *Theor. Appl. Climatol.*, 124(3–4), 919–933.

Reddy, M. J., and Ganguli, P. (2012a). “Bivariate Flood Frequency Analysis of Upper Godavari River Flows Using Archimedean Copulas.” *Water Resour. Manag.*, 26(14), 3995–4018.

Reddy, M. j, and Ganguli, P. (2012b). “Application of copulas for derivation of drought severity-duration-frequency curves.” *Hydrol. Process.*, 26(11), 1672–1685.

Renard, B., and Lang, M. (2007). “Use of a Gaussian copula for multivariate extreme value analysis: Some case studies in hydrology.” *Adv. Water Resour.*, 30(4), 897–912.

Revadekar, J. V., and Kulkarni, A. (2008). “The impact of the positive Indian Ocean dipole on Zimbabwe droughts Tropical climate is understood to be dominated by.” *Int. J. Climatol.*, 2029, 2011–2029.

Revadekar, J. V., Patwardhan, S. K., and Rupa Kumar, K. (2011). “Characteristic Features of Precipitation Extremes over India in the Warming Scenarios.” *Adv. Meteorol.*, 2011, 1–11.

Rigby, R. A., and Stasinopoulos, D. M. (2005). “Generalized additive models for location, scale and shape (with discussion).” *Appl. Stat*, 54(3), 507–554.

Sajeev, A., Deb Barma, S., Mahesha, A., and Shiau, J.-T. (2021). “Bivariate Drought Characterization of Two Contrasting Climatic Regions in India Using Copula.” *J. Irrig. Drain. Eng.*, 147(3), 05020005.

Sajeev, A., and Kundapura, S. (2023a). “Temporal Assessment of Meteorological Drought Events Using Stationary and Nonstationary Drought Indices for Two Climate Regions in India.” *J. Hydrol. Eng.*, 28(11), 1–23.

Sajeev, A., and Kundapura, S. (2023b). “A Non-stationary Hydrologic Drought Index Using Large-Scale Climate Indices as Covariates.” *Recent Dev. River Corridor Manag.*, S. Dutta and V. Chembolu, eds., Singapore: Springer Nature Singapore, 53–65.

Saji, N. H., Goswami, B. N., Vinayachandran, P. N., and Yamagata, T. (1999). “A dipole mode in the tropical Indian ocean.” *Nature*, 401(6751), 360–363.

Saji, N. H., and Yamagata, T. (2003). “Possible impacts of Indian Ocean Dipole mode events on global climate.” *Clim. Res.*, 25(2), 151–169.

Salimi, H., Asadi, E., and Darbandi, S. (2021). “Meteorological and hydrological drought monitoring using several drought indices.” *Appl. Water Sci.*, 11(2), 1–10.

Samra, J. S. (2004). *Review and Analysis of Drought Monitoring , Declaration and Management in India*. Working Paper 84. Colombo, Sri Lanka: International Water Management Institute.

Sasikumar, K., and Nair, V. G. (2016). “Temporal and Spatial Analysis of Drought over

a Tropical Wet Station of India in the Recent Decades Using the SPI Method." *Int. J. Appl. Pure Sci. Agric.*, 2(6), 12–21.

Schleiter, I. M., Borchardt, D., Wagner, R., Dapper, T., Schmidt, K. D., Schmidt, H. H., and Werner, H. (1999). "Modelling water quality, bioindication and population dynamics in lotic ecosystems using neural networks." *Ecol. Modell.*, 120(2–3), 271–286.

Shafaei, M., Adamowski, J., Fakheri-Fard, A., Dinpashoh, Y., and Adamowski, K. (2016). "A wavelet-SARIMA-ANN hybrid model for precipitation forecasting." *J. Water L. Dev.*, 28(1), 27–36.

Shamshirband, S., Hashemi, S., Salimi, H., Asadi, E., Shadkani, S., Kargar, K., Nabipour, N., and Chau, K. (2020). "Mechanics Predicting Standardized Streamflow index for hydrological drought using machine learning models Predicting Standardized Streamflow index for hydrological drought using." *Eng. Appl. Comput. Fluid Mech.*, 14, 339–350.

Sharma, T. C., and Panu, U. S. (2014). "Journal of Hydrology : Regional Studies Modeling of hydrological drought durations and magnitudes : Experiences on Canadian streamflows." *J. Hydrol. Reg. Stud.*, 1, 92–106.

Shewale, M. P., and Kumar, S. (2005). *Climatological features of drought indices in India*.

Shiau, J.-T., and Shen, H. W. (2001). "Recurrence analysis of hydrologic droughts of differing severity." *J. water Resour. Plan. Manag.*, 127(1), 30–40.

Shiau, J. (2020). "Effects of Gamma-Distribution Variations on SPI-Based Stationary and Nonstationary Drought Analyses." *Water Resour. Manag.*, 34(6), 2081–2095.

Shiau, J. T. (2003). "Return period of bivariate distributed extreme hydrological events." *Stoch. Environ. Res. Risk Assess.*, 17(1–2), 42–57.

Shiau, J. T. (2006). "Fitting drought duration and severity with two-dimensional copulas." *Water Resour. Manag.*, 20(5), 795–815.

Silverman, D., and Dracup, J. A. (2000). "Artificial neural networks and long-range precipitation prediction in California." *J. Appl. Meteorol.*, 39(1), 57–66.

Singh, Pavan, K., Nitin, S., and Richa, N. (2019). *Wind power forecasting using hybrid ARIMA-ANN technique*. Ambient Communications and Computer Systems: RACCCS-2018: Springer Singapore.

Singh, R., Devi, G., Parmar, D., and Mishra, S. (2017). “Impact of Rainfall and Temperature on the Yield of Major Crops in Gujarat State of India: A Panel Data Analysis (1980-2011).” *Curr. J. Appl. Sci. Technol.*, 24(5), 1–9.

SOI. (2020). “Southern Oscillation Index (SOI) Monthly Data.” *Boulder, CO NOAA Clim. Predict. Cent.*, <https://www.ncdc.noaa.gov/teleconnections/enso/indicators/soi/data.csv>.

Srinivasa Reddy, G. S., and Prabhu, C. N. (2017). “Natural Disaster Monitoring System – Karnataka Model.” (5), 178–187.

Srinivasareddy, G. S., Shivakumarnaiklal, H. S., Keerthy, N. G., Garag, P., Jothi, E. P., and Challa, O. (2019). “Drought vulnerability assessment in Karnataka : Through composite climatic index.” *MAUSAM*, 70(1), 159–170.

SST. (2020). “Sea Surface Temperature (SST) Niño 3.4 Index.” *Boulder, CO NOAA, Phys. Sci. Lab. Glob. Clim. Obs. Syst. Gr. Surf. Press.*, <https://psl.noaa.gov/gcos_wgsp/Timeseries/Data/nino34.long.anom.data> (May 18, 2022).

Stasinopoulos, D. M., and Rigby, R. A. (2007). “Generalized additive models for location scale and shape (GAMLSS) in R.” *J. Stat. Softw.*, 23(7), 1–46.

Surakhi, O., Zaidan, M. A., Fung, P. L., Motlagh, N. H., Serhan, S., Alkhanafseh, M., Ghoniem, R. M., and Hussein, T. (2021). “Time-lag selection for time-series forecasting using neural network and heuristic algorithm.” *Electron.*, 10(20).

Swetalina, N., and Thomas, T. (2016). “Evaluation of Hydrological Drought Characteristics for Bearma Basin in Bundelkhand Region of Central India.” *Procedia Technol.*, 24, 85–92.

Telesca, L., Lovallo, M., Lopez-moreno, I., and Vicente-serrano, S. (2012). “Investigation of scaling properties in monthly streamflow and Standardized Streamflow Index (SSI) time series in the Ebro basin (Spain).” *Physica A*, 391(4), 1662–1678.

Thirumalaiah, K., and Deo, M. C. (2000). “Hydrological forecasting using neural networks.” *J. Hydrol. Eng.*, 5(2), 180–189.

Thomas, J., and Prasannakumar, V. (2016). “Temporal analysis of rainfall (1871–2012) and drought characteristics over a tropical monsoon-dominated State (Kerala) of India.” *J. Hydrol.*, 534, 266–280.

Tigkas, D., Vangelis, H., and Tsakiris, G. (2012). “Drought and climatic change impact on streamflow in small watersheds.” *Sci. Total Environ.*, 440, 33–41.

Tijdeman, E., Stahl, K., and Tallaksen, L. M. (2020). “Drought Characteristics Derived Based on the Standardized Streamflow Index: A Large Sample Comparison for Parametric and Nonparametric Methods.” *Water Resour. Res.*, 56(10).

Todmal, R. S. (2022). “Link between monsoon rainfall variability and agricultural drought in the semi-arid region of Maharashtra, India.” *Curr. Sci.*, 122(8), 934–944.

Todmal, R. S., Koteswara Rao, K., Ingle, S., and Korade, M. S. (2022). “Impact of Southern Oscillation and Indian Ocean Dipole on rainfall variability over India: trends and interlinkages during 1871–2017.” *Meteorol. Atmos. Phys.*, 134(6), 1–19.

Tokar, B. A. S., and Johnson, P. A. (1999). “Rainfall-Runoff Modeling Using Artificial Neural Networks.” 4(JULY), 232–239.

Trenberth, K. E. (2011). “Changes in precipitation with climate change.” *Clim. Res.*, 47(1–2), 123–138.

Tsakiris, I. N. G. (2009). “Assessment of Hydrological Drought Revisited.” *Water Resour Manag.*, 23(April 2007), 881–897.

Tsanis, I., and Tapoglou, E. (2019). “Winter North Atlantic Oscillation impact on European precipitation and drought under climate change.” *Theor. Appl. Climatol.*, 135(1–2), 323–330.

Ummenhofer, C. C., Gupta, A. Sen, Briggs, P. R., England, M. H., McIntosh, P. C., Meyers, G. A., Pook, M. J., Raupach, M. R., and Risbey, J. S. (2011). “Indian and Pacific Ocean influences on southeast Australian drought and soil moisture.” *J. Clim.*, 24(5), 1313–1336.

Verdon-Kidd, D. C., and Kiem, A. S. (2009). “Nature and causes of protracted droughts in southeast Australia: Comparison between the federation, WWII, and big dry droughts.” Geophys. Res. Lett: Geophys. Res. Lett.

Vicente-serrano, S. M., López-moreno, J. I., Beguería, S., Lorenzo-lacruz, J., Azorin-molina, C., and Morán-tejeda, E. (2012). “Accurate Computation of a Streamflow Drought Index.” (February), 318–332.

Wang, C., Linderholm, H. W., Song, Y., Wang, F., Liu, Y., Tian, J., Xu, J., Song, Y., and Ren, G. (2020a). “Impacts of drought on maize and soybean production in northeast China during the past five decades.” *Int. J. Environ. Res. Public Health*, 17(7), 2459.

Wang, F., Wang, Z., Yang, H., Di, D., Zhao, Y., Liang, Q., and Hussain, Z. (2020b). "Comprehensive evaluation of hydrological drought and its relationships with meteorological drought in the Yellow River basin, China." *J. Hydrol.*, 584(January), 124751.

Wang, S., Huang, J., He, Y., and Guan, Y. (2014). "Combined effects of the Pacific Decadal Oscillation and El Niño-Southern Oscillation on Global Land Dry-Wet Changes." *Sci. Rep.*, 4, 1–8.

Wang, Y., Duan, L., Liu, T., Li, J., and Feng, P. (2020c). "A Non-stationary Standardized Streamflow Index for hydrological drought using climate and human-induced indices as covariates." *Sci. Total Environ.*, 699, 134278.

Wang, Y., Li, J., Feng, P., and Chen, F. (2015a). "Effects of large-scale climate patterns and human activities on hydrological drought: a case study in the Luanhe River basin, China." *Nat. Hazards*, 76(3), 1687–1710.

Wang, Y., Li, J., Feng, P., and Hu, R. (2015b). "A Time-Dependent Drought Index for Non-Stationary Precipitation Series." *Water Resour. Manag.*, 29(15), 5631–5647.

Wang, Y., Li, S., and Lu, D. (2009). "Seasonal response of Asian monsoonal climate to the Atlantic Multidecadal Oscillation." *J. Geophys. Res. Atmos.*, 114(2), 1–15.

Wang, Y., Quan, Q., and Shen, B. (2019). "Spatio-temporal variability of drought and effect of large scale climate in the source region of Yellow River." *Geomatics, Nat. Hazards Risk*, 10(1), 678–698.

Wilhite, D. A., and Glantz, M. H. (2019). "Understanding the drought phenomenon: The role of definitions." *Plan. Drought Towar. A Reduct. Soc. Vulnerability*, 11–27.

WMO (World Meteorological Organization). (2012). *Standardized Precipitation Index User Guide*. WMO No. 1090. Geneva: WMO.

Wolter, K., and Timlin, M. S. (1993). "Monitoring ENSO in COADS with a seasonally adjusted principal component index." *Proc. 17th Clim. Diagnostics Work.*

Wolter, K., and Timlin, M. S. (1998). "How does 1997198 rank ? events :" *Weather*, 53(9), 315–324.

Wu, D., Yoon, H. C., Lee, J. H., and Kim, J. S. (2022). "Regional Analysis of Hotspot and Coldspot Areas Undergoing Nonstationary Drought Characteristics in a Changing Climate." *Appl. Sci.*, 12(17).

Wu, J., Chen, X., Yao, H., Gao, L., Chen, Y., and Liu, M. (2017). "Non-linear

relationship of hydrological drought responding to meteorological drought and impact of a large reservoir." *J. Hydrol.*, 551, 495–507.

Wu, Z., Li, J., Jiang, Z., He, J., and Zhu, X. (2012). "Possible effects of the North Atlantic Oscillation on the strengthening relationship between the East Asian Summer monsoon and ENSO." *Int. J. Climatol.*, 32(5), 794–800.

Xu, D., Zhang, Q., Ding, Y., and Zhang, D. (2022). "Application of a hybrid ARIMA-LSTM model based on the SPEI for drought forecasting." *Environ. Sci. Pollut. Res.*, 29(3), 4128–4144.

Yadav, S. M., Bhagat, S. R., and Yadav, V. G. (2021). "Temporal analysis of precipitation in Saurashtra, Kutch, and Diu sub-division of Western Indian region." 144, 521–533.

Yang, H. (2011). "The significant relationship between the Arctic Oscillation (AO) in December and the January climate over South China." *Adv. Atmos. Sci.*, 28(2), 398–407.

Yang, Q., Ma, Z., Fan, X., Yang, Z. L., Xu, Z., and Wu, P. (2017). "Decadal modulation of precipitation patterns over eastern China by sea surface temperature anomalies." *J. Clim.*, 30(17), 7017–7033.

Yu, J., and Kim, T. (2019). "Future Hydrological Drought Risk Assessment Based on Nonstationary Joint Drought Management Index." *Water*, 11(3), 532.

Zadafiya, G., Ladavia, C. P., and Gandhi, H. (2022). "Downscaling approach for analysis and forecasting of meteorological parameters and identification of different drought years." *J. Water Clim. Chang.*, 13(8), 3119–3131.

Zamani, R., Tabari, H., and Willems, P. (2015). "Extreme streamflow drought in the Karkheh river basin (Iran): probabilistic and regional analyses." *Nat Hazards*, 76(1), 327–346.

Zhang, D. dong, Yan, D. hua, Wang, Y. C., Lu, F., and Liu, S. hua. (2015). "GAMLSS-based nonstationary modeling of extreme precipitation in Beijing–Tianjin–Hebei region of China." *Nat. Hazards*, 77(2), 1037–1053.

Zhang, J., Shi, X., Li, J., and Li, F. (2019). "Copula-based joint probability distribution of water supply and demand in Luhun irrigation district." *Water Sci. Technol. Water Supply*, 19(3), 932–943.

Zhang, L., and Singh, V. P. (2007). "Bivariate rainfall frequency distributions using

Archimedean copulas." *J. Hydrol.*, 332(1–2), 93–109.

Zhang, P. G. (2003). "Time series forecasting using a hybrid ARIMA and neural network model." *Neurocomputing*, 50, 159–175.

Zhang, Q., Li, J., Singh, V. P., Xu, C. Y., and Deng, J. (2013). "Influence of ENSO on precipitation in the East River basin, south China." *J. Geophys. Res. Atmos.*, 118(5), 2207–2219.

Zhang, R., and Delworth, T. L. (2006). "Impact of Atlantic multidecadal oscillations on India/Sahel rainfall and Atlantic hurricanes." *Geophys. Res. Lett.*, 33(17), 1–5.

Zhang, T., Su, X., and Feng, K. (2021). "The development of a novel nonstationary meteorological and hydrological drought index using the climatic and anthropogenic indices as covariates." *Sci. Total Environ.*, 786, 147385.

Zhang, X., Obrin, R., Wei, C., Chen, N., and Niyogi, D. (2017a). "Droughts in India from 1981 to 2013 and Implications to Wheat Production." *Sci. Rep.*, (October 2016), 1–12.

Zhang, Y., Li, W., Chen, Q., Pu, X., and Xiang, L. (2017b). "Multi-models for SPI drought forecasting in the north of Haihe River Basin, China." *Stoch. Environ. Res. Risk Assess.*, 31(10), 2471–2481.

Zhao, J., Xu, J., Xie, X., and Lu, H. (2016a). "Drought monitoring based on TIGGE and distributed hydrological model in Huaihe River Basin, China." *Sci. Total Environ.*, 553, 358–365.

Zhao, L., Lyu, A., Wu, J., Hayes, M., Tang, Z., He, B., Liu, J., and Liu, M. (2014). "Impact of meteorological drought on streamflow drought in Jinghe River Basin of China." *Chinese Geogr. Sci.*, 24(6), 694–705.

Zhao, L., Wu, J., and Fang, J. (2016b). "Robust response of Streamflow drought to different timescales of meteorological drought in Xiangjiang river basin of China." *Adv. Meteorol.*, 2016.

Zhou, H. C., Peng, Y., and Liang, G. H. (2008). "The research of monthly discharge predictor-corrector model based on wavelet decomposition." *Water Resour. Manag.*, 22(2), 217–227.

Zhu, N., Xu, J., Zeng, G., and Cao, X. (2021). "Spatiotemporal response of hydrological drought to meteorological drought on multi-time scales concerning endorheic basin." *Int. J. Environ. Res. Public Health*, 18(17), 9074.

PUBLICATIONS

Journals

- Arya Sajeev and Subrahmanya Kundapura, (2023) "Temporal assessment of meteorological drought events using stationary and non-stationary drought indices for two climate regions in India." *J. Hydrol. Eng.(**ASCE**) 28:1-23.* https://doi.org/10.1061/JHYEFF.HEENG-6011
- Arya Sajeev and Subrahmanya Kundapura, (2024) "Comparative evaluation of meteorological and hydrological drought using stationary and non-stationary indices in a semi-arid river basin in India." *Natural Hazards, Springer. 1-36.* https://doi.org/10.1007/s11069-024-06739-2
- Arya Sajeev and Subrahmanya Kundapura, "Performance Evaluation of ARIMA, FNN, RNN, and Hybrid models in Forecasting Meteorological drought in a semi-arid region in India." *J. Hydrol. Eng.(**ASCE**).*
  (**Under Review**)

Conference

- Arya Sajeev and Subrahmanya Kundapura, (2021) "Stream flow and Hydrological Drought Trend analysis and forecasting." Proc. Int.Conf. Hydraulics, Water Resources and Coastal Engg., (HYDRO 2020), Paramount Publishing House, ISBN: 9789390631568, Vol. 2, 1155-1165.
  (**Secured best paper award**)

- Arya Sajeev and Subrahmanya Kundapura, (2022) "A Non-stationary Streamflow Drought Index using large-scale climate indices as covariates." *2nd International Conference on River Corridor, Research & Management 2022, IIT Guwahati and IIT Jammu.*
  https://doi.org/10.1007/978-981-99-4423-1_4

BIODATA

Name	**Arya Sajeev**
Date of Birth	17.12.1993
Address	Nadukkudi House, Iramalloor P.O, Kothamangalam, Ernakulam. Kerala. 686691
Qualification	M. Tech (Water Resources Engineering and Management)
E-mail	aryasaji93@gmail.com
Publications	Journals: 3 Conferences: 2
Awards/achievements	Best paper award for International Conference on Hydraulics, Water Resources and Coastal Engg., (HYDRO 2020)